Investigation of the Mechanisms of Excitation and Contraction in Rat Pulmonary and Systemic Resistance Arteries

Rahman, Mohammad

Award date:
2010

Awarding institution:
University of Bath

INVESTIGATION OF THE MECHANISMS OF EXCITATION AND CONTRACTION IN RAT PULMONARY AND SYSTEMIC RESISTANCE ARTERIES

Mohammad Mahmudur Rahman

A thesis submitted for the degree of Doctor of Philosophy

Department of Pharmacy and Pharmacology
University of Bath

August 2010

Signed……

Acknowledgements

No scientific work is a one man job. Supports from many people and institutions made this work possible. First of all, I would like to express my sincere gratitude and appreciation to my supervisor Dr. Sergey Smirnov for his continuous guidance and kind support throughout the research and writing up of this manuscript. His always-encouraging words and relentless pursuit of scientific excellence and integrity made him an excellent mentor to me and made me love science.

I acknowledge the invaluable help of Dr. Maksym Harhun in St. George's, University of London for his contribution to the confocal microscopy experiments. Dr. Alister McNeish and Dr. Vsevolod Telezhkin must be acknowledged for their contribution to the experiments measuring membrane potential. I sincerely thank Professor Jeremy Ward and his group in King's college, London for their generosity in allowing me use of their lab for permeabilisation and western blot experiments. Thanks also to Professor Chris Garland and Dr. Kim Dora for allowing me extensive use of their wire myograph.

I would also like to express my sincere thanks to all my fellow lab colleagues, with special recognition to Dr. Kathryn Yuill and Polina Iarova who helped me by offering technical support and sincere advice.

I am especially grateful to the ORS scheme of University of Bath, Bath, UK for providing funding to support my study. I am also thankful to my colleagues in the Department of Pharmacology, Faculty of Veterinary Science; and to the authority of Bangladesh Agricultural University, Mymensingh, Bangladesh for all sorts of support during my higher study.

Special thanks are owed to my parents who have first shown me the light of education. Last but not least, I thank my family specially my wife and daughter who supported me mentally throughout the past four years of my PhD program.

Publications

Conference abstracts:

1. **Rahman MM**, Smirnov SV. (2008). 4-aminopyridine contracts pulmonary artery in voltage-dependent and voltage-independent manner. Presented at EPHAR 2008, Manchester, 13-17 July and published at ***pA2Online 6[2], 007P. 2008.*** http://www.ephar2008. org/ downloads/ EPHAR2008_ Late_ Breaking_ Abstracts.pdf.

2. **Rahman MM,** Knock GA and Smirnov SV (2009). Role of voltage-gated K^+ channels in rat pulmonary arteries: the tale of two channels. A poster communication presented in Physiology 2009, University College Dublin, RoI, 7-10 July, 2009. ***Proc. Physiol. Soc.*** **15, PC116**. Published online at http://www.physoc.org/custom2/publications/proceedings/archive/article.asp?ID= Proc Physiol Soc 15PC116.

Original paper (in preparation):

1. **Mohammad M. Rahman,** Maksym I. Harhun, Alister J. McNeish, Vsevolod S. Telezkin, Sergey V. Smirnov. Regulation of excitability in the rat pulmonary vasculature: The tale of two K^+ channels.

Abstract

In the pulmonary circulation voltage-gated K^+ (K_V) channels control resting membrane potential. Their direct contribution to the development of hypoxic pulmonary vasoconstriction (HPV), the unique response of the pulmonary artery (PA) to hypoxia, however remains controversial. KCNQ channels are thought to contribute to the control of PA excitability but their relative contribution compared to the K_V channels and the role in HPV is unknown. Recent electrophysiological evidence suggests tight coupling between K_V channels and mitochondria, a putative oxygen sensor in PA. No focussed studies to examine these questions in intact arteries were performed. Therefore, the main aims were to investigate: i) a relative role of K_V and KCNQ channels in the regulation of PA excitability and contractility, ii) relative sensitivity of these channels to hypoxia, iii) a relationship between K_V channels and mitochondria and cellular metabolism, in the intact PA. Rat mesenteric artery (MA) was used as a representative of systemic circulations. Small vessel myography, microelectrode technique, confocal imaging and western blot together with selective pharmacological agents were employed to address these questions. The main findings are: i) the presence of mutual physiological interaction between K_V and KCNQ channels in the regulation of PA excitability, ii) K_V, but not KCNQ, channels are inhibited by hypoxia in PA, iii) the existence of specific interactions between mitochondria and K_V channels which are potentiated and altered in hypoxia in PA, not in MA, iv) these interactions may contribute to contractions caused by the K_V inhibition additionally to the voltage-dependent Ca^{2+} entry and Rho-kinase dependent Ca^{2+} sensitisation, v) contractions are less metabolic dependent in PA than in MA, vi) the effects are not species dependent as some were observed in the mouse. These findings suggest the presence of specific mitochondrial-dependent mechanisms in PA which play role in physiological conditions and in HPV.

List of abbreviations and symbols

4-AP	:	4-aminopyridine
$[Ca^{2+}]_i$	:	Intracellular free Ca^{2+} concentration
2-DOG	:	2-deoxyglucose
ADP	:	Adenosine diphosphate
AMP	:	Adenosine monophosphate
AMPK	:	AMP-activated protein kinase
APS	:	Ammonium persulphate
ATP	:	Adenosine 3`,5`-triphosphate
BK_{Ca}	:	Large conductance Ca^{2+}-activated K^+ channel
BSA	:	Bovine serum albumin
cADPR	:	Cyclic adenosine diphosphate ribose
CaM	:	Ca^{2+}-calmodulin complex
cAMP	:	Cyclic 3`,5`- adenosine monophosphate
CCCP	:	Carbonyl cyanide 3-chlorophenylhydrazone
CCE	:	Capacitative Ca^{2+} entry
cGMP	:	Cyclic 3`,5`- guanosine monophosphate
CH	:	Chronic hypoxia
ChTX	:	Charybdotoxin
CICR	:	Ca^{2+}-induced Ca^{2+} release
CN^-	:	Cyanide ion
CO	:	Carbon monoxide
CO_2	:	Carbon dioxide
COPD	:	Chronic obstructive pulmonary disease
CPA	:	Cyclopiazonic acid
CPI-17	:	PKC-potentiated phosphatase inhibitor protein-17 kDa
Da	:	Dalton
DAG	:	Diacylglycerol
ddH_2O	:	Double distilled water
DMSO	:	Dimethylsulphoxide
DNA	:	Deoxy-ribonucleic acid
E-C coupling	:	Electromechanical cell coupling

EC_{50}	:	Half maximal effective concentration
ECL	:	Enhanced chemiluminescence
EDTA	:	Ethylenediamine tetraacetic acid
EGTA	:	Ethylene glycol-bis (β-aminoethyl ether)-N, N, N`, N`-tetra acetic acid
E_m	:	Cell resting membrane potential
ERG	:	Ether-a-go-go-related genes
ET-1	:	Endothelin-1
FCCP	:	Carbonyl cyanide 4-trifluoromethoxy phenylhydrazone
Glc-6-PD	:	Glucose-6-phosphate dehydrogenase
GPCRs	:	G-protein coupled receptors
H_2O_2	:	Hydrogen peroxide
HBSS	:	HEPES buffered saline solution
HEPES	:	N-2-hydroxyethylpiperazine-N-2-ethanesulphonic acid
HPV	:	Hypoxic pulmonary vasoconstriction
HRP	:	Horseradish peroxidase
Hz	:	Hertz
i.d.	:	Internal diameter
IbTx	:	Iberiotoxin
IC_{50}	:	Half maximal inhibitory concentration
I_K	:	K^+ current
I_{Kv}	:	Voltage-gated K^+ current in VSMCs
IP_3	:	Inositol 1, 4, 5-triphosphate
IP_4	:	Inositol 1, 3, 4, 5-tetrakisphosphate
IPA	:	Intra-pulmonary artery
K_2P	:	Two-pore domain K^+ channels
K_{ATP}	:	ATP sensitive K^+ channel
K_{Ca}	:	Ca^{2+}-activated K^+ channel
KCNQ	:	K_V long QT or K_V7 channel
kDa	:	Kilo Dalton
K_{ir}	:	Inwardly rectifier K^+ channel
KO	:	Knock out
K_V	:	Voltage-gated K^+ channel

L-NAME	:	N^{ω}-nitro-L-arginine methylester
LQT	:	Long QT syndrome
LSM	:	Laser scanning microscope
L-VOCC	:	L-type voltage-operated calcium channel
MA	:	Mesenteric artery
mA	:	Milliampear
MASMC	:	Mesenteric artery smooth muscle cell
mETC	:	Mitochondrial electron transport chain
MLC	:	Myosin light chain
MLCK	:	Myosin light chain kinase
mm	:	Millimetre
mM	:	Millimolar
mMA	:	Mouse mesenteric artery
mN	:	Milli Newton
mPA	:	Mouse pulmonary artery
mRNA	:	Messenger ribonucleic acid
Ms	:	Methanosulphonic acid
MYPT1	:	Myosin phosphatase targeting subunit 1
MΩ	:	Mega ohm
NA	:	Numerical aperture
NaCN	:	Sodium cyanide
NAD	:	Nicotinamide adenine dinucleotide
NADH	:	Nicotinamide adenine dinucleotide (reduced form)
NADP	:	Nicotinamide adenine dinucleotide phosphate
NADPH	:	Nicotinamide adenine dinucleotide phosphate (reduced form)
NCX	:	Sodium calcium exchanger
nM	:	Nanomolar
NO	:	Nitric oxide
NSCC	:	Non-selective cation channel
O_2^-	:	Superoxide anion
PA	:	Pulmonary artery
pA	:	Picoampear
PAGE	:	Polyacrylamide gel electrophoresis

PAH	:	Pulmonary arterial hypertension
PASMC	:	Pulmonary arterial smooth muscle cell
pCa	:	-log[Ca^{2+}] (M)
P_{CO2}	:	Partial pressure of CO_2
PH	:	Pulmonary hypertension
PIP_2	:	Phosphatidyl inositol di-phosphate
PIPES	:	Piperazine-1,4-bis-2-ethanesulfonic acid
PKA	:	Protein kinase A
PKC	:	Protein kinase C
PKG	:	Protein kinase G
PLC	:	Phospholipase C
P-loop	:	Pore-forming loop
PMCA	:	Plasma membrane Ca^{2+} ATPase
^{p}MLC	:	Phosphorylated myosin light chain
^{p}MYPT1	:	Phosphorylated myosin phosphatase targeting subunit 1
P_{O2}	:	Partial pressure of O_2
PSS	:	Physiological salt solution
rMA	:	Rat mesenteric artery
ROCC	:	Receptor operated Ca^{2+} channel
ROK	:	Rho-kinase
ROS	:	Reactive oxygen species
rPA	:	Rat pulmonary artery
RT-PCR	:	Reverse transcription polymerase chain reaction
RyR	:	Ryanodine receptor
S.E.M.	:	Standard error of the mean
SDS	:	Sodium dodecyl sulphate
SDS-PAGE	:	SDS-Polyacrylamide gel electrophoresis
SERCA	:	Sarcoplasmic-endoplasmic Ca^{2+} ATPase
SK_{Ca}	:	Small conductance Ca^{2+}-activated K^{+} channel
SMC	:	Smooth muscle cell
SOC	:	Store operated channel
SR	:	Sarcoplasmic reticulum
SUR2B	:	Sulphonyl urea receptor subunit 2B

TASK	:	TWIK-related Acid-Sensitive K^+ channel
TBS	:	Tris-buffered saline
TEA	:	Tetraethylammonium
TEMED	:	Tetramethylethylenediamine
THIK	:	TWIK-related Halothane-Inhibited K^+ channel
TIFF	:	Tagged image files
TM	:	Transmembrane domain
TP	:	Thromboxane
TRAAK	:	TWIK-related Arachidonic Acid activated K^+ channel
TREK	:	TWIK-related K^+ channels
TRPC	:	Transient receptor potential channel
TWIK	:	Tandem of P domains in Weak Inward rectifier K^+ channel
TXA_2	:	Thromboxane A_2
v/v	:	Volume/volume
V_m	:	Membrane potential
VOCC	:	Voltage-operated calcium channel
VSMC	:	Vascular smooth muscle cell
w/v	:	Weight/volume
Δp	:	Electrochemical gradient
$\Delta \Psi m$	:	Change in mitochondrial membrane potential
µM	:	Micromolar
µm	:	Micrometer

Table of contents

List of Figures

List of Tables

To the departed souls of my parents

Chapter 1

GENERAL INTRODUCTION

1.1 Physiological role of pulmonary and systemic blood vessels

The pulmonary circulation is distinguished from the systemic circulation by the fact that the pulmonary circulation handles the same cardiac output but in a very different way, enabling reoxygenation of blood at 20% of the vascular resistance seen in the systemic vasculature. This is achieved due to the unique characteristics of the pulmonary circulation, which is a low pressure and low resistance but high flow system. On the contrary, the systemic circulation delivers oxygenated blood to tissues at a high pressure and represents a high resistance system. The total resistance of the pulmonary circulation is less than one-tenth of that of the systemic circulation (Walter, 2003). The mean pressure in the pulmonary circulation is approximately 15 mmHg whereas in systemic arteries (e.g., aorta) it is approximately 95 mmHg. Similarly, pulse pressure is relatively lower in the pulmonary (~17 mmHg) than in the systemic circulation (~40 mmHg). Functional differences are supported by differences in vessel morphology. Pulmonary blood vessels are generally shorter and wider than their counterparts on the systemic side. Although the pulmonary arterioles (small resistance arteries) contain smooth muscles and can constrict, these vessels are far less muscular than their systemic counterparts, and their resting tone is low. Very small pulmonary arterioles (internal diameter <70 μm) do not have smooth muscle cell. The walls of the pulmonary vessels are as thin as the walls of veins elsewhere in the body. The thinness of vessel walls and paucity of smooth muscle make the pulmonary vessels highly compliant (Walter, 2003). The pulmonary vascular bed resembles that of the systemic circulation although the wall of larger pulmonary arteries are only 30% of the thickness of the aorta, and the small arteries have a smaller

number of smooth muscle cells than their counterparts in the systemic vascular bed. These characteristics of the pulmonary circulation are essential for the maintenance of circulating O_2 levels. When O_2 levels are compromised (partial pressure of O_2 (P_{O2}) below 60 mmHg) in an area of the lungs pulmonary arteries respond uniquely by constricting and diverting blood flow to the areas of high oxygen availability (ventilation-perfusion matching), a phenomenon known as hypoxic pulmonary vasoconstriction (HPV), also historically known as the von Euler-Liljestrand mechanism (Dumas *et al.*, 1999;Sommer *et al.*, 2008). In addition, the high partial pressure of CO_2 (P_{CO2}) and/or low interstitial pH results in pulmonary vasoconstriction (Riley, 1951). This phenomenon thereby helps optimisation of gas exchange at the blood-air interface (Riley, 1951;Marshall *et al.*, 1981;Orchard *et al.*, 1983). Conversely, the systemic circulation responds to low P_{O2}, high P_{CO2} and/or low pH by vasodilation to provide a better O_2 supply to target organs (Wadsworth, 1994;Dumas *et al.*, 1999). Features of the pulmonary vasculature in the rat and mouse are similar to that in humans, thus making these rodent species widely accepted models for study of mechanisms of HPV and pulmonary related diseases (Hislop & Reid, 1978).

1.2 Morphology of blood vessel and vascular smooth muscle

Depending on the vessel diameter and function, the pulmonary vasculature is composed of four distinct types of blood vessels: i) large extraparenchymal or conduit arteries, ii) small intrapulmonary arteries or resistance pulmonary arteries that control pulmonary vascular resistance, iii) capillaries and iv) pulmonary veins. The resistance pulmonary arteries bear special significance because they are the major site of HPV (Kato & Staub, 1966) and are also the focus for most of the pathophysiology of pulmonary arterial hypertension (Archer & Rich, 2000). For proper understanding of the pathophysiology of vascular diseases, extensive knowledge of the complex vessel structure and functional organisation in the cardiovascular system is essential (Pugsley & Tabrizchi, 2000). The morphology and functions of various vascular beds differ greatly from one to another. Despite the variation in different vascular beds, the basic structure of blood vessels is similar.

The vascular wall is composed of three distinct regions or tunicas: tunica intima, tunica media and tunica adventitia. There are four building blocks that make up these tunicas: collagen fibres, elastic fibres, smooth muscle cells (SMCs) and endothelial cells (Fig. 1.1). The major vessels in mammals consist mainly of tunica media, primarily composed of SMCs and elastic fibres. There is variation in the number of SMC layers, the larger more muscular arteries, such as aorta, have many highly organised layers separated by an elastic lamella, whereas less muscular arteries have only one SMC layer (Tennant & McGeachie, 1990). Highly extensible elastic fibres account for most of the stretch of vessels at normal pressure elsewhere in the body, as well as bearing the stretch of pulmonary tissues in the pulmonary circulation (Emile, 2003). Vascular SMCs exert tension mainly by means of active contraction that involves Ca^{2+}-calmodulin-dependent myosin light chain phosphorylation. However, relaxed vascular SMCs do not contribute to the elastic tension of the vascular wall, a function mainly regulated by the elastic and collagen fibres (Emile, 2003).

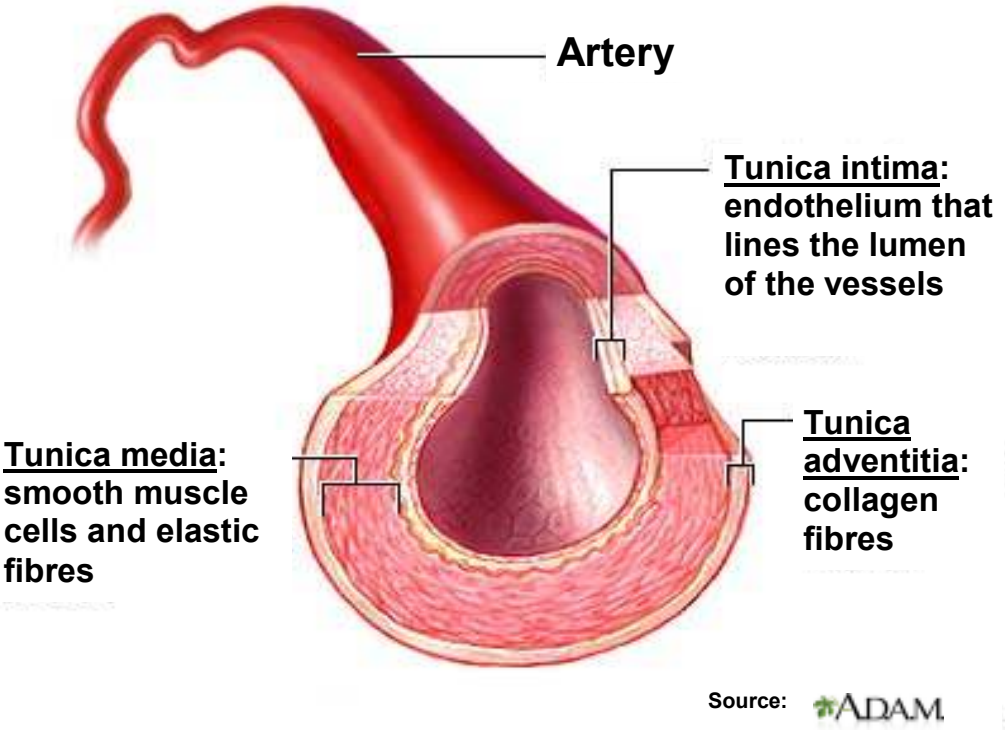

Figure 1.1 Structure of an artery.

Cross section of the arterial wall shows three distinct layers or tunicas: the innermost layer or tunica intima, the muscular middle layer or tunica media and the outer collagen layer or tunica adventitia.

Smaller arterioles (<70 µm diameter) and capillaries do not have a smooth muscle layer, rather only one intimal layer of endothelial cells resting on a basal lamina. Therefore, the control of blood flow by vasoconstriction and vasodilatation occurs in arteries of larger size (>70 µm diameter) (Christensen & Mulvany, 2001;Hester & Hammer, 2002). Vascular endothelial cells form a single, continuous layer that lines all vascular beds (Emile, 2003). Vascular endothelium acts not only as a passive barrier between plasma and extracellular fluid, but also as a source of potent mediators which actively control the contraction and relaxation of underlying smooth muscle cells (Aird, 2008).

1.3 Role of pulmonary artery with special implications to the phenomenon of HPV

The pulmonary arteries carry de-oxygenated mixed venous blood to the lungs. After arising from the right ventricle, they bifurcate as they follow the bronchial tree, and their divisions ultimately form a richly anastomosing capillary bed that supply the alveoli, the site of gaseous exchange. The pulmonary capillaries have an average internal diameter of ~ 8 μm, and each segment of the capillary network is ~10 μm in length. After gas exchange in the alveoli, the blood is eventually collected in the pulmonary veins (Walter, 2003). The typical partial pressure of oxygen (Po_2) in the alveolar air is 100 mmHg. Oxygen acts primarily on the pulmonary arterioles and a low Po_2 causes HPV (German & Stanfield, 2005). In isolated, buffer-perfused lung, HPV starts within seconds after the onset of mild hypoxia (alveolar P_{O2} <100 mmHg) (Peake *et al.*, 1981;Weissmann *et al.*, 1995;Weissmann *et al.*, 2006b). Since HPV can also occur in isolated lungs and pulmonary arteries, it does not rely on either the nervous system or systemic hormones. It is generally believed that the low Po_2 acts directly on the pulmonary vascular smooth muscle cells (Walter, 2003). Previous studies concluded that the smooth muscle layer of the precapillary resistance pulmonary arteries, located at the entrance of the acinus in close contact with alveoli, are both censor and effector cells of HPV (Kato & Staub, 1966;Staub, 1985;Hillier *et al.*, 1997). Large PA, smaller, partially muscularised PA, or postcapillary vessels are significantly less responsive to hypoxia, when compared with resistance PA (Dawson *et al.*, 1978;Madden *et al.*, 1985;Fike & Kaplowitz, 1994). Furthermore, isolated smooth muscle cells from resistance pulmonary artery contract in response to hypoxia at a P_{O2} of 25-50 mmHg, whereas smooth muscle cells from isolated cerebral arteries dilate, suggesting that SMCs could be the centre of oxygen sensing and therefore the main mediator of the HPV response (Murray *et al.*, 1990;Madden *et al.*, 1992). Although PA smooth muscle cells are considered as the primary locus of HPV, the endothelium plays important facilitatory role for sustained HPV (Ward & Aaronson, 1999;Liu *et al.*, 2001b;Aaronson *et al.*, 2002). The pulmonary artery endothelium synthesises and metabolises multiple vasoactive mediators that could potentially interact with, or augment the intrinsic rise in $[Ca^{2+}]_i$ in order to

promote sustained HPV (Aaronson *et al.*, 2002). Among the endothelium-derived vasoactive mediators nitric oxide (NO) and ET-1 are mostly considered to influence HPV. It has been suggested that hypoxic-inhibition of basal NO synthesis may uncover intrinsic vascular tone and so effectively cause HPV (Rodman *et al.*, 1990;Ogawa *et al.*, 1993;Terraz *et al.*, 1999). On the other hand ET-1 has a non-specific potentiating effect of on HPV (Ward & Aaronson, 1999).

How exactly PA constricts in response to hypoxia is mostly unknown. However, the hypothesised mechanisms including all those proposed for oxygen sensing in hypoxia by the peripheral chemoreceptor and mitochondria, will be further elaborated in section 2.7 of this chapter.

1.4 Physiology of vascular smooth muscle (VSM) contraction

Smooth muscle cells (SMCs) are small spindle or fusiform in shape and contain a single central nucleus. The cells contain contractile actin (thin) and myosin (thick) filaments; however, they are not arranged in the regular, cross-striated patterns that are visible in both cardiac and skeletal muscle fibres. As a result, these muscle fibres appear smooth or non-striated and uniformly bright under light microscope. The myofilaments (actin and myosin) fill most of the cytoplasm. There is neither banding nor T tubules, however, SMCs do have a sarcoplasmic reticulum (SR) that can sequester and release calcium. Furthermore, myosin in SMCs is different from the myosin in striated muscle, and it forms a different type of thick filament that permits more overlap with actin and thus a greater degree of contraction. Although in SMC the thick and thin filaments are arranged in parallel with each other as in skeletal muscle, they tend to run obliquely in various directions, resulting in contraction along several axes (German & Stanfield, 2005). SMCs are found in internal organs, blood vessels, and other structures that are not under voluntary control. In blood vessels SMCs are arranged in a circular pattern (Fig. 1.1) and control blood pressure by altering luminal diameters. SMCs are involuntary muscles innervated and regulated by nerves from postganglionic neurons originating from the sympathetic and parasympathetic divisions of the autonomic nervous system. SMCs also make close contact with each other via specialised connections called gap junctions, which allow rapid ionic communications between muscle cells resulting in coordinated activity of smooth muscle sheets or layers (Eroschenko, 2005).

Irrespective of muscle type (whether it is skeletal, cardiac or smooth), it is an increase in the levels of intracellular free calcium concentrations ($[Ca^{2+}]_i$) that triggers muscle contraction. The time during which $[Ca^{2+}]_i$ remains elevated determines the duration of muscle contraction. The process by which 'excitation' triggers the increase in $[Ca^{2+}]_i$ is called 'excitation-contraction coupling'. In SMCs, Ca^{2+} can enter the cytoplasm from the extracellular space through voltage-gated or ligand-gated ion channels, or alternatively, Ca^{2+} can be released from the

SR into the cytoplasm (Fig. 1.2). Thus both extracellular and intracellular sources contribute to an increase in $[Ca^{2+}]_i$ (Mickelson & Louis, 1996). However, in SMCs, L-type voltage-operated Ca^{2+} channels (L-VOCCs) are one of the most important routes for Ca^{2+} entry (Rang H.P. *et al.*, 2007). During excitation, $[Ca^{2+}]_i$ may rise from its resting level of less than 100 nM to a level greater than 10 μM , thus resulting a huge gradient, which serves as a driving force for Ca^{2+} influx (Himpens *et al.*, 1992;Orallo, 1996).

In SMCs, an increased level of $[Ca^{2+}]_i$ activates the crossbridge cycle (i.e., binding of myosin with actin) and force generation by a cascade of intracellular signals. Contractions in smooth muscle are triggered when Ca^{2+} binds reversibly to calmodulin (CaM). This binding triggers a conformational change that enables the Ca^{2+}-CaM complex to bind to and activate an enzyme called myosin light chain kinase (MLCK). The activated MLKC then catalyzes the phosphorylation of 20 kDa myosin light chain (MLC_{20}) at ser19 (Kamm & Stull, 2001;Somlyo & Somlyo, 2003). The phosphorylated MLC_{20} ($^{P}MLC_{20}$) then activates and initiates crossbridge activity (Fig. 1.2). Crossbridge cycling then proceeds resulting in smooth muscle contraction as long as the $[Ca^{2+}]_i$ level is enough to keep triggering the crossbridge cycling (German & Stanfield, 2005). The subsequent decrease in $[Ca^{2+}]_i$ is the signal to cease crossbridge cycling (Mickelson & Louis, 1996). During the crossbridge cycle, contractile proteins convert the energy of ATP hydrolysis into mechanical energy. Because ATP stores are small, the cell must regenerate the ATP needed for muscle contraction (Mickelson & Louis, 1996).

Termination of crossbridge cycling in smooth muscle requires more than just removal of Ca^{2+} from the cytosol, because the phosphate group attached to myosin is covalently bound and therefore does not dissociate easily. For this reason, termination of the crossbridge cycle in smooth muscle requires the action of myosin light chain phosphatase (MLCP), an enzyme which by removing the phosphate group inactivates myosin (Fig. 1.2). MLCP is constantly active and competes with MLCK by dephosphorylating $^{P}MLC_{20}$, thus activation (and phosphorylation) of MLC_{20} occurs only when enough Ca^{2+} is present to activate MLCK to a degree sufficient to overcome the action of MLCP (German & Stanfield, 2005).

The basic mechanism regulating VSM contractility is broadly determined by factors which increase $[Ca^{2+}]_i$ causing VSM contraction, and by factors which decrease $[Ca^{2+}]_i$ causing VSM relaxation. The mechanism responsible for increasing and decreasing in $[Ca^{2+}]$ in VSMCs will be discussed in the following section in more details.

1.5 General mechanisms regulating vascular smooth muscle (VSM) contractility

Since the main function of arteries is to regulate blood flow by changing vessel diameter, the identification and understanding of mechanisms that regulate VSM contractility is important. The contractility of smooth muscle is primarily reliant upon the levels of $[Ca^{2+}]_i$. However, vascular tone depends not only on $[Ca^{2+}]_i$ but also on Ca^{2+} sensitisation of contractile apparatus (Somlyo & Somlyo, 1994). Ca^{2+} sensitisation is a phenomenon whereby a greater contraction is produced for a given concentration of $[Ca^{2+}]_i$ with several receptor-mediated contractile stimulations (Somlyo & Somlyo, 1994). It is thought that Ca^{2+} sensitisation is an important regulator of pulmonary contractility and plays a key role in HPV (Robertson *et al.*, 1995;Robertson *et al.*, 2000a;Nagaoka *et al.*, 2004;Aaronson *et al.*, 2006;Oka *et al.*, 2008;McNamara *et al.*, 2008).

1.5.1 Mechanisms increasing $[Ca^{2+}]_i$

Two main processes are responsible for elevation of $[Ca^{2+}]_i$. The mechanism of activation of Ca^{2+} influx by changes in membrane potential is known as excitation-contraction coupling (E-C coupling) (Bauer & Sanders, 1985;Orallo, 1996). Ca^{2+} can also be increased as a result of activation of receptors by neurotransmitters or hormones, which is known as pharmacomechanical coupling (Somlyo & Somlyo, 1968;Orallo, 1996). The main mechanisms contributing to the E-C coupling and pharmacomechanical coupling are schematically shown in Figure 1.2. These mechanisms can be broadly divided into two groups: **a)** mechanisms that depend on extracellular Ca^{2+} entry and **b)** mechanisms that depend on the intracellular Ca^{2+} release. The first group of mechanisms include: **1)** voltage-dependent Ca^{2+} entry via L-type voltage operated calcium channels (L-VOCCs); **2)** voltage-independent Ca^{2+} entry via ligand-gated (or receptor-operated) Ca^{2+}-permeable channels (ROCCs); and **3)** store-operated calcium channels (SOCCs) activated by depletion of the sarcoplasmic reticulum (SR).

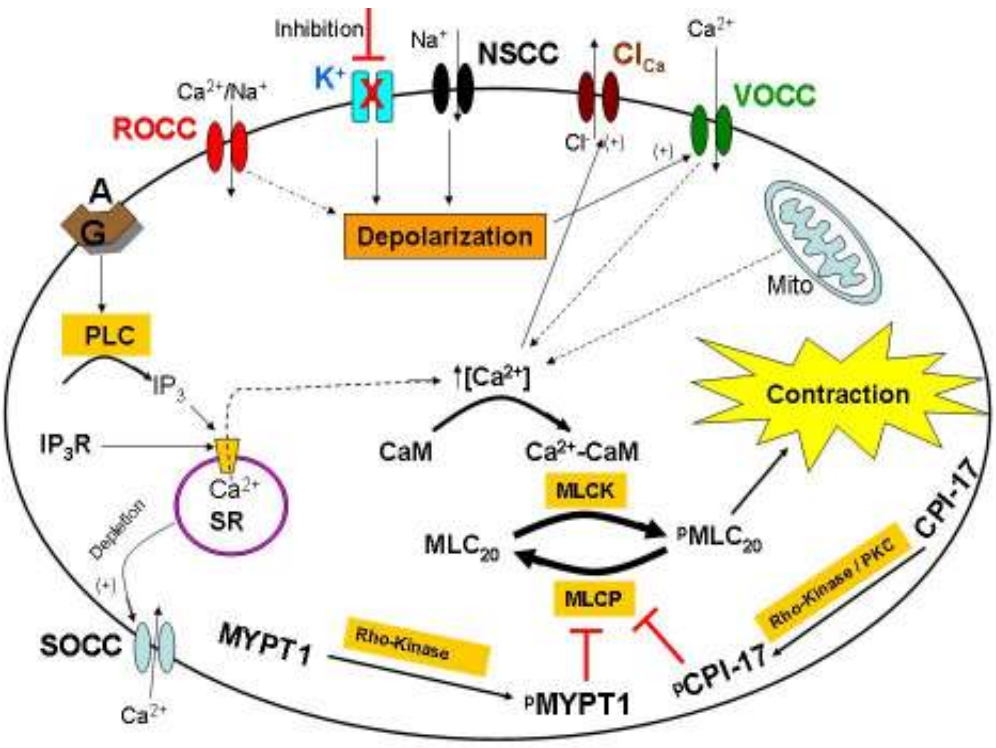

Figure 1.2 Schematic diagram showing mechanisms controlling vascular smooth muscle contraction.

SOCC- store operated calcium channel, A- agonist, G- G protein coupled receptor, ROCC- receptor operated calcium channel, K^+- potassium channel, NSCC- non-selective cation channel, Cl_{Ca}- calcium-activated chloride channel, VOCC- voltage operated calcium channel, PLC- phoshpholipase C, IP_3- inositol triphosphate, IP_3R- IP_3 receptor, SR- sarcoplasmic reticulum, Mito- mitochondria, CaM- calmodulin, MLCK- myosin light chain kinase, MLC_{20}- 20 kDa regulatory myosin light chain, $^{P}MLC_{20}$- phosphorylated 20 kDa regulatory myosin light chain, MYPT1- myosin phosphatase targeting subunit 1, ^{P}MYPT1 - phosphorylated myosin phosphatase targeting subunit 1, CPI-17 – PKC-potentiated phosphatase inhibitor protein-17 kDa, ^{P}CPI-17 – phosphorylated PKC-potentiated phosphatase inhibitor protein-17 kDa.

Two main intracellular Ca^{2+} sources, which are known to contribute to elevation of $[Ca^{2+}]_i$, are: **1)** Ca^{2+} release from intracellular stores in response to excitatory agonists and corresponding activation of G-protein coupled receptors; **2)** mitochondrial Ca^{2+} release. Recent evidence also suggests that other cellular organelles such as lysosomes may also release Ca^{2+} during hypoxia, thus contributing to the HPV responses (Kinnear *et al.*, 2008;Calcraft *et al.*, 2009).

The above mentioned mechanisms are closely interdependent. Thus, voltage-dependent Ca^{2+} entry will be determined by membrane depolarisation caused predominantly by inhibition of K^+ channels; however, activation of Cl^- channels, and/or non-selective cation channels, including ROCCs and SOCCs, can also contribute to membrane depolarisation.

In the vasculature, K^+ channels play a fundamental role in excitability by maintaining the membrane potential, a salient regulator of vascular tone (Archer & Michelakis, 2002). Ubiquitously expressed K^+ channels in VSMCs include: voltage-gated K^+ channels (K_V), large-conductance Ca^{2+}-activated K^+ channels (BK_{Ca}), ATP-sensitive K^+ channels (K_{ATP}) and inward rectifier K^+ channels (K_{ir}) (Moudgil *et al.*, 2006;Ko *et al.*, 2008). Recent evidence clearly demonstrates the presence of another group of voltage-dependent K^+ channels in VSMCs which belong to the K_V7 subfamily encoded by KCNQ genes, and commonly known as KCNQ channels (Yeung & Greenwood, 2005;Joshi *et al.*, 2006;Brueggemann *et al.*, 2007;Yeung *et al.*, 2008;Joshi *et al.*, 2009). Furthermore, two-pore domain acid-sensitive K^+ channels such as TASK, were also found in VSMCs (Gurney *et al.*, 2003;Gardener *et al.*, 2004;Olschewski *et al.*, 2006). K_V, KCNQ and BK_{Ca} channels are activated by depolarisation of cell membrane. In addition, BK_{Ca} channels are also activated by elevated intracellular free Ca^{2+}, while K_{ATP} channels are activated by Mg^{2+}ADP and inhibited by a rise in intracellular ATP level. Membrane hyperpolarisation will deactivate or close-down voltage-gated K^+ channels such as K_V, KCNQ and BK_{Ca}, but will activate K_{ir} channels (Brayden, 1996;Clapp & Tinker, 1998). Inhibition of any type of K^+ channel will result in membrane depolarisation resulting in an increase in Ca^{2+} influx through L-VOCCs and leading to VSM contraction (Weir & Archer, 1995;Nelson & Quayle, 1995;Takuwa, 1996;Sweeney & Yuan, 2000).

The resting membrane potential measured in intact blood vessels is typically between -60 and -50 mV (Berger *et al.*, 1998). As the voltage-dependence of activation of L-VOCCs is very steep in this voltage range (Brayden & Nelson, 1992), small decreases in the membrane potential could be sufficient to activate L-VOCCs, leading to VSM contraction. In different vascular beds this apparent threshold for the L-VOCC activation will be determined by the density of L-VOCCs and the type and the density of K^+ channels expressed in SMCs. In pulmonary artery SMCs, for example, the current density of K_V channels (defined as the peak current amplitude divided by the cell size determined in pF) is ~10-fold higher than in mesenteric arterial SMCs (Firth *et al.*, 2009a).

Also, agonists causing VSMC contraction may directly activate non-selective cation channels (NSCCs), and thereby result in membrane depolarisation and an increase in $[Ca^{2+}]_i$ (Guibert *et al.*, 2008). Activation of Ca^{2+}-dependent Cl^- channels by elevated $[Ca^{2+}]_i$ can also contribute to membrane depolarisation and thus to VSM contraction (Criddle *et al.*, 1997;Saleh & Greenwood, 2005).

TRP (Transient Receptor Potential) channels:

It is generally accepted that TRP channels are responsible for the voltage-independent Ca^{2+}-entry in VSMCs and represent molecular correlates for ROCCs and SOCCs. The TRP gene superfamily consists of 7 subfamilies with at least 28 mammalian homologues. The TRP gene superfamily is known to encode a wide variety of cation channels with diverse biophysical properties, activation mechanisms and physiological functions (Yang *et al.*, 2010b). Unlike voltage-gated ion channels, TRP subunits do not possess a voltage-sensing moiety, making them voltage-independent (Owsianik *et al.*, 2006). SOCCs in SMCs are not highly selective for Ca^{2+} and are considered to be non-selective cation channels. Single channel currents through SOCCs have been recorded in cells isolated from rat and mouse aorta and showed little selectivity for Ca^{2+} over monovalent cations such as Na^+ (Trepakova *et al.*, 2000). TRP subunits are divided into several subfamilies according to their activation stimuli and the presence of regulatory domains on the cytosolic C-and N-termini. The subfamilies

of TRP channels include canonical (TRPC), melastatin-related (TRPM), vaniloid receptor-related (TRPV), polycystins (TRPP), mucolipidins (TRPML), mechanoreceptor potential C (TRPN), and ankyrins (TRPA). TRPC is activated by G-protein coupled receptors, while a range of chemical and physical stimuli including capsaisin, lipids, acid, heat, shear stress and hypo-osmolarity can activate TRPV (Pedersen *et al.*, 2005;Inoue *et al.*, 2006). TRPM are activated in response to increased $[Ca^{2+}]_i$, oxidative stress, or exposure to cold (Pedersen *et al.*, 2005). Less distinctly related subfamilies such as TRPP, TRPML, TRPN and TRPA are associated with specific genetic disorder (Pedersen *et al.*, 2005).

Recent studies suggest that TRP channels (TRPC, TRPV and TRPM) play crucial roles in the regulation of vascular tone, hypoxic pulmonary vasoconstriction, smooth muscle cell proliferation, vascular remodelling, and pulmonary arterial hypertension (Firth *et al.*, 2007;Yang *et al.*, 2010b). Evidence accumulated over the past decade suggests that members of the canonical subgroup of TRP channels constitute tetramers of both ROCCs and SOCCs (Parekh & Putney, Jr., 2005;Albert *et al.*, 2007). Studies suggest that TRPC 1, 4 and 5 isoforms are sensitive to store depletion and could function as SOCCs, whereas TRPC 3, 6 and 7 isoforms function as ROCCs (Pedersen *et al.*, 2005).

More than 10 TRP isoforms including TRPC, TRPV and TRPM have been detected in various vascular preparations [reviewed in (Firth *et al.*, 2007)] including pulmonary and mesenteric artery smooth muscle cells (Walker *et al.*, 2001;Ng & Gurney, 2001;Wang *et al.*, 2004;Lu *et al.*, 2008;McElroy *et al.*, 2008). ROCCs are probably NSCCs with some degree of selectivity for divalent cations such as Ca^{2+} (Orallo, 1996). ROCCs could be activated by agonists including ATP, norepinephrine, ET and serotonin (Orallo, 1996;Nilsson *et al.*, 1998) and can also cause membrane depolarisation leading to L-VOCCs activation and Ca^{2+} influx. Several studies have presented evidence for TRPC1 being an essential component for SOCCs in VSMCs, including aorta (Xu & Beech, 2001;Brueggemann *et al.*, 2006), cerebral artery (Bergdahl *et al.*, 2005), mesenteric artery (Saleh *et al.*, 2006), portal vein (Saleh *et al.*, 2008), coronary artery (Takahashi *et al.*, 2007;Saleh *et al.*, 2008), as well as PASMCs (Sweeney *et al.*, 2002). TRPC 1 and 6 isoforms have been found to be responsible for agonist- and acute hypoxia-

induced vasoconstriction of pulmonary arteries (Lin *et al.*, 2004;Weissmann *et al.*, 2006a) as well as mesenteric arteries (Saleh *et al.*, 2006). On the other hand, expression of TRPC channels can also cause vasoconstriction via SOCC-mediated mechanisms in a wide range of vasculatures including pulmonary (McDaniel *et al.*, 2001;Ng & Gurney, 2001;Kunichika *et al.*, 2004) as well as systemic arteries (Lee *et al.*, 2002;Reading *et al.*, 2005). As mediators of influx of positively charged cations, SOCCs may also contribute to cell depolarisation and activation of L-VOCCs. In comparison to ROCCs, SOCCs are highly selective for Ca^{2+} over other cations (Hoth & Penner, 1992).

G-protein coupled receptors and SR:

A special class of intracellular ligand-gated Ca^{2+} channels (also called calcium-release channels, IP_3 and ryanodine receptors) control the release of Ca^{2+} from intracellular Ca^{2+} stores. IP_3 receptors are present on the SR in VSMCs. The predominant mechanism by which the SR can be stimulated to release Ca^{2+} is by IP_3 acting upon IP_3 receptors. IP_3 is increased after agonist receptor activation causing phospholipase C (PLC) induced hydrolysis of phosphotidylinositol bisphosphate (PIP_2) to yield IP_3 and DAG (Tasker *et al.*, 1999). An increase in $[Ca^{2+}]_i$ resulting from total agonist action or Ca^{2+} entry via ROCCs and VOCCs can induce further Ca^{2+} release from the SR via interaction of Ca^{2+} with ryanodine receptors (RyRs), a phenomenon known as calcium induced Ca^{2+} release (CICR) (Lesh *et al.*, 1998). Ca^{2+} depletion of intracellular Ca^{2+} stores triggers the SOCCs in the plasma membrane to open and allow Ca^{2+} entry. The exact mechanism by which SOCCs are activated is not completely understood (Barritt, 1999), however the role of Orai and STIM1 (stromal interaction molecule 1) proteins which can interact with certain types of TRPC have been implicated (Shuttleworth, 2009). STIM1, a 90-kDa transmembrane Ca^{2+}-binding protein, is constitutively resident in the sarco(endo)plasmic reticulum and plasma membrane, and the pore of these channels is comprised of both Orai1 and Orai3 subunits (Shuttleworth, 2009). STIM1 is thought to play a pivotal role in activation of SOCCs and store operated Ca^{2+} entry (SOCE) (Bakhramov *et al.*, 1998;Minke, 2006;Lewis, 2007;Putney, Jr., 2007). It is well documented that $[Ca^{2+}]_i$ responses to hypoxia in distal PASMCs (Ng *et al.*, 2005;Wang *et al.*, 2005a) and HPV in isolated lungs (Weigand *et al.*,

2005) require Ca^{2+}-entry through SOCCs. A recent study confirms the importance of SOCE in HPV and also provides further evidence that HPV is greater in distal (resistance) than proximal (conduit) PA because greater number and activation of SOCCs in distal PASMCs generates a bigger increase in $[Ca^{2+}]_i$ (Lu *et al.*, 2008).

Chloride channels:

Chloride (Cl^-) channels, abundantly distributed in the VSMCs, also play an important role in regulating VSM excitation and contraction (Kitamura & Yamazaki, 2001). Out of the five major categories of Cl^- channels only two types are associated with calcium signalling: (i) Cl^- channels that are activated by an increase in $[Ca^{2+}]_i$ concentration, called Ca^{2+}-activated Cl^- channels (Cl_{Ca}) and (ii) Cl^- channels that are activated by change in cell volume, called swelling-activated or volume-sensitive Cl^- channels (Cl_V) (Frings *et al.*, 2000;Hartzell *et al.*, 2005;Leblanc *et al.*, 2005). The expression of Cl_{Ca} have been found in both vascular and non-vascular smooth muscles, where they play an important role in the regulation of smooth muscle tone (Large & Wang, 1996;Leblanc *et al.*, 2005). Their molecular identity has however been elusive (Nilius & Droogmans, 2003;Hartzell *et al.*, 2009). Several molecular candidates have been proposed for vascular Cl_{Ca} channels including members of the CLCA and bestrophin gene families. CLCA1 was found to be expressed in mouse portal vein (Britton *et al.*, 2002) and CLCA4 in many VSMCs including aorta and coronary vessels (Elble *et al.*, 2002). Most recently, Manoury *et al.* (2010) provided evidence that TMEM16A (or anoctamin 1), a member of the transmembrane 16 (TMEM16) protein family, forms Cl_{Ca} channels in PASMCs (Manoury *et al.*, 2010). Cl_{Ca} channels play important roles in several cellular functions. They are of key importance in VSMCs where they are activated by a rise in the level of $[Ca^{2+}]_i$ (e.g., in response to contractile agonist). Activation of Cl_{Ca} channels leads to membrane depolarisation and thus contributes to contractile responses to constrictor hormones and neurotransmitters in vascular beds (Large & Wang, 1996;Kitamura & Yamazaki, 2001;Leblanc *et al.*, 2005). In smooth muscle cells, especially in vascular myocytes, the activation of Cl_{Ca} is believed to be an excitatory depolarising mechanism which will lead to membrane depolarisation (Greenwood & Leblanc, 2007;Ayon *et al.*, 2009). This is because Cl^- ions are

actively transported and actively accumulated within the cell by several classes of anion transporters (Chipperfield & Harper, 2000;Forrest *et al.*, 2010), yielding a rise in intracellular free Cl^- ($[Cl^-]_i$) levels ranging between 30 and 60 mM (Large & Wang, 1996;Chipperfield & Harper, 2000;Leblanc *et al.*, 2005) resulting in a reversal potential for Cl^- between -20 and -30 mV in VSMCs. As this is more positive than the resting potential (-60 to -50 mV) the net Cl^- efflux from the cell through Cl_{Ca} will lead to membrane depolarisation, which (~ -20 mV) in turn increases the open probability of L-VOCCs favouring Ca^{2+} entry into the cell and vasoconstriction (Large & Wang, 1996;Leblanc *et al.*, 2005). Apart from Ca^{2+}-induced activation, reactive oxygen species (ROS) can also activate Cl_{Ca} (Greenwood *et al.*, 1997;Greenwood *et al.*, 2002). In pulmonary arteries, the occurrence of this process could contribute to membrane depolarisation.

The Turner and Kozlowski group in Oxford first reported the existence of Cl_{Ca} in PASMCs (Salter *et al.*, 1995). Studies using rat PASMCs suggest a relationship between $[Ca^{2+}]_i$ and Cl_{Ca} channels under hypoxic conditions. Hypoxia increases $[Ca^{2+}]_i$ leading to opening of Cl_{Ca} channels, and further increases in $[Ca^{2+}]_i$. Under chronic hypoxic conditions, Cl_{Ca} may play an important role in hypoxic pulmonary hypertension and may take part in the regulation of proliferation of PASMCs (Yang *et al.*, 2006). The Cl_V channels, being activated by vascular distension caused, for example, by a rise in blood pressure in systemic arteries and veins could also lead to membrane depolarisation and subsequent opening of L-VOCCs resulting in VSM contraction (Yamazaki *et al.*, 1998;Kitamura & Yamazaki, 2001). A recent study also suggests that the inhibition of Cl_V may potentiate the EDHF-induced vasorelaxation through the K_{ir} channels (Yang *et al.*, 2010a).

Mitochondria:

Accumulation of Ca^{2+} by isolated mitochondria was first discovered in the 1950s (Slater & Cleland , 1953) and in the early seventies it was elucidated that Ca^{2+} accumulation in the mitochondria occurs due to their highly negative (inside) membrane potential ($\Delta\psi_m$) (Scarpa & Azzone, 1970;Rottenberg & Scarpa, 1974). Since then a series of works have established mitochondria as emerging

modulators of $[Ca^{2+}]_i$, having a capacity to effectively uptake, store and buffer sub-plasmalemmal Ca^{2+} (Malli *et al.*, 2003;Parekh, 2003;Szabadkai *et al.*, 2006;Szabadkai & Duchen, 2008). It is therefore suggested that mitochondria are capable of regulating all components of Ca^{2+} signalling machinery including Ca^{2+} release via IP_3 and RyR, Ca^{2+} influx via SOCCs, Ca^{2+} uptake and Ca^{2+} extrusion via the mitochondrial Na-Ca^{2+} exchangers (NCX) to contribute to ER Ca^{2+} refilling (Malli *et al.*, 2003;Szabadkai & Duchen, 2008;Walsh *et al.*, 2009). Experiments conducted in PASMCs have also shown that Ca^{2+} release from SR, via RyRs or IP_3 mediated mechanisms, increases mitochondrial Ca^{2+} levels (Drummond & Tuft, 1999). However, it is currently not fully understood to what extent mitochondria are involved in ER filling and Ca^{2+} homeostasis in the pulmonary and mesenteric circulation, although it is generally considered to be important in the regulation of Ca^{2+} homeostasis (Ward *et al.*, 2004b). It is also possible that mitochondrial regulation of Ca^{2+} may have an important role in HPV as hypoxia has indeed been shown to inhibit mitochondrial uptake of Ca^{2+} (Kang *et al.*, 2002) and to activate NADPH oxidase to increase intracellular reactive oxygen species (ROS) and $[Ca^{2+}]_i$ through the mitochondrial ROS-PKCε signalling axis in PASMCs (Rathore *et al.*, 2008). Mitochondria also contribute to K_V channel mediated cellular excitability in PASMCs (Firth *et al.*, 2009a).

1.5.2 Mechanisms decreasing $[Ca^{2+}]_i$

Mechanisms which will directly or indirectly decrease $[Ca^{2+}]_i$ can be broadly subdivided into two groups: **a)** membrane-dependent mechanisms such as i) inhibition or closure of L-VOCCs via activation of K^+ channels, ii) activation of exchangers, e.g., sodium-calcium exchanger (NCX), iii) activation of Ca^{2+}-ATPase in the plasma membrane; and **b)** Ca^{2+} sequestration mechanisms such as i) Ca^{2+} sequestration by sarco(endo)plasmic reticulum Ca^{2+} ATPase (SERCA), ii) increase in cAMP and cGMP, iii) cytosolic Ca^{2+}-binding proteins (Juhaszova *et al.*, 1996;Barritt, 1999).

The activation of K^+ channels either by voltage (K_V, KCNQ, BK_{Ca}) or by an increase in $[Ca^{2+}]_i$ (BK_{Ca}) will lead to membrane hyperpolarisation, and result in closure of L-VOCCs, leading to vasodilatation (Nelson & Quayle, 1995;Takuwa, 1996). Thus the K^+ channels limit smooth muscle contraction.

The activity of electrogenic ion exchangers, such as the NCX or the Na^+-K^+ ATPase, also affects membrane potential depending on ion gradients. Activation of the NCX working in the reverse mode, i.e. extruding excess of Na^+ may hyperpolarise the cell membrane, although its physiological role in VSMCs has been questioned (Bolton, 1979;Juhaszova *et al.*, 1996). However, inhibition of NCX during hypoxia in pulmonary arteries may contribute to the HPV response (Wang *et al.*, 2000).

The SR is the major store of intracellular calcium and its effective permeability is determined by the relative rate of influx and efflux mechanisms. The SERCA serves to sequester Ca^{2+} by removing it from the cytoplasm and refilling the internal Ca^{2+} stores (Orallo, 1996;Treiman *et al.*, 1998). The levels of $[Ca^{2+}]_i$ at each moment of time are reflective of the filling state of the internal Ca^{2+} stores (Rueda *et al.*, 2002). Thus SERCA is responsible for vasorelaxation. It has been suggested that an active SERCA pump is essential to obtain optimal Ca^{2+} release in SMCs (Gomez-Viquez *et al.*, 2003). Plasma membrane Ca^{2+}-ATPase (PMCA) pumps reduce $[Ca^{2+}]_i$ by Ca^{2+} efflux utilising energy derived from ATP hydrolysis (Gonzalez *et al.*, 1996).

Cyclic nucleotides such as adenosine 3′,5′-monophosphate (cAMP) and cyclic guanosine 3′,5′-monophosphate (cGMP) also play significant roles in lowering $[Ca^{2+}]_i$ in the VSMCs. When the inhibitory agonists (e.g., adenosine, β-agonists) bind to G-protein coupled receptors (GPCR), this leads to activation of K^+ channels and inhibition of Ca^{2+} channels and regulates the formation of cAMP and cGMP (Barritt, 1999). An increase in cytosolic levels of cAMP (by β-adrenergic agonists, PGI_2 or adenosine) or cGMP (by NO from endothelial cells) mediates vasodilatation through reduction of both $[Ca^{2+}]_i$ and Ca^{2+} sensitivity in VSMCs (Polson & Strada, 1996;Vaandrager & de Jonge, 1996). Increased levels of cytosolic cAMP reduces $[Ca^{2+}]_i$ through the activation of protein kinase A

(PKA), including inhibition of PLC and Ca^{2+} channels (Minami *et al.*, 1993b;Takuwa, 1996). The increase in cAMP also reduces myofilament Ca^{2+} sensitivity, presumably by phosphorylation of MLCK and thereby decreasing its affinity for Ca^{2+}-calmodulin complex (Takuwa, 1996). Similarly, the increase in cGMP levels leads to the activation of protein kinase G (PKG), which in turn reduces $[Ca^{2+}]_i$ through activation of SERCA, PMCA and NCX, inhibition of IP_3R/IP_3 synthesis, activation of K^+ channels and inhibition of L-VOCCs (Vaandrager & de Jonge, 1996). PKG also reduces myofilament Ca^{2+} sensitivity possibly by upregulating MLCP (Vaandrager & de Jonge, 1996;Somlyo & Somlyo, 2000).

Moreover, the myoplasma of the SMCs contains many Ca^{2+}-binding proteins such as calmodulin, troponin C, saponin, calbindin, calretinin, parvalbumin and the annexin family that may provide a mechanism for the rapid binding of Ca^{2+} and thereby reducing $[Ca^{2+}]_i$ (Heizmann, 1992;Horowitz *et al.*, 1996;Niki *et al.*, 1996). Following entry into the SR, Ca^{2+} binds to several hydrophilic proteins, such as calreticulin or calsequestrin that are capable of binding large amounts of Ca^{2+} (Marin *et al.*, 1999).

1.5.3 Mechanisms regulating Ca^{2+} sensitisation

The 'Ca^{2+} sensitisation of the contractile apparatus' can be modulated by either MLC_{20} phosphorylation-dependent or voltage-independent mechanisms. The MLC_{20} phosphorylation dependent mechanism involves two main kinases such as RhoA/Rho-kinase and PKC (Somlyo & Somlyo, 2000;Hirano, 2007).

The catalytic enzyme MLCP consists of three subunits: a catalytic subunit (PP1Cδ; ~37 kDa), a large 110-130 kDa regulatory subunit termed myosin phosphatase target subunit (MYPT1) and a 20 kDa subunit of unknown function (Hartshorne, 1998;Ito *et al.*, 2004). A small monomeric G-protein called RhoA activates Rho-kinase that phosphorylates MYPT1. Phosphorylated MYPT1

(^{P}MYPT1) inhibits MLCP's catalytic activity, increasing MLC_{20} phosphorylation and thereby VSM contraction (Feng *et al.*, 1999). Moreover, Rho-kinase as well as PKC may phosphorylate and activate CPI-17, a PKC-potentiated phosphatase inhibitor protein-17 kDa, leading to the inhibition of PP1Cδ, and thereby inhibiting MLCP (Li *et al.*, 1998;Koyama *et al.*, 2000).

Additional mechanisms of increased contractility exist in VSMCs. The MLC_{20} phosphorylation-independent mechanism depends on the regulation of cross-bridges by thin filament associated proteins, such as caldesmon and calponin (Morgan & Gangopadhyay, 2001). Phosphorylation of caldesmon and calponin leads to enhanced cross-bridge cycling and thus to an enhanced contractile response without an increase in MLC_{20} phosphorylation (Winder *et al.*, 1998). The importance of this mechanism in pulmonary function is yet not known.

1.6 Potassium channels in vascular smooth muscle cells

K^+ channels are the key regulators of cellular excitability and contractility of VSMCs. As discussed above, activation of K^+ channels results in membrane hyperpolarisation and vasodilatation, whereas inhibition of K^+ channels will lead to membrane depolarisation and vasoconstriction (Yuan, 1995;Nelson & Quayle, 1995;Ko *et al.*, 2008). In the vasculature, including the pulmonary circulation, several functionally distinct types of K^+ channel have been identified. These include: K_V, KCNQ, BK_{Ca}, K_{ATP}, K_{ir} and K_{2P} (Standen & Quayle, 1998;Moudgil *et al.*, 2005;Ko *et al.*, 2008).

1.6.1 Structure and biophysical properties of potassium channels

The majority of K^+ channels are composed of pore-forming primary α-subunits and regulatory β-subunits (Patel & Honoré, 2001). All K_V channels are homotetramers (all four α-subunits are identical), but they may also form heterotetramers from two or more distinct types of α-subunits within the same family. Formation of heterotetramers is often responsible for altering the biophysical properties from those of any of the homotetramers (Russell *et al.*, 1994;Ottschytsch *et al.*, 2002). The membrane topologies of the primary α-subunit of K^+ channels expressed in vascular smooth muscle cells are depicted in Figure1.3.

Apart from the functional properties, based solely on the structural properties of α-subunits (e.g. transmembrane domain and pore formation), K^+ channels can be divided into three main families:

6TM-1P family of K^+ channels: This family comprises the voltage-gated K_V subfamilies, the KCNQ subfamily, the EAG subfamily, the Ca^{2+}-activated Slo subfamily (e.g. BK_{Ca}) and the Ca^{2+}-activated SK subfamily (SK_{Ca}). The pore-

forming α-subunits form tetramers, and heteromeric channels may be formed within subfamilies (e.g. $K_V1.1$ with $K_V1.2$) (Wei *et al.*, 2005).

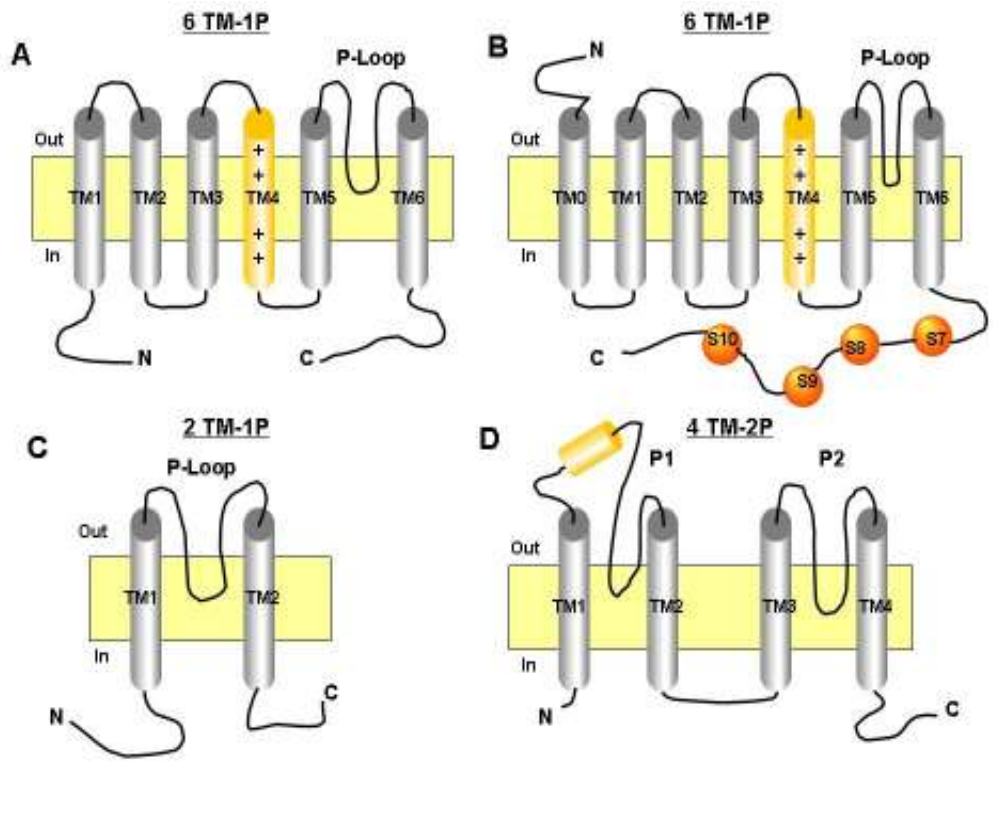

Figure 1.3 Putative topology of K^+ channel α-subunits in vascular smooth muscle cells (a planar view).

A and B, α-subunits of K_V and BK_{Ca} channels, respectively; C, K_{ir} subunit of K_{ATP} channels and D, K_{2P} channels. The pore forming loops are defined as P-Loops in A-C and P1 and P2 in D. The transmembrane (TM) domains are indicated in each subunit. TM, transmembrane; P, pore.

4TM-2P family of K^+ channels: The primary pore-forming α-subunit contains two pore domains, hence termed two pore domain K^+ channel (K_{2P}). They form functional dimers rather than the usual K^+ channel tetramers. These channels are open at all voltages and are thought to underlie many leak currents in native cells (Goldstein *et al.*, 2005).

2TM-1P family of K^+ channels: K^+ channels of this family (known as inward-rectifier K^+ channels) include strong inward-rectifier K^+ channels ($K_{ir}2.x$), G-protein-activated inward-rectifier K^+ channels ($K_{ir}3.x$) and the ATP-sensitive K^+ channels ($K_{ir}6.x$) which combine with sulphonylurea receptors. The pore-forming α-subunits form tetramers and heteromeric channels may be formed within K_{ir} subfamilies (e.g. $K_{ir}3.2$ with $K_{ir}3.3$) (Wei *et al.*, 2005;Goldstein *et al.*, 2005).

Regulatory β-subunits: The regulatory β-subunits modulate the biosynthesis, expression and gating of α-subunits (Patel & Honoré, 2001). The β-subunits are important for association with K_V types (K_V1 and K_V2) and BK_{Ca} channels. Three main regulatory K_Vβ-subunits (K_Vβ1- β3) have been identified (Pongs *et al.*, 1999). When associated with K_V α-subunits, K_Vβ subunits interact with the amino terminus of α-subunits; and thus four β-subunits interact with four α-subunits to form a functional channel (Gulbis *et al.*, 1999;Gulbis *et al.*, 2000).

Silent sub-units: There are other types of subunits called 'silent' or 'modifier' subunits for their inability to produce K^+ channel currents. Four K_V families (K_V5, K_V6, K_V8 and K_V9) encode subunits that act as silent or modifier subunits (Salinas *et al.*, 1997b). Kv9.3 belongs to this novel sub-family of electrically silent voltage-gated K^+ channels and is the first to be identified in vascular smooth muscle (Patel *et al.*, 1997). Although the silent subunits do not express a K^+ channel current by themselves, but induce profound changes in the properties of the K_V2 subfamilies by forming heterotetramers (Hugnot *et al.*, 1996;Post *et al.*, 1996;Salinas *et al.*, 1997a;Zhong *et al.*, 2010a).

Structural features and gating of different K^+ channels:

K_V channels: Among the functionally distinct five types of K^+ channels, K_V channels are the predominant group of K^+ channels expressed in pulmonary vasculature (Yuan, 1995;Ko *et al.*, 2008). K_V channels comprise the largest family, subdivided into 12 subfamilies (Table 1.1) (Goldstein *et al.*, 2005). Structurally, K_V channels are homo or hetero tetramers composed of four pour forming α-subunits, each comprising of six transmembrane spanning domains (TM1-TM6 or S1-S6) with a pore forming region called 'P-Loop' between the TM5 and TM6 (Wray, 2009). Thus symmetrically arranged four α-subunits of K^+ channel form a central pore which is highly selective for the transportation of K^+ ions across the cell membrane (MacKinnon *et al.*, 1990). The segment S4 or TM4 domain of the voltage-gated K^+ channels contains four positively charged arginine residues that are essential for depolarisation-dependent opening of the channel. The S4 segment is therefore called the voltage-sensing segment (Aggarwal & MacKinnon, 1996;Jiang *et al.*, 2003).

Upon activation, the positively charged S4 segment moves outwards, leading to conformational changes in the α-subunits and opening of K^+ channels, and the negatively charged S2 and S3 segments are also involved in this process (Wray, 2009). Membrane depolarisation may also lead to conformational changes of the cytoplasmic C- and N-domains of K_V channels altering voltage-sensitivity of some K_V channels (Kobrinsky *et al.*, 2006). $K_V\beta$ subunits interact with the amino terminus of the α-subunits to form a functional K_V channel (Gulbis *et al.*, 1999;Gulbis *et al.*, 2000). Thus heteromultimeric association of different β-subunits contributes to increase the complexity of K_V channels (Patel & Honoré, 2001).

Table 1.1 Subfamilies of K_V channels and their inhibitors[1]

Subfamily group	Subtypes	Associated subunits	Inhibitors
K_V1.x	K_V1.1-K_V1.8	$K_V\beta$1, $K_V\beta$2	TEA potent (K_V1.1), 0.3 mM TEA potent (K_V1.2), 560 nM TEA moderate (K_V1.3, 1.6), 10 mM 4-AP potent (K_V1.5), 270 μM α-dendrotoxin (K_V1.1, 1.2, 1.6), 20 nM Margatoxin (K_V1.1, 1.2, 1.3), 2 nM Charybdotoxin (K_V1.2), 14 nM Correolide (K_V1.x), 90 nM
K_V2.x	K_V2.1-K_V2.2	K_V5.1, K_V6.1-6.3, K_V8.1, K_V9.1-9.3	TEA moderate, 2.6 mM 4-AP poor (K_V2.1), 18 mM 4-AP moderate (K_V2.2), 1.5 mM
K_V3.x	K_V3.1-K_V3.4	MiRP2 (K_V3.4)	TEA potent (K_V3.1, 3.2), 100-200 μM 4-AP potent (K_V3.1, 3.2), 30-100 μM BDS-1 (K_V3.4), 47 nM
K_V4.x	K_V4.1-K_V4.3	KChiP, KChAP	-
K_V7.x (KCNQ)	K_V7.1-K_V7.5	mink, MiRP2 (K_V7.1)	TEA (K_V7.2), 0.16-0.50 mM TEA (K_V7.4), 3 mM XE991 (K_V7.1, 7.2), 0.7-0.8 μM XE991 (K_V7.4), 5 μM Linopirdine (K_V7.1-K_V7.5), 7-16 μM
K_V10.x, K_V11.x, K_V12.x (EAG)	K_V10.1-10.2 (eag1-2), K_V11.1-11.3 (eag1-3, herg1-3), K_V12.1-12.3 (elk1-3)	minK, MiRP1 (erg1)	E-4031 (K_V11.1), 7.7 nM Astemizole (K_V11.1), 1 nM Terfenadine (K_V11.1), 56 nM

[1]Modified from Alexander *et al.*, 2009, Grissmer *et al.*, 1994 and Gutman *et al.*, 2005

Table 1.2 Subfamilies of K_{Ca} channels and their inhibitors[1]

Subfamily group	Subtypes	Inhibitors
K_{Ca}1.x, **K_{Ca}4.x,** **K_{Ca}5.x ('Slo')**	K_{Ca}1.1 (Slo, BK), K_{Ca}4.1-4.2 (Slack), K_{Ca}5.1 (Slick)	TEA (200 nM) Charybdotoxin (<10 nM) Iberiotoxin (~10 nM)
K_{Ca}2.x **K_{Ca}3.x ('SK')**	K_{Ca}2.1-2.3 (SK1-SK3) K_{Ca}3.1 (SK4, IK)	Charybdotoxin (K_{Ca}3.1) (<10 nM) Apamin (K_{Ca}2.1-2.3) (<10 nM)

[1]Modified from Alexander *et al.*, 2009

BK_{Ca} channels: They also form tetramers consisting of 4 α and 4 β subunits. The α-subunit has extracellular N- and intracellular C-termini (Wallner *et al.*, 1996). Due to an additional TM domain (TM0) the N-terminus of α-subunit of this channel lies extracellularly (Fig. 1.3 B). The α-subunit is the pore forming component of the channel and is composed of 11 hydrophobic domains, including 7 membrane spanning (TM0-TM6) domains known as the 'core' region and 4 cytosolic (S7-S10) domains known as the 'tail' region (Korovkina & England, 2002a). This channel is regulated by the β-subunit which comprises of two membrane spanning domains separated by an extracellular loop. Similar to K_V channels, in the α-subunit there is a pore forming region or P-Loop between TM5 and TM6 and the TM4 contains positively charged amino acid residues that confers voltage sensitivity of the channel (Korovkina & England, 2002a).

K_{ATP} channels: are octameric complexes of two different proteins of distinct function; four pore-forming K_{ir} channel subunits (K_{ir} 6.1 or 6.2) (Fig.1.3 C) surrounded by four sulphonyl urea receptors (SURs) (Aguilar-Bryan & Bryan, 1999). SURs are ATP binding cassette proteins that bind to the pore-forming K_{ir} subunits to form a functional K_{ATP} channel. The K_{ir} subunits regulate transport of

K^+ whereas SUR subunits regulate channel activity depending on cellular ATP levels (Burke *et al.*, 2008). Binding of ATP to K_{ir} subunits results in conformational changes and thus channel closure (Tucker *et al.*, 1997) whereas interaction of phospholipids with K_{ir} activates K_{ATP} channels and thus relieves ATP inhibition (Shyng & Nichols, 1998).

K_{2P} channels: K_{2P} or two pore domain K^+ channels have four TM segments (TM1-TM4) and two pore forming domains (P1 and P2). The α-subunit has a short cytoplasmic N-terminal and a long cytoplasmic C-terminal. In addition, an extracellular loop exists between the TM1 and P1 regions (Lesage & Lazdunski, 2000) (Fig. 1.3 D). In structure, K_{2P} channels differ from any other K^+ channels in that they have a single pore-forming motif within their α-subunit, whereas K_{2P} channels have two. K_{2P} channels are believed to assemble as a dimer of two α-subunits to form functionally active channels (Nishida *et al.*, 2007). The K_{2P} channels expressed in VSMCs include TASK-1, TASK-2, TREK-2, THIK-1 and TWIK-2 (Kim *et al.*, 1998;Medhurst *et al.*, 2001;Liu & Saint, 2004;Putzke *et al.*, 2007).

1.6.2 Role of potassium channels in regulation of excitability of pulmonary and systemic arteries

Functional K^+ channels expressed in VSMCs are listed in Table1.3 and include: K_V, KCNQ, BK_{Ca}, K_{ATP}, K_{ir}, and K_{2P} channels. In addition, ERG channels have also been identified in murine portal vein smooth muscle (Ohya *et al.*, 2002;Yeung & Greenwood, 2007).

Table 1.3 Functional types of K^+ channels expressed in VSMCs

	Potassium channels					
Tissues	**K_V**	**KCNQ**	**BK_{Ca}**	**K_{ATP}**	**K_{ir}**	**K_{2P}**
Pulmonary	Yuan, 1995;Peng *et al.*, 1996	Joshi *et al.*, 2006;Joshi *et al.*, 2009	Peng *et al.*, 1996;Barman *et al.*, 2003	Clapp & Gurney, 1992		Gurney *et al.*, 2002;Gardener *et al.*, 2004
Cerebral	Robertson & Nelson, 1994	Zhong *et al.*, 2010b	Robertson *et al.*, 1993		Zaritsky *et al.*, 2000	
Mesenteric	Xu *et al.*, 1999	Mackie *et al.*, 2008	Sansom & Stockand, 1994	Quayle *et al.*, 1995		Gardener *et al.*, 2004
Coronary	Remillard & Leblanc, 1996		Tanaka *et al.*, 1997	Gollasch *et al.*, 1996	Quayle *et al.*, 1996	
Portal vein	Edwards *et al.*, 1993	Ohya *et al.*, 2003	Kirkup *et al.*, 1996	Hart *et al.*, 1993		
Aorta	Tammaro *et al.*, 2004	Yeung *et al.*, 2007	Tammaro *et al.*, 2004			

1.6.2.1 K_V Channels:

The K_V superfamily may be further subdivided into seven conserved gene families including voltage dependent K_V channels (K_V1.x-K_V4.x), the KCNQ channels (K_V7), the silent or modifier channels (K_V5, K_V6, K_V8 and K_V9 subunits), and the eag-like channels (K_V10.x-K_V12.x) (Gutman *et al.*, 2005). K_V channels are ubiquitously expressed in VSMCs including K_V1.1-1.8, K_V2.1-2.2, K_V3.1-3.4, K_V4.1-4.3, K_V7.1, 7.4 & 7.5, K_V9.1, K_V11, $K_V\beta$1.1-1.3, $K_V\beta$2.1-2.2 (Cox & Petrou, 1999;Davies & Kozlowski, 2001;Ohya *et al.*, 2003;Wang *et al.*, 2005b;Brueggemann *et al.*, 2007;Yeung *et al.*, 2007;Joshi *et al.*, 2009;Zhong *et al.*, 2010b). In pulmonary arteries K_V1.1, 1.2, 1.5, 2.1, 3.1, 9.3 and $K_V\beta$1-2; and in the mesenteric arteries K_V1.1, 1.2, 1.3, 1.5, 2.1, 3.4, 4.2, 4.3, 9.3, and $K_V\beta$1-2 appear to dominate [reviewed in (Cox, 2005)]. As voltage-gated K_V channels are activated by membrane depolarisation (which could result for example from activation of Cl_{Ca}, ROCCs or VOCCs) and will induce membrane hyperpolarisation and vasorelaxation, they act as negative feedback regulators. Thus, the main function of K_V channels is to dampen cell excitation, limit membrane depolarisation and maintain resting vascular tone (Nelson & Quayle, 1995;Jackson, 2000b;Sobey, 2001;Korovkina & England, 2002a). Inhibition of K_V channel activity resulting from sustained depolarisation could be associated with a range of pathophysiological conditions. For example, in diabetic patients, high circulating glucose levels have been associated with an increase in ROS by inducing superoxide (O_2^-) production which impaired K_V channel activity (Liu *et al.*, 2001a;Liu & Gutterman, 2002). Notably, it was found that K_V currents in mice PASMCs are more sensitive to TEA and less sensitive to 4-AP (Ko *et al.*, 2007), unlike in the rat (Smirnov *et al.*, 2002) suggesting that in different species, different K_V channel types could contribute to the regulation of cell excitability.

In general, the role of K^+ channels is crucial for maintenance of low resistance in the pulmonary circulation. It is well established that in PASMCs, K_V channels play the central role in regulation of membrane potential and are thus postulated to be a major determinant of vascular tone (Yuan, 1995;Moudgil *et al.*, 2006;Ko *et al.*, 2008). They also contribute to hypoxic pulmonary vasoconstriction (Archer & Michelakis, 2002). Decreased K_V channel expression in the pulmonary

circulation contributes to pathogenesis of pulmonary artery hypertension (Yuan *et al.*, 1998a;Yuan *et al.*, 1998b;Bonnet *et al.*, 2006) by enhancing cell proliferation and inhibiting apoptosis (Michelakis *et al.*, 2002b;Remillard & Yuan, 2004). It has also been demonstrated that decreased K_V channel activity and a subsequent rise in $[Ca^{2+}]_i$ in PASMCs leads to medial hypertrophy by stimulation of PASMC proliferation in patients with pulmonary hypertension (Platoshyn *et al.*, 2000).

Table 1.4 K_V channel subfamilies with encoding genes and tissue distribution*

K_V channels	**Gene name**	**Channel distribution**
K_V1.1	KCNA1	**Pulmonary artery**[1,2], brain, heart, retina
K_V1.2	KCNA2	**Pulmonary artery**[2], brain, atrium, ventricle, retina
K_V1.3	KCNA3	Brain, lung, islets, spleen, thymus, lymph node, testis
K_V1.4	KCNA4	**Pulmonary artery**[2], brain, skeletal muscle, heart
K_V1.5	KCNA5	**Pulmonary artery**[2], **aorta**, smooth muscle, kidney
K_V1.6	KCNA6	**Pulmonary artery**[2], brain, heart, lung, ovary, testis
K_V1.7	KCNA7	**Pulmonary artery**[3], heart, placenta, skeletal muscle
K_V1.8	KCNA10	Brain, heart, kidney, adrenal gland, skeletal muscle
K_V2.1	KCNB1	**Pulmonary artery**[2], brain, heart, lung, retina, eye
K_V2.2	KCNB2	**Mesenteric artery**[4], brain, tongue, gut muscle
K_V3.1	KCNC1	**Pulmonary artery**[2], brain, lung, skeletal muscle
K_V3.2	KCNC2	**Mesenteric artery**[4], brain, islets, Schwann cells
K_V3.3	KCNC3	**Mesenteric artery**[4], brain, central auditory nuclei
K_V3.4	KCNC4	Parathyroid, prostate, brain, skeletal muscle
K_V4.1	KCND1	**Pulmonary artery**[3], brain, lung, stomach, liver
K_V4.2	KCND2	Brain, atrium ventricle, cochlear nucleus
K_V4.3	KCND3	**Pulmonary artery**[2], heart, brain, smooth muscle
K_V5.1	KCNF1	Brain, heart, liver, kidney, skeletal muscle
K_V6.1	KCNG1	Cardiac myocytes, brain, uterus, ovary, bone, skin
K_V6.2	KCNG2	Myocardium, fetal brain, germinal centre B cells
K_V6.3	KCNG3	Brain, spinal cord, pituitary, testis, thymus
K_V6.4	KCNG4	Brain, liver, small intestine, colon

Table 1.4 continued[*]

(K_V channel subfamilies with encoding genes and tissue distribution**)**

K_V7.1	KCNQ1/KVLQT	**Pulmonary**[6]**, carotid**[7]**, femoral**[7]**, mesenteric**[7] **and cerebral arteries**[10]**; portal vein**[8], **aorta**[7,9]
K_V7.2	KCNQ2/KQT2	Brain, lung, heart, eye, small intestine, placenta
K_V7.3	KCNQ3	Brain, eye, retina, testis, colon
K_V7.4	KCNQ4	**Pulmonary**[6], **carotid**[7]**, femoral**[7]**, mesenteric**[7] **and cerebral arteries**[10], **aorta**[7]**,** cochlea
K_V7.5	KCNQ5	**Pulmonary**[6], **carotid**[7]**, femoral**[7]**, mesenteric**[7] **and cerebral arteries**[10]**; aorta**[7,9]**,** brain, sympathetic ganglia, skeletal muscle
K_V8.1	KCNV1	Brain, kidney
K_V8.2	KCNV2	Lung, liver, kidney, pancreas, spleen, thymus, testis
K_V9.1	KCNS1	**Pulmonary artery**[3], brain, lens epithelium
K_V9.2	KCNS2	**Pulmonary artery**[3], brain, retina, spinal cord
K_V9.3	KCNS3	**Pulmonary artery**[2,5], brain, heart, kidney
K_V10.1	KCNH1	Brain, melanoma cells
K_V10.2	KCNH5	Brain
K_V11.1	KCNH2	Brain, heart, kidney, liver, lung, ovary, blood cells
K_V11.2	KCNH6	Brain, uterus, rat pituitary
K_V11.3	KCNH7	Brain, sympathetic ganglia, rat pituitary
K_V12.1	KCNH8	Brain, lung, uterus, testis, sympathetic ganglia
K_V12.2	KCNH3	Brain, lung
K_V12.3	KCNH4	Brain, lung, pituitary gland

[*]Modified from Alexander *et al.*, 2009 and Gutman *et al.*, 2005

[1]Young *et al.*, 2006; [2]Wang *et al.*, 2005b; [3]Davies & Kozlowski, 2001; [4]Xu *et al.*, 1999; [5]Hulme *et al.*, 1999; [6]Joshi *et al.*, 2009; [7]Yeung *et al.*, 2007; [8]Ohya *et al.*, 2003; [9]Brueggemann *et al.*, 2007; [10]Zhong *et al.*, 2010b

K_V channel currents are inhibited by hypoxia in PASMCs (Post *et al.*, 1992;Sweeney & Yuan, 2000;Coppock *et al.*, 2001;Mandegar & Yuan, 2002;Platoshyn *et al.*, 2007). Hypoxia results in inhibition of gene expression of K_V channel α-subunits in PASMCs (Wang *et al.*, 1997;Wang *et al.*, 2005b). Chronic hypoxia selectively downregulates K_V channel expression, reduces K_V current (I_{KV}), and induces depolarisation in PASMCs (Smirnov *et al.*, 1994;Platoshyn *et al.*, 2001). A 4-AP-sensitive K_V channel was found to be involved in vasoconstriction under hypoxic conditions in rat isolated main pulmonary artery (Bardou *et al.*, 2001) and isolated rabbit lungs (Liu *et al.*, 2001c). Among the twelve subfamilies of K_V channels, K_V1.5 and K_V2.1 are thought to be the main contributors to the initiation of HPV in rat pulmonary artery myocytes (Archer *et al.*, 1998). A most recent study provides compelling evidence that K_V1.5 is an important hypoxia-sensitive K_V channel in PASMCs (Firth *et al.*, 2009b). K_V1.2, K_V1.4 and K_V1.5 are the most important α-subunits in human PASMCs because these are the K_V channel α-subunits that participate in forming functional channels in human PASMCs (Archer *et al.*, 1998;Coppock *et al.*, 2001;Archer *et al.*, 2001;Platoshyn *et al.*, 2004). Although K_V3 and K_V4 subunits have also been reported to be hypoxia sensitive, only K_V3.1b was found to be present in PA. Hypoxia inhibits K_V3.1b channels expressed in L929 cells, and the expression of these channels was demonstrated in PASMCs suggesting their potential role in O_2 sensing in PA (Osipenko *et al.*, 2000). Chronic hypoxia decreases expression of K_V1.1, K_V1.5, K_V1.6, K_V2.1, K_V4.3, and K_V9.3 α-subunits (Osipenko *et al.*, 2000;Platoshyn *et al.*, 2001). The functional characteristics and physiological role of K_V channels in relation to HPV will be further elaborated in the HPV section of this chapter.

Table 1.5 Potency of K_V channel inhibitors 4-AP and TEA in pulmonary and systemic VSMCs

	4-AP (IC_{50}) mM	TEA (IC_{50}) mM
Rat PASMCs	0.30 (Okabe *et al.*, 1987)	>100 (Okabe *et al.*, 1987)
Mouse PASMCs	>10 (Ko *et al.*, 2007)	1-5 (Ko *et al.*, 2007)
Rat PASMCs	0.35 (Smirnov *et al.*, 2002)	Insensitive (Smirnov *et al.*, 2002)
Rat MASMCs	~1 (Smirnov & Aaronson, 1992)	9.9 (Xu *et al.*, 1999;Lu *et al.*, 2001)
Rat MASMCs	5.1 (Xu *et al.*, 1999;Lu *et al.*, 2001)	

For pharmacological characterisation of the K_V1 subfamily, a wide range of specific toxins are available for individual subtypes but not for $K_V1.5$ (Table 1.1). Only 4-AP and correolide (which blocks all $K_V1.x$) are the tools available for pharmacological characterisation of $K_V1.5$, the main contributor in HPV. However, an inhibitor such as TEA is another alternative pharmacological tool to investigate the properties of K_V channels as the members of both the K_V2 and K_V3 subfamilies are sensitive to TEA. Thus, the lack of a specific inhibitor of $K_V1.5$ channels has made the investigation of these types of channels difficult in intact preparations. It is widely accepted that 4-AP is the most frequently used and most selective known inhibitor of K_V channels in vascular smooth muscle cells (Okabe *et al.*, 1987;Beech & Bolton, 1989;Volk *et al.*, 1991;Gelband & Hume, 1992;Smirnov & Aaronson, 1992;Ishikawa *et al.*, 1993;Robertson & Nelson, 1994). Therefore, 4-AP has been used to distinguish K_V currents from BK_{Ca} currents: both of which are activated by membrane depolarisation (Okabe *et al.*, 1987;Beech & Bolton, 1989;Smirnov & Aaronson, 1992). Although the IC_{50} of 4-AP in isolated PASMC is <1 mM (Okabe *et al.*, 1987;Smirnov & Aaronson, 1994;Smirnov *et al.*, 2002), much higher concentrations are necessary to cause contraction in intact pulmonary artery. For this reason, many studies using intact tissue and focussing on K_V channel responsiveness have used higher

concentrations of 4-AP. For example, 2-16 mM in rat pulmonary artery (Han *et al.*, 2007), 10 mM in mouse pulmonary artery (Xu *et al.*, 2008) and 10 mM in chicken ductus arteriosus (Greyner & Dzialowski, 2008;Cogolludo *et al.*, 2009) were used (Table 1.6). Thus, there is always a marked difference in the concentration of 4-AP used for inhibiting K_V channels in single isolated cells versus intact tissue preparations. The concentration of 4-AP is usually chosen by the experimenter depending upon the purpose and nature of the experiment.

Table 1.6 A comparison of the concentrations of 4-AP used in intact arteries in contraction studies

Tissue	**Species**	**4-AP (mM)**	**References**
Pulmonary artery	Rat	10	Karamsetty *et al.*, 1998
Pulmonary artery	Rat	2 to16	Han *et al.*, 2007
Pulmonary artery	Mouse	10	Xu *et al.*, 2008
Pulmonary artery	Lamb	10	Konduri *et al.*, 2009
Detrusor muscle	Rat	10	Ning & Liang, 2009
Diaphragm muscle	Guineapig	> 10	Ishida & Honda, 1993
Ductus arteriosus	Chicken	10	Cogolludo *et al.*, 2009
Ductus arteriosus	Chicken	10	Greyner & Dzialowski, 2008

1.6.2.2 K_V7 (KCNQ) channels:

1.6.2.2.1 KCNQ genes and the role of their expression products: a brief history:

KCNQ genes encode members of the K_V7 family of K^+ channel subunits that now includes five members: $K_V7.1$- $K_V7.5$ or KCNQ1-KCNQ5. K_V7 or KCNQ channels were first discovered in neurons and cardiac cells where they are thought to play an important role in regulation of membrane potential (Robbins, 2001;Delmas & Brown, 2005). This is a relatively recently discovered group of the K_V channel subfamily. The first publications came in 1996 (Wang *et al.*, 1996) and first non-provisional gene patent filed in 1998 (Biervert *et al.*, 1998;Charlier *et al.*, 1998;Singh *et al.*, 1998). Long before the discovery of these KCNQ channels, Brown and Adams identified a voltage-gated K^+ current that could account for a decrease of potassium conductance in frog sympathetic neurones and named 'M-current' due to its suppression by stimulation of muscarinic acetylcholine receptors (Brown & Adams, 1980). Identification of a gene product that could account for the long-established 'M-current' came in 1996 when Mark Keating and colleagues discovered K_VLQT1 (now called KCNQ1) as one of the ion channels underlying the long-QT syndrome (a potentially fatal inherited cardiac arrhythmia) (Wang *et al.*, 1996). Following the discovery of K_VLQT1, in 1998, neuronal KCNQ channels, specifically KCNQ2, 3 and 5, were cloned using the sequence homology with the important cardiac K_VLQT1 channel (Yang *et al.*, 1998). Subsequent genetic analyses revealed numerous mutations in KCNQ2 and 3 channels capable of producing a range of biophysical alterations or loss of function (Biervert & Steinlein, 1999). In 1999, mutations in another member of the family, KCNQ4, were found to be responsible for a form of autosomal dominant deafness, and this subunit (KCNQ4) was shown to play an important role in hair cell regulation in the cochlea (Kubisch *et al.*, 1999;Kharkovets *et al.*, 2000). The fifth family member, KCNQ5, was first publicly disclosed in 2000 (Lerche *et al.*, 2000;Schroeder *et al.*, 2000;Maljevic *et al.*, 2010).

Out of the five members, KCNQ1 is predominantly expressed in the cardiac muscle and in epithelial cells and is believed to be generally absent from neuronal tissue (Robbins, 2001). In cardiac tissue KCNQ1 is involved in repolarisation following an action potential. In cardiac myocytes KCNQ1 subunits assemble with the accessory β-subunit (KCNE1) and form a channel complex constituting the delayed rectifier current (I_{Ks}), which is partly responsible for terminating the cardiac action potential (Barhanin *et al.*, 1996;Sanguinetti *et al.*, 1996). Mutations in KCNQ1 may lead to dysfunction of the channel and cause the cardiac long-QT syndrome. In epithelial tissue KCNQ1 is important in regulation of water and salt transport. A lack of functional KCNQ1 channel expression has been found to have severe implications in the epithelial tissues of organs such as lung, stomach, cochlea, intestine, and kidney, where salt and water transport is crucial for proper function. Thus humans with mutations in KCNQ1 may suffer from deafness (Jervell & Lange-Nielsen, 1957;Neyroud *et al.*, 1997). Similarly, KCNQ1 knock out mice showed deafness, balance problems and morphological abnormalities in the inner ear and gastrointestinal tract (Lee *et al.*, 2000;Casimiro *et al.*, 2001).

The other four members (KCNQ2-KCNQ5) are mainly expressed in the nervous system hence they are called neuronal KCNQ channels (Jentsch, 2000;Robbins, 2001;Cooper & Jan, 2003). KCNQ2-KCNQ5 channels have been proposed to constitute the 'M-current', which is central in the control of neuronal action potential firing due to its modulation by neurotransmitters and voltage-sensitivity (Mackie & Byron, 2008). KCNQ2, KCNQ3 and KCNQ5 determine sub threshold excitability of neurons whilst KCNQ2 and KCNQ3 coassemble to form the 'M-current' in the brain (Wang *et al.*, 1998). KCNQ4 plays a physiological role in hearing by mediating potassium efflux from outer hair cells (Kubisch *et al.*, 1999;Kharkovets *et al.*, 2000). Mutations in KCNQ2 and KCNQ3 cause benign familial neonatal seizures (Biervert *et al.*, 1998;Charlier *et al.*, 1998;Singh *et al.*, 1998), whilst mutations in KCNQ4 underlie congenital deafness (Kubisch *et al.*, 1999). However, no disease has yet been found to be related to KCNQ5 (Lerche *et al.*, 2000;Schroeder *et al.*, 2000;Maljevic *et al.*, 2010).

Intriguingly, expression of 'neuronal' KCNQ4 and KCNQ5 transcripts and protein has recently been found also in vascular smooth muscle cells (Yeung *et al.*,

2007;Joshi *et al.*, 2009;Zhong *et al.*, 2010b), indicating their potential importance in the regulation of vascular excitability and contractility. This will be further elaborated below.

1.6.2.2.2 KCNQ expression and function in vascular smooth muscle:

Recent studies provide consistent evidence that KCNQ1, 4 and 5 transcripts are expressed in vascular smooth muscle cells including pulmonary, mesenteric and other systemic blood vessels (Ohya *et al.*, 2003;Yeung *et al.*, 2007;Joshi *et al.*, 2009;Zhong *et al.*, 2010b). KCNQ channels are voltage-gated channels, but their threshold for activation is substantially more negative (between -80 and -60 mV) than that for other voltage-gated K^+ channels (-30 and -40 mV) (Wang *et al.*, 1998;Gurney *et al.*, 2010). KCNQ channels are characterised by some unique features such as (i) slow activation and deactivation, and (ii) their inability to inactivate during sustained depolarisation (Brown & Adams, 1980;Gurney *et al.*, 2010). These are the main reasons why they were suggested as the background K^+ currents found in PASMCs (Evans *et al.*, 1996). The biophysical properties of KCNQ channels could be altered by a number of factors including PIP_2 hydrolysis and heterotetramer formation. Furthermore, associated subunits of KCNQ channels (e.g., KCNE1-5) may also play significant modulatory role on channel expression, biophysical and pharmacological properties of these channels especially KCNQ1 [recently reviewed in (Greenwood & Ohya, 2009)].

KCNQ channels, expressed in a variety of VSMCs, play an important role in maintaining the resting membrane potential and vascular reactivity (Yeung & Greenwood, 2005;Joshi *et al.*, 2006;Brueggemann *et al.*, 2007;Yeung *et al.*, 2007;Yeung *et al.*, 2008;Mackie *et al.*, 2008;Mackie & Byron, 2008;Joshi *et al.*, 2009;Gurney *et al.*, 2010). The expression of different subunits of the KCNQ channel subfamily in VSMCs is summarised in the Tables 1.4 and 1.7.

Table 1.7 Expression of KCNQ channel subunits in VSMCs

KCNQ subunit	Species and tissue involved	References
KCNQ1	Mouse portal vein	Ohya *et al.*, 2003
KCNQ 1, 4 and 5	Mouse aorta, carotid, femoral and mesenteric arteries	Yeung *et al.*, 2007
KCNQ5	Cultured rat aorta	Brueggemann *et al.*, 2007
KCNQ1 and 5	Rat aorta	Brueggemann *et al.*, 2007
KCNQ1, 4 and 5	Rat mesenteric artery	Mackie *et al.*, 2008
KCNQ1, 4 and 5	Rat pulmonary artery	Joshi *et al.*, 2009
KCNQ1, 4 and 5	Rat cerebral artery	Zhong *et al.*, 2010b

Role of KCNQ channels in pulmonary and mesenteric arteries:

Recent evidence suggests that in addition to their role in neurons, KCNQ channels also play an important role in maintaining resting membrane potential and cellular excitability in arteries and are expressed in both pulmonary and systemic circulations. Out of the five KCNQ genes, three subunits (KCNQ1, 4 and 5) were found to be expressed in PASMCs, with KCNQ4 being expressed in a greater degree (Joshi *et al.*, 2009). In contrast to K_V channels, specific inhibitors of KCNQ channels are available making investigation of these channels easier. Two KCNQ blockers, linopirdine and XE991, have been developed and are widely used in study of the role of KCNQ channels. Both linopirdine and XE991 were demonstrated to be potent constrictors of pulmonary artery (Joshi *et al.*, 2006) and linopirdine has been demonstrated to be a potent constrictor of mesenteric artery (Mackie *et al.*, 2008). Among the activators of KCNQ channels, flupirtine and retigabine are widely used to activate all of the subtypes of KCNQ channels except KCNQ1, that lack a transmembrane tryptophan residue which is believed to be responsible for the action of these drugs (Schenzer *et al.*, 2005;Wuttke *et al.*, 2005;Bentzen *et al.*, 2006). These recent findings suggest that KCNQ channels could contribute to the regulation of resting membrane potential in pulmonary (Joshi *et al.*, 2006) as well as mesenteric arteries (Mackie *et al.*, 2008). However,

a very recent study suggests that among the KCNQ subtypes most probably KCNQ4 makes an important contribution to the regulation of pulmonary vascular tone, with a greater contribution in pulmonary than in systemic vessels (Joshi *et al.*, 2009). It is noteworthy, however, that the whole cell KCNQ current density measured with the voltage-clamp technique is very small (≤ 1pA/pF at 0 mV) (Mackie *et al.*, 2008;Joshi *et al.*, 2009), which complicates its investigation at the single cell level. Therefore, most of the conclusions about their functional role were derived from the effects of KCNQ inhibitors and activators on intact arteries.

Table 1.8 Biophysical properties of potassium channels in VSMCs

	K_V	KCNQ
Subtypes	K_V 1.1-1.7 and 1.10; K_V 2.1; K_V 3.1b, 3.3 and 3.4; K_V 4.1, 4.2 and 4.3; K_V 5.1; K_V 6.1-6.3; K_V 9.1 and 9.3; K_V 10.1; and K_V 11.1 [1-5]	KCNQ1, 4 and 5 [16-20]
Accessory subunits	K_V β1, K_V β2 and K_V β3 [3,6]	KCNE 1-5 [19,21]
Activators	Depolarisation [7], PKC [8,9], $\downarrow pH_i$ [10]	Depolarisation[7]
Inhibitors	Hyperpolarisation[7], PKC[8], $\uparrow[Ca^{2+}]_i$ [11], Rho-kinase [12]	Hyperpolarisation[7]
Antagonists	4-AP [13], cyt P450 inhibitors (Clotrimazole)[14], Correolide[15]	Linopirdine [18,22], XE991[16,19], (Ba^{2+})[23]

[1] Archer *et al.*, 1998*; [2] Coppock & Tamkun, 2001*; [3] Platoshyn *et al.*, 2004*; [4] Smirnov & Aaronson, 1994*; [5] Smirnov *et al.*, 2002*; [6] Accili *et al.*, 1997; [7] Nelson & Quayle, 1995*; [8] Aiello *et al.*, 1996; [9] Son *et al.*, 2006; [10] Berger *et al.*, 1998; [11] Cox & Petrou, 1999; [12] Cachero *et al.*, 1998; [13] Osipenko *et al.*, 1997; [14]Yuan *et al.*, 1995b; [15]Cheong *et al.*, 2001; [16]Joshi *et al.*, 2009*; [17]Mackie *et al.*, 2008; [18]Ohya *et al.*, 2003;[19] Li *et al.*, 2006; [20]Yeung *et al.*, 2007; [21]Roura-Ferrer *et al.*, 2008; [22]Joshi *et al.*, 2006; [23]Gibor *et al.*, 2004.

* Pulmonary circulation.

Table 1.8 Continued

(Biophysical properties of potassium channels in VSMCs)

	BK_{Ca}	K_{ATP}	K_{2P}
Subtype	Slo-1 or KCNMA-1[24]	K_{ir} 6.1[46-47] K_{ir} 6.2[48]	TASK-1&2, THIK-1, TRAAK, TREK-1&2, TWIK-1&2[57-58]
Accessory subunits	β1[24-26] β2, β3,β4[3]	SUR2B[46,48]	None
Activators	PKG[27], NO[28-29], PKA[30], EETs[31-32], CO[33], AA[34], Depolarisation, ↑$[Ca^{2+}]_i$ [35]	PKA[49] CGRP[50] ↓ATP[51] PKG[7] Pinacidil[52]	Depolarisation & ↑pH_o [57] PKA[59]
Inhibitors	PKC[36-37], ROS[38], ↓pH[39], Hyperpolarisation[7], c-Src[40]	↑ATP[53-54], Ca^{2+} activated PP2B[54], PKC[55]	Hyperpolarisation & ↓pH_o[57]
Antagonists	IbTX[41-42], ChTX[41], Paxilline[43-44], 1 mM TEA[45]	Glybenclamide[56], Tolbutamide[7]	(Zn^{2+})[58] Anandamide[58]

[24]Orio *et al.*, 2002; [25]Brenner *et al.*, 2000; [26]Cox & Aldrich, 2000; [27]Barman *et al.*, 2003*;[28]Bolotina *et al.*, 1994; [29]Brakemeier *et al.*, 2003; [30]Carl *et al.*, 1991; [31]Archer *et al.*, 2003; [32]Zhang *et al.*, 2001; [33]Wang *et al.*, 1997; [34]Lu *et al.*, 2005; [35]Jackson, 2000b; [36]Barman *et al.*, 2004*; [37]Minami *et al.*, 1993a; [38]Tang *et al.*, 2004; [39]Schubert *et al.*, 2001; [40]Alioua *et al.*, 2002; [41]Gao & Garcia, 2003; [42]Giangiacomo *et al.*, 1992; [43]DeFarias *et al.*, 1996; [44]Tammaro *et al.*, 2004; [45]Li & Aldrich, 2004; [46]Cui *et al.*, 2002*; [47]Teramoto, 2006; [48]Isomoto *et al.*, 1996; [49]Sun *et al.*, 2006; [50]Wellman *et al.*, 1998; [51]Clapp & Gurney, 1992; [52]Quayle *et al.*, 1995; [53]Glavind-Kristensen *et al.*, 2004; [54]Wilson *et al.*, 2000; [55]Chrissobolis & Sobey, 2002; [56]Jackson, 1993; [57]Gardener *et al.*, 2004*; [58]Gurney *et al.*, 2003*; [59]Olschewski *et al.*, 2006.

* Pulmonary circulation.

1.6.2.3 BK_{Ca} channels:

BK_{Ca} channels, abundantly expressed in VSMC, are activated by changes in the $[Ca^{2+}]_i$ and membrane depolarisation thus contributing to the regulation of membrane potential and vascular tone especially in small myogenic vessels (Nelson & Quayle, 1995;Waldron & Cole, 1999;Korovkina & England, 2002a;Korovkina & England, 2002b). At physiological concentrations of $[Ca^{2+}]_i$ (≤100 nM), BK_{Ca} channels are generally shut, in the physiological range of membrane potentials, however when $[Ca^{2+}]_i$ is increased (e.g. to micromolar level) these channels can be activated even at hyperpolarised potentials. Thus, increased $[Ca^{2+}]_i$ enhances the voltage-dependence of BK_{Ca} channel activation by shifting it leftward to more hyperpolarised membrane potential (Stehno-Bittel & Sturek, 1992). The resultant hyperpolarisation acts to limit excessive Ca^{2+} influx by decreasing the opening of L-VOCCs. This feature makes BK_{Ca} channels an ideal candidate for feedback inhibition when levels of $[Ca^{2+}]_i$ are significantly increased (Brayden & Nelson, 1992;Nelson *et al.*, 1995;Knot *et al.*, 1998;Burg *et al.*, 2006;Yang *et al.*, 2009). Pressure- or neurotransmitter-induced depolarisation in the VSMCs can be counteracted by the efflux of K^+ that results in the activation of BK_{Ca} channels (Brayden & Nelson, 1992). BK_{Ca} channel currents are sensitive to inhibition by external toxins including iberiotoxin, charybdotoxin and TEA at IC_{50} values of ~10, <10 and 200 nM, respectively (Miller *et al.*, 1985;Langton *et al.*, 1991;Giangiacomo *et al.*, 1992;Nelson & Quayle, 1995). Amongst these, iberiotoxin is the most selective and potent blocker of BK_{Ca} channels (Wallner *et al.*, 1995). Charybdotoxin has also been widely used as another BK_{Ca} channel blocker; however, it can also affect some K_V channel subtypes (Table 1.1) as well as intermediate conductance K_{Ca} (IK_{Ca}) channels (Carl *et al.*, 1991;Gebremedhin *et al.*, 1996;Waldron & Cole, 1999).

BK_{Ca} channel properties and expression can be altered in many pathophysiological conditions including hypertension, hypoxia and diabetes (England *et al.*, 1993;Peng *et al.*, 1999;Sobey, 2001). Changes in BK_{Ca} channel properties have also been reported to be associated with coronary atherosclerosis (Bolotina *et al.*, 1991). Vascular remodelling is associated with both promotion of

VSMC proliferation and attenuation of programmed cell death or apoptosis. Activation of BK_{Ca} channels have also been shown to induce early apoptotic cell shrinkage, as well as downstream cytoplasmic casepase activation and DNA fragmentation which are essential for apoptotic cell death (Remillard & Yuan, 2004;Burg *et al.*, 2006).

Role of BK_{Ca} channels in pulmonary and mesenteric arteries:

In PASMCs, BK_{Ca} channel activity has been demonstrated to be attenuated by acute hypoxia (Post *et al.*, 1995). In PASMCs, it has been shown that chronic hypoxia decreased levels of mRNA and protein of the BK_{Ca} α-subunit, suggesting a down-regulation of BK_{Ca} activity (Bonnet *et al.*, 2003). Inhibition of BK_{Ca} channels completely restored blunted HPV in rats with experimental liver cirrhosis (Carter *et al.*, 2000). It has been reported that oxygen caused fetal pulmonary vasodilation via BK_{Ca} channel activation, which led to membrane hyperpolarisation (Cornfield *et al.*, 1996). The modulators of BK_{Ca} channels in PASMCs include: cytosolic Ca^{2+}, membrane potential, membrane stretch, fatty acids, NADH and NAD (Kirber *et al.*, 1992;Lee *et al.*, 1994). Although a BK_{Ca} channel inhibitor itself does not produce contraction, blocking of these channels significantly increased the contraction to $PGF_{2\alpha}$ in rat mesenteric arteries (Abdullah & Docherty, 1999) and also further potentiated ryanodine-induced contraction in the rat cremester arteriole (Yang *et al.*, 2009). These findings suggest an indirect influence posed by BK_{Ca} channels in the regulation of arterial tone. However, in rat intra PASMCs there is very little evidence for its contribution to the regulation of cell resting potential (Smirnov *et al.*, 1994;Smirnov & Aaronson, 1994).

1.6.2.4 K_{ATP} channels:

K_{ATP} channels represent another class of K^+ channels ubiquitously expressed in VSMCs (Noma, 1983;Nelson & Quayle, 1995), where they contribute to the maintenance of resting membrane potential and regional blood flow (Quayle *et al.*, 1997;Rodrigo & Standen, 2005). K_{ATP} channels show little or no voltage

dependency. Both *in vivo* and *in vitro* studies have shown that inhibition of K_{ATP} channels leads to vasoconstriction and membrane depolarisation in various types of VSMCs (Noma, 1983;Nelson *et al.*, 1990;Nakashima & Vanhoutte, 1995;Quayle *et al.*, 1997;Teramoto, 2006). K_{ATP} channels are inhibited by intracellular ATP and activated by nucleotide diphosphates (Beech *et al.*, 1993;Clapp, 1995). The most frequently used pharmacological inhibitor of K_{ATP} channels is glibenclamide which has an IC_{50} value between 20 and 200 nM (Beech *et al.*, 1993;Xu & Lee, 1994;Nelson & Quayle, 1995;Clapp, 1995). The inhibition of K_{ATP} channels is associated with impaired coronary and cerebral autoregulation (Narishige *et al.*, 1993;Hong *et al.*, 1994;Nelson & Quayle, 1995). On the other hand, activation of K_{ATP} channels is closely associated with several pathophysiological conditions, including systemic arterial dilation during hypoxia (Daut *et al.*, 1990;Brayden, 2002), reactive hyperemia in coronary and cerebral circulation (Kanatsuka *et al.*, 1992;Bari *et al.*, 1998;Brayden, 2002), and endotoxemic shock-induced vasodilation (Landry & Oliver, 1992;Ishizaka & Kuo, 1996;Kinoshita & Katusic, 1997). However, under basal conditions, it has been reported that the open probability of K_{ATP} channels is low (Jackson, 2000a).

Role of K_{ATP} channels in pulmonary and mesenteric arteries:

Robertson *et al.* (1992) suggested that K_{ATP} channels are normally closed in the pulmonary arteries and are not activated by the levels of hypoxia that cause a constriction (Robertson *et al.*, 1992). Several studies suggested that K_{ATP} channels may contribute to the regulation of basal blood flow in the mesenteric vascular bed (Nelson *et al.*, 1990;Moreau *et al.*, 1994;Murphy & Brayden, 1995;Gardiner *et al.*, 1996;Quayle *et al.*, 1997).

1.6.2.5 Two Pore Domain K^+ (K_{2P}) channels:

K_{2P} channels (also called KCNK or background or leak K^+-selective channels) are accredited for regulating resting membrane potential and cell excitability. These channels have been identified in a range of vascular tissues including pulmonary as well as mesenteric artery SMCs (Evans *et al.*, 1996;Gurney *et al.*,

2003;Gardener *et al.*, 2004;Olschewski *et al.*, 2006;Gonczi *et al.*, 2006). The activity of K_{2P} channels is strongly regulated by physical factors. For example, TASK-1 is highly sensitive to extracellular pH (Duprat *et al.*, 1997), volatile anaesthetics such as halothane (Gurney *et al.*, 2003) and hypoxia (Olschewski *et al.*, 2006). TREK-1, on the other hand, is temperature-sensitive (Maingret *et al.*, 2000), whilst TRAAK is stretch sensitive channel (Maingret *et al.*, 1999). Functionally expressed K_{2P} channels give rise to K^+-selective currents that are activated at all voltages, unlike K_V, K_{Ca}, or K_{ATP} channels whose activity is controlled by voltage and Ca^{2+} or metabolic regulation (Olschewski *et al.*, 2006). In other words, K_{2P} channels express a non-inactivating current, denoted I_{KN}, which is characterised by having no time or voltage dependency (Evans *et al.*, 1996). The decrease in leak K^+ conductance leads to membrane depolarisation that enhances the open probability of L-VOCCs in SMCs, resulting in Ca^+ entry and vasoconstriction (Olschewski *et al.*, 2006). It is notable that the lack of specific inhibitors of K_{2P} channels complicates studies of their roles in intact multicellular preparations (Brenner & O'Shaughnessy, 2008).

Role of K_{2P} in pulmonary and mesenteric artery:

Members of K_{2P} channels expressed in pulmonary artery are TASK-1 TASK-2, THIK-1, TREK-2, and TWIK-2 and in mesenteric artery are TASK-1 TASK-2, THIK-1, TRAAK, TREK-1, TWIK-1 and TWIK-2; (Gardener *et al.*, 2004). It is suggested that TASK-1 channels in pulmonary artery may play an important role in regulating resting membrane potential and eliciting vasoconstriction in response to hypoxia (Gurney *et al.*, 2003). TASK-2 channels also have been suggested to have a functional role in setting the membrane potential in pulmonary artery myocytes (Gonczi *et al.*, 2006). Blockade of K_{2P} channels by anandamide or bupivacaine generated a small increase in pulmonary artery tone unlike mesenteric artery (Gardener *et al.*, 2004). It is also important to note that TASK-1 channels in rat (Gurney *et al.*, 2003) and in human (Olschewski *et al.*, 2006) pulmonary artery SMCs exhibit sensitivity to hypoxia and, as such, these channels may be functionally important in mechanisms underlying HPV.

1.7 Hypoxic pulmonary vasoconstriction

Precapillary or resistance pulmonary arteries constrict during alveolar hypoxia resulting in the HPV response. HPV is a cardinal feature of the pulmonary circulation, with multiple mechanisms, one of which involves K^+ channel inhibition. HPV is an adaptive physiological mechanism of the lung that directs blood perfusion from poorly ventilated to well-ventilated lung areas to optimise gas exchange. Impairment of the HPV response under conditions of marked regional alveolar hypoxia (e.g., acute respiratory distress syndrome, or during anaesthesia) may result in poor arterial oxygenation that may lead to life-threatening hypoxemia (Marshall, 1990;Naeije & Brimioulle, 2001). Alternatively, when hypoxia is rather global (e.g., at high altitudes), generalised vasoconstriction leads to acute pulmonary hypertension (PH). If PH is chronic (e.g., chronic obstructive pulmonary disease), in addition to vasoconstriction, a process of vascular remodelling occurs leading to right-heart failure (Raj & Shimoda, 2002;Moudgil *et al.*, 2005;Stenmark & McMurtry, 2005;Weissmann *et al.*, 2006b).

Historically, indication of HPV was revealed as early as 1894 when Bradford and Dean (1894) first recognised an increase in pulmonary arterial pressure in response to alveolar hypoxia (Bradford & Dean, 1894). The physiological role of this increase in pulmonary artery pressure in response to alveolar hypoxia was not clear until 1946, when von Euler and Liljestrand (Von Euler & Liljestrand, 1946), for the first time, found that PA pressure increased in feline lungs ventilated with low O_2 mixtures, and decreased when ventilated with pure O_2. From this observation they speculated that pulmonary vasoconstriction to hypoxia could help to improve gas exchange efficiency by diverting blood flow away form poorly ventilated lung regions and towards areas with better oxygenation. Recognising this fact, they suggested that ventilation-perfusion matching was the purpose of this response. Thus, the principle of HPV is also known as von Euler-Liljestrand mechanism (Sommer *et al.*, 2008). Since then, factors modulating HPV have been identified by dissecting the mechanism of HPV using a variety of approaches including isolated organs, tissues and single cells from a range of animals including humans.

In spite of extensive research the mechanisms of HPV are still incompletely resolved. Issues addressing the questions of how O_2 levels are detected in PASMCs, what interim signalling is involved and which components act as effectors still remain controversial (Sato *et al.*, 2000;Gurney, 2002;Moudgil *et al.*, 2005;Gurney & Joshi, 2006). At present, research on HPV is driven by several hypotheses and their associated mechanisms which are briefly highlighted below.

1.7.1 Multiple mechanisms of HPV

There are several mechanisms proposed to be involved in HPV. However, currently there is no single unified hypothesis that can entirely explain this phenomenon (Aaronson *et al.*, 2006;Weissmann *et al.*, 2006b), leading to common consensus that HPV is a complex multi factorial phenomenon with more than one underlying mechanism (Ward & Aaronson, 1999;Gurney, 2002). It is currently well accepted that elevated $[Ca^{2+}]_i$ is crucial to the development of HPV. One of the proposed mechanisms involves Ca^{2+} entry via L-VOCCs (McMurtry *et al.*, 1976), which is subsequent to hypoxia-induced inhibition of K_V channels and membrane depolarisation (Archer & Michelakis, 2002;Moudgil *et al.*, 2005;Mauban *et al.*, 2005). Although the mechanism of K_V channel inhibition by hypoxia is not well understood, it may involve ROS produced by the mitochondrial electron transport chain (mETC) (Weir & Archer, 1995;Archer & Michelakis, 2002), or may engage a different mediator of mitochondrial origin, e.g. Mg^{2+} ions (Firth *et al.*, 2008;Firth *et al.*, 2009a). ROS hypothesis proposed by the Archer group relys on reduced ROS production by the mETC (Archer *et al.*, 1993;Archer & Michelakis, 2002;Michelakis *et al.*, 2002a). However, others demonstrate an increase in ROS (Waypa & Schumacker, 2006). This would rather enhance and not inhibit K_V channels (Reeve *et al.*, 1995). An increase in ROS leads to an increase in $[Ca^{2+}]_i$ and may not involve L-VOCCs (Robertson *et al.*, 2000b). Ca^{2+} release from intracellular stores triggering SOCC, the opening of Ca^{2+}-permeable cation channels, and sensitisation of the contractile apparatus to Ca^{2+} involving ROK are now increasingly postulated to be involved in the HPV response (Robertson *et al.*, 2000a;Robertson *et al.*, 2000b). Among the several

HPV hypotheses, a recent proposal suggests a role for adenosine monophosphate (AMP)-activated protein kinase (AMPK) dependent, cADP ribose activated, Ca^{2+} release from the SR via RyR (Evans *et al.*, 2005;Evans, 2006a;Evans, 2006b). However, the latest work by Gupte and colleagues proposed that glucose-6-phosphate dehydrogenase (Glc-6-PD) and NADPH redox are crucially involved in the development of HPV (Gupte *et al.*, 2010).

1.7.2 Effector components of HPV

Several effector components of HPV have been proposed. K_V channel is one of the most accepted effectors linked to Ca^{2+} entry mediated via L-VOCCs as a result of hypoxia-induced inhibition of K_V channels and consequent depolarisation (Weir & Archer, 1995;Olschewski *et al.*, 2002;Archer & Michelakis, 2002). ROS and/or changes in the cellular redox state represent another effector in HPV, but controversy exists regarding which system and what redox changes mediate the HPV response. Recently, it has been proposed that activation of Glc-6-PD is a link between hypoxia-induced inhibition of glycolysis and mitochondrial ETC and the development of HPV (Gupte *et al.*, 2010). Additionally, AMPK and RhoA/ROK have been shown to be involved in HPV mechanism.

1.7.2.1 AMP-activated protein kinase (AMPK)

Evans and his colleagues (Evans *et al.*, 2005;Evans *et al.*, 2006;Evans, 2006a;Evans, 2006b) have proposed a novel effector mechanism in PASMCs which may be particularly sensitive to the metabolic stresses induced by hypoxia. This group reported that hypoxia induced an increase in the AMP/ATP ratio with an ensuing AMPK dependent cDNA-ribose activated Ca^{2+} release from the SR via RyRs. It has also been reported that AMPK activation is necessary for the effect of hypoxia in carotid body of neonatal rat (Wyatt & Evans, 2007;Wyatt *et al.*, 2007). Evidence suggests that activation of AMPK is a key event in the initiation

of the contractile response of intra pulmonary arteries (IPAs) to acute hypoxia. Preincubation of IPAs with the AMPK inhibitor compound C (40 μM) inhibited phase II, but not phase I of hypoxia (Robertson *et al.*, 2008). Also it has been shown that hypoxia could activate AMPK via an increased mitochondrial ROS production by a mechanism independent of nucleotide concentration (Quintero *et al.*, 2006) thus providing a potential link between different effectors in the HPV response.

1.7.2.2 Rho-Kinase and Ca^{2+} sensitisation

Calcium sensitisation and desensitisation are major mechanisms regulating smooth muscle contraction (Somlyo & Somlyo, 2003). Hypoxia-induced Ca^{2+} sensitisation in VSMCs has helped, at least in part, to understand the mechanism underlying HPV. Hypoxia has been reported to increase ROK activity in PASMCs, and this increase was blocked by antagonists of Rho such as toxin B and exoenzyme C3 (Wang *et al.*, 2001). Hypoxia increased MLC phosphorylation and decreased MP activity in PASMCs (Wang *et al.*, 2003b). Specific antagonists of ROK, Y-27632 and HA-1077, have recently been used to study the involvement of RhoA and its downstream effector ROK in the signalling pathways activated by hypoxia. Y-27632 and HA-1077 block hypoxia-induced MLC phosphorylation and MP inactivation in PASMCs, phase II contraction of HVP in distal PAs, and HPV in isolated lungs and intact animals (Robertson *et al.*, 2000a;Wang *et al.*, 2001;Wang *et al.*, 2003b;Nagaoka *et al.*, 2004;Fagan *et al.*, 2004). The role of Ca^{2+} sensitisation in both acute and chronic hypoxia has been proven since the discovery of this phenomenon (McMurtry *et al.*, 2003). These findings collectively suggest that HPV requires an increase in $[Ca^{2+}]_i$, associated with increase in Ca^{2+} sensitivity which is mediated by RhoA/ROK.

However, the mechanism of hypoxia-induced activation of RhoA/ROK is currently unclear. It is speculated that either hypoxia driven increases in ROS (Waypa *et al.*, 2001) or hypoxia induced elevation of Ca^{2+} itself (Sakurada *et al.*, 2003) activates the RhoA dependent Ca^{2+} sensitisation. Further experimental

evidence advanced this hypothesis to the conclusion that PKC and ET-1 independent Ca^{2+} sensitisation is responsible for the sustained response in acute hypoxia and that it is intrinsically reliant upon an intact endothelium (Aaronson *et al.*, 2002;Robertson *et al.*, 2003). These results further suggest that an endothelium derived putative constrictor factor, which could be released in HPV, is involved in the RhoA/ROK mediated Ca^{2+} sensitisation in HPV. Since RhoA/ROK plays the a central role in HPV (Ward *et al.*, 2004a), inhaled Rho-kinase inhibitors (e.g. Y-27632) may be very promising therapeutic candidates as vasodilators in patients with pulmonary hypertension (Nagaoka *et al.*, 2005).

1.7.2.3 Mitochondrial ROS and HPV

Physiologically ROS could be formed by several different mechanisms. However, mitochondria represent an important source of ROS, an unavoidable by-product of cellular respiration. During this process, some electrons, which are passing down the mitochondrial electron transport chain (mETC), could leak away and can directly reduce oxygen molecules (O_2) to superoxide anion (O_2^-). This leak in the electron transport can occur at complexes I and III of the mETC (Turrens, 1997), although there is an agreement that the major source of ROS is complex III (Chen *et al.*, 2003), where it has been extensively explored (Turrens *et al.*, 1985). In the pulmonary circulation, it is now widely accepted that the O_2 sensor during HPV resides in the mitochondria (Ward, 2008), which are also a putative source of ROS generation. Changes in ROS in response to hypoxia are well established and there is currently support for the involvement of the mETC in oxygen sensing in PASMCs (Moudgil *et al.*, 2005;Waypa & Schumacker, 2005). However, there are two opposing hypotheses regarding ROS generation during HPV. The '***redox hypothesis***' which states a reduction of ROS in HPV (Weir & Archer, 1995;Weir *et al.*, 2002;Archer & Michelakis, 2002), whilst the '***mitochondrial ROS hypothesis***' provides evidence for an increase of ROS during hypoxia (Waypa *et al.*, 2001;Leach *et al.*, 2001).

The '***redox hypothesis***' proposed originally by Weir and Archer (Weir & Archer, 1995;Weir *et al.*, 2002;Archer & Michelakis, 2002) is based on the concept that under normoxic conditions, constitutive generation of ROS by mitochondria maintains K^+ channels in an oxidised and thus active open state. This hypothesis proposes that hypoxia suppresses the transfer of electron through the mETC causing a fall in ROS generation, thereby making the cytosol in PASMCs more reduced. The reduced cellular environment is proposed to inhibit K^+ channels, with consequent depolarisation and Ca^{2+} entry via L-VOCCs (Weir & Archer, 1995;Michelakis *et al.*, 2002a;Moudgil *et al.*, 2005). This hypothesis predicts that inhibitors of the proximal mETC (rotenone acting on Complex-I and myxothiazol acting proximal to the active site of antimycin) should mimic hypoxia, thus preventing any further response to a subsequent hypoxic challenge. In support of this prediction, some reports have shown that at least some of these agents do cause vasoconstriction, at least transiently (Rounds & McMurtry, 1981;Archer *et al.*, 1993;Archer *et al.*, 1999), while some other reports have shown no vasoconstrictor activity at all (Zhao *et al.*, 1996;Waypa *et al.*, 2001;Leach *et al.*, 2001). However, both rotenone and hypoxia have been shown to increase NADH/NAD ratio, in favour of the 'more reduced state' of the cytosol as predicted by this hypothesis (Archer *et al.*, 1993;Waypa *et al.*, 2001).

Conversely, the '***mitochondrial ROS hypothesis***' suggests that hypoxia causes a paradoxical increase in mitochondrial ROS generation from the ubisemiquinone region of complex III, and, subsequently, this increase in ROS initiates the rise in $[Ca^{2+}]_i$ (Chandel & Schumacker, 2000;Waypa *et al.*, 2001;Leach *et al.*, 2001;Waypa *et al.*, 2002). This hypothesis is arguably stronger as hypoxia has been shown to increase ROS in PASMCs; both ROS and HPV have been blocked by rotenone, myxothiazol and antioxidants; moreover oxygen sensing does not occur in mutant PA myocytes that lack functioning mETC (Waypa *et al.*, 2001). Most recently, Waypa and colleagues measured redox status in the mitochondrial matrix, the intermembrane space, and the cytosol of PASMCs during hypoxia, using targeted expression of a thiol redox sensitive ratiometric fluorescent protein sensor, RoGFP. With the help of this novel approach they detected increased ROS signalling in the intermembrane space and the cytosol during hypoxia, and concluded that hypoxia activates subcellularly compartmentalised redox

signalling, which is associated with increase in cytosolic ROS, thus leading to the development of the HPV response (Waypa *et al.*, 2010).

These two opposing hypotheses raise the obvious question as to whether ROS actually increases or decreases during hypoxia. The proponents of both hypotheses mentioned the methods used for measuring ROS as a key problem. Further work is necessary to resolve this point-counter point argument.

1.7.2.4 K^+ channels

In PASMCs, K^+ channels play a crucial role in the maintenance of negative resting membrane potential (-60 to -50 mV). As described in the earlier sections, functional K^+ channels expressed in PASMCs include K_V, KCNQ (K_V7), BK_{Ca}, K_{ATP}, and K_{2P}. The involvement and role of these channels in the mechanisms underlying HPV will be discussed in this section.

K_{2P} channels have been recently identified in PASMCs as a non-inactivating current, denoted I_{KN}, which is characterised by little time or voltage dependency (Evans *et al.*, 1996). It has been reported that K_{2P} subtype TASK-1 exhibits sensitivity to hypoxia (Olschewski *et al.*, 2006), and, therefore, these channels may be functionally important in mechanisms underlying HPV.

Another class, BK_{Ca} channels are expressed in PASMCs, though the relative contribution to the whole cell current varies between different species and in different regions of the pulmonary arterial tree (Mandegar *et al.*, 2002). Recent report suggests that during hypoxia an attenuation of BK_{Ca} currents occurs via an inhibition of cAMP/PKA dependent pathway in rat PASMCs (Barman *et al.*, 2005). In the pulmonary arteries, currently, BK_{Ca} channels are not considered to be important in HPV. However, recent study suggests that BK_{Ca} channels in PASMCs might play an indirect role in HPV. Since BK_{Ca} channels contribute to a diminished vascular tone, their increased expression in remodelled PA (e.g., in COPD) might play a role in attenuating HPV (Peinado *et al.*, 2008).

K_{ATP} is another ubiquitous class of K^+ channels, which show little or no voltage-dependence. It is believed that under basal conditions the open probability of K_{ATP} channels is low (Jackson, 2000a). Some evidences suggest that K_{ATP} may contribute to resting membrane potential in PASMCs, although the regulatory mechanisms are still to be elucidated (Cui *et al.*, 2002). There is no proposed role for K_{ATP} channels in HPV, as it has been suggested that K_{ATP} channels are normally closed in the pulmonary arteries and are not activated by the levels of hypoxia that cause a constriction (Robertson *et al.*, 1992).

KCNQ (K_V7) channels are also expressed in PASMCs, where they play an important role in contractility (Joshi *et al.*, 2006) but a role in HPV is currently not established. However, in PASMCs, KCNQ (Joshi *et al.*, 2006) and TASK-1 (Gurney & Manoury, 2009) channels are known to be open at the physiologic range of resting membrane potentials. Therefore, it is possible that if they are inhibited by hypoxia, it may contribute to membrane depolarisation in PASMCs, which will also promote activation of K_V channels and lead to HPV (Olschewski *et al.*, 2006;Gurney & Manoury, 2009).

The role of K_V channels in HPV was not established until 1992, when Post *et al.* described for the first time that hypoxia could inhibit K_V channels in pulmonary, but not systemic, SMCs, and thus cause depolarisation (Post *et al.*, 1992). This ground breaking discovery led to the K^+ channel hypothesis of HPV (Weir & Archer, 1995). Currently we have ample evidence to claim that a range of K^+ channel types may be inhibited to a greater or lesser extent by hypoxia (Lopez-Barneo *et al.*, 2001). It is well documented that the K^+ current suppressed by hypoxia in PASMCs is voltage-gated and sensitive to 4-AP, and therefore most probably are K_V channels (Post *et al.*, 1995;Osipenko *et al.*, 1997;Turner & Kozlowski, 1997;Archer *et al.*, 1998). Though the role of K_V channels in HPV is generally established (Reeve *et al.*, 2001), there is a controversy about which subtype of K_V channels or which other types of K^+ channels might contribute to HPV (Gurney *et al.*, 2002).

1.7.2.5 K_V channels

Hypoxia causes inhibition of K_V channels in pulmonary arterial SMCs but does not inhibit K^+ current in systemic arterial SMCs, such as renal or mesenteric arteries (Post *et al.*, 1992;Yuan *et al.*, 1993). In PASMCs, the degree of K^+ current inhibition and membrane depolarisation is proportional to the severity of hypoxia (Olschewski *et al.*, 2002). This study also suggests that hypoxia acts primarily on the K_V current in rat PASMCs, as after inhibition of K_V current with 4-AP (5 mM), hypoxia does not reduce the current further. Moreover, in resistance PA, pretreatment with 4-AP (10 mM) eliminates subsequent HPV, but not phenylephrine constriction (Archer *et al.*, 2004). Collectively, these observations support the hypothesis that K_V channels could play a central role in the mechanism underlying HPV. The importance of K_V channels in the regulation of HPV has further been supported by Smirnov *et al.* (1994) who showed that chronic hypoxia (pO_2 30-35 mmHg) was associated with a marked (40-50%) reduction in K_V current (I_{Kv}) amplitude. Similar to acute hypoxic episodes, chronically hypoxic animals had a resting membrane potential that was significantly more positive (-43.5±2 mV) than that observed in normoxic animals (-54.3±2 mV) (Smirnov *et al.*, 1994). Application of 1 mM 4-AP mimicked this depolarisation.

Several attempts have been made to identify the molecular properties of native PASMC O_2-sensitive K_V channel subunits (Archer *et al.*, 1996;Patel *et al.*, 1997). These studies report that in the presence of the K_V1.x channel inhibitor correolide, hypoxia exhibited reduced ability to depolarise resistance PASMCs, indicating a central role for the K_V1.x family channels in hypoxic depolarisation (Archer *et al.*, 2004). Decreased mRNA expression and attenuated protein expression of the K_V channel α-subunits (K_V1.1, K_V1.5, K_V2.1, K_V4.3 and K_V9.3) have been reported in primary cultured PASMCs but not in MASMCs (Platoshyn *et al.*, 2001). Multiple K_V channel homotetrameric subunits (K_V1.2, K_V1.3, K_V2.1 and K_V3.1) and heterotetrameric subunits (K_V1.2/ K_V1.5, K_V1.5/ K_Vβ1.1 and K_V3.1/ K_V9.3) have demonstrated sensitivity to acute hypoxia (Coppock & Tamkun, 2001). All the studies verify a potential role for the K_V α-subunits K_V1.2, K_V1.5, K_V3.1b and

K_V2.1/K_V9.3 which display similar hypoxic inhibition and are all slowly inactivating voltage-gated channels sensitive to 4-AP but not to ChTX. Several β-subunits are expressed in PASMCs and may interact with the K_V1.x family as oxidoreductase enzymes and can function as redox sensors (MacKinnon, 1991;Yuan, 2001). β-subunits may have a significant role in O_2 response as it has been demonstrated for the K_V1.2β subunit co-expressed with the K_V4.2α subunit (Archer *et al.*, 1999).

Among the K_V subunits discussed above, K_V1.5 alone or in association with K_V1.2 seem to play central role in HPV. This is supported by various studies. Thus, hypoxia inhibits K_V1.5 cloned from human PAs (Archer *et al.*, 2004) and HPV is diminished in K_V1.5 knock out mice (Archer *et al.*, 2001). Interestingly, the effects of hypoxia, apparently are not directly on the channel protein, rather it appears to be tissue specific, because, when the human K_V1.5 is overexpressed in MASMCs, hypoxia does not reduce I_K. However, when it is overexpressed in PASMCs, hypoxia reduces I_K by 40% (Platoshyn *et al.*, 2006). A recent study using single-cell reverse transcription-PCR, has shown that in PASMCs the level of expression of K_V1.5 correlates with the sensitivity of the I_K in the individual PASMC to hypoxia (Platoshyn *et al.*, 2007). This study therefore suggests that the response to hypoxia may vary between different PASMCs depending on the expression level of K_V1.5. This observation gave rise to the concept of *'pacemaker'* PASMCs, which, in response to hypoxia, may initiate contraction and pass the signal to other PASMCs through gap junctions. The central role for K_V1.5 α-subunits in HPV is also supported by the effect of chronic hypoxia on expression of mRNA and protein for K_V channels, which is decreased relatively quickly in PASMCs (Smirnov *et al.*, 1994;Osipenko *et al.*, 1998;Reeve *et al.*, 2001). In the case of K_V1.2, K_V1.5 and K_V2.1, the decrease in mRNA occurs within 6 hrs of the onset of hypoxia (Hong *et al.*, 2004). In line with the decrease in K_V channel expression, acute HPV is diminished in rats that have been exposed to chronic hypoxia (McMurtry *et al.*, 1978), and can be restored by the transfection of human K_V1.5 using an aerosol (Pozeg *et al.*, 2003), again supporting the importance of K_V1.5 in the mechanism of HPV. This notion is further supported by the findings that K_V1.5 protein is most abundant in the SMCs

of resistance PAs, even though mRNA for many other K_V channel is also present (Archer *et al.*, 2004).

Although it is widely accepted that hypoxic inhibition of K_V channels forms the core of the K^+ channel hypothesis of HPV, it's still unclear how acute hypoxia inhibits K_V channel function and how chronic hypoxia downregulates K_V channel gene expression. Potential intermediates or factors which may be involved in hypoxia-induced inhibition of K_V channel function and expression, include oxygen radicals, mETC, NADPH oxidase, redox status, metabolic inhibition, cytochrome P-450 oxidoreductase, cytochrome c, cellular redox status changes, endothelin-1 production, and conformational changes of α- and β-subunits (e.g., due to cysteine reduction of the channel protein), and phosphorylation of α- and β-subunits (Patel *et al.*, 2004).

According to the redox hypothesis cellular redox status, mitochondria, O_2 sensing and K_V channels are all linked together ultimately resulting in HPV. Archer and colleagues (1993) were the first group to propose a redox based O_2 sensor as a regulatory point in the response of pulmonary vasculature to hypoxia. They suggest that a more reduced cytosolic state due to decrease in ROS is responsible for vasoconstriction via inhibition of K^+ channels, which were demonstrated to be responsive to changes in cell redox state (Weir & Archer, 1995). Since this initial observation this group has continued extensive research in support of this hypothesis. Later they were able to demonstrate opposing effects of oxidants (which increase cellular redox state) and antioxidants (which decrease cellular redox state) on whole cell K^+ channel currents (Reeve *et al.*, 1995). Recent study also indirectly support the redox hypothesis by showing that the thiol oxidant diamide causes PA vasodilation via activation of K^+ channels and inhibition of SOCCs (Schach *et al.*, 2007). Proponents of the redox hypothesis postulate that the high basal levels of H_2O_2 in PA may actually activate K^+ channels and, therefore, in hypoxia a decrease in mitochondrial H_2O_2 production would block them (Michelakis *et al.*, 2004). This concept is supported by the finding that I_{Kv} is inhibited by mETC inhibitors, in particular those acting on complex I and III (the major sites of ROS generation) (Archer *et al.*, 1993). On the contrary, mitochondrial uncouplers, which decrease mitochondrial membrane potential

(ΔΨm) (Yuan *et al.*, 1996), and metabolic inhibitors (e.g. 2-deoxyglucose) (Yuan *et al.*, 1994) also inhibit I_{Kv} in PASMCs, suggesting the presence of multiple, presently undetermined, mitochondria-dependent mechanisms which affect I_{Kv} in PASMCs. Importantly, these studies were only focussed on the inhibition of I_{Kv} amplitude, which does not allow for discrimination between mitochondria-specific and non-specific actions of inhibitors (Searle *et al.*, 2002).

Interestingly, hypoxia also causes an enhancement of I_{Kv} at negative voltages in addition to its inhibition at positive voltages, an observation which is not discussed in studies demonstrating this phenomenon in both canine (Post *et al.*, 1992) and rat (Archer *et al.*, 1993;Turner & Kozlowski, 1997) PASMCs. This phenomenon could however be explained by recent findings where the interaction between mitochondria and K_V channels in PASMCs was studied in details. Thus, Firth *et al.* (2008) described a novel Mg^{2+}- and ATP-mediated mechanism by which mitochondria may directly regulate K_V channel activity, in such a way that inhibition of mETC enhances I_{Kv} at negative potentials but decreases current amplitude at positive potentials, in addition to any effects of intracellular ROS or redox state. This study predicts that inhibition of I_{Kv} by hypoxia may only occur following partial depolarisation. Notably, in the following study Firth *et al.* (2009) show that this mechanism is facilitated by a very close approximation of mitochondria with the PASMC membrane, whilst in systemic artery SMCs this close approximation is absent. This discovery of a difference in the spatial distribution of mitochondria specifically in PASMCs has potentially opened a new avenue for further role of K_V channels in the development of the HPV response.

1.8 Metabolic Regulation of Vascular Tone: mitochondrial oxidative phosphorylation and glycolysis

1.8.1 Role of mitochondria in metabolic regulation of vascular tone

The role of mitochondria as cellular energy provider is well established but its importance in the regulation of vascular contractility and HPV is poorly understood. Cellular energy is derived from metabolic fuels like glucose, fatty acids and amino acids. Initially these molecules are processed by anaerobic glycolysis in the cytosol and β-oxidation (fatty acid metabolism) in mitochondria. Figure 1.4 illustrates the main pathways for metabolism of glucose by glycolysis and oxidative phosphorylation. ATP, the end product of glycolysis and oxidative phosphorylation, is thus utilised to maintain cellular function as well as for the generation and maintenance of vascular tone.

1.8.2 Mitochondrial oxidative phosphorylation

The mitochondria occupy a considerable proportion of the cells cytoplasm and are crucial to cellular energy production enabling it to produce upto 38 ATP by mitochondrial oxidative phosphorylation whereas in glycolysis only 2 ATP is produced from each molecule of glucose (Leach *et al.*, 2002) (Fig. 1.4). By a chemiosmotic process, large amounts of energy are harnessed in the inner mitochondrial membrane, which is used to drive the production of ATP. This chemiosmotic process was first proposed by Mitchell in 1961 (Mitchell, 1961) who further proposed that uncouplers of oxidative phosphorylation acted as proton conductors through the mitochondrial membrane from the matrix (Reid *et al.*, 1966).

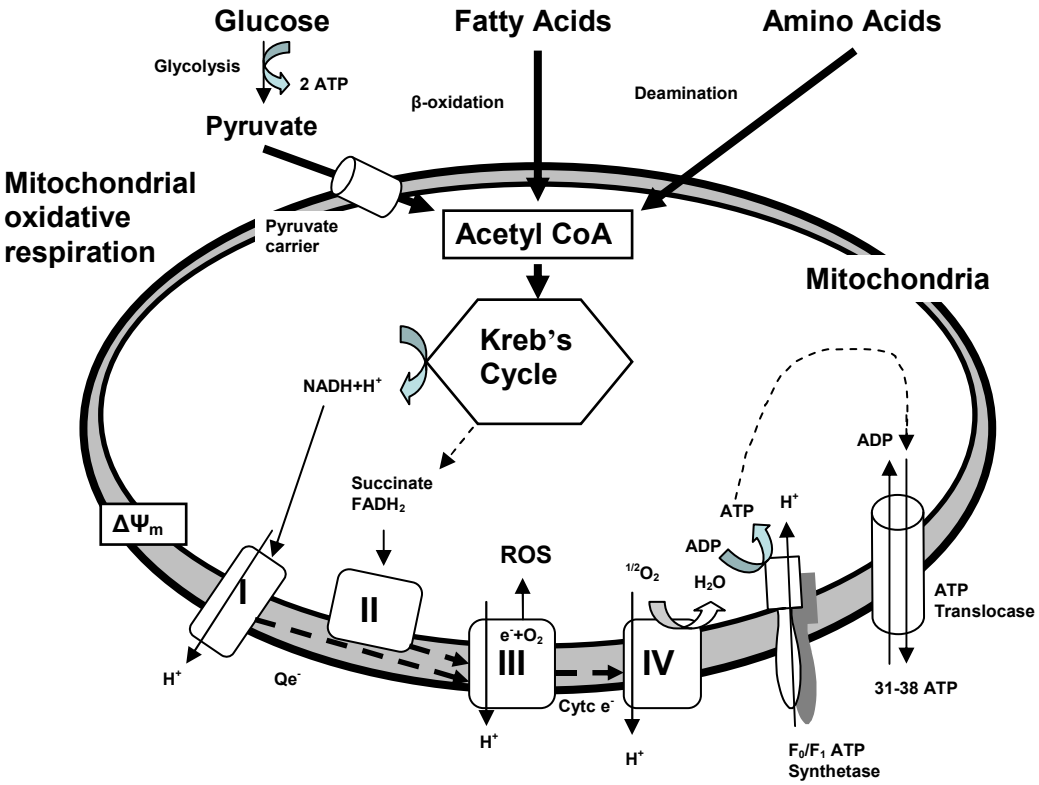

Figure 1.4 Simplified diagrams of smooth muscle metabolic pathways and cellular respiration.

Glucose undergoes glycolysis to produce pyruvate and a net 2 ATP molecules. Pyruvate is transported by a pyruvate carrier into the mitochondrion where it is converted to acetyl CoA. Acetyl CoA is also derived from fatty acids (β-oxidation) and amino acids (de-amination). Acetyl CoA then enters the Krebs cycle where the acetyl group is further oxidised to generate NADH and ubiquinon (enzyme Q). NADH acts as the reducing equivalent driving the mETC and enzyme Q additionally gains two H^+ that are also transferred to complex III, and is reduced to ubiquinol. Electrons are transported from complex I and II to III via coenzyme Q (Qe^-) and from complex III to IV via cytochrome c (cytc e^-). The electrochemical gradient (Δp) created by movement of protons into the inner mitochondrial space drives H^+ back across the membrane via the F_0/F_1 ATP synthetase, producing ATP which itself is transported out of the mitochondrion by the ATP translocase in exchange for ADP.

1.8.3 Mitochondrial electron transport chain (mETC)

The mitochondrial electron transport chain or respiratory chain (complexes I-V) is the major site responsible for ATP production by oxidative phosphorylation. Mitochondrial oxidative phosphorylation is the process by which a series of multi-subunit of enzyme complexes interact in passing electrons down a series of redox reactions and simultaneously storing energy as an electrochemical proton gradient, which will ultimately drive the generation of mitochondrial ATP. During metabolism, substrate molecules are progressively dehydrogenated producing hydrogen ions. The hydrogen ions are transferred to nicotinamide adenine dinucleotide (NAD^+) and flavin adenine dinucleotide (FAD) to form the reduced form of the co-enzymes NADH and $FADH_2$. Reoxidation of these co-enzymes releases electrons (e^-) and protons which then enter the mETC.

Complex I (NADH dehydrogenase)

The reduced co-enzymes NADH and $FADH_2$ are high energy electron carriers generated by the Krebs cycle and transferred to the inner mitochondrial membrane where NADH acts as a reducing equivalent feeding complex I. Complex I is reduced by accepting e^- from NADH which looses a H^+ to form NAD^+. Electrons are passed via flavin to ubiquinone (enzyme Q) which transports the electron to complex III. In this process ubiquinone is reduced to ubiquinol.

Complex II (cytochrome b-c complex or Co-enzyme Q reductase)

In addition to passing e^- to complex III, complex II also functions to add additional e^- to the quinone pool by removing e^- from succinate. Complex II bypasses complex I by transferring the electrons from succinate to co-enzyme Q.

Complex III

In complex III a phenomenon known as the Q cycle occurs. Ubiquinone is regenerated in complex III via ubisemiquinone, the putative site for ROS

generation, and cycles back to complex I and II within the inner mitochondrial membrane (Fig. 1.5). During the Q cycle four protons move across the mitochondrial inner membrane, adding to the proton gradient initiated in complex I (Yu *et al.*, 1998a;Hunte *et al.*, 2003). If the $\Delta\Psi_m$ is altered by metabolic inhibition or by drugs (e.g., antimycin A), the electron transport is disrupted. This might cause an increase in ROS production at this complex (Fig. 1.5).

Complex IV (cytochrome oxidase)

In the complex IV, the final acceptor of electron is the molecular O_2 which accepts four electrons and subsequently is reduced to form a water molecule (Fig. 1.5).

Complex V (F_0/F_1 ATP synthetase)

F_0/F_1 ATP synthetase is present in the mitochondrial inner membrane where the F_0 part resides in the membrane whilst the F_1 part protrudes above the membrane into the matrix. The F_0/F_1 ATP synthetase is driven by the proton gradient (Δp) that is created by complexes I, III and IV of the mETC across the mitochondrial inner membrane. Generated Δp drives the formation of ATP from ADP and inorganic phosphate (Pi) (Stock *et al.*, 2000). It can be summarised as:

$NADH + H^+ + 3ADP + 3Pi + {}^1/_2O_2 \rightarrow NAD + 3ATP + H_2O.$

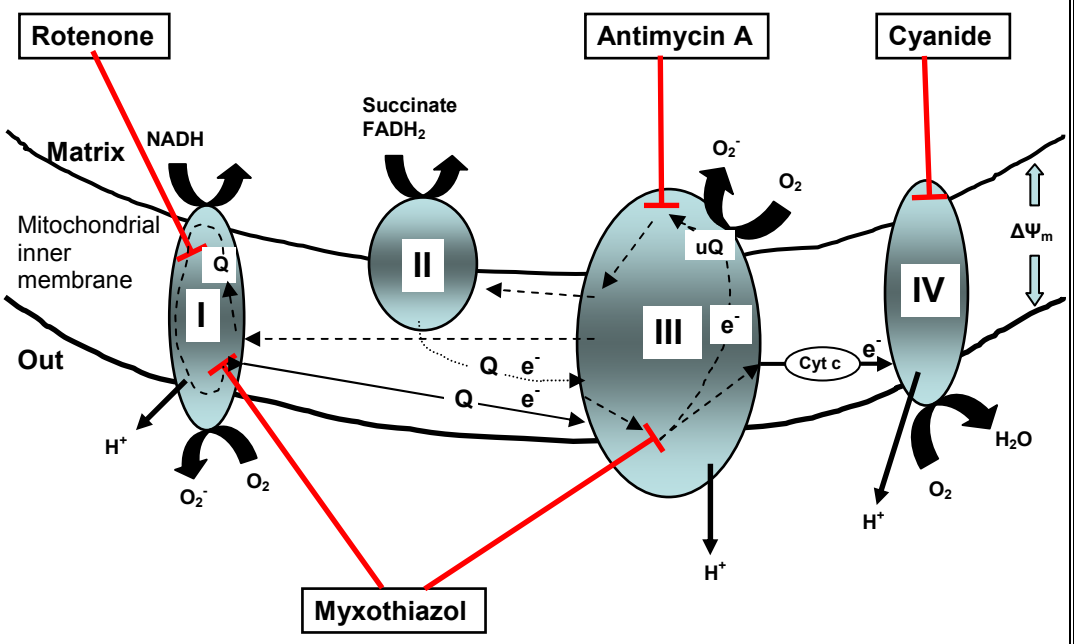

Figure 1.5 Simplified diagram of the mETC and its complexes, showing point of action of key inhibitors.

Oxidation of NADH at complex I and $FADH_2$ at complex II results in transfer of electrons by ubiquinone (enzyme Q) to complex III and then to complex IV by cytochrome c. The final electron acceptor in complex IV is molecular O_2 generating water. Superoxide radicals (O_2^-) are produced at both complexes I and III by a single electron transfer to molecular O_2. The correct functioning of the mETC complexes maintains mitochondrial membrane potential ($\Delta\Psi m$). mETC inhibitors and their site of action are rotenone (inhibiting complex I), myxothiazol (inhibiting complexes I and proximally in III), antimycin (inhibiting distally complex III) and cyanide (inhibiting complex IV). Inhibition at any point in the chain will cause proximal reduction and distal oxidation. Q, ubiquinone; e^-, electron; uQ, ubisemiquinone; Cyt c, Cytochrome c.

1.8.4 Anaerobic respiration

Adenosine triphosphate (ATP) is a molecule capable of storing and transferring large amount of energy. Energy derived from the hydrolysis of ATP is essential for muscle contraction, protein synthesis and ion transport across cell membrane. In addition to mETC, ATP is also produced from anaerobic sources by glycolysis and creatine kinase. ATP and ADP are relatively large, immobile molecules reside within the mitochondria, or close to the site of energy utilisation. On the other hand phosphocreatine (PCr) is a small, freely diffusible molecule which can carry high energy bond from the mitochondria to the sites of utilisation. In the mitochondrial outer membrane ATP phosphorylates creatine (Cr) to form phosphocreatine; the process is catalysed by creatine kinase (Clark, 1994). The PCr carries high energy bond to the sites of utilisation where the creatine kinase reaction is reversed resulting in transport of phosphate from PCr to ADP, thus forming ATP:

$$[ATP] + [Cr] \leftrightarrow [PCr] + [ADP] + [H^{+}].$$

Another anaerobic mechanism which maximises energy production by generating ATP from ADP by transforming a high energy phosphate:

$$[ADP] + [ADP] \rightarrow [ATP] + [AMP].$$

Generally mitochondria provide the majority of ATP for cell function, however, vascular smooth muscles are unusual in that they exhibit high levels of glycolysis enabling them to generate ~30% of total ATP production even during normoxia, and accounts for ~90% of the glucose utilised by the cell (Paul, 1989).

1.8.5 Pharmacological tools to intervene mitochondrial oxidative phosphorylation and glycolysis

Pharmacological tools utilised to intervene with oxidative phosphorylation, mainly target complexes I, III and IV of the mETC. The commonly used inhibitors of these complexes are shown in Fig. 1.5.

An inhibitor of complex I, rotenone, blocks electron transfer in close proximity to the ubiquinone binding site (Andreyev *et al.*, 2005). Inhibition of complex I by rotenone has already become a well established experimental model enabling mitochondria to become a pharmacological target (Szewczyk & Wojtczak, 2002). Antimycin A prevents transfer of electron by inhibiting the Q cycle distal to ubisemiquinone in (Fig. 1.5) causing accumulation of unstable semiquinone, thus stimulating superoxide production (Turrens, 2003). Myxothiazol, on the other hand, by inhibiting proximal to ubisemiquinone in the Q cycle (Fig. 1.5), prevents and/or inhibits the effect of antimycin A, leading to inhibition of superoxide production in mammalian mitochondria (Zoccarato *et al.*, 1988;Korshunov *et al.*, 1997). Mitochondrial inhibitors rotenone and myxothiazol dose-dependently inhibit HPV without mimicking the effect of HPV in normoxic conditions (Weissmann *et al.*, 2003). However, another report suggests that rotenone, cyanide, myxothiazol and oligomycin mimic the effects of hypoxia via inhibition of a background K^+ current leading to membrane depolarisation and voltage-gated Ca^{2+} entry (Wyatt & Buckler, 2004). Cyanide inhibits cytochrome c at complex IV, thus causing disruption of the mETC at the final step. Thus cyanide could be a helpful pharmacological tool to investigate the dependence of contraction on the oxidative metabolism mediated by mitochondria in intact arteries (Otter & Austin, 2000;Leach *et al.*, 2001;Swärd *et al.*, 2002). Two commonly used inhibitors of the ATP synthetase are oligomycin, which binds between the F_0 and F_1 subunits, and dicyclohexylcarbodiimide (DCCD) which binds in the F_0 subunit of the F_0/F_1 ATP synthetase. These inhibitors selectively inhibit mitochondrial oxidative phosphorylation thereby preventing oxidative ATP production (Matsuno-Yagi & Hatefi, 1993).

When the mETC is impaired, e.g. in the presence of inhibitors or uncouplers, the proton gradient will be reduced, but respiration will proceed. However, the ATP synthesis will be activated in the reverse mode resulting in ATP hydrolysis instead of synthesis, in order to maintain mitochondrial membrane potential.

Both iodoacetate and 2-deoxyglucose (2-DOG) inhibit anaerobic production of ATP by blocking glycolysis (Stanbrook & McMurtry, 1983), and therefore were used to assess the role of glycolysis in intact preparations (Gasser *et al.*, 1993;Conway *et al.*, 1994;Leach *et al.*, 2001;Fukumoto *et al.*, 2005). The combination of cyanide with 2-DOG is also useful to obtain a complete inhibition of both glycolysis and oxidative phosphorylation, thus preventing the majority of ATP production (Lancaster & Harrison, 1998).

1.9 Aims and objectives of the thesis

Studies carried out in isolated cells undoubtedly support the proposal for the leading role of K_V channels in the regulation of resting membrane potential in the pulmonary circulation. The close link between the K_V channels and mitochondria, specifically in the pulmonary artery, has also been proposed. This hypothesis is based on electrophysiological studies performed in single myocytes, but whether such a relationship exists in intact arteries is not known. The KCNQ channels have also recently been considered as the regulator of the pulmonary vascular tone. However, the relative contribution of K_V and KCNQ channels to the regulation of the cell membrane potential in intact pulmonary artery has not been addressed.

The main aims of this thesis therefore were: to investigate the relative contribution of the K_V and KCNQ channels in the regulation of pulmonary artery excitability and contractility under normal and hypoxic conditions and to establish a potential interaction between the K_V channels and mitochondria in intact pulmonary arteries. To determine the specificity of the observed effects to the pulmonary circulation, the rat mesenteric artery was used as a representative of the systemic circulation.

Thus, the initial objectives of this thesis were:

1. To identify the relative role of K_V and KCNQ channels in vascular contractility using selective pharmacological inhibitors, small vessel myography, microelectrode technique and confocal imaging.

2. To investigate the involvement of K_V and KCNQ channels in acute hypoxia-induced pulmonary vasoconstriction.

3. To assess the relative contribution of the voltage-dependent and voltage-independent (Ca^{2+} sensitisation) pathways in contractions induced by the

inhibition of K^+ channels using specific inhibitors, western blot analysis and tissue permeabilisation technique.

4. To determine the relative role of mitochondria and cellular metabolism in contractions induced by the inhibition of K_V channels using selective inhibitors.

5. To identify species differences by comparing contractile responses to K^+ channel inhibitors of the arteries in the rat and mouse.

Chapter 2

MATERIALS AND METHODS

2.1 Isolation of blood vessels

Male Wistar rats (weighing 250-300 g) and male CD mice (weighing 35-40 g), were killed by cervical dislocation in accordance with UK Home Office guidelines. The heart and lungs were removed *en bloc* after opening of the chest cavity from the diaphragm and cutting the rib cage. Subsequently the abdominal area was opened midline and the whole mesenteric bed was removed. All tissues were placed in 100 ml of Krebs solution and kept on ice for micro dissection. Rat intrapulmonary arteries (internal diameter 300-500 μm) and 3rd order mesenteric arteries (internal diameter 250-400 μm) were micro dissected, cleaned of connective tissues whilst remaining intact in the organ. Mouse arteries were collected in the similar way except that the main intrapulmonary arteries (diameter 250-350 μm) and 1st order mesenteric arteries (internal diameter 150-250 μm) were collected. Arteries were cut into sections of ~2 mm length while maintaining in the ice cold Krebs solution in the dissection Petri dish. A piece of 40 μm diameter stainless steel wire (DMT/AS) was carefully inserted through the lumen of the piece of the artery which was subsequently mounted into the jaws of wire myograph following the procedure as described in details bellow. All of the above procedures were carried out using a microscope (Leica, Zoom 2000 or Meiji, Optech Scientific Instruments, Japan) and KL 1500 LCD light source (Olympus, UK).

A. Rat intra pulmonary arteries **B. Mouse intrapulmonary arteries**

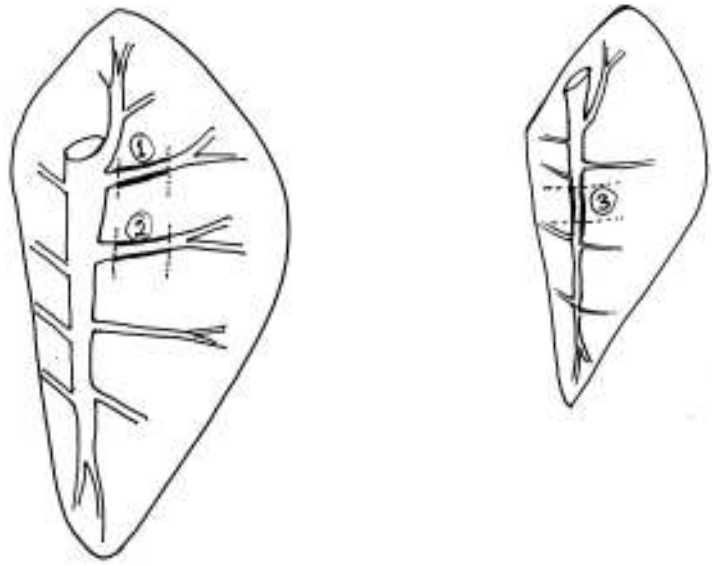

Figure 2. 1 Micro-dissection of rat and mouse intra pulmonary arteries.

A piece of ~ 2 mm long intra pulmonary artery was collected from the indicated area (1) and (2) from rat lung and area (3) from mouse lung. From the mouse lung the main intra pulmonary artery was taken instead of taking side branch because the diameter of the later was very small which made small vessel mounting more difficult with less reliable level of success.

2.2 Myography

The contraction was measured using small vessel wire myograph (Mulvany *et al.*, 1982;Mulvany, 1988;Mulvany & Aalkjaer, 1990;Buus *et al.*, 1994;Mulvany, 1999). The myograph is a form of organ bath which is composed of a horizontal stainless steel chamber containing two opposing stainless steel 'jaws'. Each jaw has a pair of 'teeth' between which the arterial ring will be positioned with the help of two pieces of stainless steel wire. The jaw on the right is attached to a micrometer for adjusting the distance between the two jaws (Fig. 2.2).

Figure 2. 2 Jaws of myograph.

Original photograph shows the arrangements of one pair of jaws of a wire myograph. One of the jaws is attached to the force transducer (left), and the other jaw (right) is attached to the micrometer which is manually adjusted to apply tension on the mounted vascular ring.

These micrometers are manually operated for the normalisation procedure. The jaw on the left is attached to a force transducer via a steel rod that passes through a hole in the side of the chamber. The hole through which the rod passes is sealed with vacuum grease provided by Danish Myotechnology (Aarhus, Denmark). The ring of artery was mounted on two pieces of 40 μm stainless steel wire, attached to each of the two jaws. The detailed procedure of mounting the tissue is described below (section 2.2.2). The two vessel Mulvany-Halpern myograph (also called dual myograph) is equipped with two pairs of jaws enabling mounting of two pieces of arterial ring in the same bath solution at the same time. In my study I used one pulmonary and one mesenteric artery ring in parallel to investigate the differences in tissue responses being simultaneously challenged with the same substance under the same experimental conditions. In some experiments I also used multi myograph system (four channel myograph, Model 610M, Danish Myotechnology, Denmark). In that system two pulmonary and two mesenteric artery rings were mounted in four chambers and the rest of experimental conditions was identical. The responses were repeated in a dual chamber myograph and no significant difference in tissue responses was observed. I also used multi myograph system for the membrane permeabilisation experiments that I carried out at King's College London, because this procedure required different approach (as described in Section 2.3 below).

2.2.1 Solutions used in myography

Table 2.1 Composition of solutions used in wire myography (in mM)

Composition	Standard Krebs (PSS)	20 mM KCl	30 mM KCl	40 mM KCl	80 mM KCl
NaCl	118	102	92	82	42
NaHCO3	24	24	24	24	24
$MgSO_4$	1	1	1	1	1
NaH_2PO_4	0.5	0.5	0.5	0.5	0.5
KCl	4	20	30	40	80
Glucose	11	11	11	11	11
$CaCl_2$	1.8	1.8	1.8	1.8	1.8

pH = 7.35

2.2.2 Vessel mounting procedure

Before starting the mounting procedure myograph chamber(s) was filled with 10 ml (dual myograph) or 5 ml (four-channel myograph) PSS at room temperature; chamber and solutions were continuously gassed with 95% O_2/5% CO_2 mixture. Pieces of stainless steel wire were freshly cut ready to be used for mounting the vessel. In the dissection Petri dish under low magnification the first wire was inserted through the lumen of the arterial ring with great care to avoid any damage to the lumen wall. Once the first wire was inserted the arterial ring was then transferred from Petri dish to the myograph chamber holding the two edges of the wire with blunt forceps. The first wire along with the arterial ring was attached to one of the two jaws. The wire was first hold tightly between the jaws and then one end was secured under one of two screws. The wire was placed under the screw such that when the screw is tightened, always in a clockwise direction, the wire

will be tighten up further by the movement of the screw (Fig 2.3 i). In the same way the other end of the wire was also secured under the other screw of the same jaw (Fig 2.3 ii). Care was taken so that both ends of the wire were secured tightly and that there was no slack in the wire. This was achieved by holding the free end of the wire tightly with blunt forceps and pulling it taut while manoeuvring it under the screw, and continuing to hold it taut while tightening the screw with the other hand. The wire was passed under the side of the screw that will result in the wire being pulled tighter when the screw is tightened clockwise (Fig 2.3 i and ii).

Once the first wire was secured the jaws were opened and the second wire was then passed through the lumen of the artery already secured by the first wire (Fig 2.3 iii). The wire was held in the middle with blunt forceps and held in such a way that it lied parallel to the bottom of the chamber and in parallel with the artery ring. By placing the tip of the second wire at the opening at either end of the mounted artery a simple wrist action was all that was required for this wire to pass through the lumen of the artery. Care was taken to keep the tip of the second wire straight and to keep it parallel with the first wire (Fig 2.3 iii).

Once the second wire had been passed through the artery ring such that the artery sits roughly in the middle of it, the jaws were re-closed in order to clamp onto the second wire and render it immobile (Fig 2.3 iv). Then the two ends of the second wire were secured under the two screws of the second jaw. The first end was secured with the jaw closed; tightening the screw over the wire such that the wire was pulled tight as the screw was tightened (fig 2.3 vi-x). The jaws were then re-opened just enough to loosen the hold over the second wire (Fig 2.3 vii), and as with the first wire, the free end was held tightly with forceps and pulled taut to take up all slack as it was passed under the remaining screw and as the screw is tightened (Fig 2.3 viii-x). If the two wires were not perfectly parallel, the elevation of one or the other at one end or the other was carefully adjusted with blunt forceps in order to properly align it with the other. While warming up the myograph before normalisation, the jaws were set slightly apart to prevent the two wires from touching, but not enough to begin stretching the arterial ring.

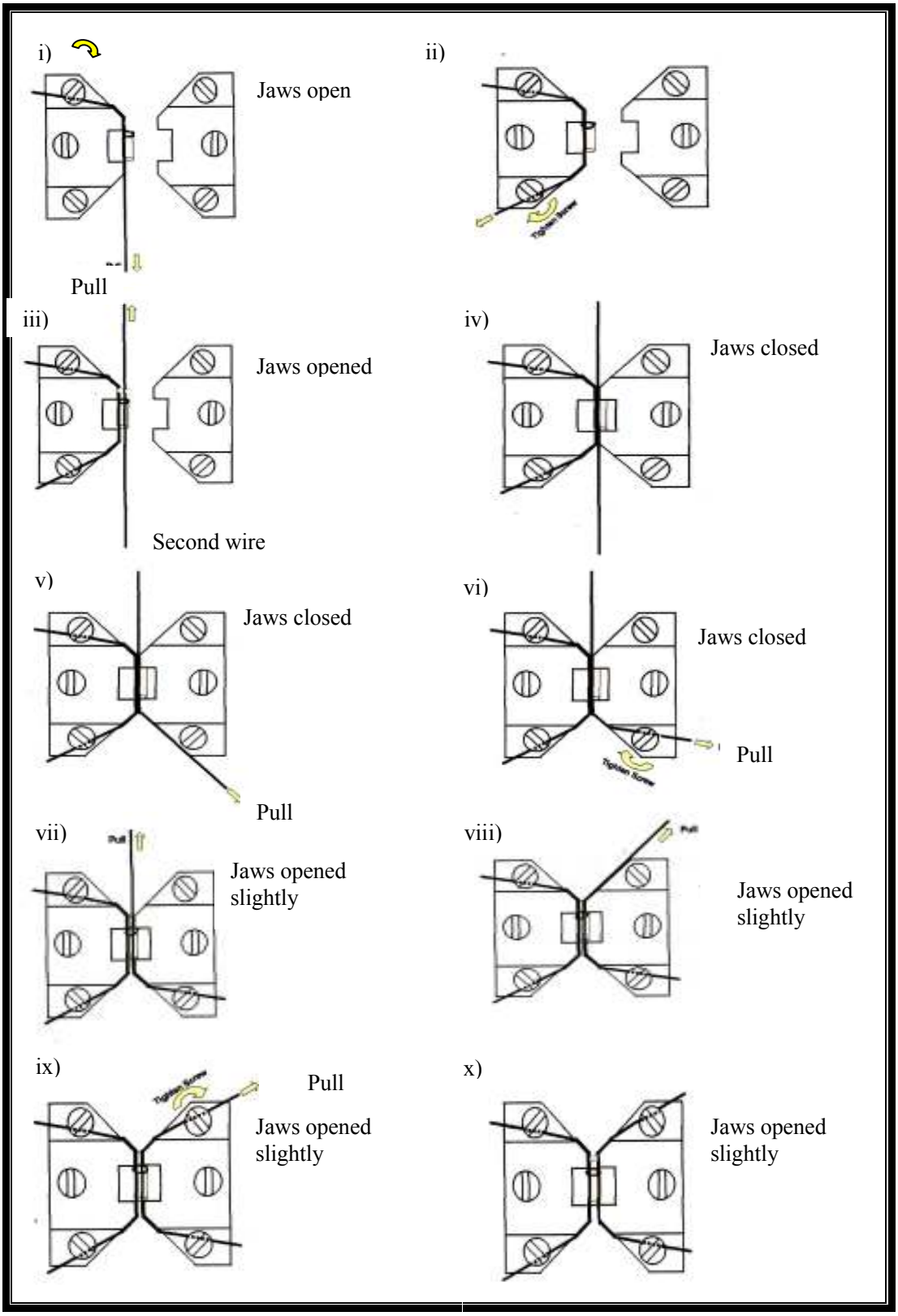

Figure 2. 3 Step-by-step diagrams demonstrating vessel mounting procedure on a wire myograph.

2.2.3 Normalisation of the tension

Tension was normalised using a normalisation protocol which also enables to obtain circumference, diameter of the vessel ring, and tension (mN/mm) under a specified transmural pressure. After mounting, the vessel rings were stabilised in Krebs with continuous bubbling with a gas mixture of 95% O_2 and 5% CO_2 at 37^{o}C for 1h. The temperature was controlled and maintained by the built-in heater. Following stabilisation vessel rings were set to an internal circumference at which they were just held under tension. The micrometer was adjusted manually and the resting tension-internal circumference relation was determined using the custom written program called NORMALIZE (McPherson, 1985). The vessel rings set to a normalised tension by re-adjusting the micrometer in a position determined by the software. This software allows the calculation of transmural pressure for a vessel. By re-adjusting the level of stretch on a vessel by small increments, pressure was increased or decreased until the optimum physiological pressure was achieved which in rodent intra pulmonary artery is ~15 mmHg (Herget *et al.*, 1978;MacLean & McCulloch, 1998;Boer *et al.*, 2004;Baliga *et al.*, 2008;Kelland *et al.*, 2010) and small mesenteric artery is ~100 mmHg (Mulvany & Halpern, 1977;Madhani *et al.*, 2003;Baliga *et al.*, 2008).

2.2.4 General experimental procedure in myography

Following a one hour stabilisation period the vessels were checked for viability using 80 mM KCl for 3 min each. At least three to four consecutive high K^+ (80 mM KCl) applications were carried out to establish a contraction of reproducible maximal amplitude. Only vessels developing a tension of >3 mN for rPA and >6 mN for rMA were deemed suitable for tension recording. For mouse tissue a slightly less tension with high K^+ (>2 mN for mPA and >4 mN for mMA) was deemed acceptable because of comparatively smaller diameter of mouse vessels. Because the main focus of this work was the role of ion channels in smooth

muscle cells, the endothelial function was suppressed by using 100 μM L-NAME (N^{ω}-nitro-L-arginine methylester) to block nitric oxide synthase and 10 μM indomethacin to inhibit cycloxigenase. To verify that endothelium is not interfering with the observed responses to 4-AP, these were compared with the responses obtained following the mechanical removal of the endothelium by a gentle rubbing of the endothelial lumen with a human hair. A single dose of 10 μM acetylcholine was used to verify the lack of endothelium-dependent relaxation. As no difference was observed, all experiments were performed in the presence of L-NAME and indomethacin.

In majority of experiments, the procedure composed of 3 steps: control, pretreatment with agonist and recovery; each are described in the relative chapters. In between different steps, tissue contractility and viability was re-established by regular wash-out with Krebs and 80 mM KCl (approximately every 10 to 15 min). Each subsequent experimental step was applied only when the amplitude of contraction to 80 mM KCl was established. The maximal contraction to 80 mM KCl response (measured at the end of 3 min for PA or as the peak contraction in MA) immediately prior to an experimental procedure was considered as 100%. Tension developed in the response to a vasoactive substance or an inhibitor was expresses as percentage of 80 mM KCl contraction (unless otherwise stated).

Table 2.2 Vasoactive mediators used in tension study

Compound	Function(s)	Stock and solvent	Final concentration
KCl	Depolarising agent, receptor-independent vasoconstrictor	4X (H_2O)	20 - 80 mM
4-AP	K_V channel blocker	0.5 M (H_2O)	0.5-10 mM
Linopirdine	KCNQ channel blocker	10mM (Ethanol)	10 μM
Y-27632	Rho-kinase inhibitor	10mM (H_2O)	10 μM
U-46619	TxA_2 mimetic, vasoconstrictor	1mM (DMSO)	10 nM -1 μM
L-NAME	e-NOS blocker	100mM (H_2O)	100 μM
Indomethacin	COX inhibitor	10mM (DMSO)	10 μM
Diltiazem	L-type Ca^{2+} channel blocker	10mM (H_2O)	10 μM
Nifedipine	L-type Ca^{2+} channel blocker	1mM (DMSO)	1 μM
ACh	e-NOS stimulant, vasodilator	10mM (H_2O)	10 μM
TEA	K_V channel blocker, vasoconstrictor	2M (H_2O)	1-20 mM

2.3 Membrane permeabilisation

Vascular smooth muscle cell membrane permeabilisation is a valuable technique for the direct control of cytoplasmic solute composition and for understanding of contractile mechanism (Kitazawa *et al.*, 1989;Kobayashi *et al.*, 1989). In this study, two different methods of membrane permeabilisation, that produces different levels of membrane skinning, were carried out: α-toxin permeabilisation and β-escin permeabilisation. α-toxin permeabilisation was carried out with a commercially available α-toxin (Sigma-Aldrich Co. Ltd, Poole, UK). It is a widely used technique to study effects of drugs and action of transmitters in smooth muscle for exploring in a near-physiological condition as α-toxin makes cells permeable to low molecular weight solutes of upto 1000 Da (Ahnert-Hilger & Gratzl, 1988). β-escin permeabilisation was carried out with a commercially available agent called β-escin which is one of the saponin esters. β-escin permeabilisation yields smooth muscle preparations with an apparently intact, coupled receptor-effector cascade and a cell membrane that is permeable to higher molecular weight (at least 17,000 Da) compounds than does α-toxin (Kobayashi *et al.*, 1989).

2.3.1 Procedure of tissue permeabilisation

Due to different experimental approach used, most notable differences in myography technique for permeabilised arteries compared to non-permeabilised vessels were: 1) experiments were conducted at 26ºC rather than 37ºC; 2) because external solutions were buffered with PIPES instead of bicarbonate, organ bath was gassed with compressed air and not with 5% CO_2 and 95% O_2. Arteries were mounted on a myograph as described in section 2.2.2. After obtaining three consecutive contractile responses to 80 mM KCl the arteries were equilibrated in normal relaxing solution (G10) containing 10 mM EGTA. Details of the solutions used are described below in the section 2.3.2. Free Ca^{2+} concentration in bath

solutions (expressed as pCa=-log[Ca^{2+}] in M) was achieved by mixing K_2EGTA and CaEGTA in appropriate proportions. Due to high cost of α-toxin, a special technique was adopted for α-toxin permeabilisation in Jeremy Ward's Lab. The solution in the myograph chamber was completely removed using a pressure suction tube (great care was taken not to touch the arteries during this procedure). Approximately 150 µl of pCa 6.5 solution containing 60 µg ml^{-1} α-toxin was applied directly on the mounted artery; this volume was sufficient to form a large drop of solution around the artery with a stable surface tension. During the following 30 min, ~25 µl of the same permeabilisation solution was added to the drop every 10 min to prevent drying of arteries. The degree of permeabilisation was monitored by a slow development of tension. Permeabilisation process considered to be completed when tension reached a plateau level. The artery was then relaxed with two consecutive washes with the relaxing G10 solution (termed as it has very low pCa <10). When tension returned to the baseline level, submaximal contraction was brought about by application of a test solution with pCa 7.2 (in rPA) or with pCa 6.4 (in rMA). Vasoactive agents were added to the bathing solution once contraction in the test solution reached steady state level. Since β-escin is not an expensive chemical, it was added directly in the bath solution (50 µM) and left for 30 min to permeabilise the tissue. Both α-toxin and β-escin are washed off in G10.

2.3.2 Solutions and chemicals used for membrane permeabilisation

In membrane permeabilisation experiments three main solutions were used, the tissue relaxing solution G10 and pCa 4.5 (CaG), and other pCa solutions of different concentration. The stock solutions and recipe for G10 and pCa 4.5 are described in this section. Different concentration of pCa solutions were prepared by mixing CaG (pCa 4.5) and G10 solutions in the corresponding ratios shown in the table 2.5 at the end of this section.

Table 2.3 Stock solutions used for permeabilisation study

100 mM CaEGTA (500 ml)

100 mM $CaCO_3$	5.0 g
100 mM EGTA	19.02 g
195 mM KOH	5.47 g

Ionic strength = 495 mM

$CaCO_3$ and EGTA were dissolved in ~450 ml doubled distilled water (ddH_2O), stirred for 30 min. Then KOH was added and stirred slowly until solution turned into a clear one (1-2 hours). The solution left stand for CO_2 to leave the solution. Finally the volume was made up to 500 ml with ddH_2O and the pH was left as it was. Stored in the fridge.

100 mM K_2EGTA (500 ml)

100 mM EGTA	19.02 g

Ionic strength = 300 mM

EGTA was dissolved in ddH_2O and pH was adjusted to 7.1 by carefully adding KOH pellets. Stored at room temperature.

200 mM PIPES, KOH (500 ml)

200 mM PIPES	30.24 g

Ionic strength = 400 mM

PIPES was dissolved in ddH_2O and pH was adjusted to 7.1 by carefully adding KOH pellets. Stored at room temperature.

Table 2.3 continued.

100 mM $Mg(Ms)_2$ (500 ml)

100 mM MgO	2.015 g
200 mM methanosulfonic acid	9.61 g

Ionic strength = 300 mM

MgO was dissolved in ~400 ml ddH_2O and then methanosulfonic acid was added and waited for MgO to dissolve slowly. Volume was made up to 500 ml with ddH_2O but pH was left as it was. Stored at room temperature.

1 M KMs (500 ml)

1 M methanosulfonic acid	48.05 g
1 M KOH	32.6 g

Ionic strength = 2000 mM

Methanosulfonic acid was dissolved in ~400 ml ddH_2O and then a KOH was added and stirred slowly. Volume was made up to 500 ml with ddH_2O but pH was left as it was. Stored at room temperature.

Table 2.4 Recipe for G10 and pCa 4.5

	G10 (1L)	pCa 4.5 (500 ml)
PIPES (200 mM)	150 ml	75 ml
$Mg(Ms)_2$ (100 mM)	53 ml	26.5 ml
KMs (1 M)	46.6 ml	23.3 ml
K_2EGTA (100 mM)	100 ml	---------
CaEGTA (100 mM)	--------	50 ml
Na_2ATP	2.806 g	1.404 g
Na_2creatinine phosphate	2.55 g	1.276 g
pH adjusted with KOH	pH 7.1	pH 7.1
Storage	2-8 ºC (fridge)	-20 ºC (freezer)

To give total $[Mg^{2+}]$ = 5.3 mM
To give total $[Ca^{2+}]$ = 10 mM (pCa 4.5 only)
To give total [EGTA] = 10 mM
To give total [ATP] = 5 mM

Table 2.5 Ionic strengths of G10 and pCa 4.5

G10

400 (PIPES)*150/1000	=	60 +
300 ($Mg(Ms)_2$)*53/1000	=	15.9 +
2000 (KMs)*46.6/1000	=	93.2 +
300 (K_2EGTA)*100/1000	=	30 +
15 (Na_2ATP)	=	15 +
30 (NaP-Cr)	=	30 +
Total ionic strength	**=**	**244.1 mM**

pCa 4.5

400 (PIPES)*150/1000	=	60 +
300 ($Mg(Ms)_2$)*53/1000	=	15.9 +
2000 (KMs)*46.6/1000	=	93.2 +
495 (CaEGTA)*100/1000	=	19.5 +
15 (Na_2ATP)	=	15 +
30 (NaP-Cr)	=	30 +
Total ionic strength	**=**	**263.6 mM**

Table 2.6 Ratios to obtain corresponding pCa solutions

pCa	[CaG]	[G10]
20.0	0.00000	10.00000
8.0	0.34935	9.65065
7.5	1.02715	8.97285
7.4	1.25961	8.74039
7.3	1.53568	8.46432
7.2	**1.85938**	**8.14062**
7.1	2.23332	7.76668
7.0	2.65792	7.34208
6.9	3.13071	6.86930
6.8	3.64585	6.35415
6.7	4.19402	5.80598
6.6	4.76288	5.23712
6.5	5.33800	4.66201
6.4	**5.90434**	**4.09566**
6.3	6.44776	3.55224
6.2	6.95638	3.03362
6.1	7.42149	2.57851
6.0	7.83787	2.16231
5.9	8.20362	1.79638
5.8	8.51963	1.48037
5.7	8.78884	1.21116
5.6	9.01551	0.98449
5.5	9.20458	0.79542
5.4	9.36119	0.63881
5.3	9.49030	0.50970
5.2	9.59655	0.40345
5.1	9.68408	0.31592
5.0	9.75658	0.24342
4.9	9.81726	0.18273
4.8	9.86896	0.13104
4.7	9.91415	0.08585
4.6	9.95506	0.04493
4.5	9.99378	0.00622

2.4 Measurement of membrane potential (E_m)

A segment (~2 mm) of intrapulmonary or small (3rd order) mesenteric artery was mounted in a two vessel Mulvany-Halpern myograph (Model 400A; Danish Myotechnology, Aarhus, Denmark) in Krebs solution containing (mM/L): NaCl, 118.0; $NaCO_3$, 25; KCl, 3.6; $MgSO_4 \cdot 7H_2O$, 1.2; KH_2PO_4, 1.2; glucose, 11.0; CaCl, 2.5; and gassed with 95% O_2 and 5% CO_2 at 37ºC. The vessel was allowed to equilibrate for 1 hour and was then stretched to a tension equivalent to 15 mmHg (pulmonary artery) or 70 mmHg (mesenteric artery) wall tension using a normalisation protocol as described above (in section 2.2.3). Smooth muscle tension and membrane potential (E_m) were measured simultaneously as previously described (Garland & McPherson, 1992). The experiment was performed in a Faraday cage and on an anti-vibration table. A conventional glass microelectrode (borosilicate with filament, inside diameter 0.69 mm and outside diameter 1.2 mm, tip resistance 80-120 MΩ) filled with 2 mol/L KCl was used to impale individual smooth muscle cells in rat pulmonary and mesenteric arteries. The microelectrode was positioned by an EXFO 1W-812 Stepmotor driven by an 82000-1-0 series EXFO controller (Burleigh, USA). Once in position the electrode was impaled by gentle tapping on the anti-vibration table or by a pulse of negative capacitance that vibrates tip of electrode. Successful impalement was deemed as a sharp downward deflection on the recording followed by maintenance of a steady negative membrane potential and returned to near baseline upon removal of electrode. The measurement of resting membrane potential (RMP) was taken immediately before application of K^+ channel blockers and in some experiments also after wash out and recovery. Tension and membrane potential data were captured by using a commercially available software package (Powerlab/Chart5, ADInstruments Ltd, Oxphordshire, UK).

2.5 Western blot analysis

Western blot or Immunoblot is a method to detect a specific protein in a given sample of tissue homogenate or extract. This method depends on the use of a high quality antibody directed against a desired protein(s) that have been separated by gel electrophoresis according to their size. Tissues containing target protein are first broken mechanically using a homogeniser and then lysed using different buffers containing detergents, solubilising agents and different protease and phosphatase inhibitors. Detergents, salts and buffers are employed to enhance lysis of the cells and to solubilise proteins. Protease and phosphatase inhibitors are added to prevent the digestion of the sample by its own enzymes. To fully dissociate proteins of the sample into their polypeptide subunits, samples are heated with sodium dodecyl sulphate (SDS) and thiol reagent. SDS-PAGE (SDS polyacrylamide gel electrophoresis) maintains polypeptides in a denatured state once they have been treated with strong reducing agents to remove secondary and tertiary structure of protein and thus allows separation of proteins by their molecular weight. Sampled proteins become covered in the negatively charged SDS and move to the positively charged electrode through the acrylamide mesh of the gel. Smaller proteins migrate faster through this mesh and the proteins are thus separated according to their size. Following electrophoresis, separated proteins are transferred into a nitrocellulose membrane. The gel is placed next to the membrane and application of an electrical current induces the proteins in the gel to move to the membrane where they adhere. The membrane is thus turned into a replica of the gel's protein pattern, and is subsequently probed with primary antibodies raised against specific proteins. Secondary antibodies, tagged with an enzyme called horseradish peroxide (HRP), are then added to bind specifically to the already bound primary antibodies. HRP-linked secondary antibody is used with a chemiluminescent agent (known as enhanced chemiluminescence or ECL) that produces luminescence in proportion to the amount of target protein. A photosensitive film, placed against the membrane, captures the exposure of light from the reaction and thus creates an image of the antibodies bound to the blot.

2.5.1 Treatment protocol and tissue preparation for Western blot

Rat intrapulmonary and small mesenteric arteries were dissected and combined from a few animals to minimise individual variation and to maximise the amount of protein. Tissues were placed in 1.5 ml eppendorph tubes containing Krebs solution and subjected to the following treatment protocol (Table 2.7). The protocol was designed to mimic the experimental procedure used in myography experiments. To test the effect of tissue stretching main extra-pulmonary artery rings were mounted in the myograph and were treated with the same drugs as mentioned in the following protocol (Table 2.7).

Table 2.7 Tissue treatment protocol for Western blot analysis

Treatment group	Treatment protocol
Control	Bubbling with carbogen (95% O_2+5% CO_2) in Krebs solution for 50 min.
4-AP	Bubbling with carbogen in Krebs solution for 10 minutes. In continued bubbling 10 μM linopirdine for 20 min followed by 10 mM 4-AP for 20 min.
Y+4-AP	In continued bubbling 10 μM Y-27632 for 10 min followed by 10 μM linopirdine for 20 min followed by 10 mM 4-AP for 20 min.

After treatment, either non-stretched or stretched, the tissues were collected, snap frozen in liquid nitrogen, and stored at -80ºC until used. To prepare protein samples for Western blotting vascular tissue samples were mechanically homogenised using PowerGen 125 homogeniser (Fisher Scientific, UK) in 10 volumes per weight (between 200-400 μl) of an ice-cold lysis buffer (Table 2.8). Homogenates were centrifuged at 14000 rpm at 4ºC for 15 minutes and supernatant was collected.

Table 2.8 Buffers used in Western blot analysis and their composition

Buffer	Composition
Lysis buffer	150 mM NaCl, 1 mM EDTA, 50 mM Tris HCl pH 7.5, 1% Nonidet-P40, 10% glycerol, 1 mM sodium orthovenadate, 10 mM sodium fluoride, 1 mM PMSF and 1% protease inhibitor cocktail
SDS sample buffer	10% SDS, 200 mM Tris HCl pH 6.8, 50% glycerol, 0.01% bromophenol blue and 5% 2-mercaptoethanol (freshly added)
SDS-PAGE running buffer	192 mM glycine, 25 mM Trizma base, 0.1% (w/v) SDS, ultrapure water
Semi-dry transfer buffer	39 mM glycine, 48 mM Trizma base, 0.0375% SDS, 20% (v/v) methanol, ultrapure water
Tris-buffered saline (TBS)	20 mM Tris-HCl pH 7.5 and 150 mM NaCl
TBS-N	TBS+0.05% Nonedate-P40

2.5.2 Determination of protein concentrations in lysate samples

To minimise the variation in loading of lysate samples on the electrophoresis gel the protein concentration in the samples must be identical. To achieve equal loading protein concentration was determined with the BioRad protein assay (BioRad, Hercules, USA); this is a modified form of Bradford protein quantification assay (Bradford, 1976;Zor & Selinger, 1996). Standard curve was constructed with a 1 μg μl^{-1} solution of bovine serum albumin (BSA) at the concentrations ranging from 0 to 64 μg μl^{-1} in a 96-well microtitre plate. 250 μl of 1x Quickstart Bradford dye reagent (BioRad) was added in each well to be used. Then, standard BSA solutions (0-64 μl) or unknown lysate samples (2 μl) were added in triplicate in the microtitre plate. The volume in the wells used for BSA and unknown sample was adjusted by adding MiliQ water (e.g., in a well

containing 1 µl BSA: Bradford reagent 250 µl + BSA 1 µl + MilliQ 63 µl = 314 µl total volume; in a well containing 2 µl unknown sample: Bradford reagent 250 µl + unknown sample 2 µl + MilliQ 62 µl = 314 µl total volume). Protein concentration was measured at 595 nm OD (optical density) using Versamax tunable microplate reader with the help of Softmax Pro software (Molecular Devices, USA). Protein concentration in each of the lysate samples was then calculated from the standard curve by linear regression. To equalise protein concentration between all samples, the volumes of samples containing higher levels of proteins were adjusted with a necessary amount of ice-cold lysis buffer that they will be equal to that in the lysate sample with the minimum concentration of protein.

2.5.3 Sample preparation for gel electrophoresis

Antibodies typically recognise a small portion of the protein of interest and this domain may reside within the 3D conformation. To enable the antibody to access to this portion of a certain protein, it is necessary to unfold or denature the protein; this can be done by heating with an anionic denaturing detergent such as SDS. The lysate samples were mixed with 5x SDS sample buffer at the ratio of 4:1 (e.g. 25 µl sample buffer added in 100 µl lysate sample) in eppendorph tubes, incubated at 100ºC for 5 minutes using Techno dri-block DB-2A (Techno Cambridge Ltd., Cambridge, UK). Subsequently, eppendorph tubes containing the protein samples were placed on ice for 5-10 minutes and then stored at -20ºC until used for running into the gel.

2.5.4 SDS-PAGE electrophoresis

One dimensional SDS-PAGE electrophoresis (Sodium Dodecyl Sulphate PolyAcrylamide Gel Electrophoresis) was carried out using BioRad mini Protean

II gel electrophoresis with attached Powerpack 300 unit (BioRad Laboratories, Hemel Hempstead, UK). Using pre-cleaned glass plates gel chambers or cassettes were assembled according to the manufacturer's guideline. This technique is a standard means for separating proteins according to their molecular weight. The separation of molecules within a gel is determined by the relative size of the pores formed within the gel. Smaller proteins migrate through the gel faster than larger protein. This dictates the composition of the gel; the smaller the size of the protein of interest, the higher the percentage of acrylamide in the gel to be used. Conversely, the bigger the size of the protein of interest, the lower the percentage of acrylamide in the gel should be used. For the proteins of interest in this study (MYPT1, 130 kDa; MLC_{20}, 20 kDa) 7.5% gel was chosen (El-Awady *et al.*, 2008).

2.5.4.1 Preparation of SDS-PAGE gels

The running or resolving gel was prepared with 7.5% and the stacking gel with 5% acrylamide according to the following recipe (Table 2.9). The total volume of the running gel was sufficient for three 1 mm thick mini gels, while the stacking gel was sufficient for four 1 mm thick mini gels. Polymerisation is initiated by the addition of ammonium persulphate (APS) along with tetramethylethylenediamine (TEMED). A 50 µM APS (10% w/v) and 20 µl TEMED were added to running and stacking gel mixtures immediately before pouring them into the gel cassette.

Table 2.9 Recipes for electrophoresis gels

	Running gel 7.5%	**Stacking gel 5%**
30% acrylamide/bis-acrylamide	3.75 ml	1.67 ml
MilliQ water	5.6 ml	6.0 ml
1 M Tris-HCl pH 8.8	5.6 ml	-
1 M Tris-HCl pH 6.8	-	1.25 ml
10% SDS	0.25 ml	0.15 ml

Pre-cleansed glass plates were fixed in the gel cassette holder and the running gel was poured between the glass plates. The top layer of the running gel was overlaid with MilliQ water to achieve a uniform line while preventing from drying out and left to polymerise for 40 minutes. After polymerisation of the running gel water was aspirated carefully and the stacking gel was poured on top with a 10-well comb inserted between the plates to create the wells for the loading of protein samples, and left for 20 minutes to polymerise. Following polymerisation of the stacking gel the comb was removed carefully and the wells were thoroughly cleaned with MilliQ water to remove any residual stacking gel that might distort the band. Then the wells in the stacking gel were filled with 1x SDS-PAGE running buffer (Table 2.8). Stacking gel is necessary to provide a series of separate lanes for loading of the standard and unknown protein samples.

2.5.4.2 Loading samples and markers and running the gel

Using special loading tips (1- 200 µl, Gel Saver II tip natural, Fisherbrand, UK) samples (25 µl per lane) were loaded into the mini-gel wells with one well loaded with 10 µl of pre-stained molecular weight marker (Precision Plus Protein® Standards; Bio-Rad, UK) to determine the protein size and also to monitor the progress of an electrophoretic run. Ready-to-run gels were then placed into a gel tank with 1x SDS-PAGE running buffer in the top and bottom reservoirs and electrophoresis were run at 80 volts until the bromophenol blue present in the lysate samples entered the running gel. At this point, the voltage was increased to 180 volts. Gels were run until the bromophenol blue dye reached the bottom of the running gel or the desired separation of bands in reference to the molecular weight markers was achieved. Then the gels were carefully separated from the gel holders with a gel knife and placed into semi-dry transfer buffer (Table 2.8).

2.5.5 Transfer of protein to nitrocellulose membrane

Transfer of protein from gel to nitrocellulose membrane was done by semi-dry transfer using BioRad Transblot SD cell (BioRad, USA). The membrane was placed next to the gel and the two were sandwiched between absorbent materials. To achieve an efficient and smooth transfer of protein to the membrane, the positive graphite electrode (bottom) was first dampened with semi-dry transfer buffer and then the sandwich was placed on it. The sandwich was made on the bottom positive electrode by placing four 3MM Whatman paper, a piece of nitrocellulose membrane, a gel and finally another four pieces of Whatman paper, all of the similar size as the gel and all pre-soaked in the semi-dry transfer buffer. After sandwiching the gel and membrane between papers air bubble between the gel and membrane was removed by gently rolling them out with a hand-roller. Then the upper negative electrode was dampened with transfer buffer and gently lowered into place to maintain a tight contact between the gel and membrane. The rate of transfer was set at 0.8 mA cm^{-2} or 40 mA per gel for 1 hour 6 min.

2.5.6 Visualisation of protein and antibody probing

To check successful protein transfer, the membrane was washed with TBS-N (Table 2.8) and then Ponceau Red (1:10 dilution) was applied onto the membrane that revealed clear bands of proteins on it. The Ponceau Red stain was removed by washing the membrane with TBS-N and then the molecular weight standards were marked with a ball point pen. To block the non-specific background binding of the primary and/or secondary antibodies to the membrane, it was incubated with TBS-N containing 5% skimmed milk (Oxoid Ltd., Basingstoke, Hampshire, England) with gentle shaking on a Stuart rocking platform (Sterilin Ltd, Staffordshire, UK) for 1 hour at room temperature. After blocking, membranes were washed with TBS-N three times for 5 minutes each on a rocking platform at room temperature. The membranes were then incubated overnight at 4 ºC with

primary antibodies with gentle shaking. On the following morning, membranes were washed three times with TBS-N for 5 minutes each and then incubated for 1 hour with HRP-conjugated secondary antibodies (1: 5000 dilution in TBS-N with 2% skimmed milk, Dako, Glostrup, Denmark). The immunoreactive protein bands were illuminated with chemiluminescence substance ECL or advanced ECL kit (Amersham Biosciences, UK) and were developed on X-Ray film (Fujifilm Corporation, Tokyo, Japan) in a dark room. ECL kit was used for pan antibodies (e.g., MYPT1, MLC_{20}) while advanced ECL kit was used for phospho antibodies (e.g., phospho-MYPT1, phospho-MLC_{20}). The stable hard copy results on the film were quantified by densitometric analysis using ImageJ software (ImageJ 1.43, http://rsb.info.nih.gov/ij/).

Table 2.10 Conditions of primary antibodies used

Target protein for antibody	Primary antibody species	MW (kDa)	Primary antibody conc.	Secondary antibody conc.
MYPT1	Rabbit	130	1: 1000	1: 5000
Phospho-MYPT1 (Thr 850)	Rabbit	130	1: 5000	1: 5000
MLC_{20}	Rabbit	20	1:1000	1:10000
Phospho-MLC_{20}	Rabbit	20	1:1000	1:10000

All antibodies used were polyclonal. Primary antibodies were diluted in TBS-N with 0.01% (w/v) sodium azide to protect from microbial growth and applied 10 ml per each membrane. Secondary antibodies were diluted in TBS-N with 2% skimmed milk and applied 10 ml per each membrane.

2.5.7 Membrane stripping and re-probing

After taking the images for a particular protein (e.g., phospho-MYPT1), membranes subjected to reuse to probe another protein (e.g., pan MYPT1) were

washed with TBS-N for 10 minutes at room temperature on a rocking platform. Before re-probing with another primary antibody all previous antibodies were striped from the membrane using a striping solution Re-Blot Plus (Chemicon, USA). To do so, the membranes were treated with 1x Re-Blot plus solution on a rocking platform for exactly 15 minutes at room temperature. After stripping the membranes were washed thoroughly with TBS-N for 5-6 times for 5 minutes each on a rocking platform at room temperature. Membranes were then blocked with 5% skimmed milk and re-probed with primary and secondary antibodies as described before. This procedure of stripping and re-probing was used for examining equal loading of phospho proteins (e.g., ^{P}MYPT1) using antibodies specific for their non-phospho proteins (e.g., MYPT1). It has been used to get the ratio of phospho over non-phospho proteins (^{P}MYPT1/MYPT1) for quantification of changes in phosphorylation of that protein.

2.6 Calcium imaging with confocal microscopy

2.6.1 Isolation of single cell

Rat intrapulmonary and small mesenteric arteries were collected by the procedure described in section 2.1 in this chapter. For the isolation of pulmonary PASMCs and MASMCs the fragments of arteries were kept separately in HEPES buffered saline solution (HBSS) containing (mM): KCl 6, NaCl 119, $MgCl_2$ 1.2, $CaCl_2$ 2, D-glucose 12 and HEPES, 10; pH was adjusted to 7.3 with NaOH. The fragments were then transferred into 1.5 ml plastic tube with nominally Ca^{2+}-free HBSS containing 0.5 mg/ml protease type X and 1.5 mg/ml collagenase type IA. Tissue digestion was done in a water bath with gentle shaking for 15 min at 37 ºC. The tissue was then washed with warmed HBSS for 5 min and dispersed by gentle trituration with a blunt-ended, fire-polished glass Pasteur pipette. Dispersion was done in warmed nominally calcium free HBSS and the resulting suspension was pipetted onto glass coverslips, attached with vacuum grease to experimental chambers for viewing under confocal microscope. Cells were allowed to adhere for 30 min and the dispersion solution was then replaced several times with HBSS with gradually increasing concentration of $CaCl_2$. All experiments were conducted in HBSS containing 2 mM $CaCl_2$ at room temperature (20-23 ºC).

2.6.2 Confocal imaging

Confocal microscopy was performed using a Zeiss Axiovert 100M microscope attached to an LSM 510 laser scanning unit (Carl Zeiss, Oberkochen, Germany). An X40 oil immersion plan-neofluar objective (NA=1.3) was used to image cells. The pinhole was set to provide a confocal optical section (z resolution) of 0.8-1.0 μM. Temporal changes in fluorescence were imaged by repeating x-y scanning of

either a whole confocal field. Zeiss LSM files (.lsm) were exported as tagged image files (TIFF; .tif) for further analysis of the data.

2.6.2.1 Chamber system

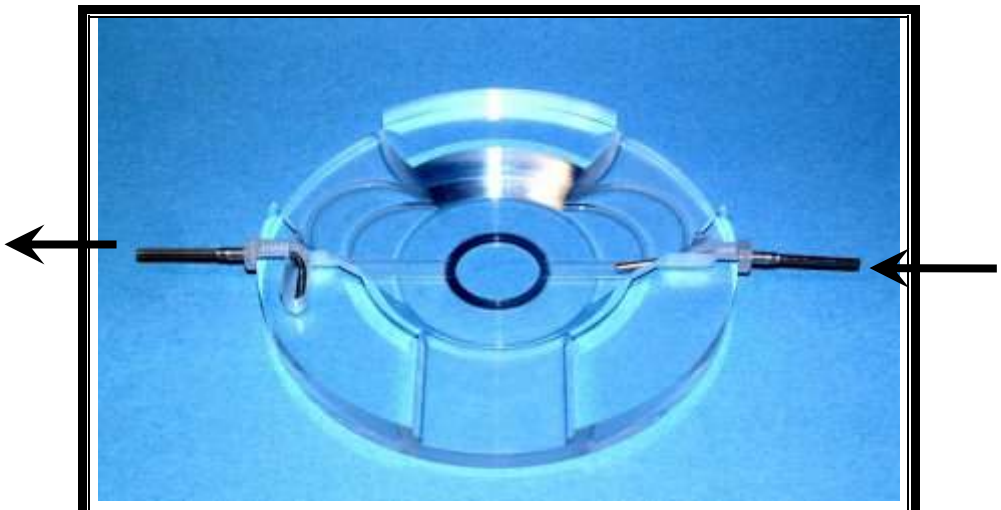

Figure 2. 4 Chamber system used for confocal microscopy. Arrows indicate the inflow and outflow of solutions.

A circular chamber was used for confocal microscopy, which consisted of three separate plastic pieces assembled as outer ring, an inner placement ring, and the bath (Figure 2.4). The bath consisted of a ring closed by a circular glass coverslip attached with vacuum grease. The capacity of the bath was ~300 µl and a series of baths were prepared so that all the cell suspension could be aliquoted among them, straight after trituration. The bath seated at the bottom of the outer ring and was held in place by the placement ring above it. Several small sections of rigid tubing were stuck around the edge of outer ring to accommodate a solution application/suction system. For solution application thin tubing was connected at one end to a 1 ml syringe (with needle) and at the other end to a small length of pulled glass capillary tube, by which it was slotted into the outer ring tubing. A

separate syringe/tube/capillary was used for each different solution (e.g., one for normal bath solution, one for 4-AP, one for linopirdine). Suction was with a similar piece of tubing connected to length of capillary tubing at one end and an aquarium pump at the other (via an air pocket).

2.6.2.2 Calcium imaging

For calcium imaging PASMCs and MASMCs were incubated for 30 minutes at room temperature with 5 μM of cell permeant calcium sensitive fluorophore, fluo-3AM (Abs/Em = 506 nm/526 nm) (Invitrogen, Paisley, UK). This was followed by a 30-min wash in HBSS to allow time for de-esterification. The fluo-3 AM was diluted from a stock solution containing 2 mM fluo-3 AM and 0.025% pluronic F-127. Pluronic F-127 is normally used in such experiments since it prevents aggregation of fluo-3 AM in HBSS solution and helps uptake of the dye by cells. Further procedures were carried out at room temperature. After loading with this Ca^{2+}-sensitive indicator , fluo-3 fluorescence was excited by the 488 nm line of Argon ion laser (Siemens, Munchen, Germany) and changes in fluorescence (an indicator of intracellular free calcium) were detected by the confocal detector at wavelengths <515 nm.

The response (fluorescence signal) was measured as the maximal change in fluorescence ΔF (F-F_0, where F is the maximum level of fluorescence reached in the presence of the stimulus, and F_0 is the initial fluorescence, immediately before the stimulus) divided by the initial fluorescence F_0. Thus, the change in the fluorescence ($\Delta F/F_0$) is an arbitrary unit. This normalisation approach removes variability due to any imprecision in loading of fluorescence indicator dye. x-y time-series imaging was performed. The final figures were produced using MicroCal Origin (MicroCal Software, Inc., USA) and Corel-Draw 7.0 (Corel Corporation, Canada).

2.6.3 Solutions and chemicals

HEPES buffered saline solution (HBSS)

Composition of HBSS (mM): 119 NaCl, 6 KCl, 1.2 $MgCl_2$, 2 $CaCl_2$, 10 D-glucose, 10 HEPES, adjusted to pH 7.35 with NaOH.

Table 2.11 Chemicals and drugs used in confocal imaging

Compound	Function	Stock and Solubility	Final concentration
fluo-3AM	Ca^{2+}-sensitive dye	2 mM (DMSO)	5 μM
4-AP*	K_V channel blocker	0.5M (H_2O)	0.5-10 mM
Linopirdine	KCNQ channel blocker	10 mM (Ethanol)	10 μM

* 4-AP stock was pH adjusted with HCl (pH=7.10)

2.6 Data analysis and statistics

Data are expressed as mean±standard error of mean (S.E.M.), where *n* equals number of animals, except in confocal (Ca^{2+} imaging) experiments, where *n* equals number of VSMCs from 3 to 4 animals. Vascular contraction and relaxation was calculated as % of maximum steady state contraction induced by 80 mM KCl or other vasoactive agents (e.g., 4-AP) as described in details in relevant chapters. In some of the experiments the absolute tension (mN) produced with vasoactive agent was taken into consideration and compared with standardised 80 mM KCl contraction. Unless otherwise stated, tension and Ca^{2+} imaging were compared between pulmonary and systemic mesenteric arteries. Significant differences between groups were determined using paired or unpaired Student's *t*-test as appropriate. Multiple comparisons were performed with one way ANOVA followed by Bonferroni, Dunnett or Tukey-Kramer post-hoc test as appropriate. Bonferroni test was used when it was necessary to compare certain selected pairs of treatment groups. Dunnett test was chosen to compare control versus all treatment groups whilst Tukey-Kramer test was used for comparing all groups (Motulsky, 1999).

Chapter 3

REGULATION OF EXCITABILITY IN THE RAT PULMONARY AND SYSTEMIC VASCULATURE: THE TALE OF TWO K^+ CHANNELS

3.1 Introduction

Under normal level of alveolar oxygen the pulmonary arterial circulation is a low-pressure, low-resistance system that carries deoxygenated blood into the pulmonary microcirculation where gas exchange can occur. In hypoxic conditions, however, pulmonary arteries constrict thus diverting blood flow from poorly ventilated to better ventilated regions of the lung to match ventilation with perfusion. The control of pulmonary vascular resistance and hypoxic pulmonary vasoconstriction resides in small intra-pulmonary arteries and depends on the level of intracellular Ca^{2+}.

Potassium channels are recognised as an important regulator of pulmonary vascular tone. For nearly two decades the investigation was focussed on one group of K^+ channels, voltage-gated K^+ (K_V) channels. This interest was driven by the following main reasons: ***i***) K_V channels are inhibited by acute hypoxia in single PASMCs (Post *et al.*, 1992;Yuan *et al.*, 1993;Olschewski *et al.*, 2002), ***ii***) the selective inhibitor of the K_V channels, 4-AP, caused membrane depolarisation (mimicking the depolarising effect of hypoxia) and attenuated HPV (Hasunuma *et al.*, 1991;Karamsetty *et al.*, 1998;Archer *et al.*, 2004), ***iii***) the inhibitors of K_{ATP} or BK_{Ca} channels did not alter basal tissue reactivity or HPV in intact pulmonary arteries and lungs (Hasunuma *et al.*, 1991;Karamsetty *et al.*, 1998), and ***iv***) the K_V channel current is the dominant K^+ current in PASMCs with a relatively little

component of BK_{Ca} or K_{ATP} currents (Smirnov *et al.*, 1994;Smirnov & Aaronson, 1994;Smirnov *et al.*, 2002).

Although the above mentioned findings overall support the proposal for the leading role of K_V channels in the regulation of membrane potential in the pulmonary circulation, they are chiefly based on the evidence obtained in single isolated cells. In intact PA, the role of the K_V channels alone in the regulation of the cell membrane potential at rest has been however challenged (Gurney *et al.*, 2002). One of the key arguments against K_V channels is that their apparent threshold of activation (between -40 and -30 mV) measured in isolated myocytes is more positive than the resting potential in intact PAs (between -52 and -59 mV) (Casteels *et al.*, 1977;Suzuki & Twarog, 1982;Bonnet *et al.*, 2001). Additionally, there is a mismatch between the effect of 4-AP, a selective K_V channel inhibitor, that produces contraction of intact isolated PA at concentrations typically above 5 mM (Doggrell *et al.*, 1999;Bonnet *et al.*, 2002) while the EC_{50} for the inhibition of K_V channels in single PASMCs ranges between 0.11 to 0.35 mM (Smirnov & Aaronson, 1994;Smirnov *et al.*, 2002).

The presence of background K^+ currents mediated by KCNQ channels has been recently demonstrated in vascular smooth muscles (Yeung & Greenwood, 2005;Mackie *et al.*, 2008), including PA (Joshi *et al.*, 2006;Joshi *et al.*, 2009). KCNQ channels are voltage-dependent K^+ channels, which activate at more negative membrane voltages (-60 to -80 mV) compared for K_V channels. Activation of KCNQ channels is also slower than other K_V channels, taking hundreds of milliseconds or even seconds to fully activate and they do not inactivate during sustained depolarisation (Gurney *et al.*, 2010). Therefore, KCNQ channels are ideal for setting the resting potential in cells (Mackie & Byron, 2008;Gurney *et al.*, 2010). Nevertheless, the large size of the K_V channel currents measured in small resistance PASMCs (Smirnov *et al.*, 2002) suggests that they can be also active at membrane potentials negative to -40 mV and be involved in the regulation of cell resting potential. The relative contribution of the K_V and KCNQ channels to contractility of PA has not been yet directly investigated.

In this chapter I have investigated the relative contribution of K_V and KCNQ channels to contraction, changes in membrane potentials and intracellular $[Ca^{2+}]_i$ in rat small PAs and isolated PASMCs using pharmacological tools, small vessel myography, microelectrode technique and confocal imaging. The tissue specificity of the responses was assessed using rat mesenteric artery recorded under identical experimental conditions. Single cells were isolated from the similar calibre arteries for experiments with confocal imaging.

3.2 Results

3.2.1 Role of K_V and KCNQ channels in the regulation of the basal tone in rat PA and MA

The effect of increasing concentrations of 4-AP from 0.5 to 10 mM applied cumulatively for 5 min each on contraction of PA and MA is shown in Fig. 3.1 A and C, respectively. Overall, in 8 PA, increasing concentrations of 4-AP caused progressive increases in tension which becomes significant only at 10 mM (22.5±7.5%) of 4-AP (compared to 0.5 mM, $p<0.001$) (Fig. 3.2 A). Under the same experimental conditions, 4-AP did not cause significant contraction in 8 MA at any concentration (Fig. 3.2 C).

To compare the effect of 4-AP in the depolarised condition which should promote a greater activation of 4-AP-sensitive K_V channels, 20 mM KCl was added to the myograph chamber for 20 min. This produced a significant increase in contraction in PA, but not in MA, as it can be seen from representative traces in Fig. 3.1 B and D. In PA and MA, 20 mM K^+ caused 20.2±5.8% and 0.87±0.21% contraction, respectively. Fig. 3.2 summarises the effect of 4-AP in 8 PA and 8 MA in the absence and in the presence of 20 mm KCl. In the presence of 20 mM KCl, progressive increases in concentration of 4-AP caused further increases in tension at all concentration tested, becomes significant at 5 and 10 mM of 4-AP in PA (compared to 0.5 mM, $0.001<p<0.05$; Fig. 3.2 B). This effect was not observed in MA, where 4-AP was able to significantly increase tension only at 10 mM (compared to 0.5 mM, $p<0.001$; Fig. 3.2 D).

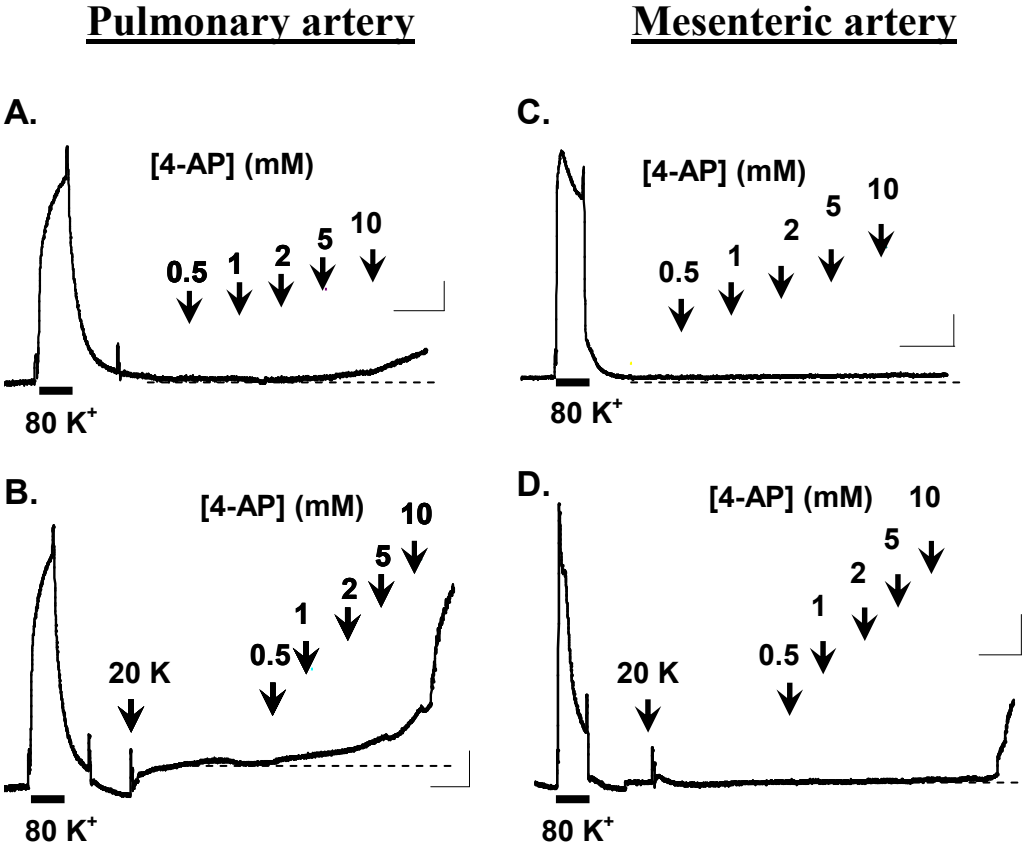

Figure 3.1 Effect of 20 mM KCl on 4-AP-dependent contraction in rat PA and MA.

A-D, Representative traces from PA (A-B) and MA (C-D) compare contractile responses induced by increasing concentrations of 4-AP (0.5-10 mM) in the absence (A, C) and presence (B, D) of 20 mM KCl. PA and MA internal diameters (i.d.) were 422 and 270 μm, respectively. Horizontal and vertical scale bars represent 5 min and 1 mN, respectively.

To compare statistically the effect of 20 mM KCl on the 4-AP-induced responses in the same tissue and between two types of arteries, data were re-arranged and are presented in Fig. 3.3. This analysis show that in the presence of elevated K^+, in PA, further contraction to increasing concentrations of 4-AP was substantially increased becoming significant at 5 and 10 mM compared to the control conditions (Fig. 3.3 A, filled circles). Significant potentiation of the 4-AP-induced contraction was also observed in MA, albeit only at 10 mM (Fig. 3.3 B, filled squares). Notably, as it can be seen from the comparison in Fig. 3.3 A and B, the 4-AP-induced contraction was greater in PA than in MA (relative to the peak 80 mM KCl responses). A significant difference in the 4-AP-induced contraction between these arteries (PA vs. MA) in the absence and presence of 20 mM KCl was observed only at 10 mM 4-AP ($0.001<p<0.01$) (Fig. 3.3 C and D, respectively).

In contrast, no apparent enhancement of contraction in PA and MA by 20 mM KCl was observed for TEA concentration-responses (1, 2, 5, 10 and 20 mM) (n=2, Fig. 3.4). In both PA and MA responses to TEA were small suggesting insignificant contribution of TEA sensitive K_V channels to contractility in these vessels. This observation is consistent with the key role of the 4-AP sensitive and TEA-insensitive K_V channels (i.e. $K_V1.5$), but rules out a significant contribution of TEA-sensitive K^+ conductances such as BK_{Ca} or TEA-sensitive K_V channels (i.e. $K_V2.1$) under this experimental conditions (Archer *et al.*, 1996;Osipenko *et al.*, 2000;Smirnov *et al.*, 2002).

The capability of 4-AP to significantly constrict PA is consistent with the recognised role of K_V channels in the control of the pulmonary vascular tone (Sweeney & Yuan, 2000;Weir & Olschewski, 2006). On the other hand, the ability of 20 mM KCl to significantly enhance the tissue sensitivity to low concentrations of 4-AP suggests the presence of additional K^+ conductances which contribute to the control of the basal tone. Recently, background KCNQ channels have been proposed to play a critical role in this process in both PA and MA (Mackie *et al.*, 2008;Joshi *et al.*, 2009;Gurney *et al.*, 2010). If this is the case under my experimental conditions, then the inhibition of KCNQ channels should also potentiate the 4-AP concentration dependence in a similar manner as did

elevated K^+. To check this hypothesis, the responses to different concentrations of 4-AP were assessed in the absence and presence of 10 μM linopirdine, a specific inhibitor of the KCNQ channels. This concentration of linopirdine was chosen to induce maximal inhibition of the KCNQ channels in intact arteries based on previous studies (Joshi *et al.*, 2006;Mackie *et al.*, 2008;Joshi *et al.*, 2009).

It is noteworthy that in this study only linopirdine was used as a reliable and selective inhibitor which has been used previously in other studies specifically measuring tension in intact arteries (Joshi *et al.*, 2006;Mackie *et al.*, 2008;Joshi *et al.*, 2009). Another reason for using a single KCNQ inhibitor was that inhibition of KCNQ channels served as an experimental tool to facilitate activation of K_V channels in the whole tissue. However, it would be interesting and useful to investigate the effect of other inhibitors, for example XE991 which is considered to be more potent (Earl *et al.*, 1998) than linopirdine, although its concentration range used in the experiments (Yeung & Greenwood, 2005;Yeung *et al.*, 2007;Yeung *et al.*, 2008;Ng *et al.*, 2010;Zhong *et al.*, 2010b) is not that dissimilar to linopirdine used in my study. It is also notable that 4-AP was found to be ineffective on KCNQ currents tested for KCNQ1, KCNQ2, KCNQ3 and KCNQ2/KCNQ3 channels (Robbins, 2001).

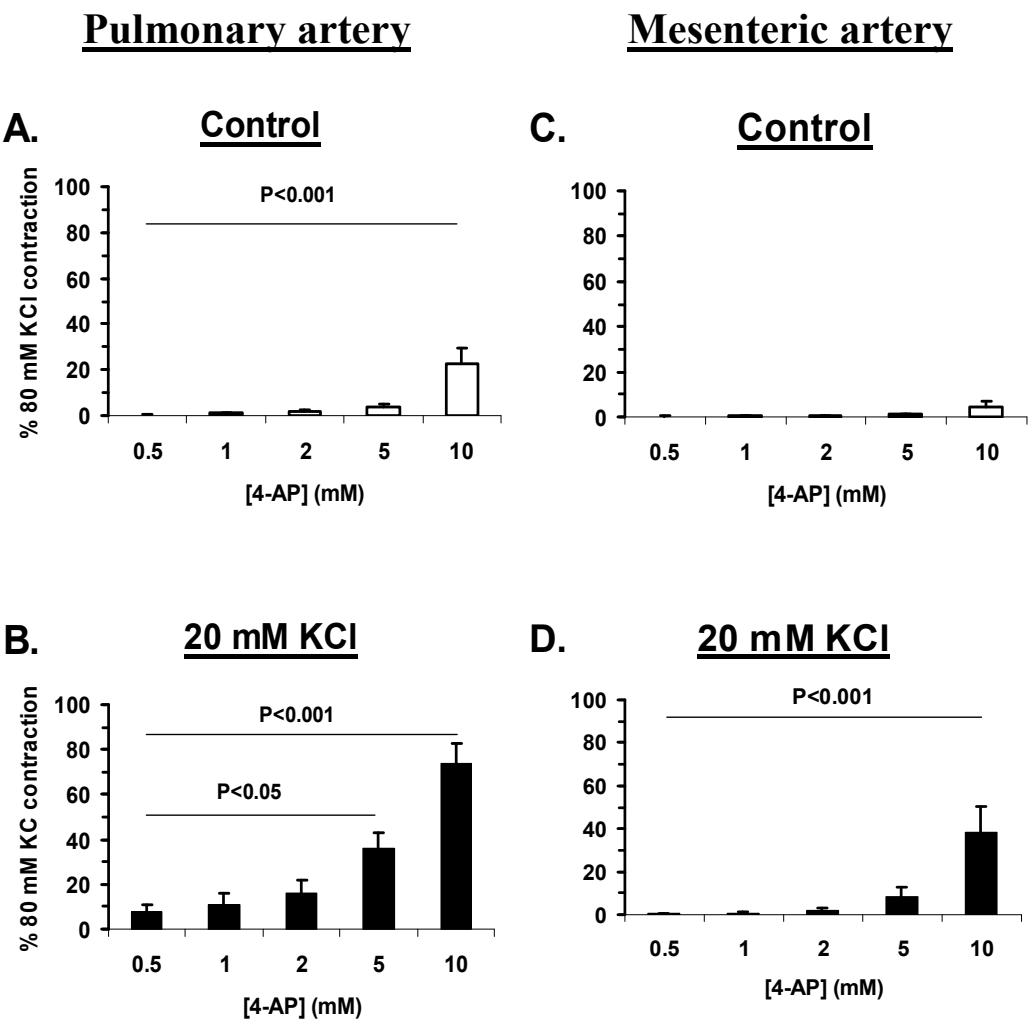

Figure 3.2 Summary of the 4-AP responses in control and depolarised rat PA and MA.

Column graphs summarise concentration-contraction relationship to 4-AP in the absence and presence of 20 mM KCl in PA (A-B) and MA (C-D). Responses to 1 to 10 mM 4-AP were compared with that produced with 0.5 mM 4-AP in control conditions and under depolarised conditions (in 20 mM KCl) (One-way ANOVA with Dunnett post-hoc test, $n = 8$).

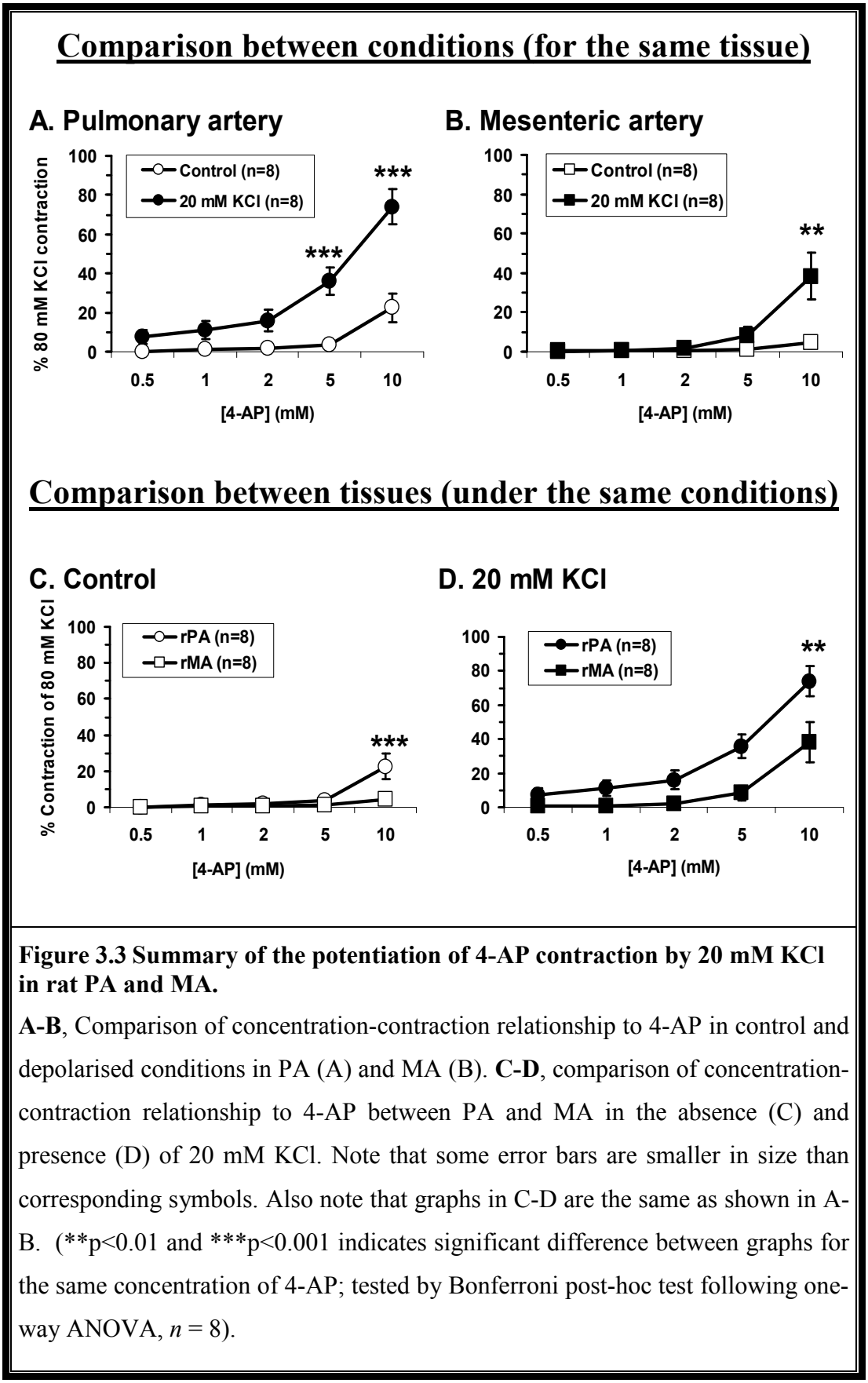

Figure 3.3 Summary of the potentiation of 4-AP contraction by 20 mM KCl in rat PA and MA.

A-B, Comparison of concentration-contraction relationship to 4-AP in control and depolarised conditions in PA (A) and MA (B). **C-D**, comparison of concentration-contraction relationship to 4-AP between PA and MA in the absence (C) and presence (D) of 20 mM KCl. Note that some error bars are smaller in size than corresponding symbols. Also note that graphs in C-D are the same as shown in A-B. (**$p<0.01$ and ***$p<0.001$ indicates significant difference between graphs for the same concentration of 4-AP; tested by Bonferroni post-hoc test following one-way ANOVA, $n = 8$).

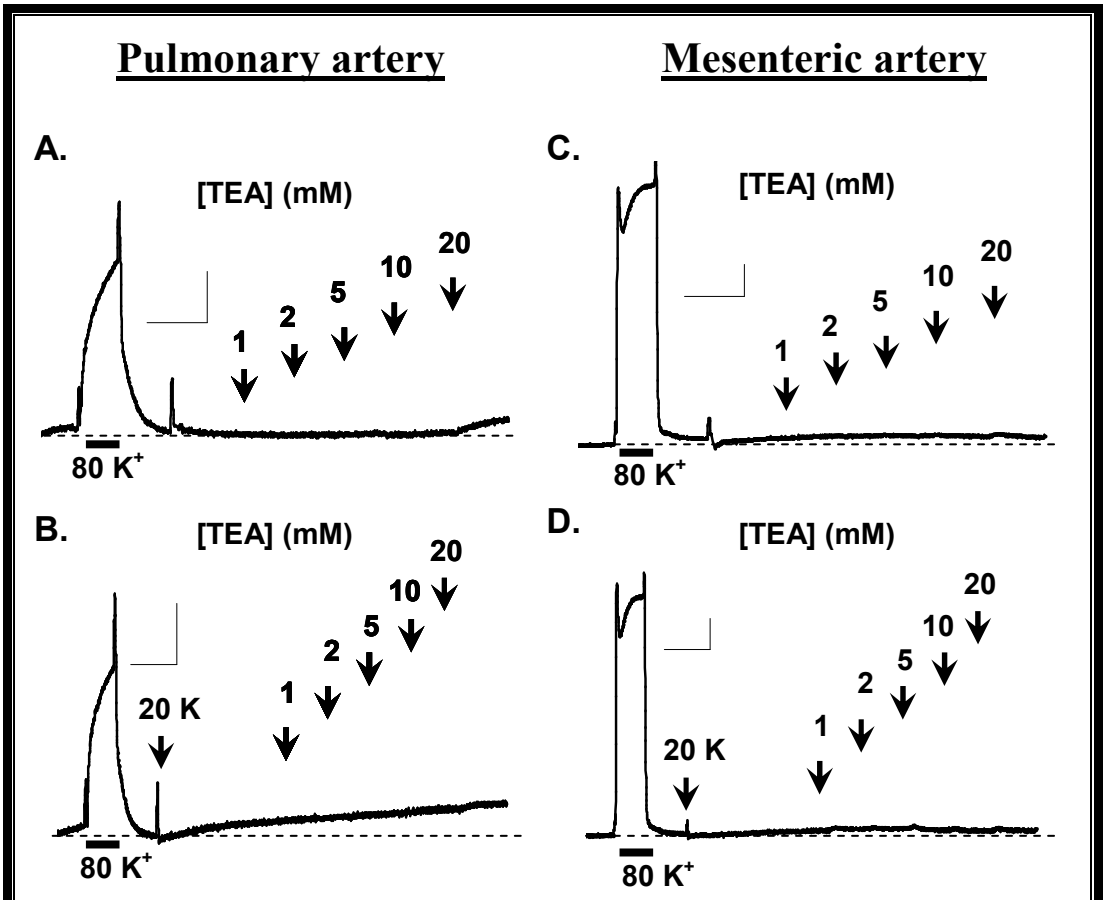

Figure 3.4 TEA concentration-responses in control and depolarised rat PA and MA.

A-D, Representative traces from PA (A-B) and MA (C-D) demonstrating the effect of increasing concentrations of TEA (1-20 mM) on contraction in the absence (A, C) and presence (B, D) of 20 mM KCl. PA and MA internal diameter were 340 and 175 μm, respectively. Horizontal and vertical scale bars represent 5 min and 1 mN, respectively.

Figure 3.5 A-D shows representative traces recorded from PA and MA in the absence and presence of 10 μM linopirdine applied for 20 min prior to application of increasing concentrations of 4-AP. As it can be clearly seen from these recordings, 4-AP-induced contraction was markedly increased in PA following the inhibition of KCNQ channels (Fig. 3.5 A and B), mimicking the effects observed in the elevated K^+. It is noteworthy that linopirdine itself caused a small but significant (14.6±2.4%, n = 28, $p<0.0001$) contraction of the PA. No significant effect of linopirdine alone was observed in the MA (1.1±0.2%, n = 26, Fig. 3.5 C and D). Fig. 3.6 summarises the effect of linopirdine on the 4-AP-induced contraction in 8 PA and 8 MA, demonstrating a significant enhancement of contraction to 5 and 10 mM 4-AP in PA in the presence of linopirdine compared to the control conditions (Fig. 3.6 A) and compared to MA measured in control conditions (Fig. 3.6 C) and in the presence of the KCNQ inhibitor (Fig. 3.6 D). Linopirdine also enhanced 4-AP-induced contraction in MA only at 10 mM (Fig. 3.6 B).

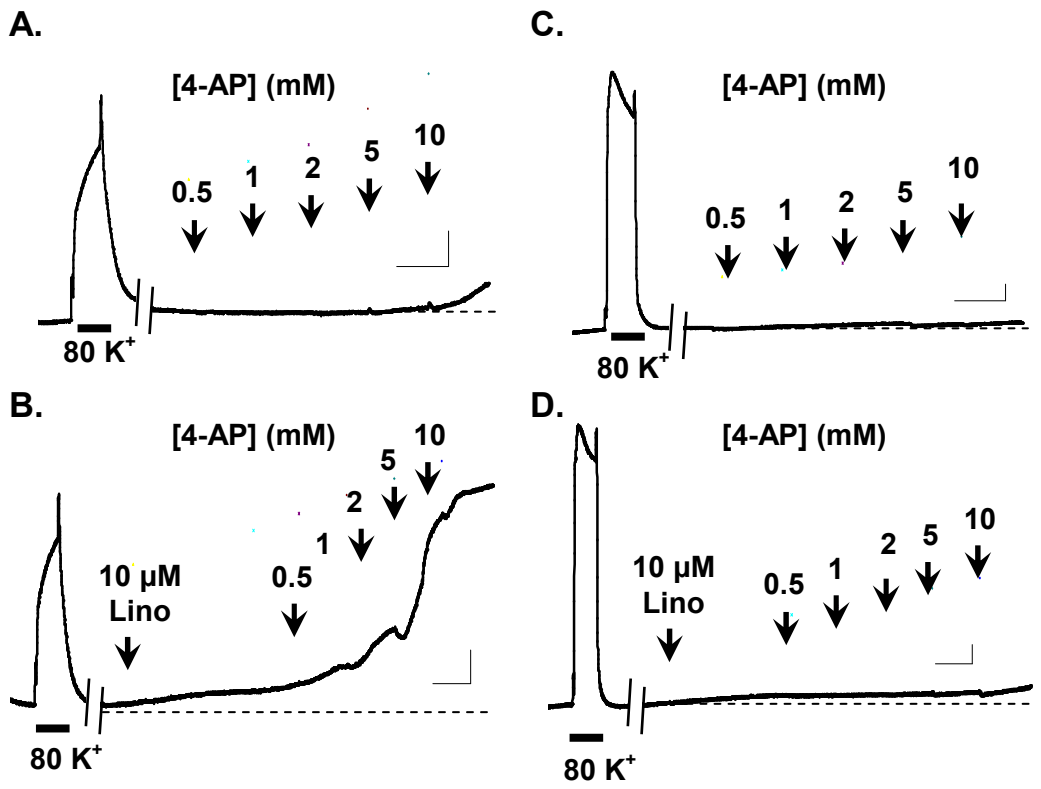

Figure 3.5 Effect of the KCNQ channel inhibitor linopirdine on 4-AP-induced contraction in rat PA and MA.

Representative traces obtained from PA (A-B) and MA (C-D) compare contractions in response to increasing concentrations of 4-AP (0.5-10 mM) in the absence (A, C) and presence (B, D) of 10 µM linopirdine (Lino). PA and MA i.d. were 412 and 242 µm, respectively. Horizontal and vertical scale bars represent 5 min and 1 mN, respectively.

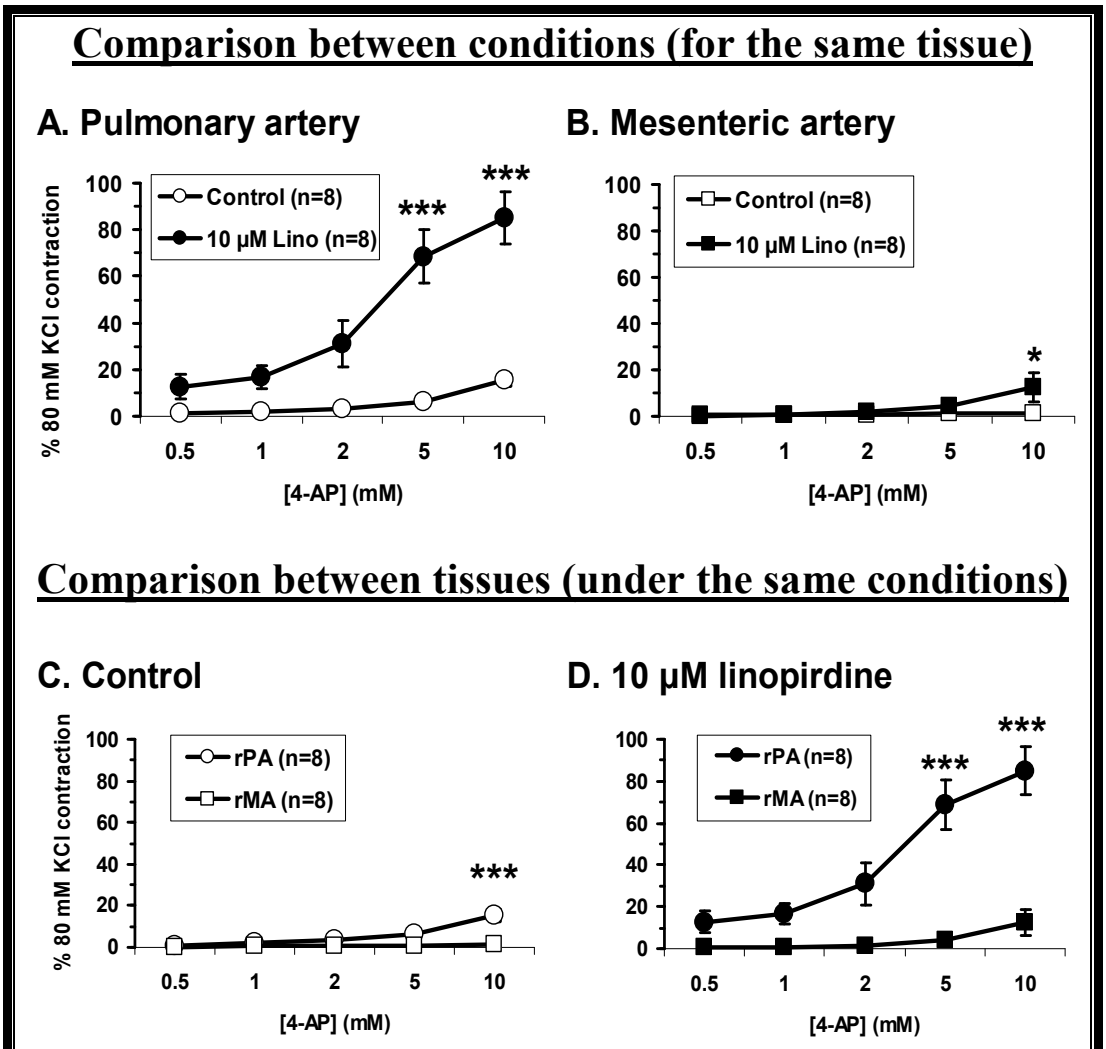

Figure 3.6 Summary of the potentiation of 4-AP contraction by linopirdine in rat PA and MA.

A-B, Comparison of concentration-contraction relationship to 4-AP between the control conditions and after linopirdine treatment in PA (A) and MA (B). **C-D**, comparison of concentration-contraction relationship to 4-AP between PA and MA in the absence (C) and presence (D) of 10 µM linopirdine. Note that some error bars are smaller in size than corresponding symbols. Also note that graphs in C-D are the same as shown in A-B. (*$p<0.05$ and ***$p<0.001$ indicates significant difference between graphs for the same concentration of 4-AP; tested by Bonferroni post-hoc test following one-way ANOVA, $n = 8$).

3.2.2 Effect of the K_V and KCNQ channel blockade on the resting membrane potential in rat PA and MA

The above described findings are consistent with the relatively greater contribution of the K_V and KCNQ channels to the regulation of the resting potential in the PA than in the MA. To assess the effect of the inhibition of the K_V and KCNQ channels on the resting membrane potential directly, changes in the membrane potential were measured using sharp microelectrodes in the presence of 10 mM 4-AP, 10 μM linopirdine and the combination of the both inhibitors. Fig. 3.7, A and B, show the effect of 10 mM 4-AP followed by the addition of 10 μM linopirdine on the tension (A) and membrane potential (B) in the PA. Application of 10 mM 4-AP caused slowly developing membrane depolarisation from the resting level of -58.3 mV to -50.0 measured after 10 min paralleled by the tension development. The addition of 10 μM linopirdine rapidly depolarised the membrane to -23.9 mV (Fig. 3.7 B). This depolarisation was associated with a significant contraction (Fig. 3.7 A). Interestingly, fluctuations in the membrane potential were observed (Fig. 3.7 B, inset). No fluctuation in tension was however seen. Such fluctuations in membrane potential were observed only in one other PA preparation.

In the MA, 4-AP caused a small depolarisation from -67.8 mV to -66.3 mV with no significant development of contraction (Fig. 3.7 C and D). Addition of linopirdine caused further membrane depolarisation which was associated with regular bursts of the spike-like activity (Fig. 3.7 D). In contrast to the PA, these fluctuations in the membrane potential mirrored by oscillations in tension (compare the inserts in Fig. 3.7 C and D). These effects were consistently observed in all MA studied. Here it is worth mentioning that in my experimental set up the resting membrane potential measured in MA was more hyperpolarised compared to the values previously reported in MA [RMP ~-57 to -60 mV; (Mulvany *et al.*, 1982;Garland & McPherson, 1992)]. This could be due to difference in the methods, especially applying different levels of resting tone. In my experiments the vessel was set at a tension equivalent to that generated at 0.9

times the diameter of the vessel at 70 mmHg. In the previous studies which showed more depolarised resting membrane potential of rat small mesenteric artery (~-57 mV to -60 mV), the vessel was set at 100 mmHg as the effective transmural pressure (Mulvany *et al.*, 1982;Garland & McPherson, 1992).

The mean changes in the membrane potential in 5-10 PA obtained from 6 rats and in 3-8 MA from 4 animals are compared in Fig. 3.8, A and B, respectively. In PA, 10 μM linopirdine evoked depolarisation from -57.8±3.9 mV to -53.3±5.1 mV and 10 mM 4-AP depolarised from -57.8±3.9 to -45.2±6.3 mV while combination of 10 μM linopirdine and 10 mM 4-AP caused significant depolarisation from -57.8±3.9 to -31.2±5.6 mV. In MA, on the other hand, 10 μM linopirdine depolarised very little from -67.8±1.8 mV to -67.0±2.5 mV, 10 mM 4-AP depolarised from -67.8±1.8 to -57.0±3.3 mV while combination of 10 μM linopirdine and 10 mM 4-AP resulted significant depolarisation from -67.8±1.8 to -47.0±4.3 mV. Combination of 10 μM linopirdine and 10 mM 4-AP significantly depolarised both tissues although the extent of depolarisation was greater in the pulmonary (~46%) than in the mesenteric artery (~31%). Fig. 3.9 A and B compare the correlation between the relative changes in the membrane potential (measured as the difference of the average membrane potential before addition and in the presence of the inhibitors) and the force of contraction. In both PA and MA, a significant correlation between the two parameters was found: correlation coefficient equal to 0.77 ($p<0.0005$) and 0.55 ($p<0.033$), respectively. This regression analysis suggests that the amount of contraction is proportional to membrane depolarisation and is independent of the way (i.e. type of K^+ channel blocker) this depolarisation was produced. It does also support the additive role of KCNQ and K_V channels in the regulation of the resting membrane potential in these arteries.

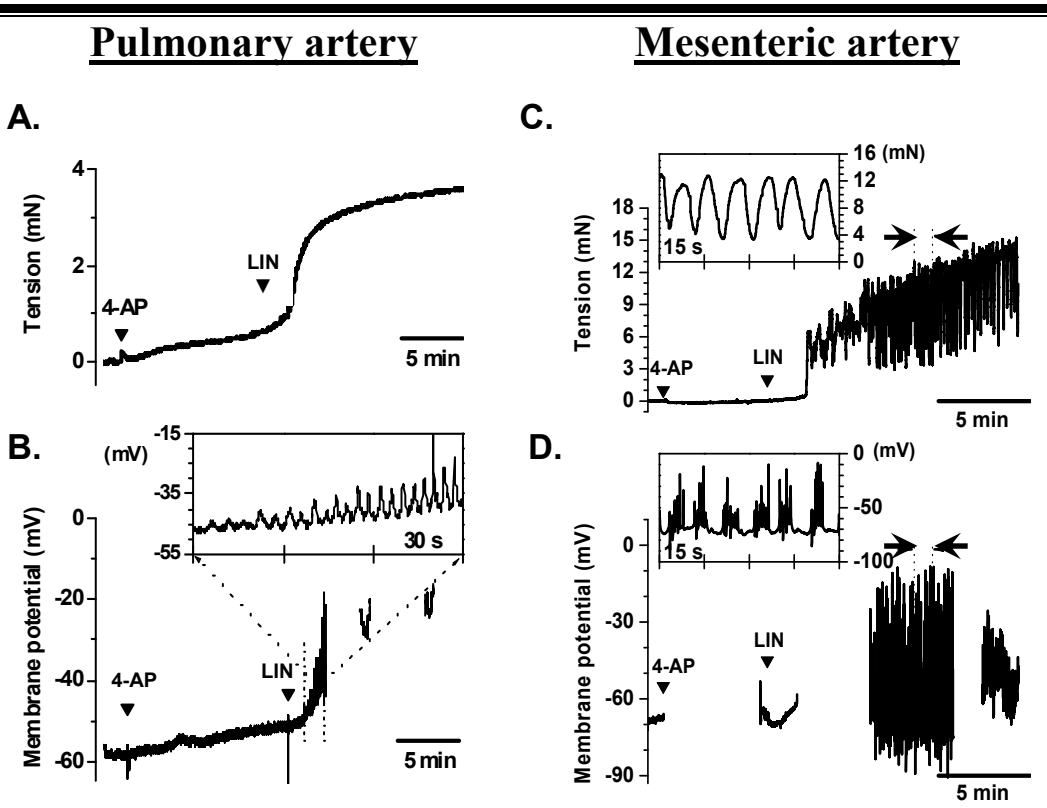

Figure 3.7 Effects of K_V and KCNQ channel blockers on tension and corresponding membrane potential in rat PA and MA.

A, C- Contraction traces obtained from PA (A) and MA (C) of 379 And 315 μm i.d. showing contraction in response to 10 mM 4-AP followed by 10 μM linopirdine (15 min each). B, D- Membrane potential traces obtained from PA (B) and MA (D) showing changes in the membrane potential upon application of 10 mM 4-AP followed by 10 μM linopirdine (15 min each). Inserts show oscillations of contraction in MA (inset in C), and fluctuations of membrane potentials in PA (inset in B) and MA (insert in D) at the expanded time scale. Note that in the panels B and D the discontinuation in the traces indicates the time when microelectrode came out from the cell during recordings due to tissue contraction.

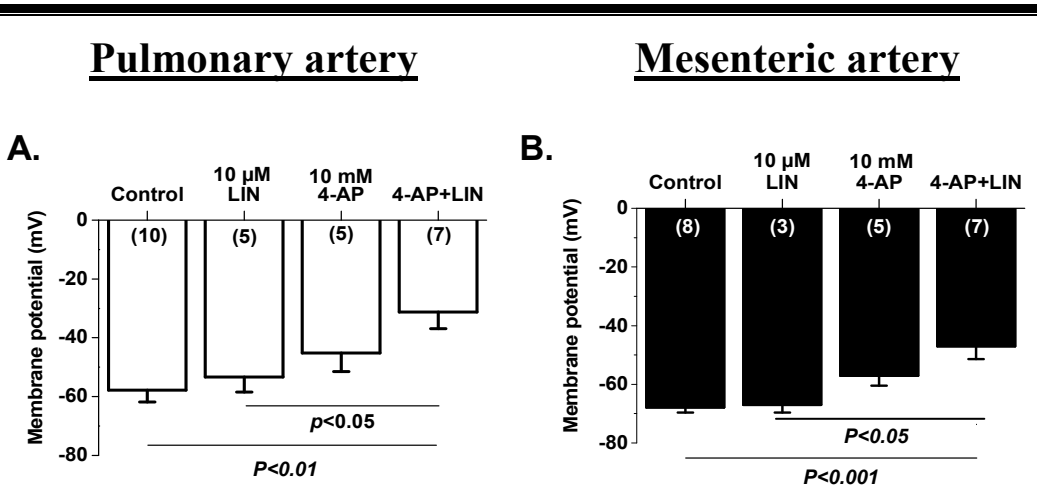

Figure 3.8 Summary of the effects of K_V and KCNQ channel blockers on membrane potential in rat PA and MA.

A-B, Mean depolarisations induced by KCNQ channel inhibitor linopirdine (10 µM) alone, K_V channel blocker 4-AP (10 mM) alone or combination of these two are shown in PA (A) and MA (B). LIN, linopirdine. Differences between groups were tested by Tukey-Kramer post-hoc test following one-way ANOVA; *n* values are indicated on the respective columns.

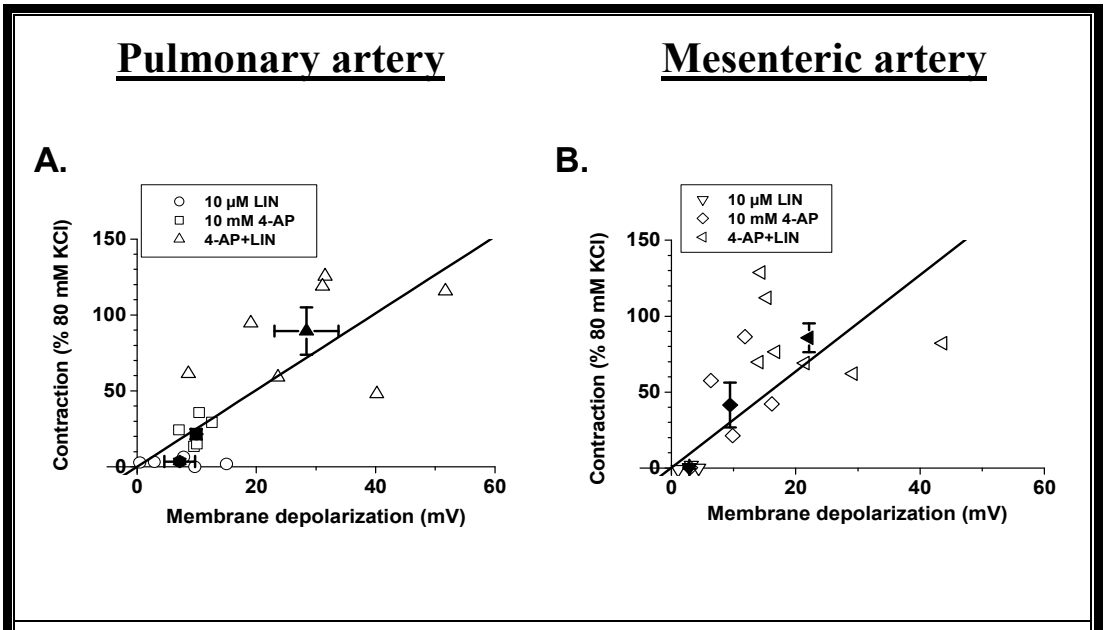

Figure 3.9 Correlation between membrane potential and contraction induced by K_V and KCNQ channel blockers in rat PA and MA.

A and B compare the correlation between the relative changes in the membrane potential and the force of contraction in PA (A) and MA (B). Each open symbol represents the result of an individual experiment, whereas filled symbols represent the mean values for each group of treatment. The regression analysis was performed using individual values. Correlation coefficient for PA and MA is equal to 0.77 ($p<0.0005$) and 0.55 ($p<0.033$), respectively.

3.2.3 Effect of the K_V and KCNQ channel inhibitors on intracellular Ca^{2+} in single myocytes from rat PA and MA

The correlation between the membrane depolarisation and the force of contraction in the presence of K_V and KCNQ channel inhibitors, 4-AP, linopirdine and their combination, directly supports the combined role of the two channel types in the regulation of the resting membrane potential. The ability of the K_V and KCNQ channel inhibitors to change $[Ca^{2+}]_i$ was evaluated in single myocytes isolated from rat PA and MA using confocal imaging. Figure 3.10, A and C, shows representative images of 2 PASMCs and 2 MASMCs loaded with Fluo-3. Figure 3.10, B and D, depicts recordings of fluorescent intensities before and after application of 2 and 10 mM 4-AP in the above mentioned 2 PASMCs and 2 MASMCs, respectively. In PASMCs application of 2 mM 4-AP caused a moderate sustained increase in $[Ca^{2+}]_i$. In one cell (marked ***a***) this response was further enhanced by 10 mM 4-AP; this represents typical responses seen in most PASMCs. In another cell (marked ***b***) 10 mM 4-AP caused slow transient responses. In MASMCs, oscillations in $[Ca^{2+}]_i$ were typically observed in both concentrations of 4-AP. The effects of 4-AP were completely reversible in both cell types. Figure 3.11, A and B, summarises the time course of this experiment in 22 PA and 41 MA myocytes. The sustained averaged response in MA could be explained by the lack of synchronicity in oscillations between individual myocytes.

Figure 3.12 statistically analyses the effects of 2 and 10 mM 4-AP on $[Ca^{2+}]_i$ in PASMCs and MASMCs. Fig. 3.12, A and C, compares the effects of 4-AP on the mean intensities, whilst Fig. 3.12, B and D, compares the mean area under the curve (AUC). Both types of analysis show that 4-AP causes significant increases in $[Ca^{2+}]_i$ in the two cell types.

When similar experiments were performed in the presence of 10 μM linopirdine and 2 mM 4-AP (Fig. 3.13), similar significant changes in $[Ca^{2+}]_i$ in PASMCs were observed as summarised in Fig. 3.13, A and B.

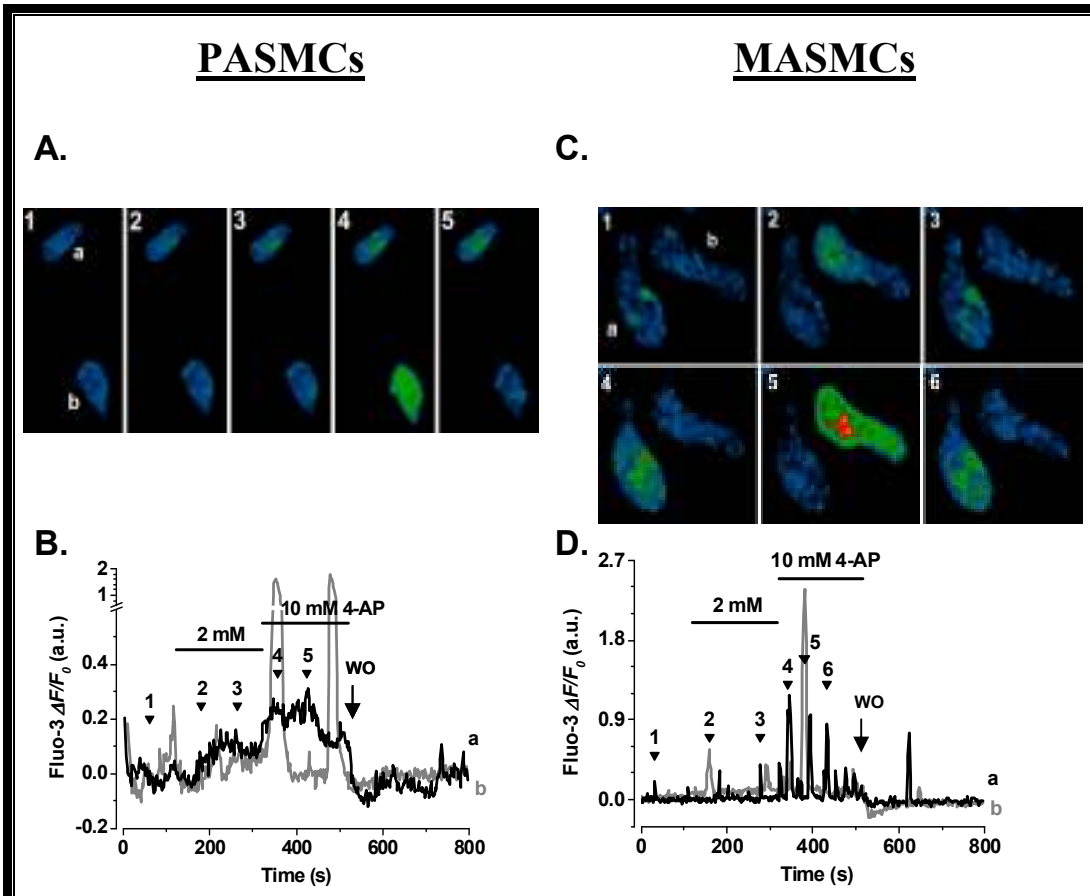

Figure 3.10 The effect of 4-AP on changes in $[Ca^{2+}]_i$ in isolated PASMCs and MASMCs.

A) Shows a series of 5 x-y confocal optical slices of two PASMCs loaded with Fluo-3 before (1) and at different times following the addition of 2 and 10 mM 4-AP as indicated. B) Shows the time course of changes in the fluorescence intensities for the two cells shown in A. Note that only cell b demonstrate a slow oscillations. Likewise, C and D represent a series of confocal x-y optical slices and corresponding time courses for fluorescence intensities, respectively, for 2 isolated MASMCs. Fluorescent intensity was expressed as $\Delta F/F_0$ where $\Delta F = F - F_0$ (F is fluorescence intensity at a given time point and F_0 is baseline fluorescence). a.u., arbitrary units. WO, wash out.

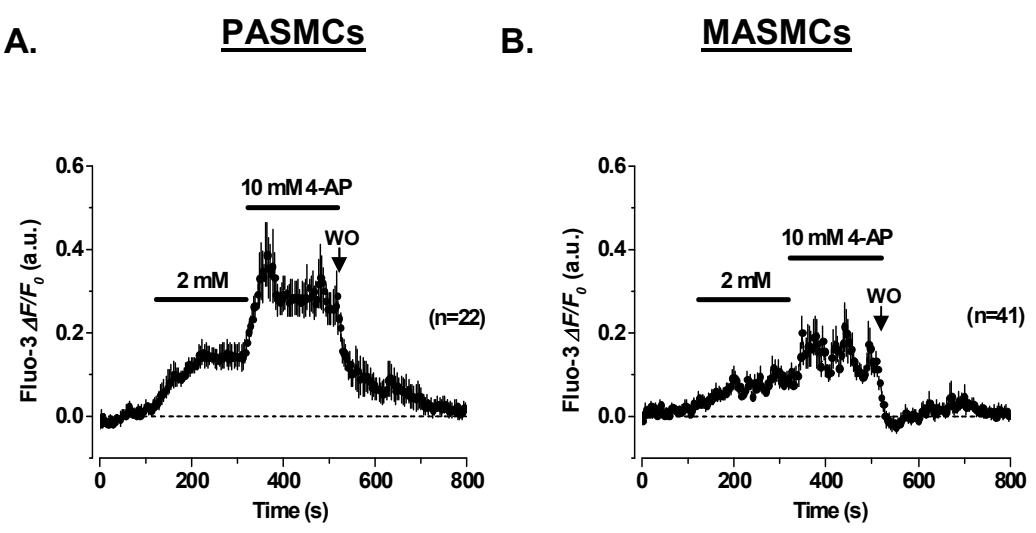

Figure 3.11 Comparison of the effect of 4-AP on $[Ca^{2+}]_i$ in isolated PASMCs and MASMCs.

Relative fluorescent intensities, expressed as $\Delta F/F_0$, and recorded in each cell using the experimental protocol shown in Fig.3.10 were averaged for 22 PASMCs (A) and 41 MASMCs (B). Vertical bars represent S.E.M. Note that in MASMCs individual cell oscillations summate causing sustained elevation of $[Ca^{2+}]_i$.

Interestingly, in MASMCs, $[Ca^{2+}]_i$ was also significantly increased in 10 μM linopirdine and 2 mM 4-AP (Fig. 3.13, C and D), the effect was smaller than in PASMCs. Indeed, the difference in changes in fluorescence ($\Delta F/F_0$) in the presence of both 10 μM linopirdine and 2 mM 4-AP was significantly greater in PASMCs than in MASMCs ($p<0.00001$). Because fluorescence intensities are presented as $\Delta F/F_0$, i.e., normalised in respect to the baseline, changes in fluorescence reflect changes in $[Ca^{2+}]_i$ and not differences in cell loading.

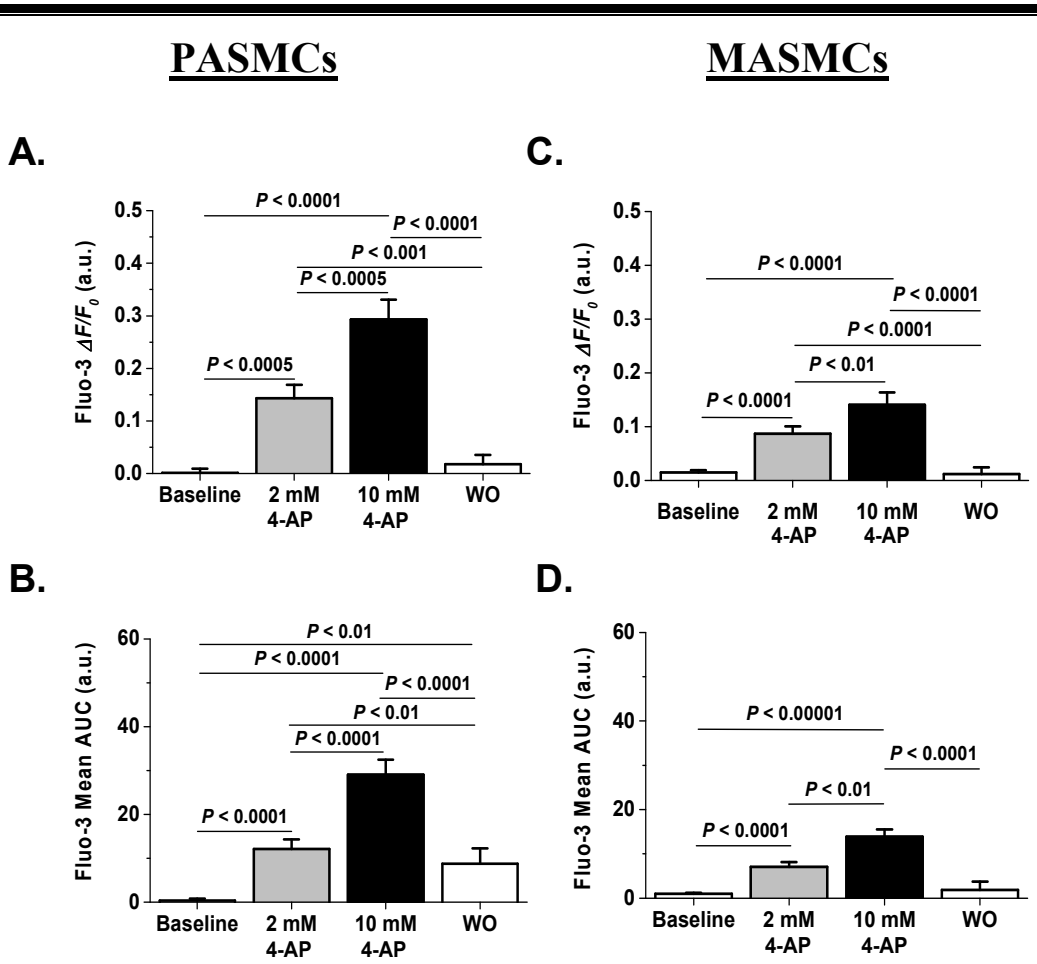

Figure 3.12 Comparison of the effect of K_V channel inhibitors on $[Ca^{2+}]_i$ in isolated PASMCs and MASMCs.

To analyse the differences statistically two approaches were used. Firstly, fluorescent intensities (averaged at the end of each treatment in each cell) were averaged and statistically compared for 22 PASMCs (A) and 41 MASMCs (C). Secondly, fluorescent intensities were taken as area under the curve (AUC) in each cell for the duration of each treatment, averaged and compared in B and D for PASMCs and MASMCs, respectively. Note that the two types of analysis gave similar results.

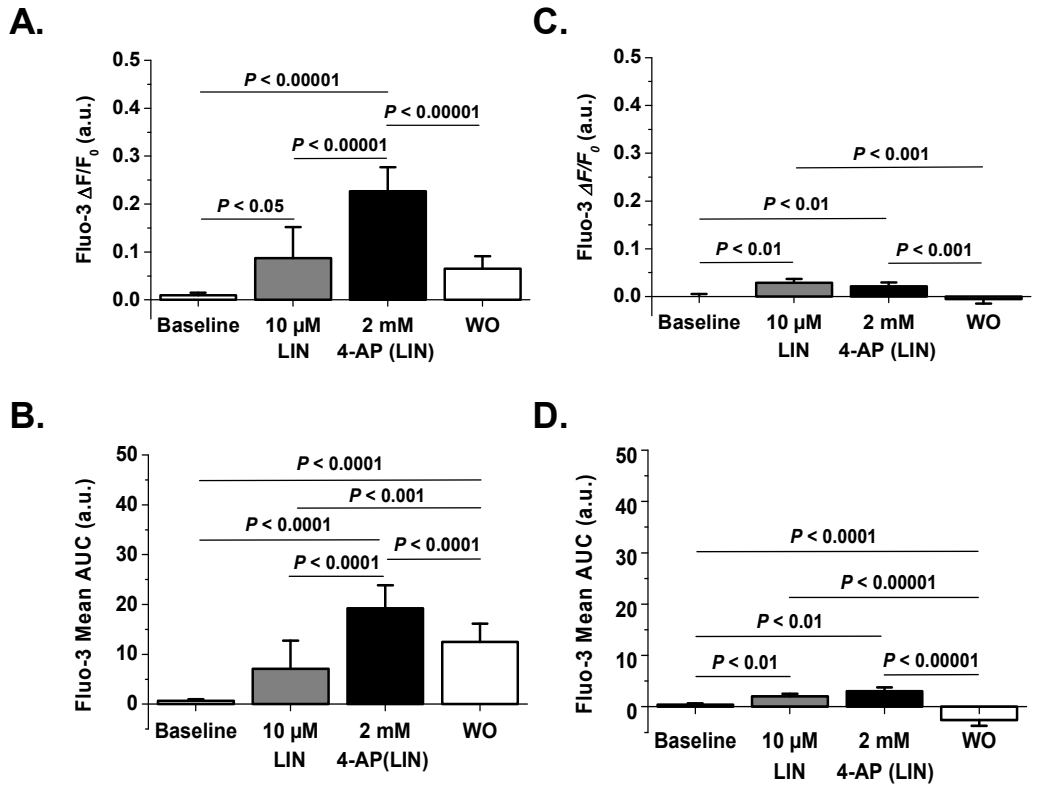

Figure 3.13 Comparison of the effect of K_V and KCNQ channels inhibitors on $[Ca^{2+}]_i$ in isolated PASMCs and MASMCs.

The experimental protocol was identical to that described in Fig. 3.10 and 3.11 except that 10 μM linopirdine and 2 mM 4-AP were respectively used instead of 2 and 10 mM 4-AP. To analyse the differences statistically two approaches were used in a same way as described in Fig. 3.12, using averaged fluorescent intensities (A and C) and the mean area under the curve (AUC) (B and D) for 42 PASMCs and 65 MASMCs, respectively. Note, no qualitative differences were observed between the two types of analysis.

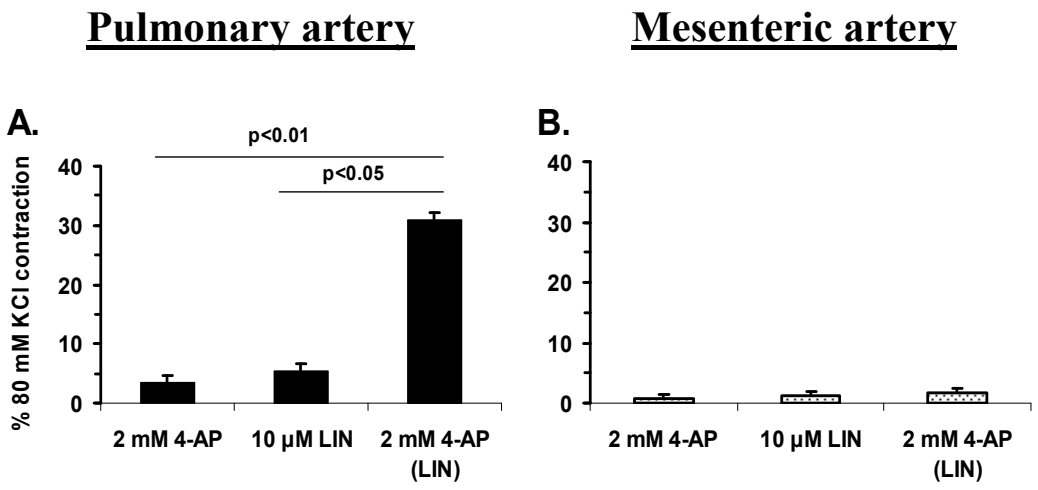

Figure 3.14 Comparison of the contractions induced by low concentration of 4-AP in the presence of linopirdine between rat PA and MA.

A and B compare the effect of pretreatment with 10 µM linopirdine on 2 mM 4-AP-induced contractions in intact PA and MA, respectively. Tension produced by 2 mM 4-AP alone and 10 µM linopirdine alone are also shown for comparison. LIN, 10µM linopirdine. Differences between groups were tested by Tukey-Kramer post-hoc test following one-way ANOVA, $n = 8$.

Functional studies of intact artery rings using wire myograph reveals that the effect of linopirdine pretreatment on low concentration (2 mM) of 4-AP-induced contraction matches the above imaging data specifically in the PA (Fig. 3.14 A). In intact MA however the pretreatment with linopirdine did not potentiate the contraction induced by 2 mM 4-AP (Fig. 3.14 B), which may be due to the fact that isolated cells are generally more depolarised, than intact tissue preparations.

3.2.4 Time-dependent potentiation of 4-AP responses: a comparison between rat PA and MA

During experiments with repetitive applications of 4-AP, time-dependent potentiation of 4-AP-induced contraction was observed specifically in MA and not in PA. This effect was consistently observed, for example, during 3rd application of 4-AP (*recovery*) compared to the first application (*control*) in the studies of the effect of L-VOCC blocker and Rho-kinase inhibitor where 3 consequent applications of 4-AP (in combination with 20 mM KCl or 10 μM linopirdine) were used: control, during treatment and recovery. Time-dependent potentiation was independent on the way the tissue was preconstricted and observed for both 20 mM KCl + 10 mM 4-AP (Figures 3.15 and 3.16) and 10 μM linopirdine + 10 mM 4-AP (Figures 3.17 and 3.18). This effect was not due to drug treatment, as in a separate series of experiments (n = 2) where 3 subsequent applications of linopirdine+4-AP or 20 mM KCl+4-AP were assessed, similar potentiation of the 4-AP-induced contraction was observed.

In this section I characterise this effect and compare the effect of 4-AP during its 1st (*control*) and during its 3rd (*recovery*) application in the presence of either 20 mM KCl (Fig. 3.15) or 10 μM linopirdine (Fig. 3.17) were compared with those following the *recovery*. Figures 3.16 and 3.18 summarise and statistically compare the responses. The effect of 10 mM 4-AP alone in both tissues is also shown for comparison. Although the exact reason(s) for this phenomenon is not clear, one may speculate that availability of K_V channels is becoming greater with time (perhaps due to tissue depolarisation). This is supported by the observation that the effects of 20 mM KCl and 10 μM linopirdine were not significantly different. Further studies with membrane voltage (V_m) measurements will be needed to clarify this question.

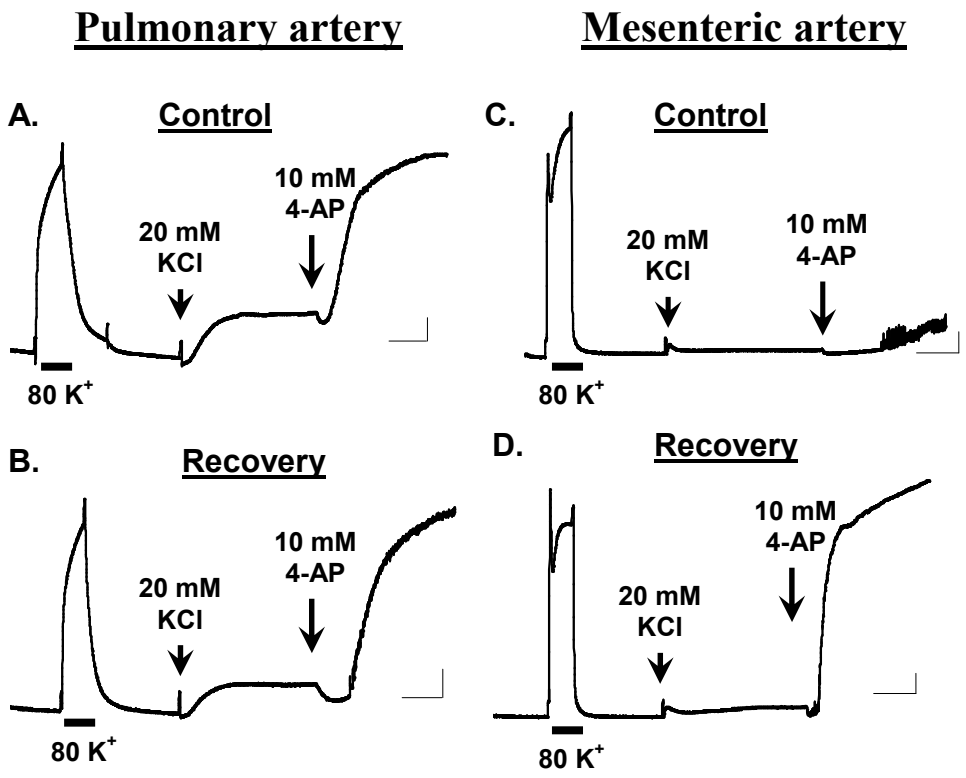

Figure 3.15 Time-dependent potentiation of 4-AP responses in the presence of 20 mM KCl in rat PA and MA.

Representative traces obtained from PA of 593 μm i.d. (A-B) and MA of 270 μm i.d. (C-D) show the control and recovery responses to 4-AP in the presence of 20 mM KCl. Note, a significant potentiation in the recovery response in MA (D) and not in PA (B). Horizontal and vertical scale bars represent 5 min and 1 mN, respectively.

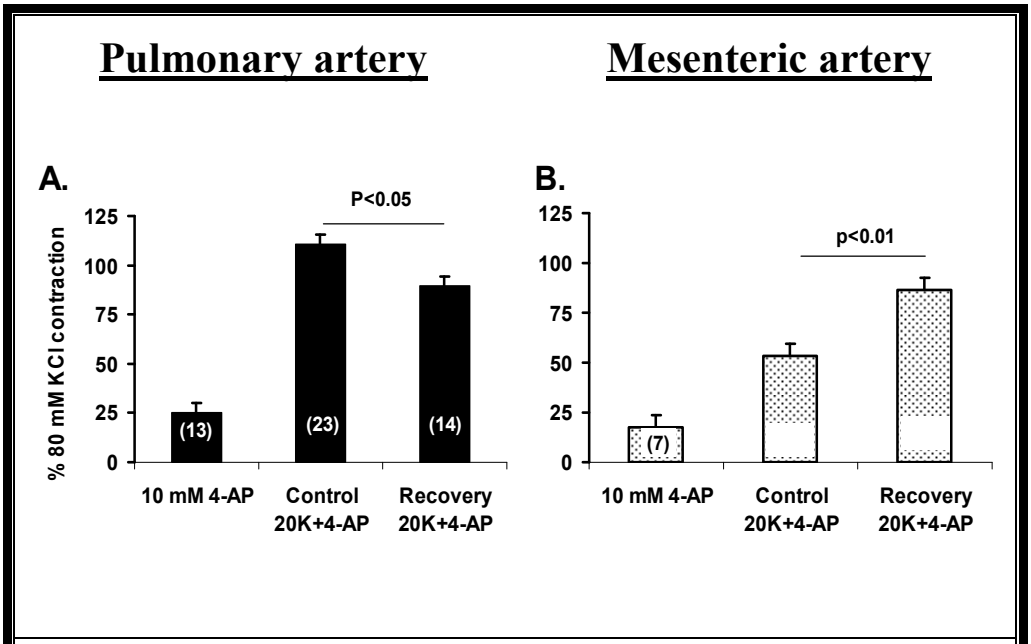

Figure 3.16 Comparison of the time-dependent potentiation of 20 mM KCl and 4-AP-induced responses between rat PA and MA.

The graphs summarise and compare the time-dependent potentiation of 4-AP responses in PA and MA in the presence of 20 mM KCl. No potentiation, rather significant decrease in recovery tension was observed in PA (A) while significant potentiation in recovery tension was observed in MA (B). The mean response to 10 mM 4-AP alone is shown for comparison. Unpaired Student's *t*-test. Respective *n* values are shown on the graphs.

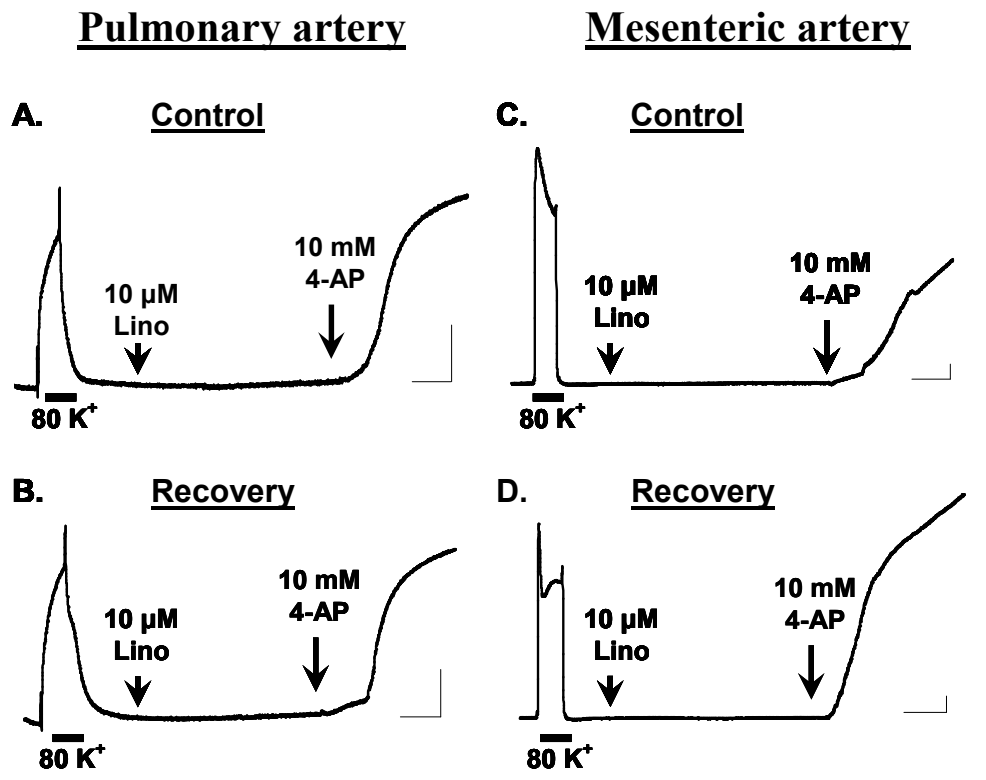

Figure 3.17 Time-dependent potentiation of 4-AP responses in the presence of 10 µM linopirdine in rat PA and MA.

Representative traces obtained from PA of 324 µm i.d. (A-B) and MA of 259 µm i.d. (C-D) show the control and recovery responses to 4-AP in the presence of 10 µM linopirdine. Note, a significant potentiation in the recovery response in MA (D) and not in PA (B). Horizontal and vertical scale bars represent 5 min and 1 mN, respectively.

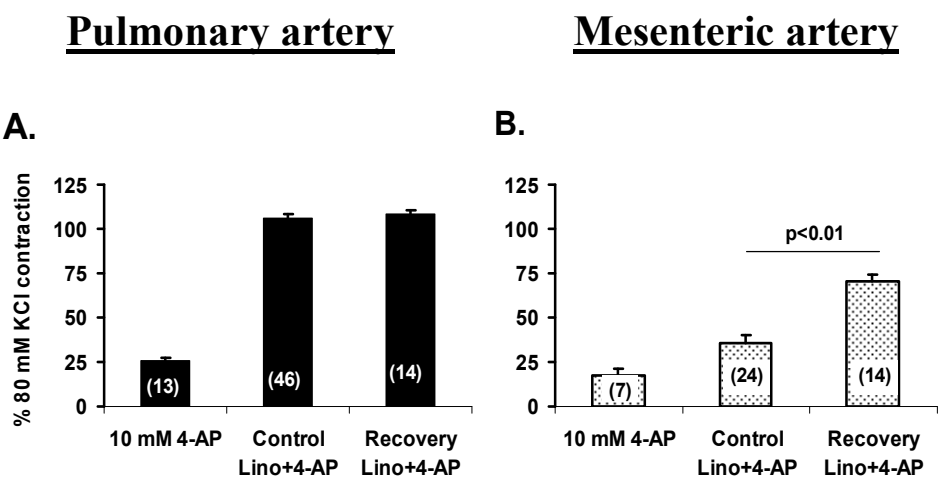

Figure 3.18 Comparison of the time-dependent potentiation of linopirdine and 4-AP-induced responses between rat PA and MA.

The graphs summarise and compare the time-dependent potentiation of 4-AP responses in PA (A) and MA (B) in the presence of 10 μM linopirdine. No potentiation was observed in PA (A) but only in MA (B). The mean response to 10 mM 4-AP alone is shown for comparison. Unpaired Student's *t*-test. Respective *n* values are shown on the graphs.

3.3 Discussion

The main findings of this chapter can be summarised as:

1) K_V and KCNQ channels differently contribute to the regulation of the basal tone in pulmonary and systemic mesenteric arteries, with significantly less contribution in the latter. In pulmonary artery, both K_V and KCNQ channels play role to maintain low resistance and low contractile state in rest.

2) In the regulation of resting membrane potential, K_V and KCNQ channels play a greater role in pulmonary than in mesenteric artery. Significant correlation between membrane potential and force of contraction was observed in both pulmonary and mesenteric artery.

3) Consistent with the ability of the K_V and KCNQ channel inhibitors to produce more depolarisation in pulmonary than in mesenteric artery, it was observed that the inhibition of K_V and KCNQ channels leads to a significantly higher level of $[Ca^{2+}]_i$ increases in isolated PASMCs than in MASMCs.

4) Time-dependent potentiation of 4-AP-induced responses was absent in pulmonary but significant potentiation observed in mesenteric artery.

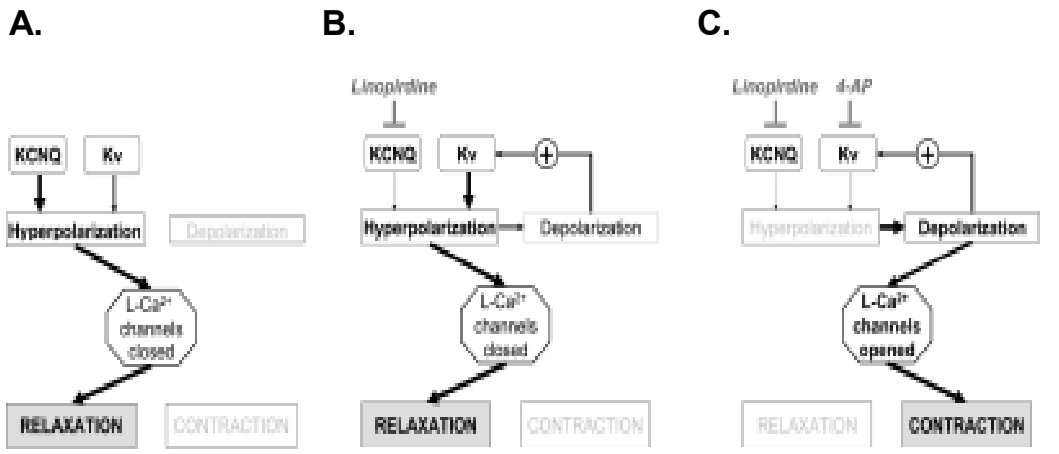

Figure 3.19 Physiological interaction between K_V and KCNQ channels in pulmonary artery.

A) Both K_V and KCNQ are active at rest keeping the cell membrane hyperpolarised. B) Inhibition of KCNQ channels alone (e.g. with linopirdine) will promote activation of K_V channels, which in turn will maintain the cell membrane hyperpolarised. Likewise, inhibition of K_V channels alone (e.g. with low concentrations of 4-AP) may not be sufficient to cause significant contraction due to the background activity of KCNQ channels. C) Inhibition of both K_V and KCNQ channels removes these key hyperpolarising forces, causing depolarisation leading to nearly maximal contraction of the artery. Further explanations are in the text.

The results presented in this chapter demonstrate that both K_V and KCNQ channels are important in the regulation of the basal tone in PA. Although this has been hypothesised previously (Gurney *et al.*, 2010), here, for the first time, I demonstrated the reciprocal interaction between the K_V and KCNQ channels in controlling pulmonary vascular contractility. This is summarised in Fig 3.19. At rest, the activity of K_V and KCNQ channels keep the cell membrane hyperpolarised and the tissue is relaxed (Fig. 3.19 A). Inhibition of only KCNQ channels (e.g. with linopirdine as shown in Fig. 3.19 B) or, likewise, inhibition of

only K_V channels (e.g. with 4-AP) will cause only small, if any, depolarisation which may or may not be accompanied by a small contraction. This is likely to occur because the additional activation of K_V or KCNQ channels (both are voltage-dependent) will tend to stabilise the cell membrane at hyperpolarised levels. However, the combined inhibition of both K_V and KCNQ channels will eliminate these two key K^+ conductances leading to the development of nearly maximal contraction in PA (Fig. 3.19 C). Any depolarising stimulus (e.g. low concentrations of KCl used in this study or activation of Cl^- or non-selective cation conductance) will cause greater activation of K_V channels thus increasing a potency of the K_V channel inhibitors. Such interaction between the two types of K^+ channels will keep the cell membrane hyperpolarised, thus maintaining pulmonary arteries relaxed and pulmonary vascular resistance low, which is one of the main features of the pulmonary circulation.

The above proposed model, however, is not fully applicable for MA. The possible reasons could be: ***i)*** relatively small expression of K_V channel current in MA compared to that in PA (Firth *et al.*, 2009a), ***ii)*** K_V channels in MA are activated at more positive potentials compared to PA (Firth *et al.*, 2009a), ***iii)*** relatively small contribution of KCNQ channels (Joshi *et al.*, 2006), and ***iv)*** other K^+ conductance (e.g., BK_{Ca}) can be activated in the presence of combined action of KCNQ and K_V inhibitors (Asano & Nomura, 2002). All these factors keep MA in more hyperpolarised state resulting in lesser responsiveness to 4-AP and linopirdine compared to PA. Interestingly, with time the effect of 4-AP is enhanced in MA (the phenomenon of time-dependent potentiation of contraction), and in that case the proposed model is becoming applicable for MA too. It is may be possible that with time and during consecutive contractions, K_V channel activation is shifted to more negative potentials, leading to greater availability of K_V channels and hence greater contraction.

The above stated reciprocal relationship between the two channels is supported by the lack of each inhibitor to cause a significant contraction in intact PA when applied alone (Figures 3.5 and 3.6). Conversely, when added together, they induced the contraction which was comparable to that produced by 80 mM KCl. In addition, combination of the two inhibitors produced larger membrane

depolarisation compared to that produced by each blocker alone (Fig. 3.8). The ability of linopirdine to enhance the effect of a low concentration of 4-AP on $[Ca^{2+}]_i$ and tension development (Fig. 3.13 and 3.14, respectively) is also supportive. On the other hand, the important contribution of the K_V channels to the regulation of the resting tone in PA is supported by the ability of high concentrations of 4-AP to cause significant contraction (Figures 3.1 A and 3.2 A). The ability of 20 mM KCl (which would be expected to cause depolarisation of the cell membrane by ~39.66 mV according to the Goldman equation) to enhance the contraction to various concentrations of 4-AP in a similar manner as does linopirdine is also consistent with the presence of active 4-AP-sensitive K_V channels. Finally, 4-AP at 10 mM alone caused larger membrane depolarisation (Fig. 3.8 A) and larger increases in $[Ca^{2+}]_i$ (Fig. 3.12) compared to that seen with the KCNQ channel inhibitor alone.

The role of both channels in the regulation of the cell resting potential is also supported by the electrophysiological measurements of the KCNQ and K_V channel currents at negative voltages in PASMCs indicating that they might be comparable in sizes. For example, using selective KCNQ activator retigabine a significant increase of 24 pA in the whole-cell current in PASMCs was observed in the negative voltages between -60 and -40 mV (Joshi *et al.*, 2009). Smirnov *et al.* has previously demonstrated similar size of K_V current in normoxic PASMCs (Smirnov *et al.*, 1994).

It is noteworthy that the level of contraction caused by 10 μM linopirdine (0.53±0.07 mN or 14.6±2.4% of 80 mM KCl) in PA is overall substantially lower than that reported by Joshi *et al.* in similar preparation (~2 mN or ~85% of 50 mM KCl) (Joshi *et al.*, 2006). This discrepancy is likely due to differences in the experimental conditions used in my and Joshi *et al.*'s study. Firstly, the resting tension was set at 5 mN (Joshi *et al*.) compared to 1-2 mN (my study). It is possible that high resting tension can activate stretch-activated non-selective channels (Kirber *et al.*, 2000) promoting greater depolarisation. Secondly, Joshi *et al.* used HEPES-based buffer, whereas bicarbonate buffer was used in my experiments. Indeed when I used HEPES buffer in one experiment 10 μM linopirdine caused contraction as big as 65% of 80 mM KCl, which is comparable

to that reported by Joshi *et al.* It is apparent that both factors are contributive to the difference, between the two studies, however further experiments are necessary to clarify the exact mechanisms behind these differences.

In MA, used in this study as a representative of the systemic circulation, increasing concentrations of 4-AP had a significantly smaller effect than in PA either in the control conditions or in the presence of 20 mM KCl or linopirdine (Figures 3.1-3.3 and 3.5-3.6), suggesting that it is not only due to the lack of KCNQ channels in MA but also due to relatively less contribution of 4-AP sensitive K_V channels. One of the contributing factors could be the differences in the expression of functional K_V channels in MA compared to PA (Firth *et al.*, 2009a). In addition, the K_V current in rat MASMCs is activated at more positive voltages than that in PASMCs (Firth *et al.*, 2009a). Another factor could be activation of other K^+ conductances, e.g. BK_{Ca} channels (Asano & Nomura, 2002). The latter might be activated by membrane depolarisation in the presence of either inhibitor (Fig. 3.8) thus limiting vasoconstriction in MA compared to PA.

Interestingly, in MA subsequent applications of 10 mM 4-AP either in the presence of 20 mM KCl or 10 μM linopirdine resulted in time-dependent increases in 4-AP-induced contraction. Such potentiation however was not observed in PA (Figures 3.15-3.18). The phenomenon of potentiation of 4-AP-induced contraction is interesting and to the best of my knowledge has not been previously reported. As the relaxation of 4-AP-induced contractions to diltiazem and Y-27632 was not apparently affected with time, it is likely that the number of K_V channels becoming increasingly available in this tissue with time. Further work is required to identify the exact mechanisms responsible for this potentiation. Although the exact mechanism for this effect is currently not known, it may contribute to the increased sensitivity of isolated MASMCs to 4-AP in calcium measurements (Fig. 3.12) compared to contractile responses measured in intact arteries (Figures 3.1-3.3 and 3.5-3.6). The less significant effect of 4-AP in the presence of linopirdine in MA is also consistent with previous observations where KCNQ channel blockers were less potent in MA in comparison to PA (Joshi *et al.*, 2006).

The proposed model of interaction between the two channels could also explain an increased sensitivity of intact PA isolated from chronic hypoxic animals to low concentrations of 4-AP (Doggrell *et al.*, 1999;Bonnet *et al.*, 2002). It is well documented that chronic hypoxia is associated with membrane depolarisation which will lead to augmented availability of 4-AP-sensitive K_V channels despite the fact that the expression of K_V channels is decreased under such conditions (Smirnov *et al.*, 1994;Osipenko *et al.*, 1998;Platoshyn *et al.*, 2001).

One of the critical points could be the use of 4-AP as the inhibitor of K_V channels. 4-AP is considered as non-selective inhibitor which may cause other effects (Petkova-Kirova *et al.*, 2000). However, the use of the same experimental design, when recordings were made from both PA and MA simultaneously under the same experimental conditions, argues against such possibility. Similar correlation between the force of contraction and membrane depolarisation depicted in Fig. 3.9 also argues against the non-specificity of 4-AP in my experimental settings. Furthermore, tissue pretreatment with 10 μM diltiazem virtually eliminated 4-AP-induced contractions in both preparations. I have also used correolide, a selective K_V1 type channel inhibitor, at concentrations up to 20 μM. However it was able to produce only ~0.2 mN force in PA (n = 2; data not shown). This value is similar to that seen at 100 μM correolide in resistance PA reported previously by Archer and colleagues (Archer *et al.*, 2004). No significant effect of correolide on contraction was observed in MA in my experimental conditions. One of the reasons for the difference between 4-AP and correolide could be in the time course of the onset of their action. Depolarisation increases the effectiveness of 4-AP because 4-AP is an open channel blocker and will effectively and potently inhibit all open K_V channels (Armstrong & Loboda, 2001). This notion is also supported by my experimental evidence. Correolide however is a slow acting blocker (Koo *et al.*, 1999) and does not completely eliminate K_V channel currents in PASMCs even at 10 μM (Dr. Smirnov's unpublished observations). Thus, very slow onset of action (>20 min) and recovery made this blocker unsuitable for the purpose of this study in characterisation of K_V channels. Therefore, 4-AP represents an adequate and useful pharmacological tool to investigate the role of K_V channels in intact preparations.

The proposed model of the interaction between two channel types, in addition to providing the basic understanding of pulmonary function, can also serve as a useful experimental tool to investigate a relative contribution of the two types of channels in the HPV response.

In this chapter it has been established that both KCNQ and K_V channels are essential for maintenance of PA in low contractile state. Using this experimental approach, I have then tested the hypothesis whether KCNQ channels are inhibited by hypoxia in intact PA, which will be presented in Chapter 4.

Chapter 4

THE ROLE OF K_V AND KCNQ CHANNELS IN HYPOXIA-INDUCED RAT PULMONARY AND SYSTEMIC VASOCONSTRICTION

4.1 Introduction

In resistance intra pulmonary artery of the rat, acute hypoxic response is biphasic in nature consisting of an initial transient contraction (phase-I) followed by a slowly developing sustained contraction (phase-II) (Kovitz *et al.*, 1993;Leach *et al.*, 1994;Lazor *et al.*, 1996;Leach *et al.*, 2000;Robertson *et al.*, 2000a;Robertson *et al.*, 2000b;Dipp *et al.*, 2001). The phase-II contraction is entirely dependent on the presence of intact endothelium (Leach *et al.*, 1994;Robertson *et al.*, 2003) but was not inhibited by nitric oxide synthase (NOS) inhibitors (Leach *et al.*, 1994). In isolated rat small MA, which is widely used as a representative of the systemic circulation, the transient phase-I contraction was observed in response to hypoxia under similar experimental conditions followed by vasodilation instead of contraction observed in contrast to the PA (Leach *et al.*, 1994).

It is generally agreed that HPV is triggered by an increase in $[Ca^{2+}]_i$ in the vascular smooth muscle cells via multiple mechanisms (Ward & Aaronson, 1999;Weissmann *et al.*, 2001;Gurney, 2002;Ward & McMurtry, 2009). The hypoxia-dependent increase in $[Ca^{2+}]_i$ has two components: an initial Ca^{2+} release from intracellular stores followed by Ca^{2+} influx from the extracellular compartment via voltage -dependent and -independent mechanisms (Means, 1994;Abe *et al.*, 1996;Ward & McMurtry, 2009). The importance of the elevated $[Ca^{2+}]_i$ for HPV is supported by the observation that a small degree of pretone

(which is independent of the type of vasoconstrictor used, e.g., high K^+, $PGF_{2\alpha}$ or U-46619) was often required to obtain a reproducible HPV response (Leach *et al.*, 1994;Ward & Robertson, 1995;Ozaki *et al.*, 1998;Robertson *et al.*, 2000b). Although the exact reason is not clear, moderate elevation of $[Ca^{2+}]_i$ is apparently necessary for initiation of the HPV response, hence the requirement for a pretone.

A significant body of evidence suggest that hypoxia-induced Ca^{2+} release from intracellular stores is an early and essential event required for initiation of HPV (Jabr *et al.*, 1997;Dipp *et al.*, 2001;Morio & McMurtry, 2002). Ca^{2+} being released from intracellular stores activates SOCCs and capacitative Ca^{2+} entry (CCE) in PASMCs (Robertson *et al.*, 2000b;McDaniel *et al.*, 2001;Wilson *et al.*, 2001;Snetkov *et al.*, 2003;Wang *et al.*, 2004).

On the other hand, it is well known that blockers of L-VOCCs suppress HPV as well as the associated rise in $[Ca^{2+}]_i$ (Salvaterra & Goldman, 1993;Vadula *et al.*, 1993;Cornfield *et al.*, 1994;Leach *et al.*, 1994), supporting the hypothesis that L-VOCCs play an important role in the initiation of the HPV response. Membrane depolarisation can be triggered by the inhibition of K^+ channels; as well as by activation of non-selective cation channels involved in CCE and by Ca^{2+}-activated chloride channels. Hypoxia-dependent inhibition of K_V channels is well documented (Weir & Archer, 1995;Olschewski *et al.*, 2002;Archer & Michelakis, 2002). K_V channels are the most abundant type of K^+ channels and an important contributor to the resting membrane potential in the pulmonary vasculature (Archer *et al.*, 1993;Smirnov *et al.*, 1994;Yuan, 1995;Smirnov *et al.*, 2002;Olschewski *et al.*, 2002;Archer *et al.*, 2004). The K_V channel currents in PASMCs are also inhibited by hypoxia (Post *et al.*, 1992;Archer *et al.*, 1993;Weir & Archer, 1995;Olschewski *et al.*, 2002;Archer & Michelakis, 2002;Platoshyn *et al.*, 2006) and therefore can contribute to membrane depolarisation and activation of L-VOCCs.

Another type of voltage-gated K^+ channels, KCNQ, is recently recognised to be also important in the regulation of resting membrane potential in vascular smooth muscle cells (Yeung & Greenwood, 2005;Brueggemann *et al.*, 2007;Yeung *et al.*, 2007;Yeung *et al.*, 2008;Mackie *et al.*, 2008) including PASMCs (Osipenko *et al.*,

1997;Joshi *et al.*, 2006;Joshi *et al.*, 2009). However, whether KCNQ channels can contribute to the HPV response has not been yet demonstrated. Furthermore, although the inhibition of K_V channels in the isolated pulmonary arterial cells has been well documented as mentioned above, their role in hypoxia-induced responses in intact pulmonary arteries remains largely unknown.

As described in the previous chapter, the combined use of linopirdine, a selective KCNQ channel blocker, and 4-AP, a selective K_V channel inhibitor, in intact tissue preparation allows the investigation of the contribution of K_V and KCNQ to excitability and contractility of intact pulmonary and mesenteric arteries. Here, I employed this approach to investigate the role of K_V and KCNQ channels in hypoxia-induced responses in intact pulmonary and mesenteric arteries of rat.

The main objectives of this chapter were:

- To investigate the relative sensitivity of K_V and KCNQ channels to hypoxia-induced responses in PA and MA.
- To compare the nature and extent of hypoxia-induced responses between PA and MA.

4.2 Methods

Contraction was measured using dual wire myograph as described in detail in Chapter 2. Hypoxia was induced by switching from the oxygen rich gas mixture of 95% O_2/5% CO_2 to nitrogen rich gas mixture of 95% N_2/5% CO_2 for 20 min followed by reoxygenation (when the effect of hypoxia was studied in the presence of vasoconstrictor or channel inhibitor) or by washing out the chamber with oxygenated PSS. The level of hypoxia was measured using an ISO_2 oxygen meter (WPI Incorporation, USA) in a separate set of experiments. The mean level of P_{O2} was 30±3 mmHg (n = 6, with variation ranging from 22-40 mmHg). During hypoxia experiments the chamber was covered with a plastic cover to minimise diffusion of ambient O_2. All experiments were performed in the presence of 100 μM L-NAME and 10 μM indomethacin. In a separate set of experiments with K^+ channel blockers hypoxia was continued for 60 min to investigate the effect of prolonged hypoxia on PA and MA under conditions when KCNQ and K_V channels were inhibited. Tissue was allowed at least 60 min to recover between hypoxic challenges (Leach *et al.*, 1994;Robertson *et al.*, 1995). Contractile responses were expressed as a percentage of the maximum tension obtained in response to 80 mM KCl (3 min) applied prior to the application of vasoconstrictors, channel blockers or hypoxia.

4.3 Results

4.3.1 Biphasic nature of hypoxia-induced vasoconstriction in isolated rat arteries in the presence of K^+ channel blockers

Following the application of KCNQ and K_V channel blockers (10 μM linopirdine and 2 mM 4-AP, respectively) the PA and MA were challenged simultaneously with hypoxia for 60 min. In this and the subsequent experiments (unless otherwise stated) low concentration of 4-AP (2 mM) was used instead of 10 mM to elicit a small pretone and thus leaving a potential room to observe further contraction in response to hypoxia for the investigation of its nature and extent. In both tissues, hypoxia produced two distinct phases of contraction: the initial transient phase-I contraction developed within first 5 to 6 minutes and then tissue was relaxed maximally in 10 to 15 minutes followed by a slowly developing phase-II contraction until the end of 60 min. The tissue was immediately relaxed to the pretone level upon re-oxygenation. The trend of hypoxic contraction in both PA and MA was similar although the level of contraction in MA was much less than that observed in PA. Also contraction during phase-II in MA was often associated with oscillations both in short exposure (20 min) to hypoxia (9 out of 13 experiments) as well long exposure to hypoxia (60 min). In both cases (short and long exposure) the oscillations usually started after the transient phase-I was subsided (i.e. 10-12 min after exposure to hypoxia). Such an oscillatory response is exemplified in Fig. 4.1 B. Here, however, I will be focussing mainly on phase-I where the role of K^+ channels has been implicated and also comparing the hypoxia-induced responses between PA and MA. Since the phase-I of hypoxic contraction subsided within 15 min; in the subsequent experiments the duration of the exposure to hypoxia was therefore limited to 20 min.

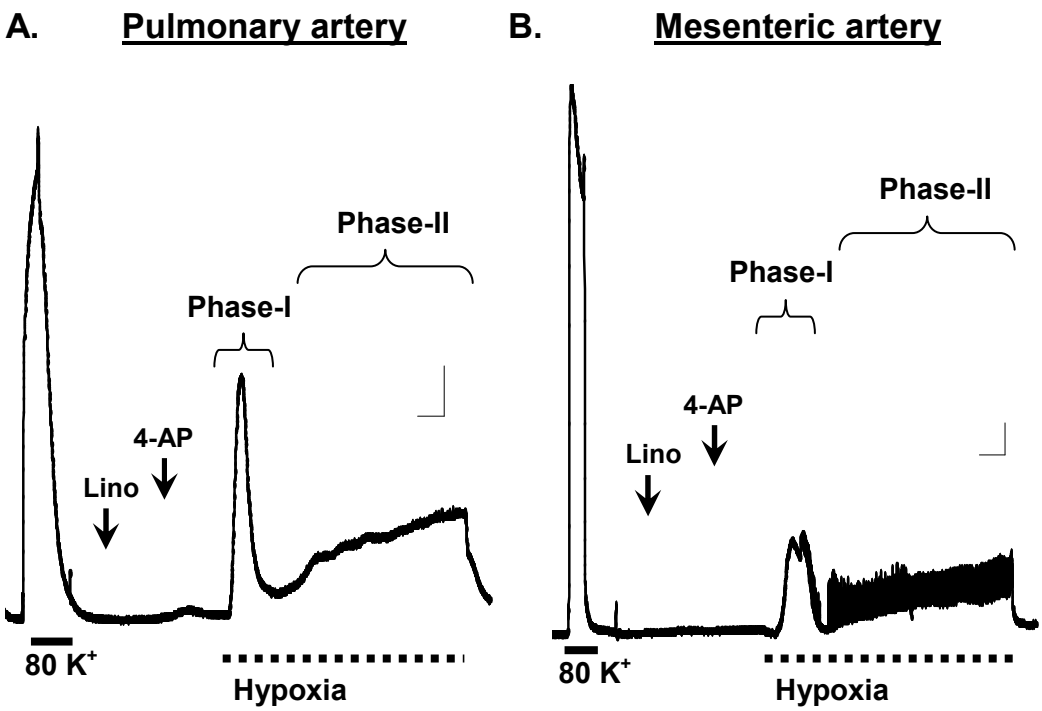

Figure 4.1 Typical biphasic responses of hypoxia-induced vasoconstriction in rat PA and MA.

Both in PA (A) and MA (B), hypoxia produced two distinct phases of contraction: the initial sharp contraction of phase-I followed by a slow and sustained phase-II. Representative traces were obtained from PA and MA of 276 and 242 μm internal diameters (i.d.), respectively. Lino, linopirdine (10 μM); 4-AP, 4-aminopyridine (2 mM); 80K+, 80 mM KCl. Horizontal and vertical scale bars represent 5 min and 1 mN, respectively.

4.3.2 Effects of K_V and KCNQ channel blockers on hypoxia-induced contraction in rat PA and MA

To evaluate the role of K_V and KCNQ channels, the effect of hypoxia was assessed in intact arteries in three different conditions: i) in the presence of 10 μM linopirdine to completely block the KCNQ channels, ii) in the presence of 2 mM 4-AP to partially inhibit K_V channels while leaving KCNQ channels intact, and iii) in the presence of both 10 μM linopirdine and 2 mM 4-AP to block both channel types in order to induce depolarisation and some level of constriction (pretone). In the presence of 2 mM 4-AP the balance between K_V and KCNQ channels will be shifted towards KCNQ channels (as described in the previous chapter). Thus, one would expect, if KCNQ channels are inhibited by hypoxia, then the HPV response will be greater in the presence of low concentration of 4-AP compared to the control.

Representative traces obtained from PA and MA are shown below in the Fig. 4.2. The mean absolute and normalised hypoxia-induced contractions in PA and MA are statistically compared in Fig. 4.3 A-D. In PAs, hypoxia alone produced a small sustained contraction which was only 0.4±0.1 mN (n = 8) (Fig. 4.3 A). A similar effect (0.4±0.05 mN, n = 4) was observed when hypoxia was applied following the pretreatment of the tissue with 2 mM 4-AP for 15 minutes (Fig. 4.3 A). Interestingly, the pretreatment of PA with 10 μM linopirdine for 20 min caused a transient hypoxia-induced contraction which was 3 times greater (1.2±0.3 mN, n = 4, Fig 4.3 A) compared to those measured in the absence of the inhibitors and in the presence of 4-AP, although this difference was not significant (one-way ANOVA). However, when the artery was pre-treated with a combination of linopirdine (10 μM for 20 min) followed by 4-AP (2 mM for 15 min), hypoxia caused a transient contraction with a peak of 4.4±0.7 mN (n = 6, Fig. 4.3 A), i.e., a response which was comparable to that evoked by 80 mM KCl (Fig. 4.2 D).

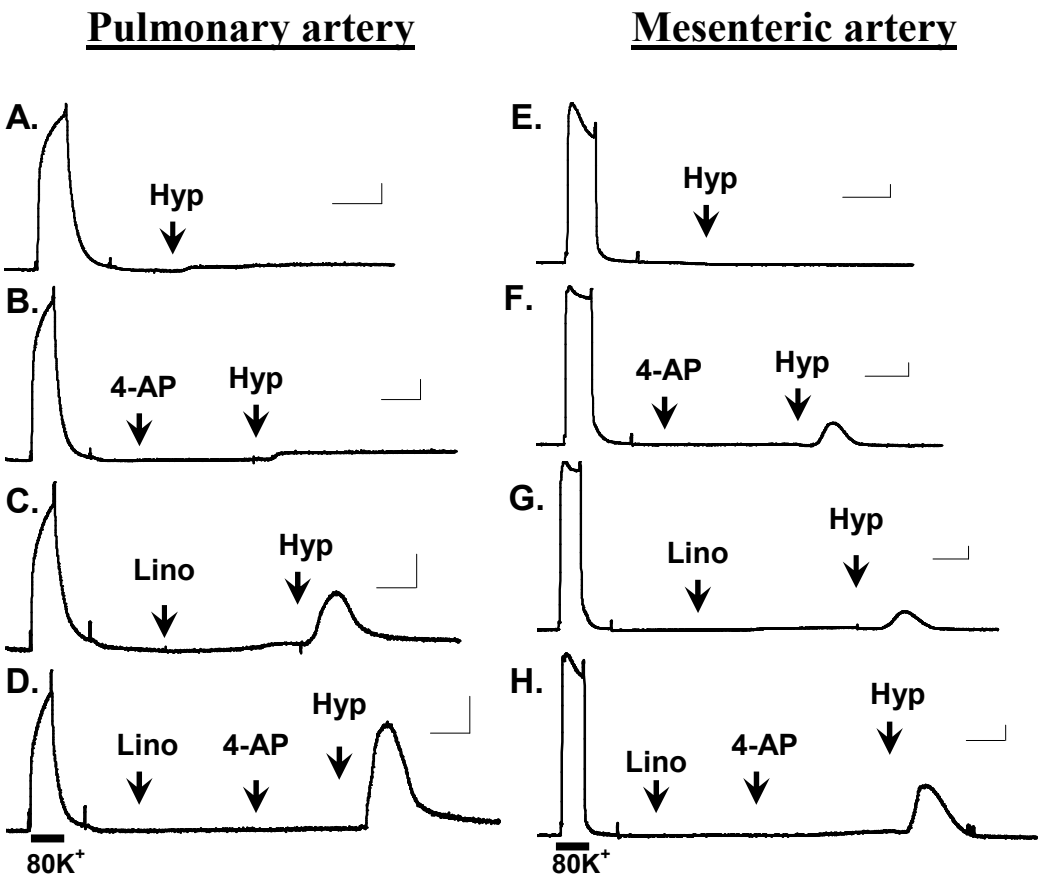

Figure 4.2 Effect of K_V and KCNQ channel blockers on hypoxia-induced vasoconstriction in rat PA and MA.

Representative traces showing the effect of hypoxia at different treatment conditions in PA (A-D) and MA (E-H). After obtaining the control hypoxia-induced responses (A and E), inhibitors were applied cumulatively as shown by arrows followed by hypoxia. A and B is from the same PA with an i.d. 309 μm while C and D is from a different PA with an i.d. 389 μm. Similarly, E & F is from the same MA with an i.d. 309 μm while G and H is from a different MA with an i.d. 314 μm. Hyp, hypoxia; 4-AP, 4-aminopyridine (2 mM); Lino, linopirdine (10 μM). Horizontal and vertical scale bars represent 5 min and 1 mN, respectively.

This effect was significantly greater than the responses measured in the control conditions (an increase by 12-fold, $p<0.001$), in the presence of 2 mM 4-AP (an increase by 11-fold, $p<0.001$), or 10 μM linopirdine (an increase by 4-fold, $p<0.001$) (Fig 4.3 A).

In MAs, on the other hand, hypoxia alone induced very little contraction of 0.03±0.02 mN (n = 8) (Fig. 4.3 C). However, in the presence of 2 mM 4-AP and 10 μM linopirdine alone, and linopirdine+4-AP, hypoxic response was increased to 1.3±0.7 mN (n = 4), 1.7±0.6 mN (n = 4) and 2.2±0.5 mN (n = 6), respectively (Fig. 4.3 C). Only in the combined presence of 4-AP and linopirdine, hypoxia caused a significant increase in tension compared to that in the absence of the inhibitors ($p<0.05$, Tukey-Kramer post-hoc test following one-way ANOVA; Fig. 4.3 C).

The MA has an ability to produce much greater contraction than PA, therefore a comparison between PA and MA based on normalised (to 80 K^+) contraction can provide a more valid assessment. When the tension was normalised to 80 K^+ to account for the difference between different treatments, similar differences were observed in PA but no difference was observed in MA (Fig. 4.3 B and D, respectively).

Notably, when comparing the hypoxic responses between PA and MA, statistical analysis (Bonferroni post-hoc test for comparison between selected pairs following one-way ANOVA) revealed that in the presence of 10 μM linopirdine and 2 mM 4-AP hypoxia produced significantly bigger responses in PA than in MA in both absolute (4.4±0.7 vs. 2.0±0.5 mN, respectively; n = 6, $p<0.01$) as well as normalised tension (70±10% vs. 10±4%, respectively; n = 6, $p<0.001$) (Fig. 4.3).

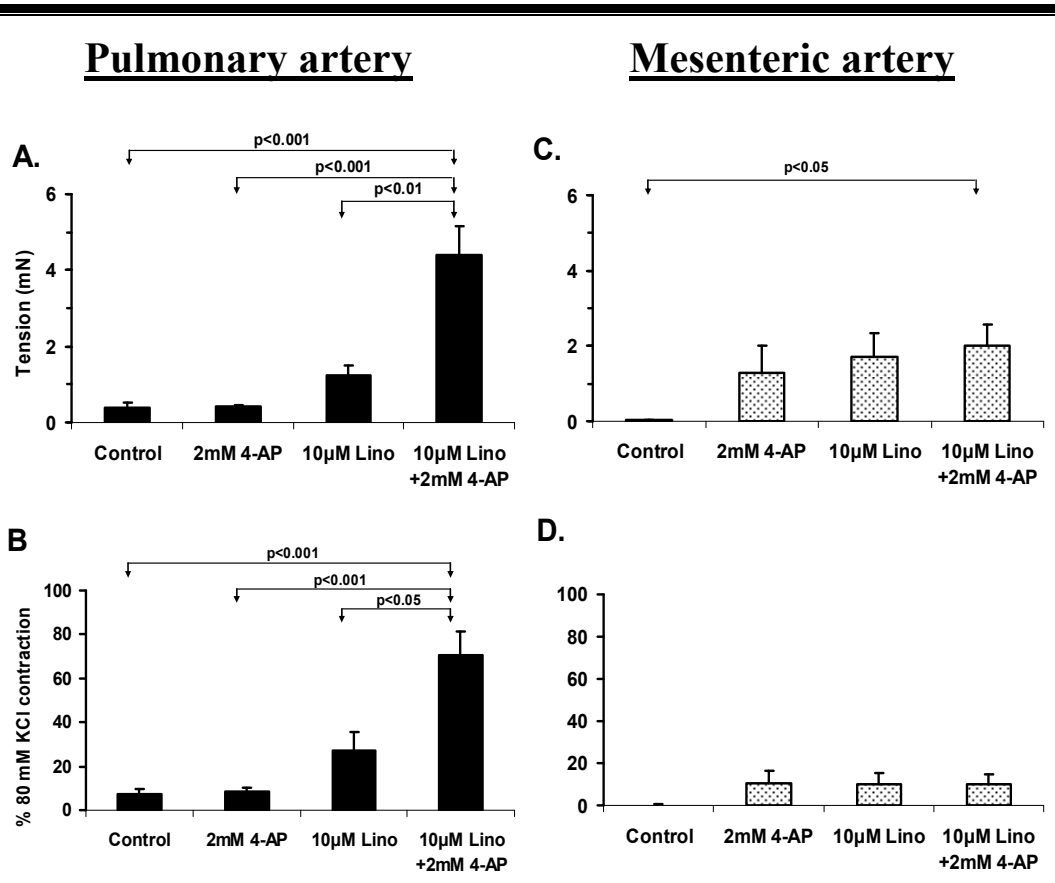

Figure 4.3 Effect of K_V and KCNQ channel blockers on hypoxia-induced vasoconstriction in rat PA and MA.

Absolute (A and C) and normalised (B and D) hypoxia-induced contractions in PA (A-B) and MA (C-D) in the presence of K^+ channel inhibitors. Lino, linopirdine; 4-AP, 4-aminopyridine. Differences between groups were tested by Tukey-Kramer post-hoc test following one-way ANOVA; n = 4-8.

4.3.3 Effect of pre-exposure to hypoxia on linopirdine and 4-AP-induced contraction in rat PA and MA

To investigate the effect of hypoxia on contraction under conditions when both KCNQ and K_V channels were virtually inhibited, linopirdine (10 μM) and 4-AP (10 mM) were used to block KCNQ and K_V channels, respectively. As the application of both inhibitors caused nearly maximal contraction, the following experimental protocol was applied. Both arteries were first treated with 10 μM linopirdine (20 min) followed by 10 mM 4-AP (15 min). The contraction thus recorded was used as a *control* response. Inhibitors were washed out until the baseline was restored. Both arteries were exposed to hypoxia for 20 min followed by the addition of the inhibitors in the same sequence and contraction was recorded as a *hypoxic response*. After at least 60 minutes of recovery period the first step was repeated and the response was recorded as a *recovery* response. Fig. 4.4 shows representative traces obtained from PA (A-C) and MA (D-F). Fig. 4.5 summarises the absolute and normalised results for PA (A-B) and MA (C-D). In PA, a combined application of 10 μM linopirdine and 10 mM 4-AP produced 5.0±0.9 (n = 6) mN tension in control which was reduced to 1.7±0.5 (n = 6) mN in hypoxia. Following wash-out and reoxygenation, the effect of hypoxia was nearly completely recovered (4.0±0.5 mN, n = 5). In this artery, hypoxia significantly reduced the contraction induced by the inhibitors compared to the control and recovery conditions (Fig 4.5 A). Similar significance was reached when the tension was normalised to 80 mM KCl contraction (Fig 4.5 B).

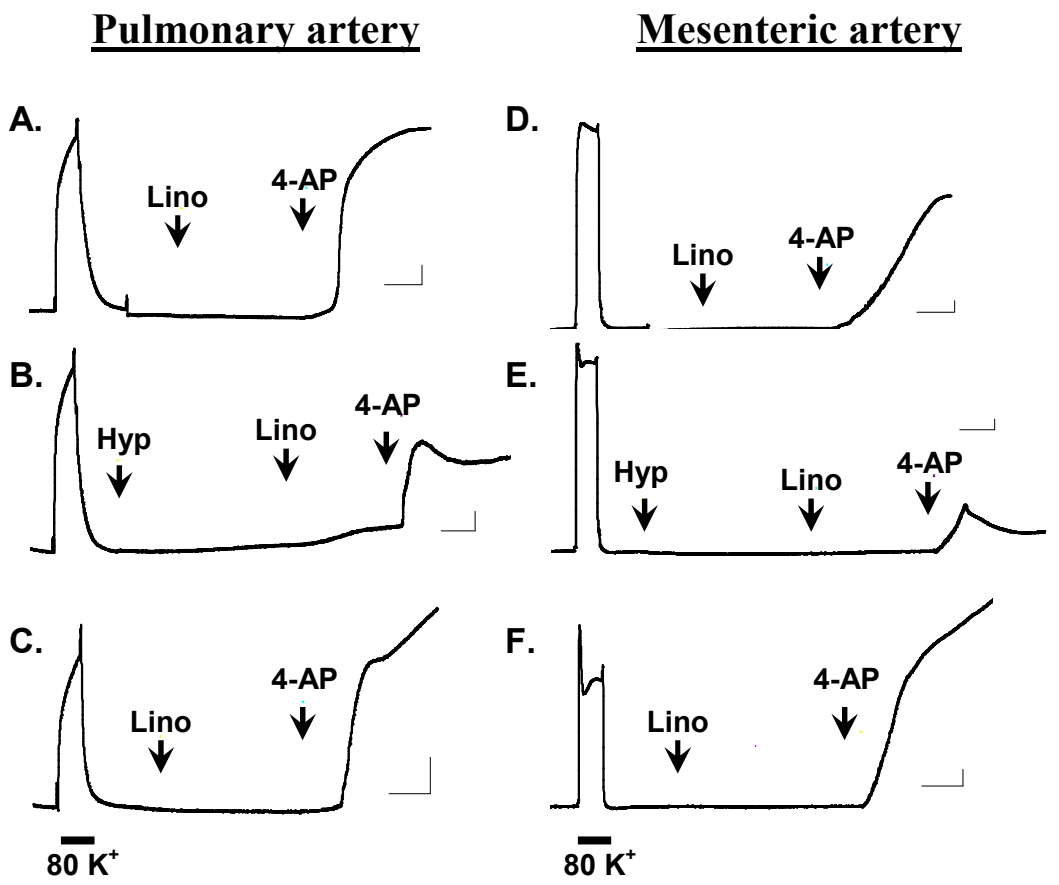

Figure 4.4 Effect of hypoxia on tension resulted from the inhibition of KCNQ and K_V channels in rat PA and MA.

Representative traces obtained from PA (A-C) of 305 μm i.d., and MA (D-F) of 199 μm i.d. show linopirdine+4-AP-induced contraction in control (A and D), in the presence of hypoxia (B and E) and after recovery from hypoxia (C and F). Note that as time of the exposure to inhibitors was limited (20 min for linopirdine and 15 min for 4-AP), some traces (e.g., C, D and F) did not reach a steady-state level. Lino, linopirdine (10 μM); 4-AP, 4-aminopyridine (10 mM); Hyp, hypoxia. Horizontal and vertical scale bars represent 5 min and 1 mN, respectively.

Under similar experimental conditions, the absolute tension in MA was also significantly reduced by hypoxia compared to the control run (from 7.4±1.3 mN to 1.3±0.5 mN, $n = 6$) (Fig. 4.5 C). The size of the contraction was recovered fully (7.4±2.0 mN, $n = 5$). The phenomenon termed 'time-dependent potentiation' described in previous chapter, could have contributed for the full recovery in this artery. Overall, in MA pre-exposure to hypoxia had a similar effect to that observed in PA on 4-AP-induced contraction, reducing significantly both absolute and normalised tension (Fig 4.5 C-D).

Interestingly, hypoxia potentiated linopirdine-induced contraction specifically in PA (Fig. 4.4 B). Pre-exposure to hypoxia for 20 min significantly potentiated linopirdine-induced contractions in PA from 1.4±1.1% (control) to 6.2±1.8% (hypoxic) ($n = 6$, $p<0.05$). However, in MA, no significant effect was observed (0.27±0.06% vs. 0.78±0.35% in control and hypoxic conditions, respectively; $n = 6$, $p>0.05$) (Fig. 4.6). As KCNQ channels should be completely blocked by 10 μM linopirdine, the increased in tension in the presence of KCNQ channel blocker is likely to be due to a greater availability of the K_V channels which are known to be blocked by hypoxia (Post *et al.*, 1992;Archer *et al.*, 1993;Weir & Archer, 1995;Olschewski *et al.*, 2002;Archer & Michelakis, 2002;Platoshyn *et al.*, 2006).

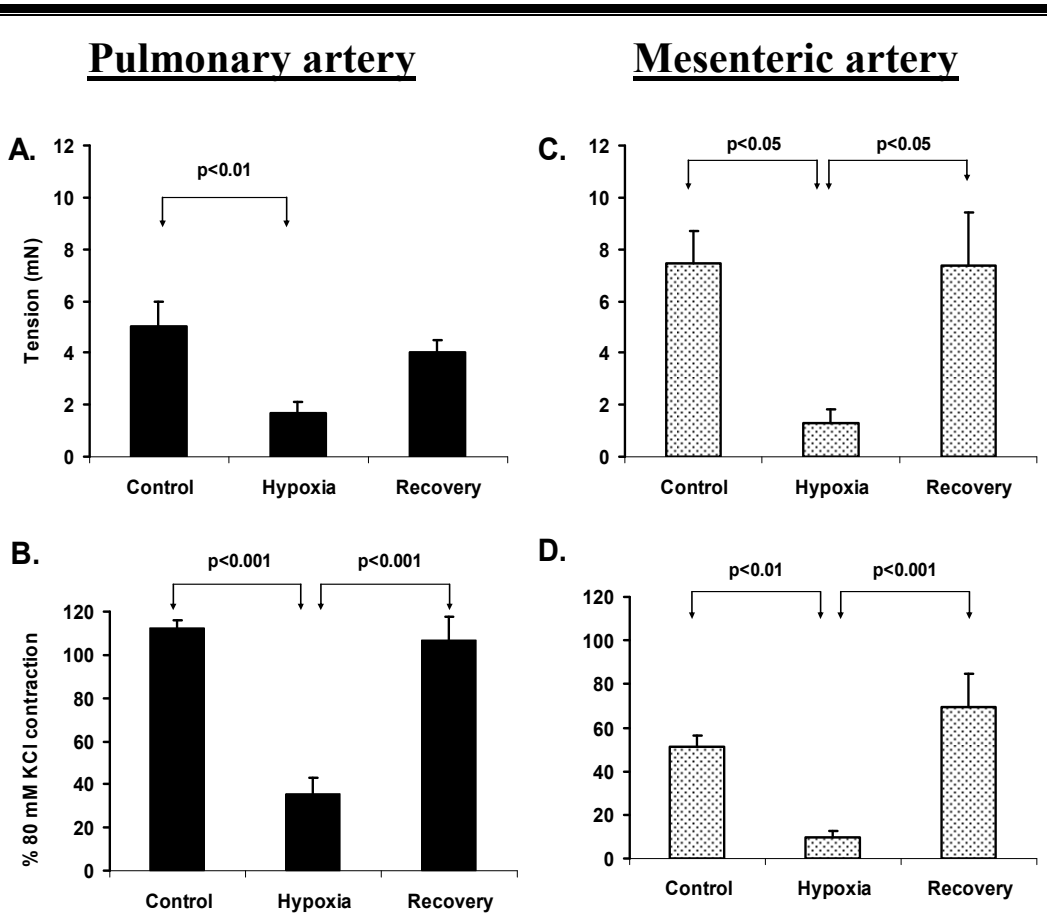

Figure 4.5 Hypoxia significantly blocks vasoconstriction induced by KCNQ and K_V channel blockers in rat PA and MA.

Graphs summarise and compare data obtained in control, hypoxic and recovery conditions in PA (A-B) and MA (C-D). A and C represent absolute tension, B and D represent normalised tension. Data were normalised to maximum contraction produced by 80 mM KCl applied prior to addition of inhibitors or hypoxia and expressed as a percentage of 80 mM KCl contraction. Differences between groups were tested by Tukey-Kramer post-hoc test following one-way ANOVA; n = 5-6.

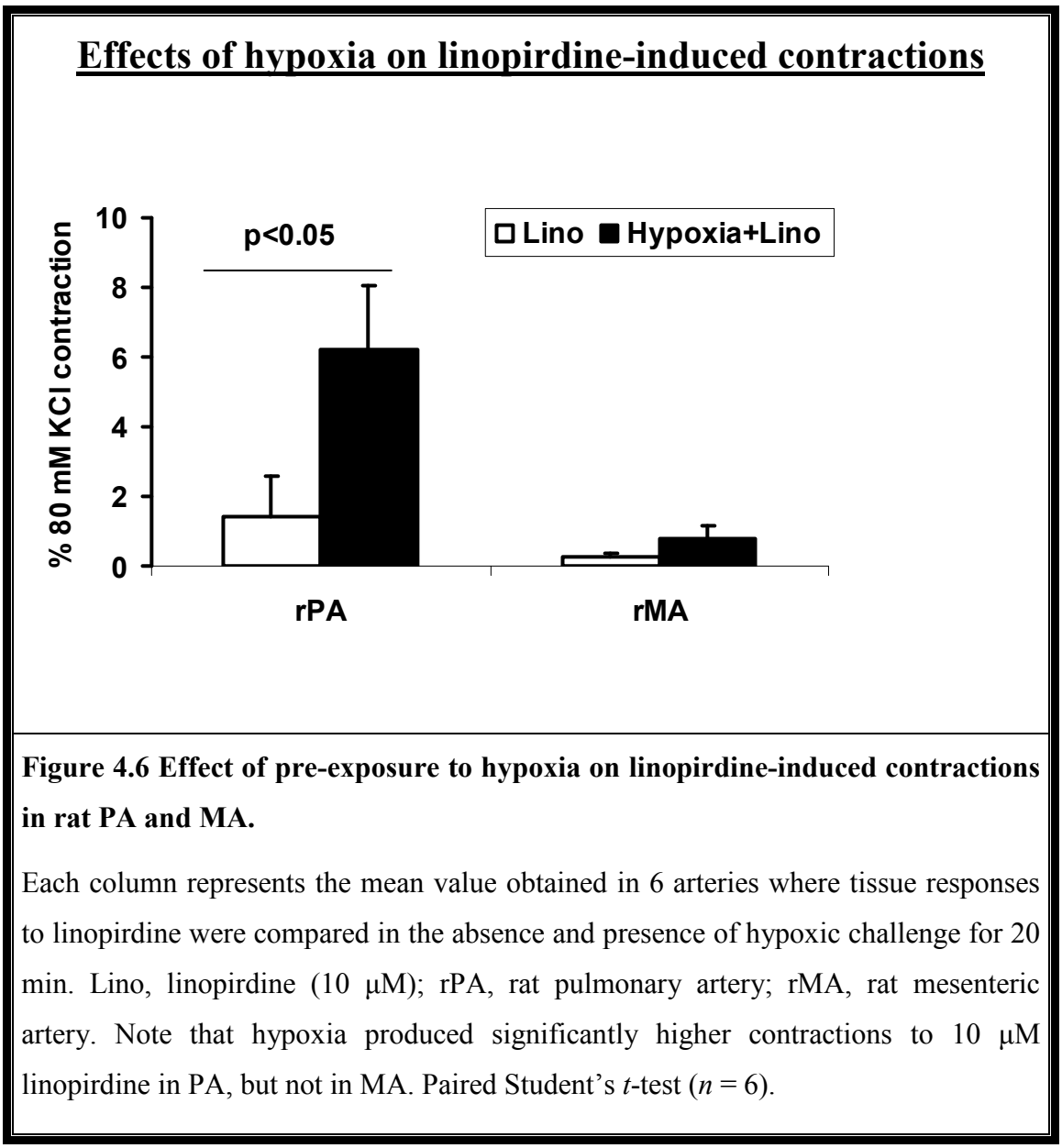

Figure 4.6 Effect of pre-exposure to hypoxia on linopirdine-induced contractions in rat PA and MA.

Each column represents the mean value obtained in 6 arteries where tissue responses to linopirdine were compared in the absence and presence of hypoxic challenge for 20 min. Lino, linopirdine (10 μM); rPA, rat pulmonary artery; rMA, rat mesenteric artery. Note that hypoxia produced significantly higher contractions to 10 μM linopirdine in PA, but not in MA. Paired Student's *t*-test ($n = 6$).

4.3.4 Hypoxia-induced contraction in the presence of thromboxane A_2 analogue U-46619 in rat PA and MA

Since I have demonstrated above that hypoxia in the presence of linopirdine and low concentration of 4-AP (which act via the voltage-dependent pathway) caused a transient hypoxic vasoconstriction in both PA and MA (Fig. 4.2 and 4.3), the effect of hypoxia was investigated in the presence of the stable thromboxane A_2 analogue U-46619 which is known to activate contraction via both voltage-independent and voltage-dependent pathways as well as by releasing Ca^{2+} from intracellular Ca^{2+} stores (Wilson *et al.*, 2005;Alapati *et al.*, 2007;McKenzie *et al.*, 2009).

Since a small degree of pretone of the intact tissue is known to enhance hypoxia-induced contraction (Leach *et al.*, 1994;Ward & Robertson, 1995;Ozaki *et al.*, 1998) and, also, the level of pretone has significant effect on the size of the subsequent hypoxic constrictor response (Rodman *et al.*, 1989;Ward & Robertson, 1995), it is therefore important to maintain the level of pretone constant by adjusting concentrations of agonist to provide adequate comparison between different protocols. In this set of experiments where U-46619 was used to elicit pretone, both diltiazem (used to block the voltage-dependent component of contraction to U-46619) and Y-27632 (used to inhibit a component of U-46619-induced contraction due to Ca^{2+} sensitisation) reduced the level of pretone. To adjust for that and to maintain a constant level of pretone, concentration of U-46619 was increased from 10 nM to 50 nM in experiments involving the use of diltiazem or Y-27632.

The experimental protocol was similar to that described in section 4.3.2. Hypoxia was applied for 20 min after obtaining a stable pretone with U-46619 applied for 20 min. Representative traces of such experiments are depicted in Fig. 4.7. It is noteworthy that hypoxia caused a transient contraction in both PA (Fig. 4.7 A) and in systemic MA (Fig. 4.7 D).

To explore a possible role of L-VOCC-mediated Ca^{2+} influx in these hypoxic responses in the presence of U-46619, arteries were pre-treated with the L-VOCC blocker diltiazem (10 μM) for 10 min prior to application of U-46619. Diltiazem was preferred to nifedipine because the former is readily reversible compared to the later. Diltiazem caused a significant attenuation of the peak hypoxic vasoconstriction by 47% in PA (mean 31.3±5.4 %, n = 5, $p<0.05$) compared to the control hypoxic response, whereas in MA this degree of inhibition was much greater, i.e. 90% (mean 85.1±2.8 %, n = 5, $p<0.05$) (traces in Fig. 4.7 B and E, respectively; summarised in Fig. 4.8).

The role of Rho-kinase in Ca^{2+} sensitisation is well known in vascular smooth muscle cells (Sauzeau *et al.*, 2000;Swärd *et al.*, 2000;Somlyo & Somlyo, 2003;Kizub *et al.*, 2010) and has also been implicated in HPV (Leach *et al.*, 1994;Robertson *et al.*, 1995;Robertson *et al.*, 2000a;Wang *et al.*, 2001;McMurtry *et al.*, 2003;Wang *et al.*, 2003b;Fagan *et al.*, 2004). To investigate whether Rho-kinase is involved in hypoxia-induced responses in the presence of U-46619, the specific inhibitor of Rho-kinase Y-27632 (10 μM) was applied for 10 minutes prior to addition of U-46619 followed by 20 min hypoxia. The effect of Y-27632 significantly reduced the hypoxic response by 67% (mean 75.6±3.4 %, n = 5, $p<0.001$) in PA and by 84% (mean 86.8±2.2 %, n = 5, $p<0.05$) in MA (traces in Fig. 4.7 C and F, respectively; summarised in Fig. 4.8).

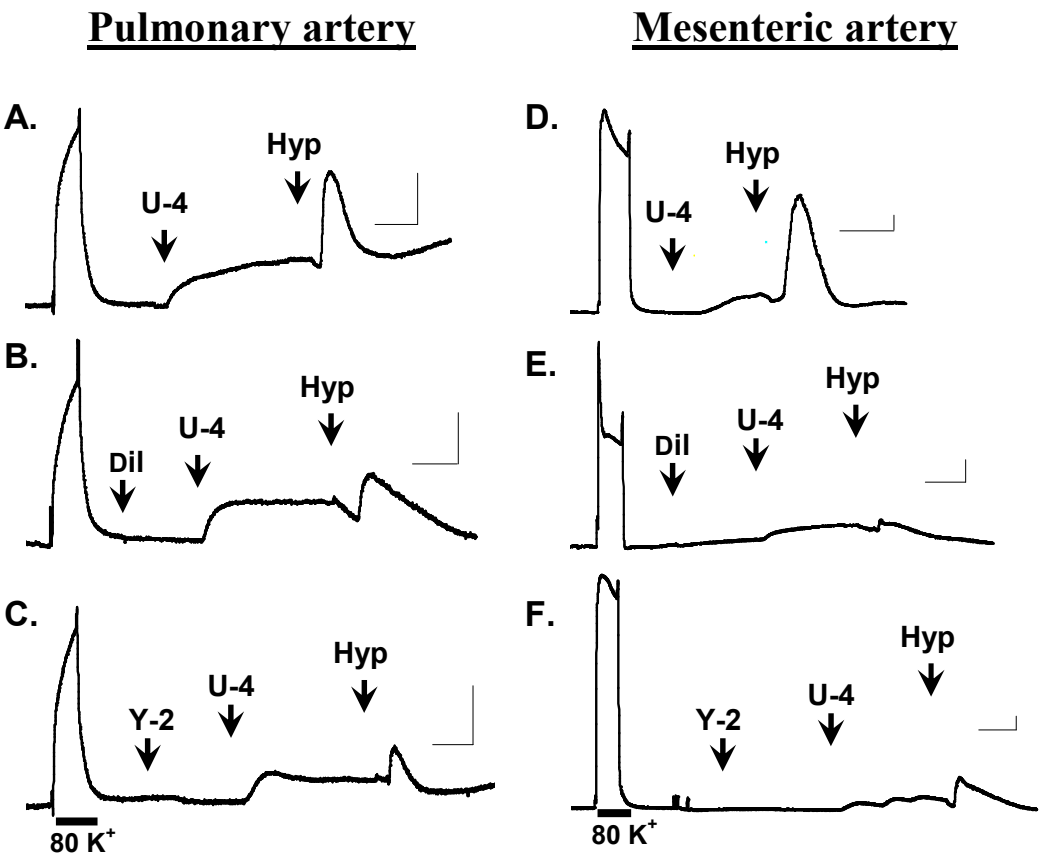

Figure 4. 7 Effect of hypoxia on U-46619-induced constriction: Role of Rho-kinase-mediated sensitisation and L-VOCC-mediated Ca^{2+} entry in rat PA and MA.

Representative tension recordings were obtained from PA (A-C) of 380, 377 and 380 μm i.d. and MA (D-F) of 243, 294 and 209 μm i.d., respectively. U-4, U-46619 (10 nM in A, D; 50 nM in B, C, E and F); Dil, diltiazem (10 μM); Y-2, Y-27632 (10 μM); Hyp, hypoxia. Horizontal and vertical scale bars represent 5 min and 1 mN, respectively.

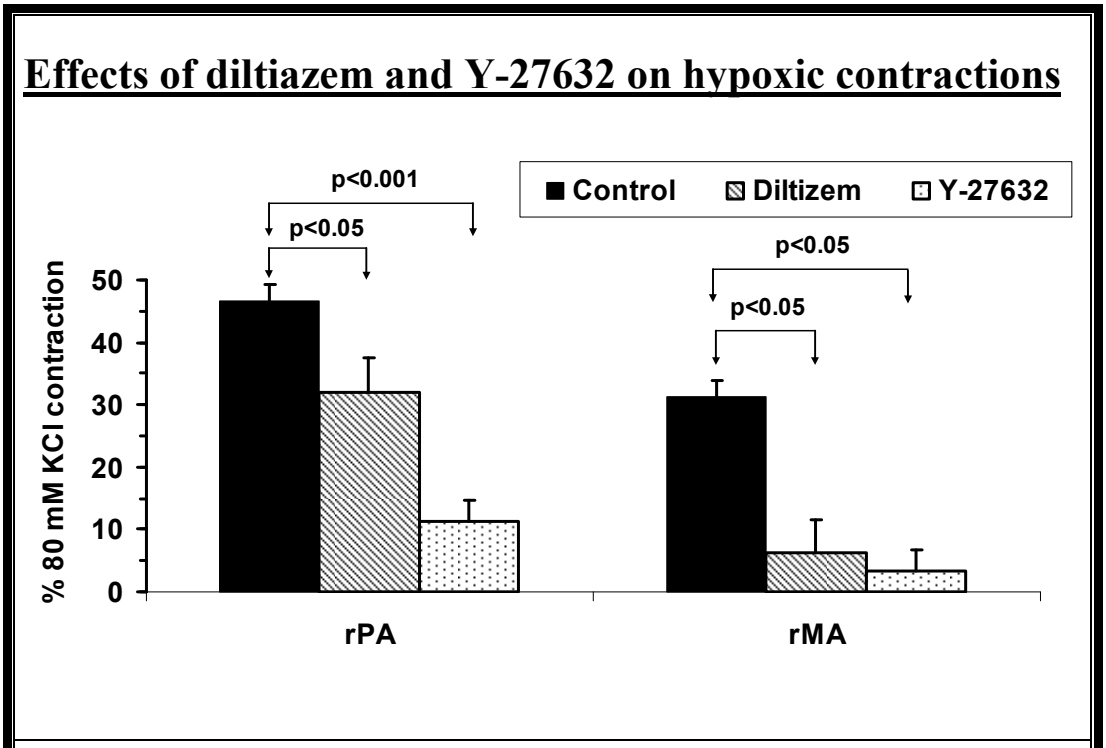

Figure 4.8 Statistical comparison of the hypoxia-induced contraction in the presence of diltiazem and Y-27632 in rat PA and MA.

Data obtained in three conditions: hypoxia in the presence of U-46619 alone (control), diltiazem+U-46619 or Y-27632+U-46619. Data expressed as a percentage of 80 mM KCl applied for 3 min before each protocol. Differences between groups were tested by Tukey-Kramer post-hoc test following one-way ANOVA, $n = 5$.

The average results are summarised and statistically compared in Fig. 4.8. It can be seen that, in PA, the inhibition of Rho-kinase had apparently a greater effect on hypoxic vasoconstriction compared to the inhibition of the L-VOCC, albeit non-significant (although significant with *t*-test when compared between the two treatment groups only). In contrast, in MA, no apparent differences between the two inhibitors were found. Overall, however, both inhibitors significantly suppressed hypoxia-induced transient contraction in both arteries, suggesting the important role played by L-VOCCs and Ca^{2+} sensitisation in hypoxia-induced vasoconstriction.

4.3.5 Effect of hypoxia in the presence of different concentrations of KCl in rat PA and MA

The results presented above suggest that hypoxia can induce a significant transient contraction in both types of arteries under conditions when the KCNQ channels and to a lesser degree the K_V channels are inhibited. The effect of hypoxia was significantly greater in PA than in MA. However, when both types of channels were completely blocked causing maximum depolarisation and contraction, pre-exposure to hypoxia caused significant attenuation of contraction induced by both the inhibitors. In the previous chapter I demonstrated that low concentration of KCl (20 mM) selectively potentiated 4-AP dependent contraction. Increasing concentrations of KCl will progressively depolarise the cell membrane, activate L-VOCCs and cause progressively increasing contraction. I therefore investigated the effect of hypoxia in the presence of increasing concentrations of KCl to induce contraction solely via the voltage-dependent pathway.

To quantitatively compare the effects produced by hypoxia in the presence of 20, 30, 40 and 80 mM KCl hypoxia-induced contractions (when occurred) and relaxations were expressed as percentage of the pretone measured before changing to hypoxia in each concentration of KCl (new baseline). Hypoxia-induced relaxations which were observed particularly when pretone was increased were measured by calculating the difference between the peak of the transient hypoxic contraction and the response measured at the end of the hypoxic challenge. Representative traces obtained from PA and MA show hypoxia-induced effects in the presence of increasing concentrations of KCl in PA (Fig. 4.9 A-D) and MA (Fig. 4.9 E-H).

In PA, at low concentration of KCl (20 mM and 30 mM), hypoxia caused transient contraction of 108±30% (n = 5) and 11±4% (n = 4), respectively (calculated as percentage of the pretone elicited by KCl). The amplitude of contraction was decreased with increased concentration of KCl (7±4%, n = 3 and 1±1%, n = 3 in 40 and 80 mM KCl, respectively). The contraction in each case was followed by gradual relaxation of 120±32% (n = 5), 29±2% (n = 4), 32±8% (n = 3) and 25±7% (n = 3) for 20, 30, 40 and 80 mM KCl, respectively (Fig 4.9 A-D; summarised in Fig.4.10).

In MA, the effect of hypoxia in increasing concentrations of KCl was associated predominantly with hypoxia-induced relaxations of 97±19% (n = 5), 91±14% (n = 4), 83±15% (n = 3) and 81±6% (n = 3) % in 20, 30, 40 and 80 mM KCl, respectively (Fig. 4.9 E-H). Note, that in MA, low concentration of KCl (20 mM) failed to induce any significant contraction (Fig. 4.9 E).

Fig. 4.10 summarises the relationship between KCl concentration and hypoxia-induced contraction and relaxation in PAs and MAs. As can be seen from this comparison, hypoxia caused significant contraction only in PA, where the hypoxia-induced contractions were maximal at low KCl concentrations and were decreased when KCl concentration was increased (Fig. 4.10 A, filled bars). In MA, hypoxia did not cause significant contraction at any KCl concentration tested (Fig. 4.10 A, open bars).

At lower KCl concentration hypoxia-induced relaxation was prevailed, and hypoxia-induced relaxations in PA were quantitatively comparable to those observed in MA (Fig. 4.10 B, filled bars). At higher concentrations of KCl, however, hypoxia-induced relaxation in MA was significantly greater than that observed in PA (Fig. 4.10 B, open bars).

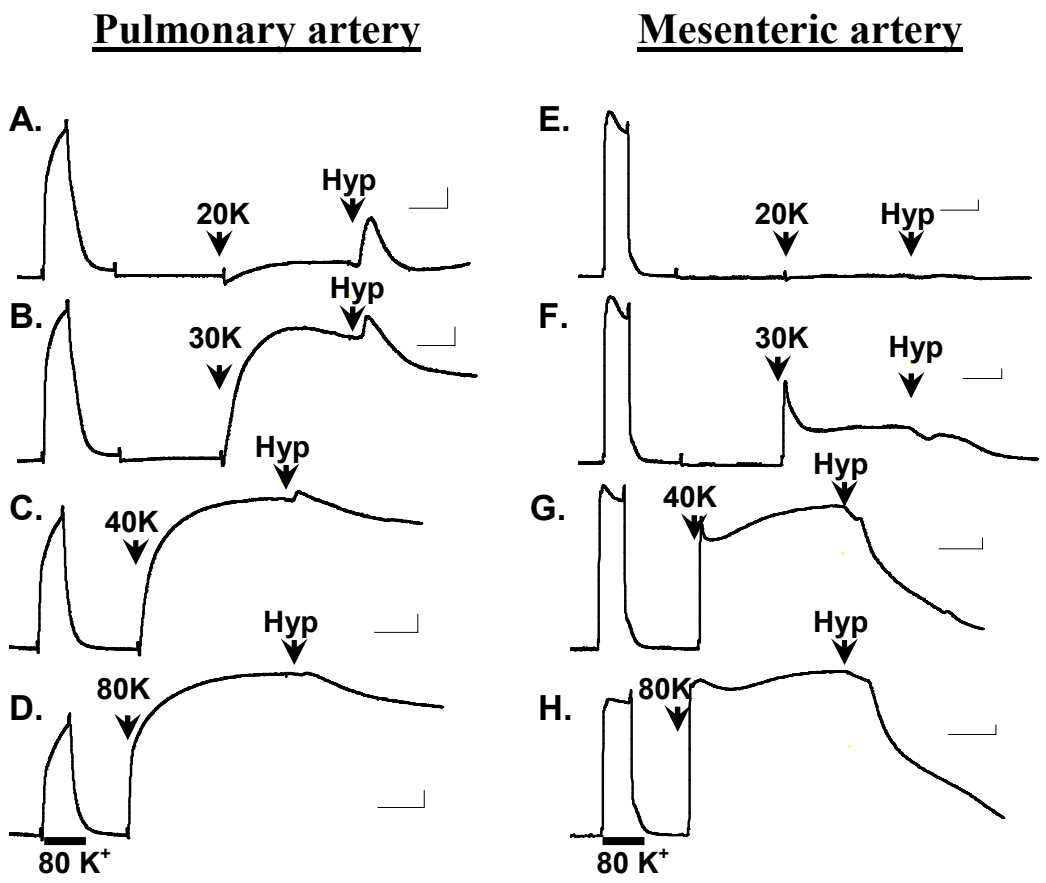

Figure 4.9 Hypoxia-induced contraction and relaxation at progressively increased pretone produced by different concentrations of KCl in rat PA and MA.

Representative traces were obtained from rat pulmonary (A-D) and mesenteric (E-H) arteries of 321 μm and 303 μm i.d., respectively. 20K, 30K, 40K and 80K indicate extracellular concentration of KCl in mM. Hyp, Hypoxia. Horizontal and vertical scale bars represent 5 min and 1 mN, respectively.

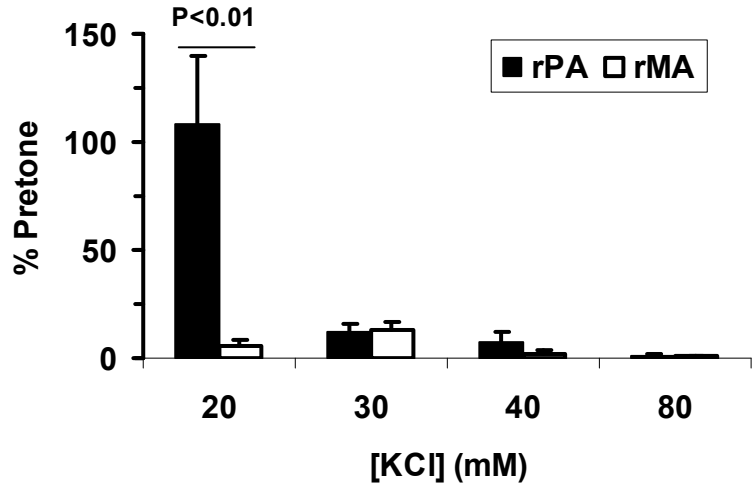

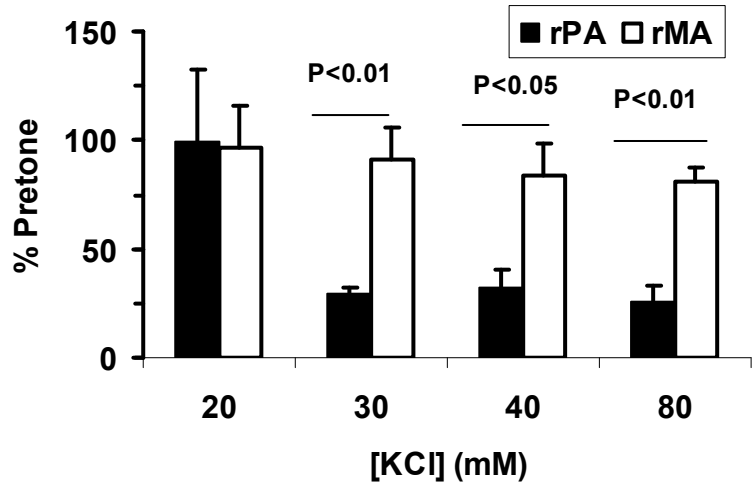

Figure 4.10 Dependence of hypoxia-induced contractions and relaxations on KCl concentration in rat PA and MA.

Each column represents the mean value obtained in 3-5 arteries. Statistical comparison between the two arteries was performed with paired Student's *t*-test.

4.3.6 Hypoxia-induced relaxation depends on the type of a preconstrictor agent

The results described in the previous section showed that, when the maximal contraction was achieved with 80 mM KCl, both arteries (PA and MA) were predominantly relaxed by hypoxia. However, the relaxation was significantly greater in MA than in PA. This may indicate that hypoxia-induced relaxation in PA and MA could involve different mechanisms. To investigate this phenomenon directly, the effect of hypoxia was studied in the presence of 80 mM KCl (to depolarise the cell membrane and maximally stimulate L-VOCC-mediated Ca^{2+} entry), 10 μM linopirdine+10 mM 4-AP (to inhibit both types of voltage-gated K^+ channels contributing to the membrane potential and cause contraction via L-VOCC-dependent pathway) and 1 μM U-46619 (a thromboxane A_2 analogue to activate contraction via receptor-mediated pathway) under conditions when maximal contraction was developed and maintained.

In this set of experiments arteries were first preconstricted using agents described above for 20 min to achieve a sustained level of contraction. Hypoxia was then applied for 20 min, followed by reoxygenation for 20 min. Relaxation responses were measured as a percentage of contraction induced by the preconstricting agent immediately prior to the hypoxic challenge.

The representative traces shown in Fig. 4.11 indicate that in PA the degree of relaxation to hypoxia depends on the way tissue was preconstricted. Thus, the hypoxic challenge relaxed KCl-induced contraction by 39%, linopirdine+4-AP-induced contraction by 69% and U-46619-induced contraction by 88% (Fig. 4.11 A-C). In contrast, hypoxia caused more complete and similar relaxation in preconstricted MA, causing 84%, 99% and 100% relaxation in the presence of KCl, K^+ channel inhibitors (linopirdine+4-AP) and U-46619, respectively (Fig. 4.11 D-F). Notably, the degrees of hypoxia-induced relaxations in MA under all three conditions were similar to that observed in PA in the presence of U-46619.

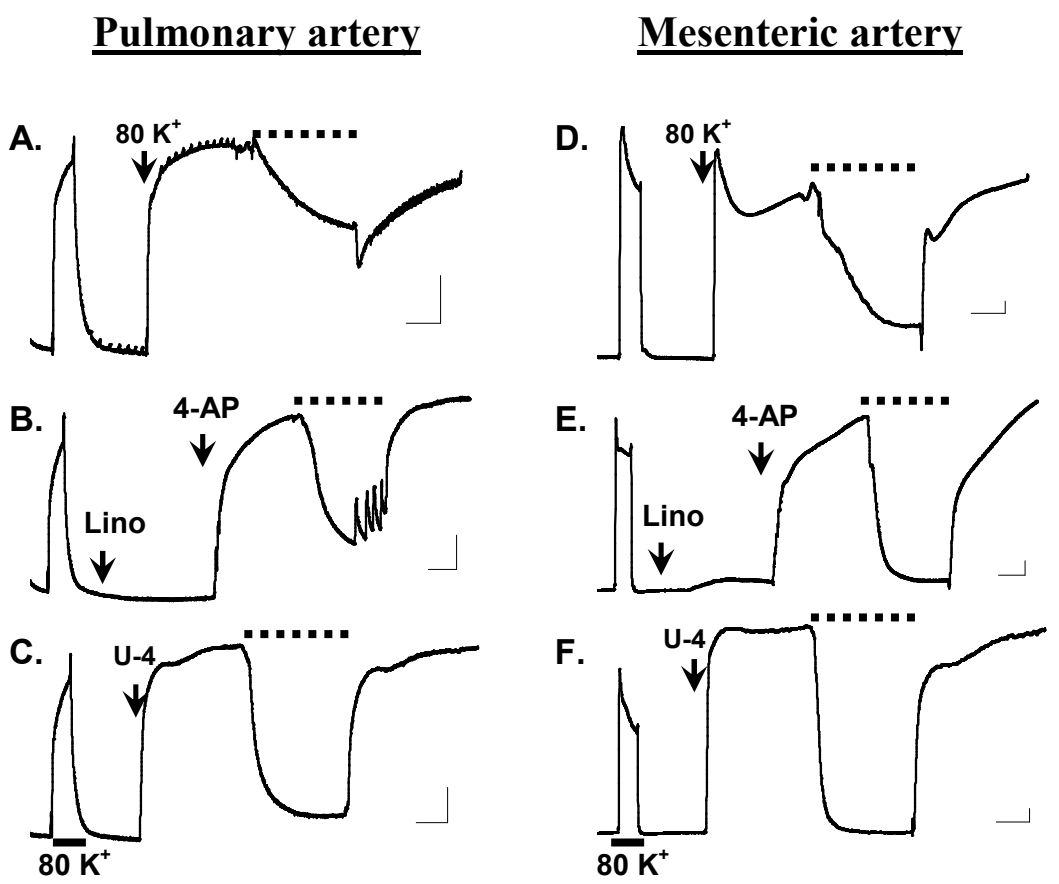

Figure 4.11 Effect of hypoxia on agonist-induced contractions in rat PA and MA.

Traces show relaxation effect of hypoxia on the maximal contraction induced by 80 mM KCl (A, D), the K^+ channel inhibition (B, E) and the thromboxane A_2 analogue U-46619 (C, F) in PA (left panel) and MA (right panel). Representative traces were obtained from PA of 313 μm (A) and 375 μm (B and C) i.d., and MA of 198 μm (D) and 277 μm (E and F) i.d. Area under dotted line indicates exposure to hypoxia. Lino, linopirdine (10 μM); 4-AP, 4-aminopyridine (10 mM); U-4, U-46619 (1 μM). Horizontal and vertical scale bars represent 5 min and 1 mN, respectively.

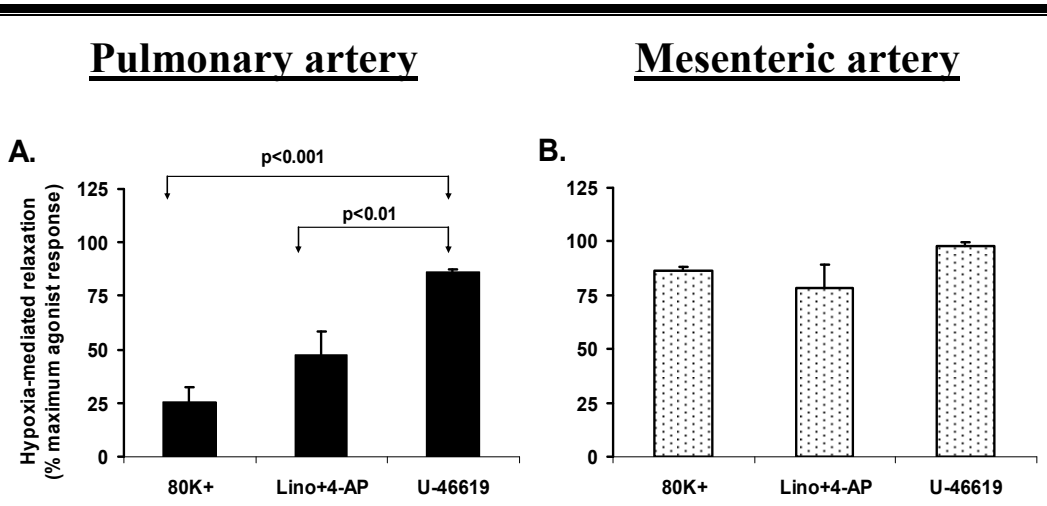

Figure 4.12 Hypoxia-induced relaxation depends on the type of agonist in rat PA and not in MA.

Relaxation to hypoxia was measured in the presence of 80 mM KCl ($80K^+$), 10 μM linopirdine+10 mM 4-AP (Lino+4-AP) and 1 μM U-46619 in PA (A) and MA (B). Relaxation response was calculated as described in the text. Differences between groups were tested by Tukey-Kramer post-hoc test following one-way ANOVA ($n = 3$).

Fig. 4.12 compares the hypoxia-induced relaxation obtained in all three conditions. In PA, hypoxia-induced relaxation in the presence of KCl and K^+ channel inhibitors (both causing the contraction via the voltage-dependent Ca^{2+} entry pathway) was significantly smaller than that in the presence of U-46619 (which causes contraction predominantly via voltage-independent mechanisms) (Fig. 4.12 A). On the other hand, in MA, the relaxation effect of hypoxia was independent on mechanism of preconstriction (Fig. 4.12 B). The comparison of hypoxia-induced relaxation between PA and MA demonstrates that, relaxation is significantly greater in MA than in PA in all three conditions (Fig. 4.13). Despite being significant (Fig. 4.13, $p<0.01$) the hypoxia-induced relaxations observed in U-46619-preconstricted arteries might have little functional significance as their degree of relaxation is similar between two arteries.

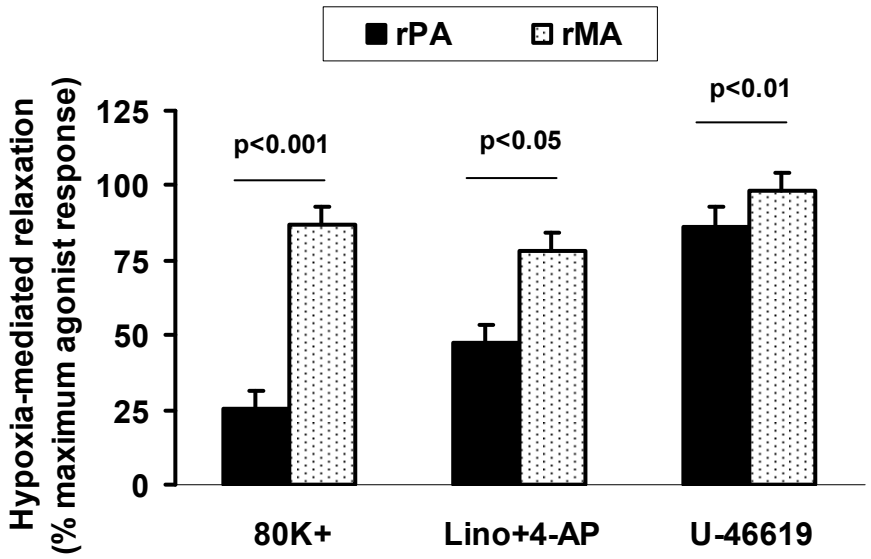

Figure 4.13 Comparison of hypoxia-induced relaxation between rat PA and MA.

Hypoxia-induced relaxation is significantly greater in MA irrespective of vasoconstrictor used. Paired Student's *t*-test; $n = 3$.

4.4 Discussion

The main observations described in this Chapter can be summarised as following:

1) Complete inhibition of KCNQ channels with 10 μM linopirdine, but not K_V channels with low (2 mM) concentration of 4-AP, stimulated a transient contraction to a short hypoxic challenge which was similar to the phase-I of HPV. This contraction was significantly greater when both inhibitors were used together. Interestingly, a transient contraction to hypoxia was also observed in systemic mesenteric arteries, although proportionally the effect was smaller than in pulmonary arteries.

2) The transient hypoxia-induced contraction was observed at the low level of pretone and was independent on the type of vasoconstrictor used (the K^+ channel inhibitors, low concentrations of KCl or U-46619) or tissue type.

3) When submaximal contraction was achieved with high concentrations of vasoconstrictor agents, hypoxia caused vasodilatation in both types of artery. In the pulmonary artery, the hypoxia-induced vasodilatation was dependent on the type of vasoconstrictor, and was less prominent in the presence of 80 mM KCl and the K^+ channels inhibitors (acting via the voltage-dependent Ca^{2+} entry pathway) than U-46619 (acting predominantly via the voltage-independent pathway). No such differences were observed in the mesenteric arteries. This could indicate the presence of a hypoxia-resistant component in contraction evoked by depolarisation which is specific to the pulmonary artery.

4.4.1 Role of K_V and KCNQ channels in hypoxia-induced contraction

The current view on the role of the K_V channels in the HPV response is that their inhibition by hypoxia and subsequent membrane depolarisation contribute to the initial rise of $[Ca^{2+}]_i$ during the first phase of HPV [recently reviewed in (Moudgil *et al.*, 2006;Weissmann *et al.*, 2006b;Ward & McMurtry, 2009)]. This hypothesis is mainly based on the well documented observation that hypoxia inhibits K_V channel currents in single isolated PASMCs (Post *et al.*, 1992;Archer *et al.*, 1993;Archer *et al.*, 1996;Olschewski *et al.*, 2002;Platoshyn *et al.*, 2006). This effect is considered to be specific to PASMCs because hypoxia does not affect K_V currents in systemic arteries (Yuan *et al.*, 1993;Michelakis *et al.*, 2002a). Surprisingly, the involvement of K_V channels in the initiation of HPV response in intact PA has not been studied previously. There could be two major reasons for the lack of studies in the intact tissues: ***i)*** the absence of commercially available specific inhibitors of the $K_V1.5$ channel isoform [the main isoform which encodes K_V channel currents in PAs (Archer *et al.*, 1998;Archer *et al.*, 2001;Smirnov *et al.*, 2002;Brevnova *et al.*, 2004;Platoshyn *et al.*, 2006)] and ***ii)*** the ability of the selective but non-specific K_V channel inhibitor 4-AP (the most widely used K_V channel inhibitor to study the role of K_V currents in the vasculature) to cause a significant contraction of isolated PAs in adult normoxic animals typically at concentrations of 5-10 mM (Priest *et al.*, 1998;Doggrell *et al.*, 1999;Doi *et al.*, 2000;Bonnet *et al.*, 2001;Bonnet *et al.*, 2002). Such low sensitivity of the intact preparations to 4-AP is in disagreement with electrophysiological findings where K_V channel currents are more sensitive to 4-AP in isolated PASMCs with an EC_{50} ranging between 0.11 to 0.35 mM (Smirnov & Aaronson, 1994;Smirnov *et al.*, 2002). The main reason for this discrepancy between single cells and whole tissue preparations is due to activity of the KCNQ channels at the resting condition and has been resolved in this study (see Chapter 3).

The understanding of the relationship between these two voltage-dependent K^+ channels provides an important opportunity to address the role of each type of channel in HPV response which was one of the main aims of this Chapter. As shown in Fig. 4.2 and 4.3, a partial inhibition of K_V channels with 2 mM 4-AP did

not enhance the HPV response in PAs. Under such conditions it could be expected that KCNQ channels are activated completely and in control of the resting potential. If hypoxia caused a significant inhibition of KCNQ channels, this would have lead to membrane depolarisation and contraction. This was not the case, leading to a suggestion that KCNQ channels in PASMCs are not significantly affected by hypoxia. On the other hand, when KCNQ channels were inhibited by 10 μM linopirdine (which should promote a greater activation of the K_V channels to enable control of the resting potential) the HPV response was augmented. Furthermore, both observations are in line with the above mentioned hypothesis that K_V channels are inhibited by hypoxia. The lack of significant differences is likely to be due to variation between the tissue responses which can be explained by the observations that hypoxia enhances the K_V current in the negative voltage range, whereas the current is inhibited at more positive potentials (Dr. SV Smirnov's unpublished observations). Such effect was also previously demonstrated (but not discussed) in canine PASMCs [Fig.7 in (Post *et al.*, 1992)] and in rat PASMCs [Fig.7 in (Archer *et al.*, 1993)]. Interestingly, this effect on the K_V channel current is very similar to that seen in the presence of mitochondrial inhibitors (Firth *et al.*, 2008). The implications of such dual effect of hypoxia on the K_V channels could be that enhanced K_V current at negative voltages stabilises the resting potentials. When the cell membrane is depolarised further, however the inhibitory effect on the K_V current will prevail leading to membrane depolarisation and contraction. This notion is supported by the observation that in the presence of 10 μM linopirdine and 2 mM 4-AP (the combination which will promote such depolarisation) hypoxia caused a significantly greater contraction (Figs. 4.2 and 4.3). Also, hypoxia significantly enhanced the contraction in the presence of 10 μM linopirdine specifically in PA (Fig. 4.4 B and Fig. 4.6).

4.4.2 Tissue specificity of HPV response

Interestingly, in MAs hypoxia was also able to induce a transient contraction in the presence of K_V channel inhibitors (Figs. 4.2 F-H and 4.3 C-D). The ability of systemic vessels to transiently constrict in response to acute hypoxia is not new and has been previously observed in porcine mesenteric (Nankervis & Miller, 1998) and coronary (Shimizu *et al.*, 2000) arteries, canine basilar (Elliott *et al.*, 1989) and sheep middle cerebral (Klaas & Wadsworth, 1989) arteries. Transient contraction to hypoxia was also observed in rat small MA (Leach *et al.*, 1994;Robertson *et al.*, 2003). The ability to compare the effect of hypoxia in pulmonary and systemic arteries under the same experimental conditions represents one of the main advantages of this study. Such comparison clearly demonstrates that the transient contractile effect of hypoxia is present in both types of arteries and importantly, this contraction is independent on the way the tissue is stimulated; either with K^+ channel inhibitors (Fig. 4.2) or with a receptor agonist U-46619 (Fig. 4.7). The independence of the hypoxic vasoconstriction on the type of stimulant was previously reported only in PAs (Rodman *et al.*, 1989), but no direct comparison between PAs and systemic arteries has yet been reported. In this Chapter I also showed for the first time that, although the transient hypoxic contraction in MA was qualitatively similar to that seen in PA, it was significantly smaller than in PAs under my experimental conditions. The hypoxia-induced responses between PA and MA although qualitatively look similar, statistical comparison of these data indicates that in the presence of linopirdine and 4-AP hypoxia produced significantly bigger responses in PA than in MA in both absolute as well as the normalised tension (Fig. 4.3). This suggests that the ability of MA to contract in response to hypoxia is less than that of PA. This conclusion does not therefore contradict the common notion that PA more readily contract in response to hypoxia although both PA and MA may share the mechanism responsible for the initial transient hypoxic contraction.

One critical difference in my study, however, is the observation of similar pattern of biphasic nature of HPV (a transient phase I followed by a slow and sustained

phase II) both in PA and MA (Fig. 4.1). The presence of the sustained phase II with occasional oscillations in MA was somewhat unexpected since most previous studies reported the relaxation of systemic arteries during prolonged effect of hypoxia (Leach *et al.*, 1994;Robertson *et al.*, 2000b;Robertson *et al.*, 2003). One possible reason for such discrepancy could be due to differences in the experimental approach. The previous studies employed $PGF_{2\alpha}$ to produce pretone whilst in my experiments linopirdine and 4-AP were used to stimulate the arteries. However, it is currently not known if this sustained phase of contraction is only the result of using K^+ channel blockers, or other factors may be involved. Although 100 μM L-NAME and 10 μM indomethacin were present in the myograph solutions in all experiments, the role of endothelium in this process is not clear. Whether endothelium-derived constricting factors (EDCF), which are released in response to various stimuli (Vanhoutte *et al.*, 1991) and are considered to be mediators of HPV (Holden & McCall, 1984;Rubanyi & Vanhoutte, 1985), are also involved in MA need to be addressed further in a separate study.

The presence of oscillations in contractions in MA is also interesting. In almost two third of the experiments, where application of linopirdine and 4-AP was followed by hypoxia, oscillations were observed in MAs, but not in PAs. Oscillations in contraction is known to be associated with oscillations of smooth muscle membrane potential (Gustafsson *et al.*, 1993) and of $[Ca^{2+}]_i$ (Peng *et al.*, 1998), whilst K^+ channels play a modulatory role in this mechanism (Gustafsson *et al.*, 1994;Edwards & Griffith, 1997). In this study, simultaneous recordings of membrane potential and vessel contraction demonstrated oscillations both in V_m and contraction in MA more frequently than in PA (Chapter 3). Also it has been reported that oscillation was promoted after removal of the endothelium (or inhibition of NO synthase) in the rabbit mesenteric (Omote *et al.*, 1993) and rabbit ear arteries (Griffith & Edwards, 1993), rat aorta (Marchenko & Sage, 1994) and rat mesenteric arteries (Sell *et al.*, 2002). Thus, it cannot be excluded that in my experiments the use of L-NAME and indomethacin are triggering such oscillations when tissue is stimulated. The absence of oscillations in PAs could be due to difference in the gap junctions and variation in synchronised oscillatory mechanisms between PAs and MAs (Aalkjaer & Nilsson, 2005).

4.4.3 Differences in hypoxia-induced relaxation in rat PA and MA

The results shown in Fig. 4.9 (A-D) and 4.10 (A) clearly demonstrate that the degree of the transient hypoxic contraction of PA strongly depends on the level of pretone which was elicited by increased concentrations of KCl and decreases as KCl-induced tension increases. The transient contraction was followed by relaxation, which progressively increased as pretone was increased. Similar biphasic effects of hypoxia were previously reported in large extra-pulmonary arteries of the rat (Bennie *et al.*, 1991;Jin *et al.*, 1992;Shigemori *et al.*, 1996) and rabbit (Bonnet *et al.*, 1989) preconstricted with KCl or an agonist. In the phase-II of HPV this initial relaxation will be followed by a slow contraction if hypoxia is persisted and the endothelium is intact (Bennie *et al.*, 1991;Jin *et al.*, 1992;Leach *et al.*, 1994). It is however worth mentioning that although hypoxia-induced relaxation was focus of many studies in systemic arteries, in PA it has not been widely investigated. Reduction in intracellular ATP during hypoxia leading to an increase in outward K_{ATP} current (Noack *et al.*, 1992) may be responsible for relaxation caused by U-46619 and linopirdine+4-AP, as was proposed for agonist (e.g. U-46619, angiotensin II, 5-HT and noradrenaline) induced contraction in PA (Wanstall & O'Brien, 1996), but would not explain relaxation in high K^+ which render these channels inactive. This mechanism may be responsible for the difference between hypoxia-induced relaxation in PA and MA in 80 mM KCl. Experiments using K_{ATP} inhibitors like glibenclamide could answer the question whether K_{ATP} channels are involved in any of those responses. In any case, the dependence of the relaxation to hypoxia on the way tissue is preconstricted in PA, but not as much in MA, could indicate differences in the way contraction is maintained in the two artery types.

In systemic arteries preconstricted with agonists or high K^+, hypoxia is known to cause relaxation (Namm & Zucker, 1973;Klaas & Wadsworth, 1989;Marriott & Marshall, 1990;Otter & Austin, 1999;Bruce *et al.*, 2004). The exact mechanism of hypoxia-dependent relaxation in systemic circulations remained unresolved and a range of mechanisms including the release of vasodilator metabolites, such as adenosine from hypoxic tissues (Berne, 1980), opening of glibenclamide-

sensitive K_{ATP} channels leading to K^+ efflux and hyperpolarisation (Daut *et al.*, 1990;Bonnet *et al.*, 1991;Mellemkjaer & Nielsen-Kudsk, 1994), inhibition of L-VOCCs (Herrera & Walker, 1998), possible dependence on cellular metabolism (Otter & Austin, 1999), the inhibition of non-voltage-dependent Ca^{2+} entry and intracellular Ca^{2+} release or the enhanced activity of SERCA (Guibert *et al.*, 2002) have been proposed. As in case of HPV, multiple factors such as the tissue type, the type of vasoconstrictor, the presence of endothelium and others are likely to contribute to hypoxic systemic vasodilatation.

Since the functional responses to hypoxia in the pulmonary and systemic circulations are different, comparison of hypoxia-induced relaxation in addition to hypoxia-induced contractions between PA and MA recorded under the same experimental conditions can reveal important differences in the responses of the two different types of arteries. Indeed, as shown in Figs. 4.11 and 4.12, the hypoxia-induced relaxation in PAs was dependent on the way tissue was pre-constricted being the weakest when PAs were pre-constricted with high K^+ and with K^+ channel inhibitors and the strongest in the presence of U-46619. On the other hand, no significant differences in hypoxia-induced relaxation were observed in MAs in the three groups. Furthermore, the relative degree of relaxation was significantly smaller in PAs than in MAs (Fig. 4.13), suggesting that the ability of MAs to relax to hypoxia is significantly greater than that of PAs. Interestingly, the weakest relaxation in PAs was observed under conditions when K^+ fluxes across the cell membrane were impaired, i.e. in 80 mM KCl or in the presence of linopirdine and 4-AP. This may indicate that the differential effect of hypoxia in PA compared to MA is most pronounced when K^+ channels (K_V in particular) are inhibited. These differences are unlikely to be due to the use of 95% O_2 as normoxia (this level of oxygen was chosen because of the joint use of PA and MA in the same chamber) because previous study demonstrated that there is no significant difference in HPV responses in PAs between 95%O_2/5CO_2 and air/5%CO_2 (Leach *et al.*, 1994).

The greater susceptibility of the phase-I of HPV measured in the presence of U-46619 to both the L-VOCC blocker diltiazem and the Rho-kinase inhibitor Y-27632 in MA, compared to PA (Fig. 4.7 and 4.8), may indicate the crucial

involvement of these two pathways in the differential regulation of contractility in these two types of vessels. The investigation of the relationship between the voltage-dependent pathway and Ca^{2+} sensitisation in the control of PA and MA contraction caused by the inhibition of the K_V channels will be the subject of the next chapter.

Chapter 5

VOLTAGE-DEPENDENT AND VOLTAGE-INDEPENDENT MECHANISMS OF 4-AP-INDUCED CONTRACTION IN RAT PULMONARY AND SYSTEMIC MESENTERIC ARTERIES

5.1 Introduction

The contractile response of intact artery rings is the result of vascular smooth muscle contractions, which are primarily due to elevation of intracellular Ca^{2+} concentration. This occurs as a result of activation of either the release of Ca^{2+} from the intracellular stores or due to Ca^{2+} influx from the extracellular space in the voltage-dependent and voltage-independent manner (Karaki *et al.*, 1997). The voltage-dependent Ca^{+} entry depends on membrane potential which in turn is determined by K^{+} efflux (Standen & Quayle, 1998). Changes in the cell membrane potential lead to changes in $[Ca^{2+}]_i$ and ultimately to the changes in the contractile state of the cell. A body of evidence suggests that, in PASMCs, K_V channels play a significant role in regulating the resting membrane potential (Yuan, 1995;Yuan *et al.*, 1998c;Mauban *et al.*, 2005). Under resting conditions, some K_V channels are active resulting in an efflux of K^{+} ions, which contributes to the negative resting membrane potential. Membrane depolarisation caused by the inhibition of K_V channels (i.e., by hypoxia or 4-AP) causes Ca^{2+} influx through L-VOCCs, which increases $[Ca^{2+}]_i$ resulting in vascular smooth muscle cell contraction and thus increasing in pulmonary tone (Weir & Archer, 1995;Sweeney & Yuan, 2000).

The results presented in this chapter, could however, suggest that contraction produced as a result of application of the K_V channel blockers in intact pulmonary arteries may be at least partly voltage-independent. The important questions are: i) whether any difference in the levels of voltage-dependent and voltage-independent components of contraction exists between the pulmonary and systemic blood vessels; and ii) what possible mechanism might be involved in the voltage-independent component? It is well documented that Ca^{2+} sensitisation due to activation of the RhoA/Rho-kinase pathway is responsible for the augmented vascular contraction in animal models (Uehata *et al.*, 1997;Mukai *et al.*, 2001;Chrissobolis & Sobey, 2001;Weber & Webb, 2001;Kitazono *et al.*, 2002;Jin *et al.*, 2006;Hilgers *et al.*, 2007) as well as in humans (Masumoto *et al.*, 2001;Seasholtz *et al.*, 2006). Therefore, the contraction of the vascular smooth muscle is subjected to the dual regulation by the Ca^{2+} signal and alteration of the Ca^{2+} sensitivity. This has been well documented for the sustained phase of agonist-induced smooth muscle contraction which is dependent on Rho-kinase activation and the phosphorylation of myosin phosphatase regulatory subunit (MYPT1) of MLCP (Swärd *et al.*, 2000;Dimopoulos *et al.*, 2007). Notably, simultaneous measurements of the force and intracellular Ca^{2+} in canine coronary arteries revealed a possibility that KCl depolarisation could increase contractility of this tissue via Ca^{2+} sensitisation (Yanagisawa & Okada, 1994). Ca^{2+} sensitisation was also implicated in the KCl-dependent augmentation of endothelin-1-induced contraction in the same preparation (Okada *et al.*, 1992).

Therefore, this chapter will be focussed on the investigation of the effects of K_V channels inhibition using a combination of 4-AP and linopirdine and membrane depolarisation using high K^+ on isometric tension in isolated PA and MA to test the following questions:

1) Whether contraction induced by blockers of K^+ channels and high K^+ involves voltage-dependent and voltage-independent pathways?
2) What is the role for Rho-kinase mediated Ca^{2+} sensitisation in these contractions?

5.2 Results

5.2.1 Effect of L-VOCC blocker (diltiazem) and a specific Rho-kinase inhibitor (Y-27632) on 4-AP-induced contraction in rat PA and MA

Contractile responses to 10 mM 4-AP were produced in PA and MA in the presence of 10 μM linopirdine to completely block KCNQ channels and to maximise 4-AP responses. In this and the subsequent experiments 10 mM 4-AP was always preceded by 10 μM linopirdine unless otherwise stated. When 4-AP-induced contraction reached the steady state level (20 min), 10 μM diltiazem, an L-VOCC blocker, was applied for 10 min followed by the application of 10 μM Y-27632, a selective inhibitor of Rho-kinase. The relaxation to both inhibitors was then calculated as the percentage of the maximal steady state 4-AP contraction. Representative examples of such experiments are shown in Fig. 5.1. It can be clearly seen that diltiazem alone blocked the 4-AP contraction only partly by 46% in PA (fig. 5.1 A), but contraction in MA was blocked nearly completely by 98% (Fig. 5.1 C). Although application of Y-27632 in the presence of diltiazem further reduced 4-AP-induced contraction in PA, it failed to block it completely (Fig. 5.1 A). This contrasts to the effect of Y-27632 in MA which was completely relaxed to the basal level in the presence of the inhibitor (Fig. 5.1 C). Application of the inhibitors in the reversed order showed that Y-27632 (when applied first) was a relatively less effective relaxant compared to the diltiazem, relaxing 4-AP-induced contraction by 31% in PA (Fig. 5.1 B) and by 65% in MA (Fig. 5.1 D). Notably, the effect of Y-27632 was greater in MA than in PA. Consecutive application of diltiazem completely relaxed the 4-AP-induced contraction in MA (Fig. 5.1 D), whereas the combined effect of Y-27632 and diltiazem in PA was similar to that when applied in the reversed order, causing only partial relaxation in PA.

Fig. 5.2 summarises and statistically compares the relaxatory effects of the two inhibitors. On average, in the PA, the 4-AP-induced contraction was reduced by

48.6±2.3% (n = 11) in the presence of diltiazem. In the presence of diltiazem, application of Y-27632 further suppressed the contraction by approximately two-thirds (62.0±5.4%, n = 6) (Fig. 5.2 A and B). Although the change of the Y-27632-dependent relaxation was less than that by diltiazem (31.7±8.7%, n = 6), the resulting effect of the two inhibitors when applied together was virtually the same in PA, leaving about 35% of contraction which was insensitive to diltiazem and Y-27632. In MA, Y-27632 alone relaxation mounted to 77.2±4.0% (n = 6), which was significantly greater than that in PA ($p<0.001$, n = 6). The combination of both inhibitors completely relaxed MA independent on the order of their application (Fig. 5.2 C and D). Because diltiazem blocks contraction via inhibition of L-VOCCs whilst Y-27632 selectively inhibits intracellular Rho-kinase responsible for Ca^{2+} sensitisation and due to their additiveness (at least in PA), the diltiazem- and Y-27632- sensitive components will be referred to as the voltage-dependent and voltage-independent components, respectively.

The above comparisons clearly show that 4-AP contracts both arteries in a complex manner involving voltage-dependent and voltage-independent components in the maintenance of the sustained contraction. The distinguishing features between the pulmonary and systemic artery are a lesser sensitivity to Rho-kinase inhibition and the presence of the additional component of contraction (in PA) which is apparently insensitive to voltage-dependent Ca^{2+} entry and Ca^{2+} sensitisation.

It is worth mentioning here that removal of extracellular Ca^{2+} blocked 4-AP-induced contraction and cyclopiazonic acid also did not prevent the contraction to 4-AP (data not shown) indicating that this additional component is not due to Ca^{2+} release from the intracellular Ca^{2+} stores.

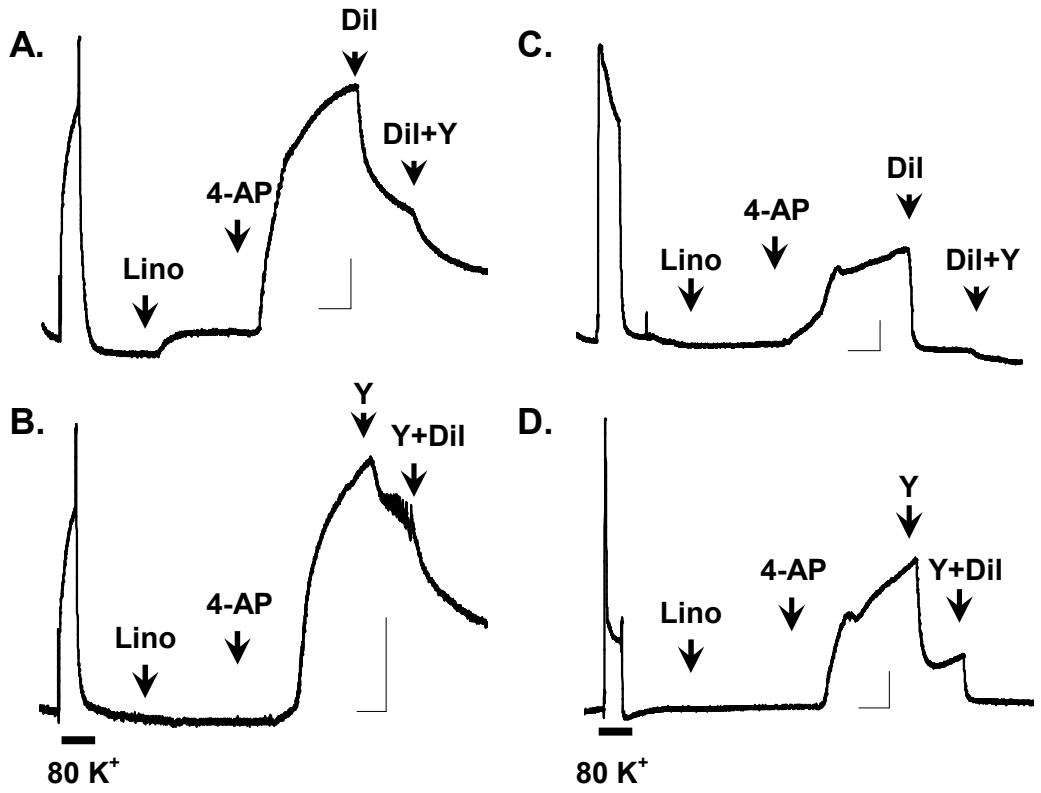

Figure 5.1 Effects of diltiazem and Y-27632 on 4-AP-induced contraction in rat PA and MA.

Traces show the effects of L-VOCC blocker (diltiazem) or a specific Rho-kinase inhibitor (Y-27632) or combination of these two inhibitors on relaxation of 4-AP-induced contraction in PA and MA. Representative traces were obtained from PA of 392 and 263 μm i.d. (A and B, respectively) and MA of 286 and 198 μm i.d. (C and D, respectively). Lino, 10 μM linopirdine; 4-AP, 10 mM 4-aminopyridine; Y, 10 μM Y-27632; Dil, 10 μM diltiazem. Horizontal and vertical scale bars represent 5 min and 1 mN, respectively.

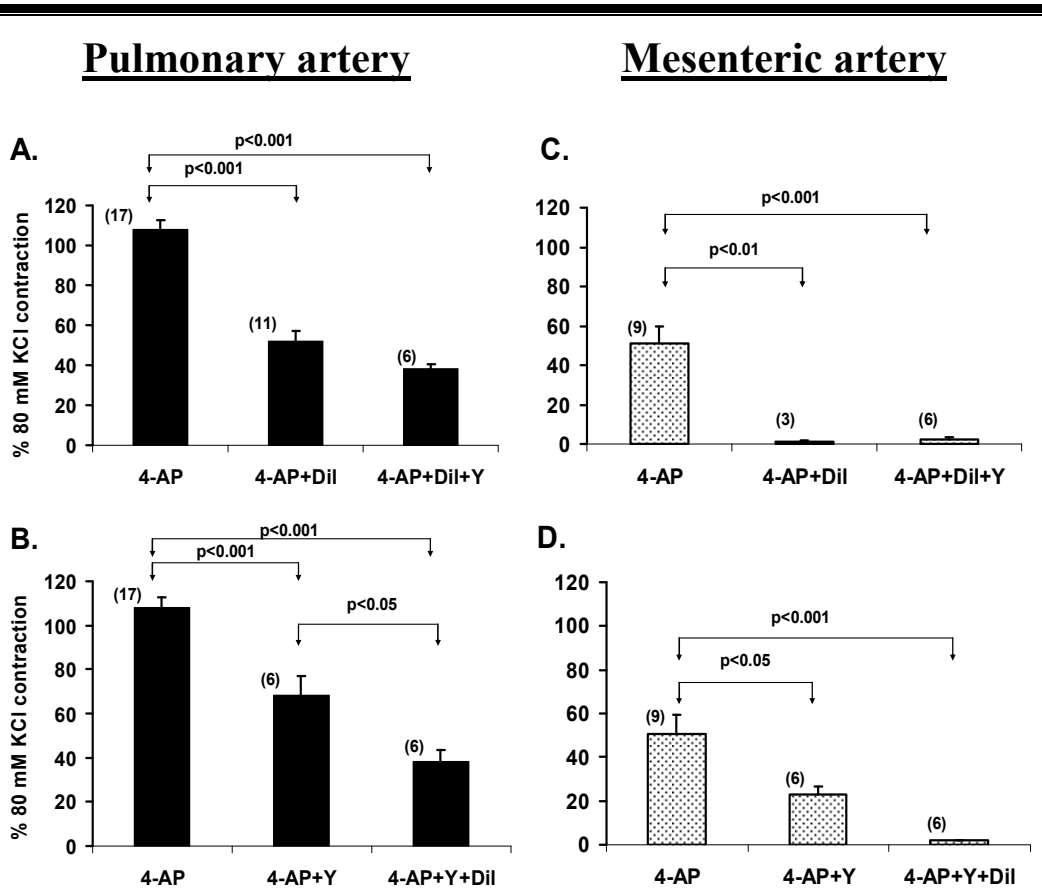

Figure 5.2 Comparison of the inhibitory effects of diltiazem and Y-27632 alone or in combination on 4-AP-induced contraction in rat PA and MA.

A and **C,** Statistical comparisons of the effects of diltiazem and diltiazem+Y-27632 on 4-AP-induced contraction in PA (A) and MA (C). **B** and **D,** Statistical comparisons of the effects of Y-27632 and Y-27632+diltiazem on 4-AP-induced contraction in PA (B) and MA (D). All 4-AP responses were carried out in the presence of 10 μM linopirdine applied for 20 min prior to 4-AP. Note that the order of the drugs listed on x-axis indicates the order of their application in the experiment. Lino, linopirdine (10 μM); 4-AP, 4-aminopyridine (10 mM); Y, Y-27632 (10 μM); Dil, diltiazem (10 μM). Differences between groups were tested by Tukey-Kramer post-hoc test following one-way ANOVA; *n* values are shown on the graph in brackets.

5.2.2 Effect of the pretreatment with diltiazem, Y-27632 or combination on the 4-AP-induced contraction in rat PA and MA

The results presented in the previous section demonstrate that in PA, in contrast to MA, the 4-AP-induced contraction was: i) less sensitive to either diltiazem or Y-27632; ii) not completely blocked by the combined application of diltiazem and Y-27632; and iii) significantly less sensitive to Y-27632. To further investigate a causal relationship between the voltage-dependent Ca^{2+} entry and Ca^{2+}-dependent sensitisation in the 4-AP-induced contraction the following experimental protocol was used for the two types of arteries: a) contraction was induced by 10 mM 4-AP (*control*); b) arteries were treated with 10 μM Y-27632 for 10 min prior to the addition of 4-AP (*Y+4-AP*); c) arteries were treated with 10 μM diltiazem for 10 min prior to the addition to 4-AP (*Dil+4-AP*); and d) 10 mM 4-AP was applied alone after wash-out of the inhibitors (*recovery*). All the experiments were performed in the presence of 10 μM linopirdine in order to maximise the 4-AP-induced responses.

Representative traces from the first set of experiments are shown in Fig. 5.3. As can be seen in this Figure, in PA, the 4-AP-induced contraction was blocked partly by the pretreatment with Y-27632 or diltiazem with the effect being smaller in the presence of Y-27632 (~61%) compared to diltiazem (~85%). Under same conditions, in MA, the contraction caused by 10 mM 4-AP was blocked more profoundly by Y-27632 (~74%) or by diltiazem (~97%) (Fig. 5.3 F and G, respectively) compared to PA. Complete recovery of the 4-AP-induced contraction was observed in both tissues. A greater recovery in MA was due to potentiation phenomenon described in details in Chapter 3. The greater inhibition of the 4-AP-induced contraction in the presence of diltiazem in both tissues is consistent with the depolarisation-induced Ca^{2+} entry required for the initiation of tension.

The results of the experiments where both arteries were pretreated with diltiazem+Y-27632 (10 μM each) are shown in Fig 5.4. As can be seen from the representative traces the 4-AP-induced contraction was completely abolished by

the pretreatment with diltiazem+Y-27632 in both PA (Fig. 5.4 A-C) and MA (Fig. 5.4 D-F). These effects were fully reversible. It is worth noting that combination of diltiazem and Y-27632 was able to completely block the 4-AP response in PA when applied prior to induction of the contraction, conversely, when the contraction induced by 10 mM 4-AP was already developed combination of both inhibitors failed to completely relax PA (Fig. 5.1 A-B; and Fig. 5.2 A-B), suggesting the necessity of the elevated intracellular Ca^{2+}.

The normalised responses obtained in these two sets of experiments are statistically compared in Fig.5.5. As can be seen from this comparison, all the effects of the L-VOCC blocker or Rho-kinase inhibitor on 4-AP-induced contraction were significantly different from the control and recovery responses (Fig. 5.5 A and B). In MA significant differences were only observed between the test data and the recovery for 10 μM Y-27632 and diltiazem pretreatments due to less consistent amplitude of 4-AP-induced contraction in control conditions (Fig. 5.5 C). Although, in principle, this can be overcome by increasing the number of experiments, however, this was not considered practical due to prolonged duration of these experiments. Moreover, consistent results showing complete blockade of 4-AP responses with L-VOCC blocker diltiazem and Rho-kinase inhibitor Y-27632 pretreatment also provided evidence in favour of additiveness of these two inhibitors. Since the combination of the diltiazem and Y-27632 completely and consistently blocked contraction in MA (Fig. 5.5 D), the difference reached significance between the test and both the control and the recovery sets of data, despite a relatively smaller control contractions. It is important to note that, in the MA, the contraction in the presence of Y-27632 reduced by 69% (from 33±9% to 10±2%) which is similar to that observed in the PA. Notably, the 4-AP-induced contraction in PA was inhibited more effectively by the pretreatment with Y-27632 by 61% (from 104±4% in the control to 41±12% in the presence of the inhibitor). This was two times greater than the effect of Y27632 on the steady state 4-AP-induced contraction compared in Fig.5.2 B. In contrast, in MA, the effects of the Rho-kinase inhibitor were similar in both conditions.

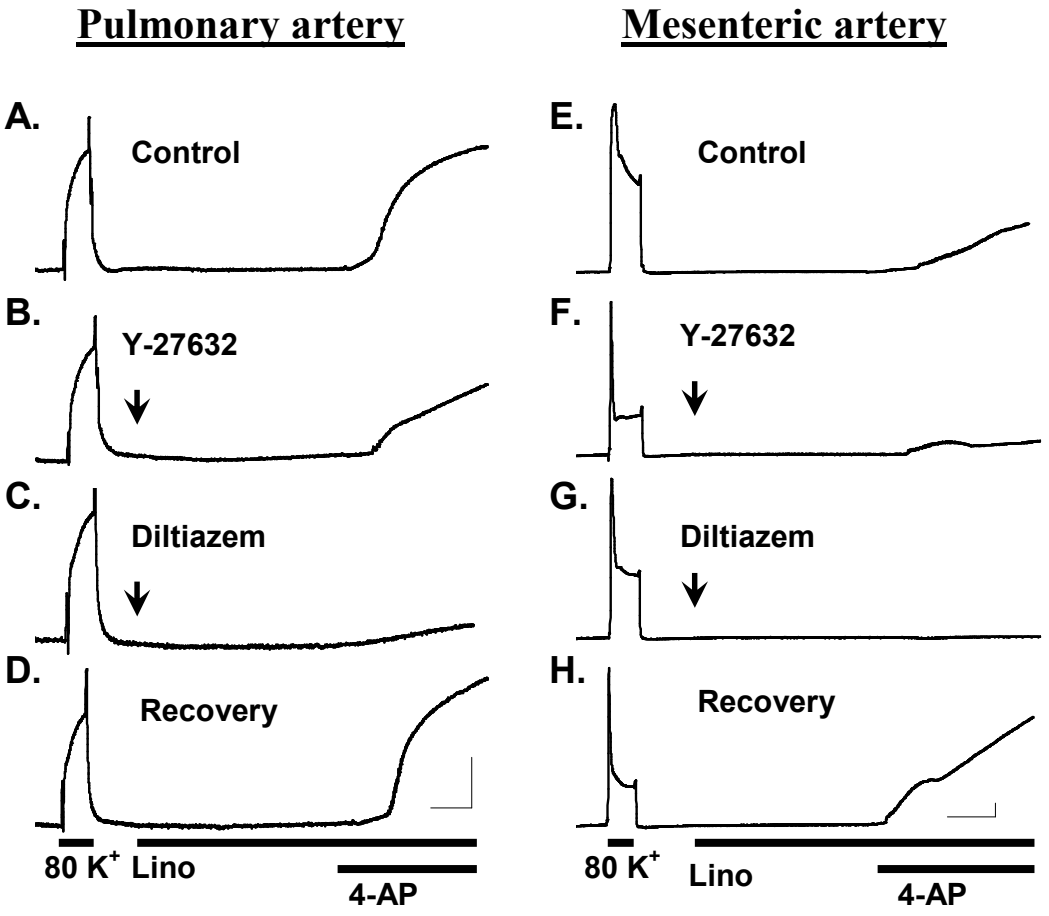

Figure 5.3 Effect of pretreatment with Y-27632 or diltiazem on 4-AP-induced contraction in rat PA and MA.

Representative traces were obtained from PA (A-D) of 263 μm i.d. and MA (E-H) of 198 μm i.d. Lino, linopirdine (10 μM); 4-AP, 4-aminopyridine (10 mM). Horizontal and vertical scale bars represent 5 min and 1 mN, respectively.

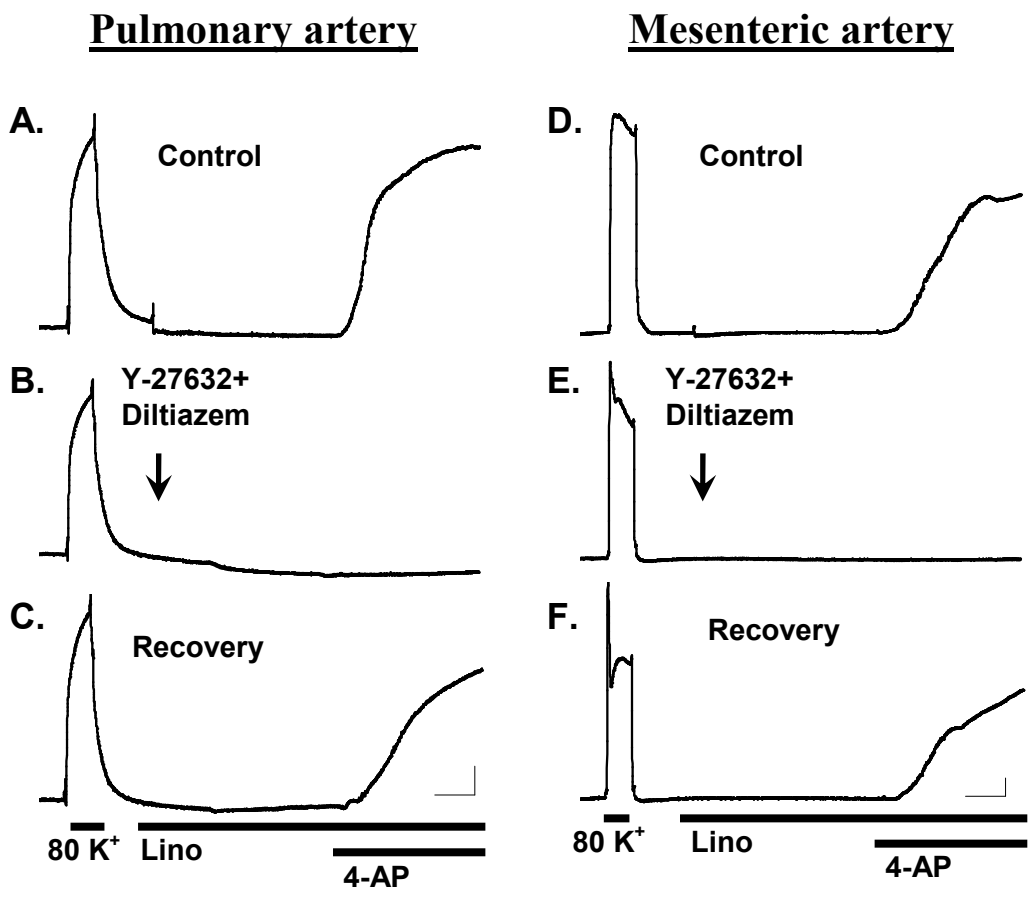

Figure 5.4 Effect of pretreatment with a combination of Y-27632 and diltiazem on 4-AP-induced contraction in rat PA and MA.

Representative traces were obtained from PA (A-C) of 330 μm i.d. and MA (D-F) of 203 μm i.d. Lino, linopirdine (10 μM); 4-AP, 4-aminopyridine (10 mM). Horizontal and vertical scale bars represent 5 min and 1 mN, respectively.

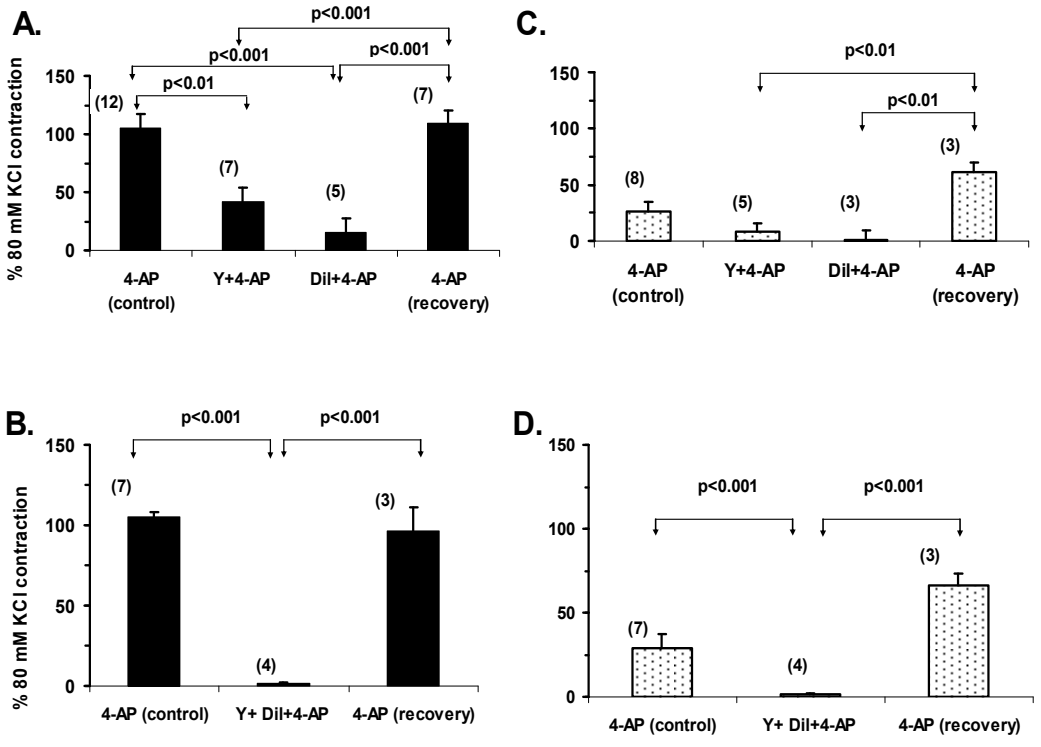

Figure 5.5 Comparison of the inhibitory effects of single and combined pretreatment with Y-27632 and diltiazem on the subsequent contraction elicited by 4-AP in rat PA and MA.

A and **C**, pretreatment with 10 μM Y-27632 alone or 10 μM diltiazem alone blocked 4-AP response only partly in PA (A) while in MA (C) the same concentration of Y-27632 alone blocks 4-AP response partly but diltiazem alone blocks this response completely. **B** and **D**, pretreatment with the combination of Y-27632 and diltiazem (10 μM each) completely blocked 4-AP response in both tissues. All 4-AP responses were carried out in the presence of 10 μM linopirdine applied for 20 min prior to 4-AP. Note that the order of the drugs listed on x-axis indicates the order of their application in the experiment. 4-AP, 4-aminopyridine; Y, Y-27632; Dil, diltiazem. Differences between groups were tested by Tukey-Kramer post-hoc test following one-way ANOVA; *n* values are shown on the graphs in brackets.

5.2.3 Dependence of the effect of Y-27632 on the level of 4-AP-induced contraction in rat PA and MA

The results described in the previous two sections may suggest that the relaxatory effect of Y-27632 depends on the level of 4-AP-induced contraction. To investigate this possibility, the effect of Y-27632 (10 μM) was compared in the presence of increasing concentrations of 4-AP (0.5, 1, 2.5, 5 and 10 mM) applied in the presence of 10 μM linopirdine. Fig. 5.6 shows representative traces recorded with this protocol in PA (Fig. 5.6 A-E) and MA (Fig. 5.6 F-J). In PA, Y-27632 completely relaxed 4-AP at contractions between 0.5 and 2.5 mM, while had only partial effect at 5 and 10 mM. Although similar trend was observed in MA, the effect of Y-27632 was always greater in MA than in PA, becoming significantly different at 10 mM of 4-AP contraction ($p<0.05$, $n = 4$) (Fig. 5.7).

It is notable that contractions produced by low concentrations of 4-AP (i.e., 0.5 and 1.0 mM) in PA was completely ablated by 10 μM Y-27632. On the other hand, consistently with the observations described in Chapter3, similar low concentrations of 4-AP produced no contraction in MA. Therefore, the degree of Y-27632-induced relaxation was compared between PA and MA only for the higher concentrations of 4-AP (i.e., 2.5, 5 and 10 mM) (Fig. 5.7).

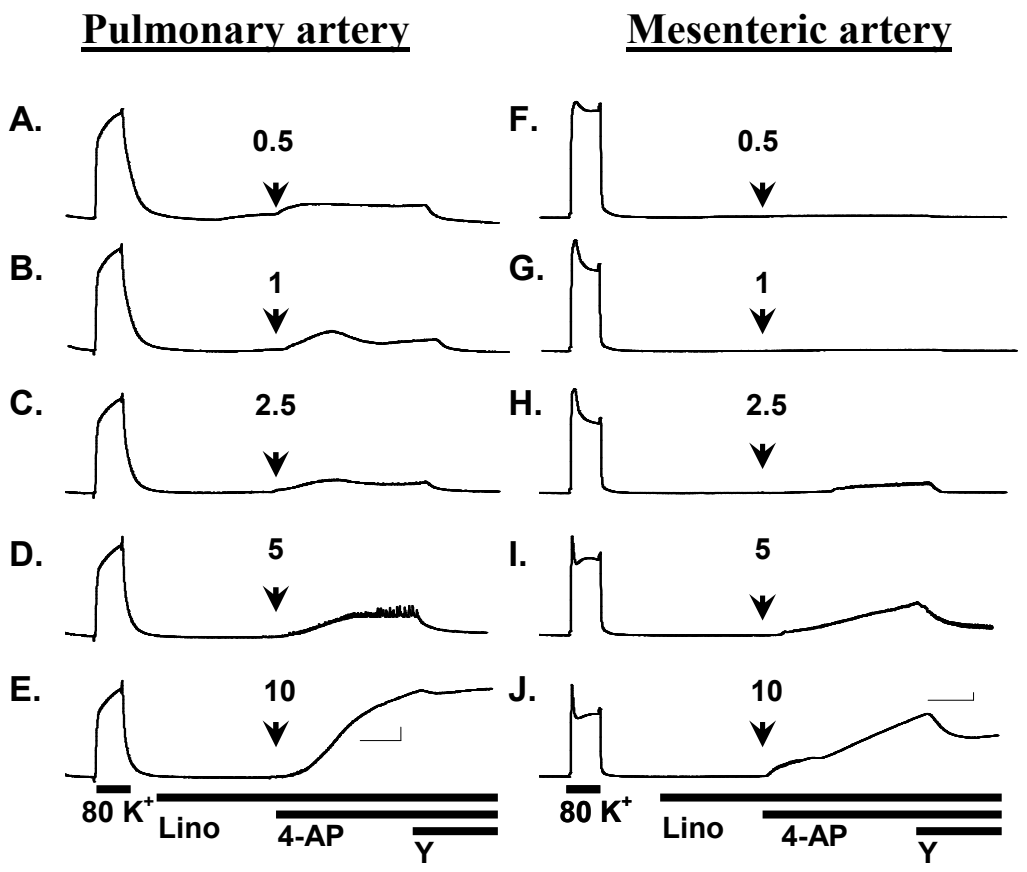

Figure 5.6 Inhibition by Y-27632 of contractions induced by different concentrations of 4-AP in rat PA and MA.

Representative traces obtained from PA (A-E) of 388 μm i.d. and MA (F-J) of 243 μm i.d. showing relative relaxation by 10 μM Y-27632 on contraction produced with different concentrations of 4-AP. All 4-AP responses were carried out in the presence of 10 μM linopirdine applied for 20 min prior to 4-AP. The time of application and the concentration of 4-AP in mM are shown by arrows. Lino, linopirdine (10 μM); 4-AP, 4-aminopyridine; Y; Y-27632 (10 μM). Horizontal and vertical scale bars represent 5 min and 1 mN, respectively.

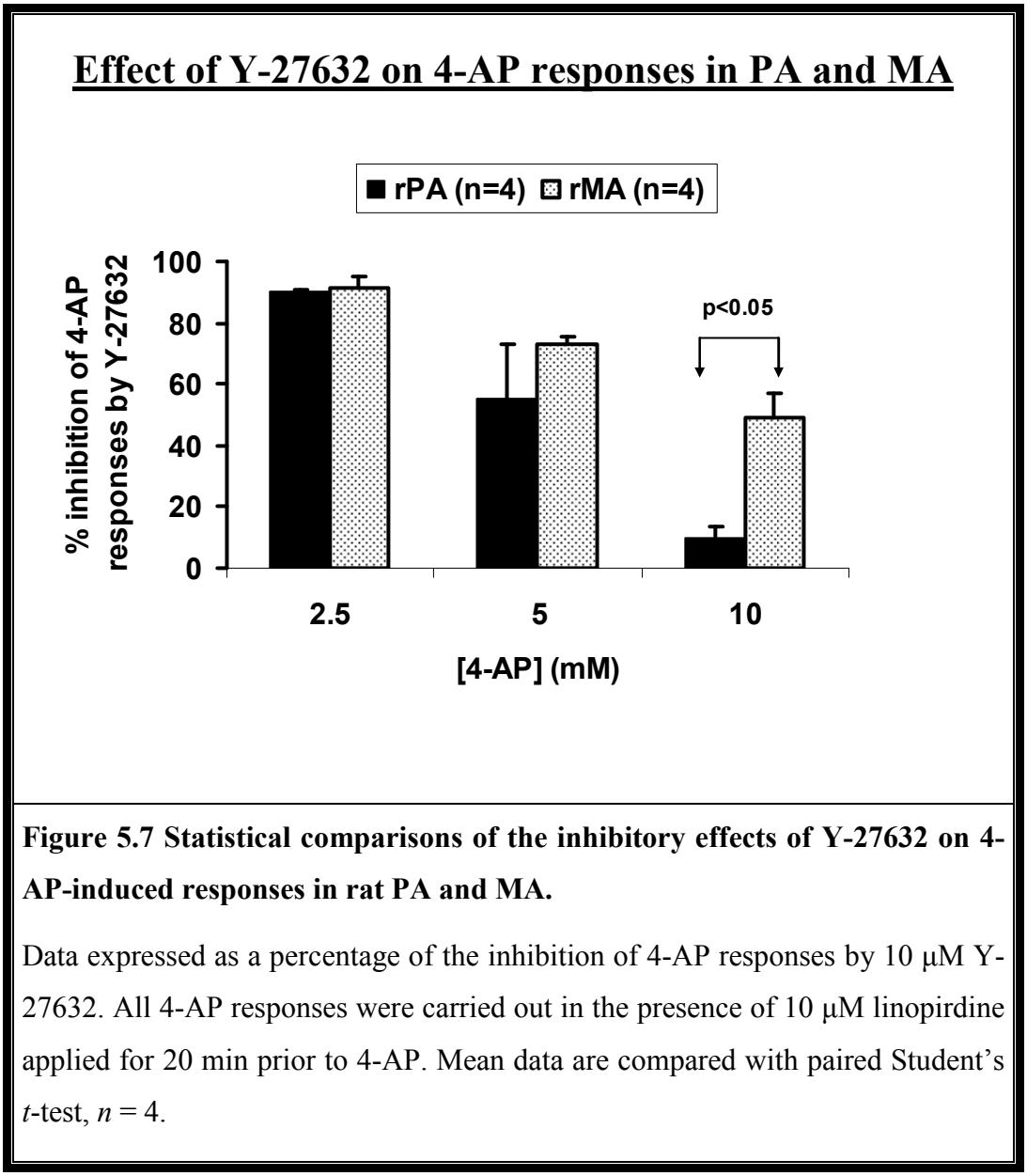

Figure 5.7 Statistical comparisons of the inhibitory effects of Y-27632 on 4-AP-induced responses in rat PA and MA.

Data expressed as a percentage of the inhibition of 4-AP responses by 10 μM Y-27632. All 4-AP responses were carried out in the presence of 10 μM linopirdine applied for 20 min prior to 4-AP. Mean data are compared with paired Student's *t*-test, $n = 4$.

5.2.4 Effect of Y-27632 on 4-AP-induced phosphorylation of myosin phosphatase target subunit (MYPT1) and MLC_{20}

In the section 5.2.1 of this chapter I demonstrated that in PA combined application (post-treatment) of diltiazem and Y-27632 or Y-27632 and diltiazem blocked the 4-AP response only partly, leaving nearly one third of the contraction insensitive. Moreover, in the section 5.2.2 I also demonstrated that pretreatment with Y-27632 alone blocked 4-AP response by ~61% ($p<0.01$, $n = 3$). Thus, I hypothesised that 4-AP was associated with Ca^{2+} sensitisation which indirectly support the idea that the myosin phosphatase target subunit (MYPT1), the downstream effector component of Rho-kinase, could have been phosphorylated in response to the treatment with 4-AP. Therefore, 4-AP might increase levels of phosphorylated MYPT1 and pretreatment of the vascular tissue with Y-27632 might reduce the phosphorylation. Freshly isolated pieces of PA and MA were divided into three groups: i) the control (no inhibitor), ii) treated with 10 mM 4-AP, and iii) treated with 10 mM 4-AP+10 μM Y-27632. Pieces of arteries were incubated in Krebs solution under continuous gassing. Following the incubation, arteries were subjected to Western blot analysis to measure level of phosphorylated MYPT1 as described in Chapter 2. In the 4-AP treated groups, 10 μM linopirdine was also present to match the contraction experiments. Rho-kinase phosphorylates MYPT1 at two different sites including Thr695 and Thr850 (mammalian sequence), and the later site is reported to be preferred by Rho-kinase (Muranyi *et al.*, 2005). I, therefore, used antiphospho MYPT1 (Thr850) antibody in this study.

Although pretreatment of the arterial tissues with 4-AP failed to show an increase in phosphorylation of MYPT1 the level of phosphorylated MYPT1 in Y-27632+4-AP treated groups was significantly reduced in PA ($p<0.05$, $n = 3$; Fig. 5.8 A).

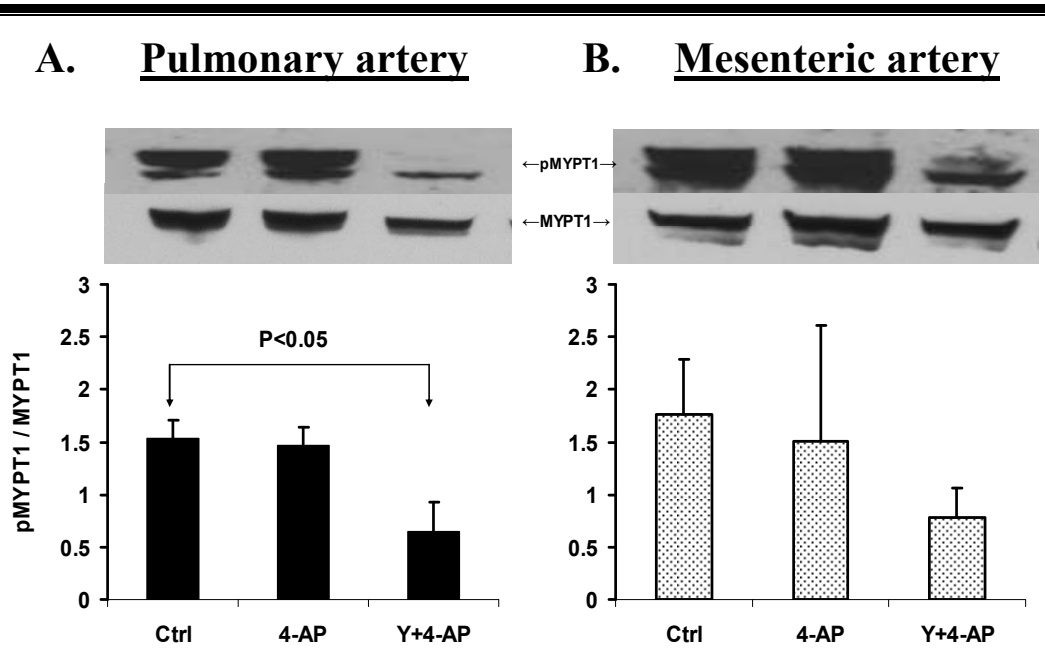

Figure 5.8 Effect of Rho-Kinase inhibitor Y-27632 on the level of phosphorylated MYPT1 in rat PA.

A combined pretreatment with 10 mM 4-AP and 10 μM Y-27632 significantly reduced phosphorylated MYPT1 in PA (A) and not in MA (B). Differences between control versus treatment groups were tested by Dunnett post-hoc test following one-way ANOVA, $n = 3$.

The above results showing the absence of 4-AP-induced phosphorylation of MYPT1 does not fit with the observation that 4-AP evokes contraction in intact PA and MA and that the 4-AP-induced contraction is sensitive to the Rho-kinase inhibitor Y-27632. One of the possible explanations could be the differences in the experimental conditions and that, in the contraction experiments arteries were under certain level of tension. It was previously shown that mild stretching of blood vessels resulted in vasoconstriction mediated by RhoA/Rho-kinase pathway (McGregor *et al.*, 2002). To test this hypothesis main extra PA rings were mounted in myograph under 5 mN of tension (hence termed *stretched*) and treated as follows: i) normalisation and stimulation 3 times with high K^+ followed

by leaving it with normal Krebs solution for an equal duration of the other treatment groups (control); ii) following normalisation and stimulation, tissue was treated with 10 μM linopirdine (20 min) and 10 mM 4-AP (20 min) (4-AP); iii) in addition to the treatment with 4-AP in this group, tissue was exposed to 10 μM Y-27632 for another 10 min (Y+4-AP). Similar treatment was given to another 3 groups without mounting them on the myograph hence termed *non-stretched*. At the end of each treatment protocol tissues were collected and snap frozen for Western blot analysis. For these *non-stretched* and *stretched* tissues, protein expression of phosphorylated 20 kDa myosin light chain ($^{P}MLC_{20}$) was measured by Western blot as $^{P}MLC_{20}$ is the ultimate indicator of tissue contraction.

Pretreatment with 4-AP showed a greater increase in the $^{P}MLC_{20}$ (Ser^{19}) levels in the *stretched* PA in comparison to *non-stretched* preparations (Fig. 5.9 B). Pretreatment with Y-27632, however, tends to decrease the $^{P}MLC_{20}$ (Ser^{19}) levels. However, neither in the *stretched* nor in the *non-stretched* tissue these differences were significant (Fig. 5.9 A and B, respectively). More experiments are necessary to determine if the difference exists in the phosphorylation levels under these conditions.

Also, the experiments with the stretched tissue were carried out in main PA rings [external diameter ~2 mm (Hislop & Reid, 1978)] whereas contraction studies were performed in small resistance arteries. Although the mechanism of contraction and Rho-kinase-dependent sensitisation supposed to be similar, the sensitivity to 4-AP could differ between the two tissues (conduit vs. resistance). The observation of two subtypes of K^{+} currents, 4-AP sensitive and 4-AP insensitive in arteries isolated from the main PA (Smirnov *et al.*, 2002) supports this possibility.

Finally, phosphorylation of MYPT1 of a different site (Thr695) also cannot be entirely excluded. Future focussed work will help to identify the exact molecular pathway involved in the 4-AP-induced contraction.

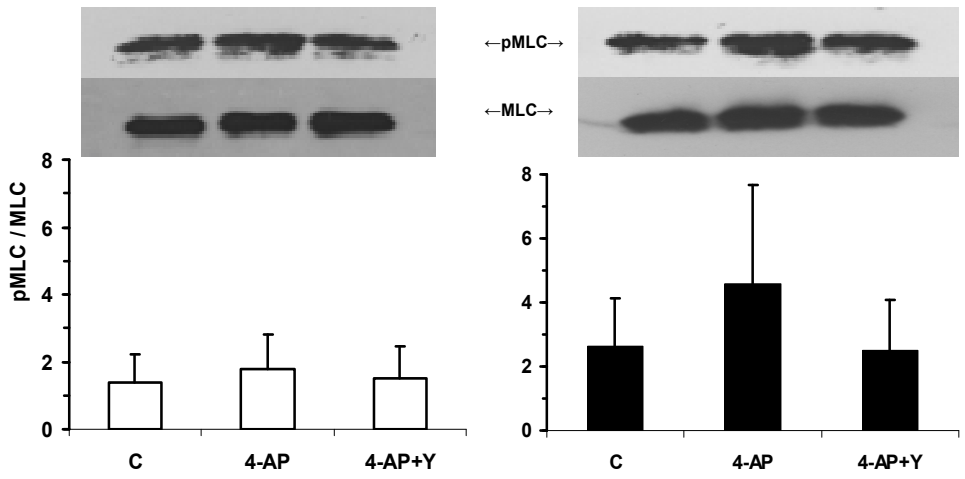

Figure 5.9 Effect of tissue stretching on 4-AP-induced phosphorylation of MLC_{20} in rat main PA.

Pretreatment with 10 mM 4-AP changed phosphorylation of MLC_{20} in stretched PA (B), but not in non-stretched PA (A). Data were not significant (one-way ANOVA, $n = 3$).

5.2.5 Effects of diltiazem and Y-27632 on high K^+ (80 mM KCl)-induced contraction in rat PA and MA

The previous sections characterised vascular response to 4-AP which acts via inhibition of K_V channels thus causing membrane depolarisation and contraction. On the other hand, use of 4-AP was criticised due to lack of its complete specificity. High concentrations of extracellular K^+ cause contraction via similar mechanism: depolarising the cell membrane due to decrease of K^+ gradient across the cell membrane and thus impairing the activity of all K^+ channels independent of their molecular or biophysical properties. To explore whether high K^+-induced contraction engages Ca^{2+}-sensitisation in addition to the established voltage-dependent mechanism similar to that observed with 4-AP in my experimental conditions, the effect of the L-VOCC blocker diltiazem and Rho-kinase inhibitor Y-27632 on the steady-state contraction induced by high concentration of K^+ was assessed in PA and MA.

Arteries were exposed to 80 mM KCl for 15 min to obtain sustained contraction followed by addition of 10 μM diltiazem, 10 μM Y-27632, or their combination for 10 min each in a similar fashion as described for 4-AP in the previous sections. In PA, diltiazem alone blocked high K^+-induced contraction by 89% (mean 84±3.6%, n = 10, $p<0.001$). Subsequent application of Y-27632 completely abolished the tension (Fig. 5.10 A). In MA, on the other hand, diltiazem alone completely blocked the total contraction (mean 99.7±0.3%, n = 10, $p<0.001$) produced with high K^+ (Fig. 5.10 C). When the application sequence was reversed, 10 μM Y-27632 blocked high K^+ contraction only by 35% (mean 35.4±2.1%, n = 11, $p<0.001$) in PA (Fig. 5.10 B), and by 85% (mean 90.6±1.4%, n = 11, $p<0.001$) in MA (Fig. 5.10 D). In both tissues, however, the tension was totally abolished in the presence of the two inhibitors added together (Fig. 5.11 A-D).

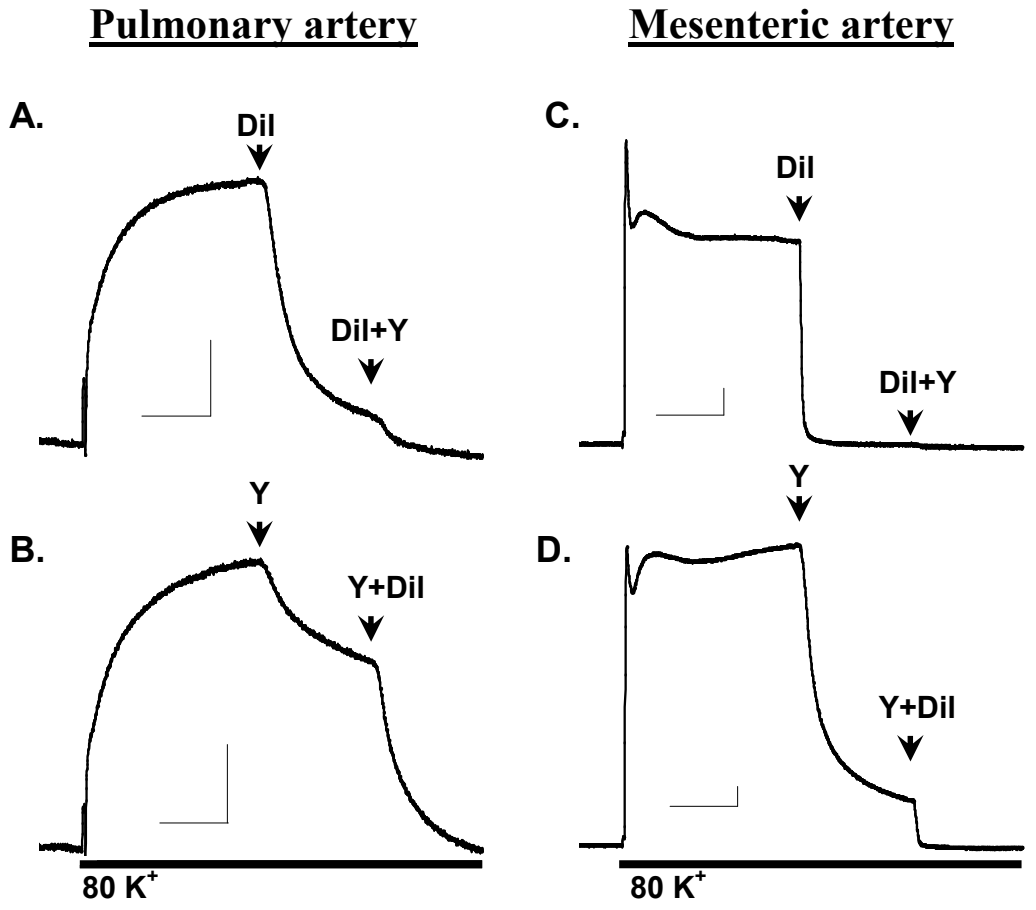

Figure 5.10 Effects of diltiazem or Y-27632 or combination of these two drugs on high K^+-induced contraction in rat PA and MA.

Representative traces were obtained from PA of 294 and 363 μm i.d. (A and B, respectively) and MA of 262 and 194 μm i.d. (C and D, respectively). 80 K^+, 80 mM KCl; Y, Y-27632 (10 μM); Dil, diltiazem (10 μM). Horizontal and vertical scale bars represent 5 min and 1 mN, respectively.

The average results of the effect of diltiazem and Y-27632 on KCl-induced contraction in 11 PA and 10 MA are statistically compared in Figure 5.11. This comparison and those reported in the previous sections demonstrate principal similarity between the relaxation induced by the two inhibitors in the presence of high K^+ and 4-AP. Notably, the degree of inhibition of the steady state contraction by Y-27632 was very similar in high K^+ (35.4±2.1%, n = 11) and 4-AP (31.7±8.7%, n = 6), suggesting that the levels of Ca^{2+} sensitisation are similar in both conditions. Also, similar to 4-AP, MA showed greater sensitivity to both diltiazem and Y-27632 in the presence of high K^+ in comparison to PA. On the other hand, the combination of both inhibitors completely relaxed high K^+-induced contraction in PA, whereas a significant component of 4-AP-induced contraction was insensitive in their presence in this preparation. Also, in MA, the degree of relaxation to diltiazem alone was very similar and nearly complete in high K^+ as well as in 4-AP-induced contractions. However, surprisingly Y-27632 completely relaxed high K^+-induced contraction (in MA), but only partially the 4-AP-induced contraction in this artery (compare Fig. 5.2 D with Fig. 5.11 D).

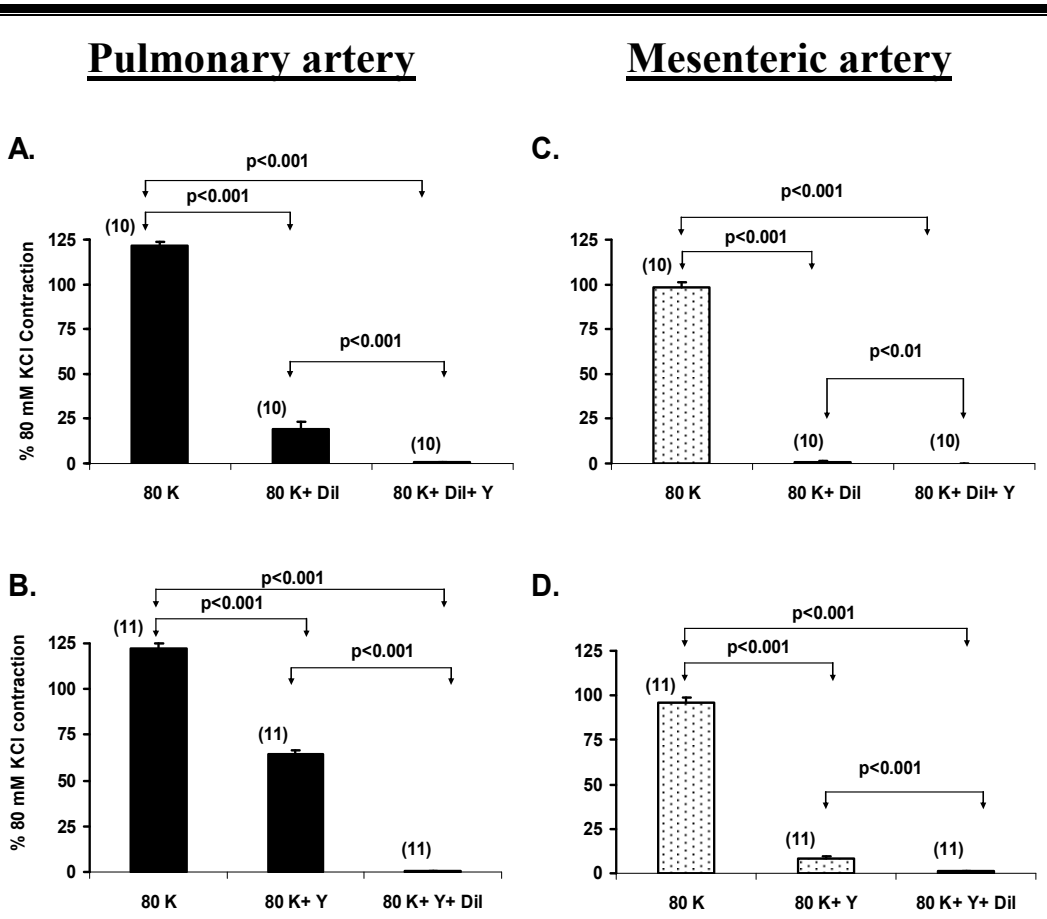

Figure 5.11 Comparison of the inhibitory effects of diltiazem and Y-27632 on high K^+-induced contraction in rat PA and MA.

A and **C,** Statistical comparisons of the effects of diltiazem and diltiazem+Y-27632 on high K^+-induced contraction in PA (A) and MA (C). **B** and **D,** Statistical comparisons of the effects of Y-27632 and Y-27632+diltiazem on high K^+-induced contraction in PA (B) and MA (D). A combination of diltiazem and Y-27632 (10 μM each) ablated high K^+ response completely in both tissue types. Note that the order of the drugs listed on x-axis indicates the order of their application in the experiment. 80 K, 80 mM KCl; Y, Y-27632; Dil, diltiazem. Differences between groups were tested by Tukey-Kramer post-hoc test following one-way ANOVA; *n* values are shown on the graphs in brackets.

5.2.6 Effect of pretreatment of PA and MA with diltiazem, Y-27632 or their combination on high K^+-induced contraction

To investigate whether the pretreatment of arteries with the two inhibitors (alone or in combination) will affect high K^+-induced contraction in a similar fashion as it did for the 4-AP-induced responses, diltiazem and Y-27632 at 10 μM each were applied for 10 min prior to the addition of 80 mM K^+. The effect of the drugs was compared with both the control and the recovery responses. Fig. 5.12 shows traces from a representative experiment. Interestingly, in PA, while a partial block of high K^+ contraction (56%) following the pretreatment with Y-27632 alone (Fig. 5.12 B) is expected based on the previous findings, an incomplete inhibition of high K^+ response by diltiazem (70%, Fig. 5.12 C) is somewhat unusual. Conversely, in MA, pretreatment with either of the inhibitors blocked high K^+ response almost completely (Fig 5.12 F and G), suggesting that the difference between PA and MA are unlikely to arise from a less potent action of diltiazem in PA, since both arteries were exposed to the same concentration of the L-VOCC blocker.

Interestingly, in the presence of Y-27632, contraction to high K^+ in MA was transient, suggesting that Ca^{2+} sensitisation is important for maintaining of contraction in this tissue. In PA, however, the amplitude of contraction was reduced, without significant changes in the time course. Similar to the 4-AP-induced contraction, the pretreatment with a combination of Y-27632 and diltiazem (10 μM each) virtually completely blocked high K^+ response both in PA (96.9±1.1, n = 3, Fig. 5.13 B) and in MA (100%, n = 3, Fig. 5.13 E).

The normalised average results statistically compared in Figure 5.14, demonstrating significant difference between the control responses and those in the presence of the inhibitors.

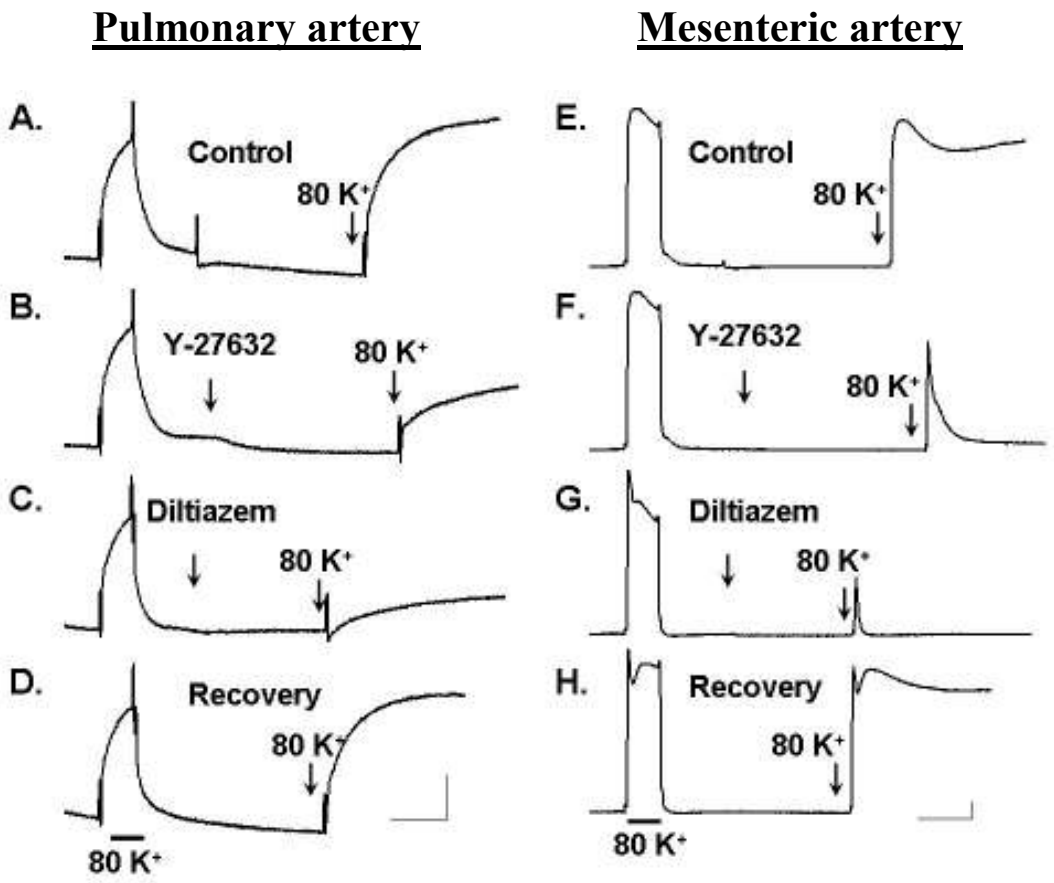

Figure 5.12 Effects of pretreatment with Y-27632 or diltiazem on high K^+-induced contraction in rat PA and MA.

Representative traces obtained from PA (A-D) of 390 μm i.d. and MA (E-H) of 240 μm i.d. showing response to 80 mM KCl in control, in the presence of 10 μM Y-27632 or 10 μM diltiazem and recovery. 80 K^+, 80 mM KCl. Horizontal and vertical scale bars represent 5 min and 1 mN, respectively.

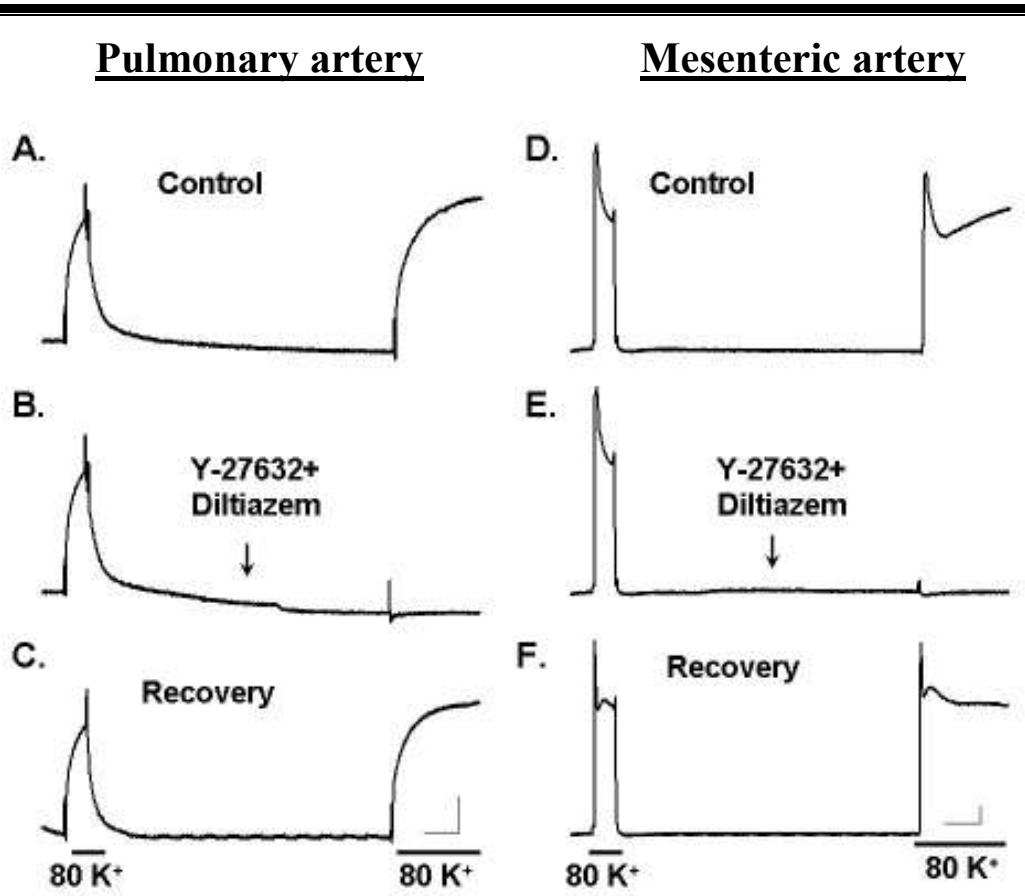

Figure 5.13 Effect of pretreatment with a combination of Y-27632 and diltiazem on high K^+-induced contraction in rat PA and MA.

Representative traces obtained from PA (A-C) of 294 μm i.d. and MA (D-F) of 262 μm i.d. showing response to 80 mM KCl in control, in the presence of Y-27632+diltiazem (10 μM each) and recovery. 80 K^+, 80 mM KCl. Horizontal and vertical scale bars represent 5 min and 1 mN, respectively.

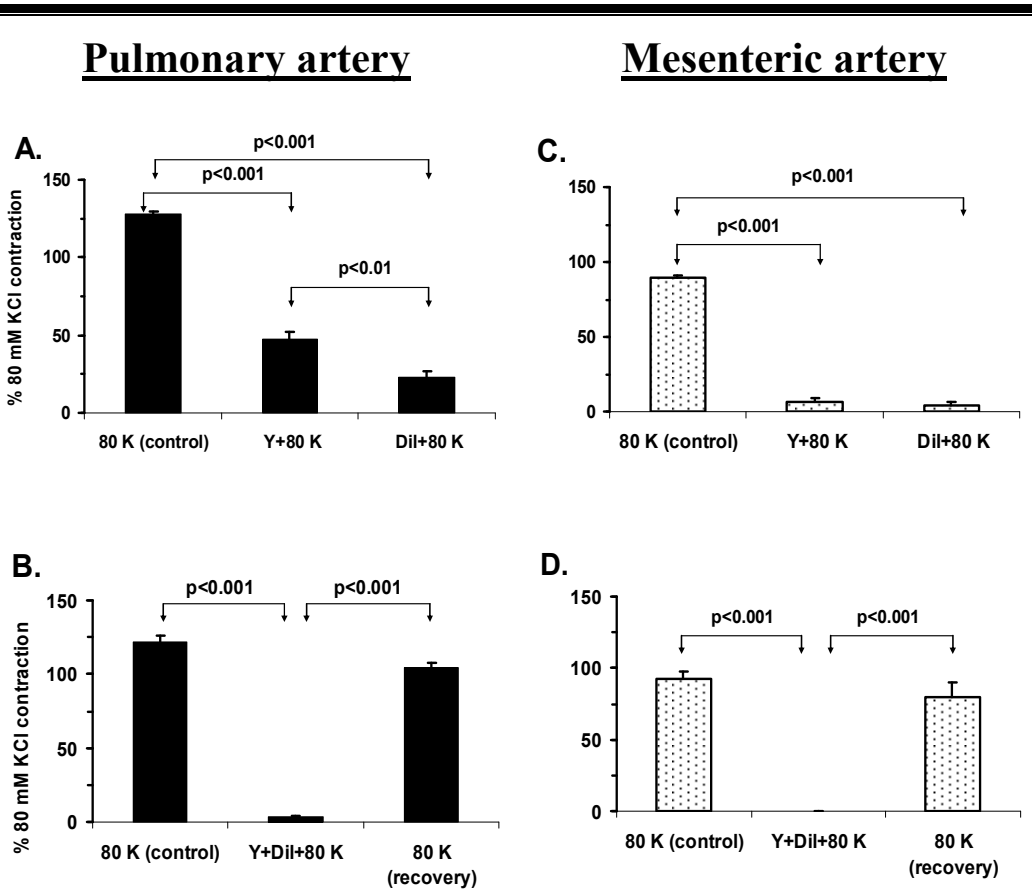

Figure 5.14 Summary of the effects of pretreatment with Y-27632 and diltiazem alone or a combination of the two inhibitors on high K^+-induced contraction in rat PA and MA.

A and **C,** Statistical comparisons of the effects of pretreatment with Y-27632 or diltiazem alone on high K^+-induced contraction in PA (A) and MA (C). **B** and **D,** Statistical comparisons of the effects of pretreatment with Y-27632+diltiazem on high K^+-induced contraction in PA (B) and MA (D). Note that the order of the drugs listed on x-axis indicates the order of their application in the experiment. 80 K, 80 mM KCl; Y, Y-27632 (10 μM); Dil, diltiazem (10 μM). Differences between groups were tested by Tukey-Kramer post-hoc test following one-way ANOVA (n = 3). Note that, as the pretreatment of the tissues with Y-27632+diltiazem resulted in the complete inhibition of contraction no further experiments were carried out.

5.2.7 Effects of Y-27632 on increasing levels of KCl-induced contractions in rat PA and MA

In the section 5.2.3 I have demonstrated that the effect of Y-27632 on the 4-AP-induced contraction depends on the level of preconstriction. It was, therefore, logical to check if a similar dependency exists for contractions induced by high K^+. In this set of experiments, increasing concentrations of KCl (20, 30, 40 and 80 mM) were applied for 15 min to obtain various levels of contractions followed by application of 10 μM Y-27632. Fig. 5.15 A-D shows representative traces in PA, where Y-27632-dependent relaxation was comparatively larger at lower than at high concentrations of KCl. In MA, on the other hand, the effect of Y-27632 was equally potent at all levels of KCl contractions (Fig. 5.15 E-H).

The statistical analysis of these differences recorded in 4 PA and 4 MA is shown in Fig. 5.16. This comparison clearly shows that the ability of the Rho-kinase inhibitor to reduce contraction depends on the level of tone in PA but not in MA. This dependence is even more pronounced than the similar trend seen at different levels of 4-AP-induced contraction (Fig. 5.7), suggesting that this effect may be specific for PA and is independent on the way the contraction is initiated. The differences between PA and MA may therefore indicate towards the different role Ca^{2+} sensitisation plays in the initiation and maintenance of contraction in these two preparations.

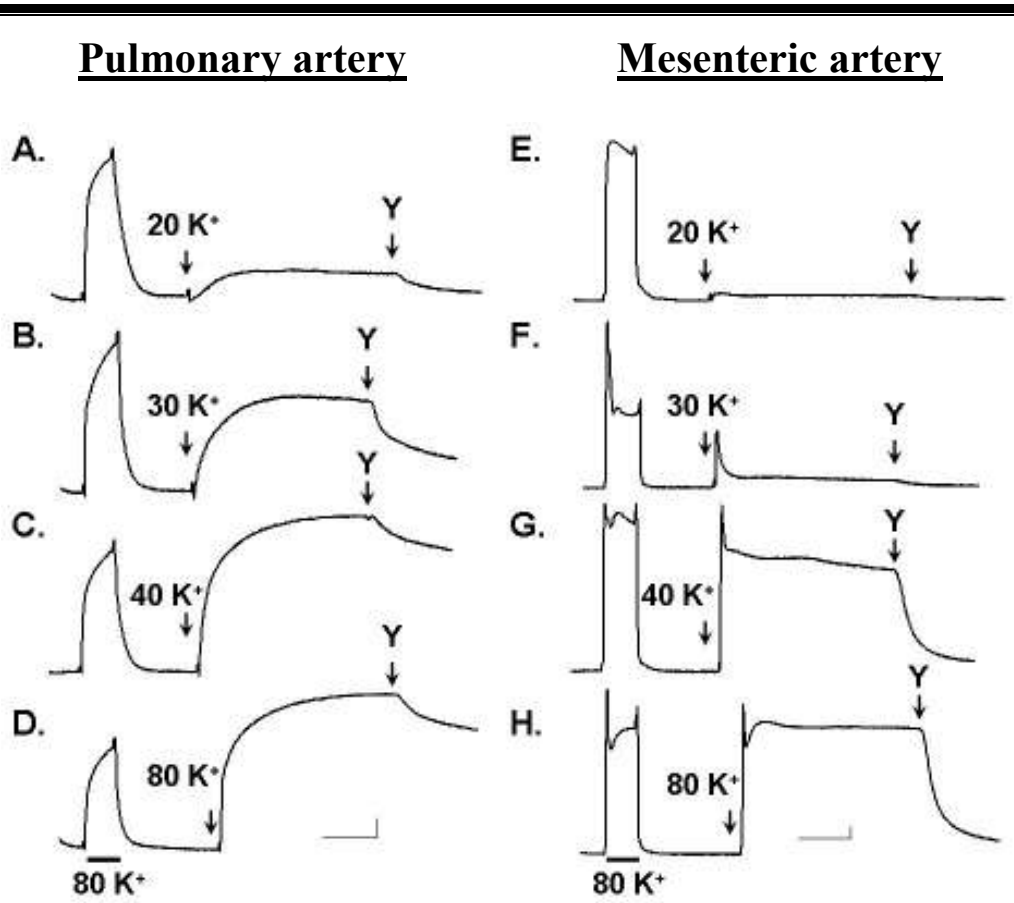

Figure 5.15 Inhibition of contraction induced by various concentrations of KCl by Y-27632 in rat PA and MA.

Representative traces obtained from PA (**A-D**) of 374 μm i.d. and MA (**E-H**) of 230 μm i.d. showing relative relaxation by 10 μM Y-27632 on contractions produced with gradual increase in concentration of KCl. **A-D**, in PA, Y-27632 relaxed contraction to 20 mM KCl completely, while contraction elicited by 30 mM or higher concentrations of KCl, Y-27632 only partly blocked the response. **E-H**, in MA, Y-27632 virtually completely blocked KCl contraction at all concentrations. 20 K^+, 30 K^+, 40 K^+ and 80 K^+ indicates extracellular concentration of KCl in mM; Y, Y-27632 (10 μM). Horizontal and vertical scale bars represent 5 min and 1 mN, respectively.

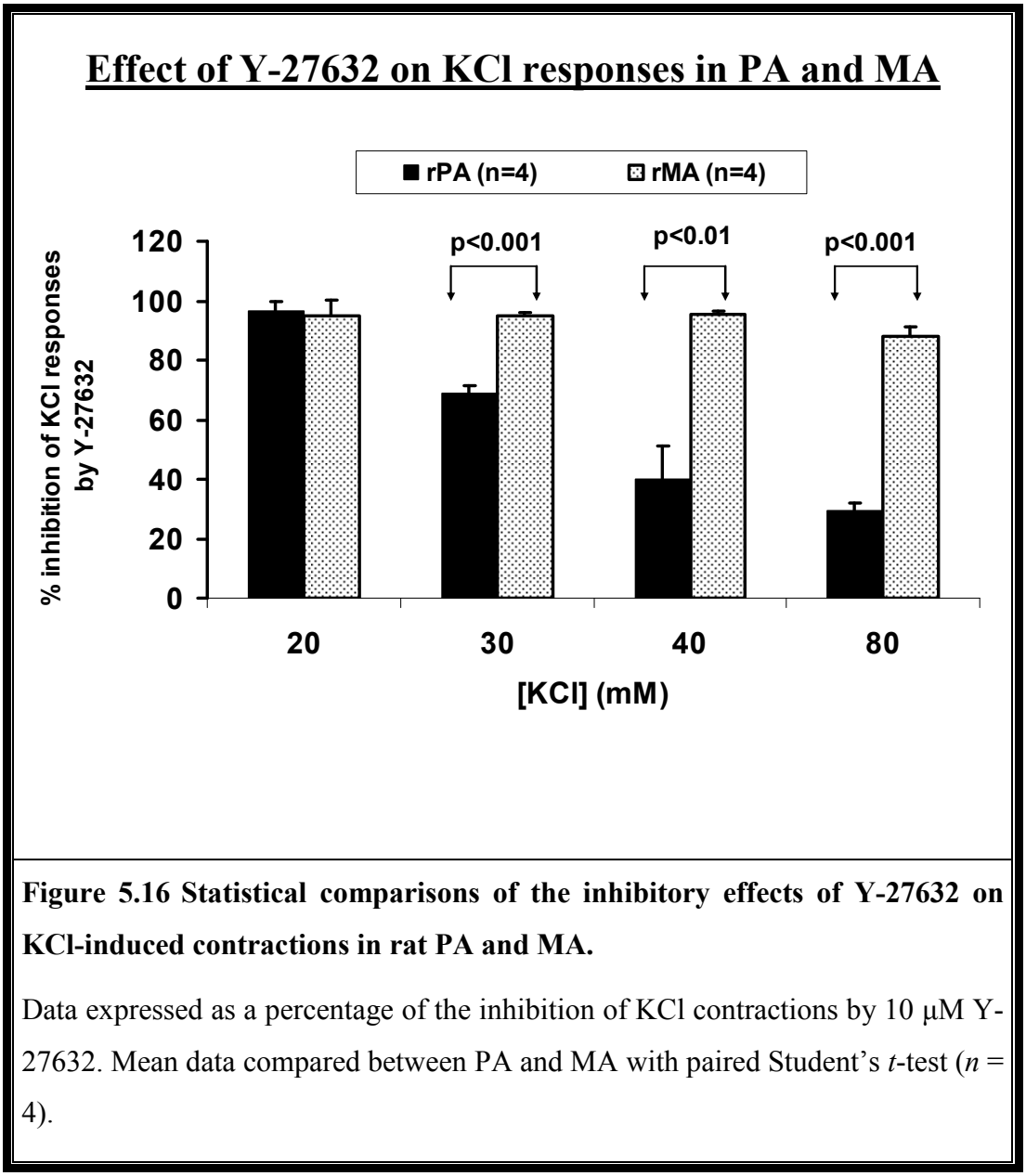

Figure 5.16 Statistical comparisons of the inhibitory effects of Y-27632 on KCl-induced contractions in rat PA and MA.

Data expressed as a percentage of the inhibition of KCl contractions by 10 μM Y-27632. Mean data compared between PA and MA with paired Student's *t*-test (n = 4).

5.2.8 Effects of Y-27632 and diltiazem on U-46619-induced contraction in rat PA and MA

The thromboxane A_2 mimetic U-46619 is a potent vasoconstrictor acting via thromboxane prostanoid (TP) receptor that triggers smooth muscle contraction via Ca^{2+}/calmodulin/MLCK pathway and RhoA/Rho-kinase pathway (Wilson *et al.*, 2005;Alapati *et al.*, 2007). U-46619-induced vasoconstriction also has a voltage-dependent component as it is reported that entry of extracellular Ca^{2+} was inhibited by nicardipine, an L-VOCC blocker (Wilson *et al.*, 2005). I, therefore, investigated the contractile responses to 1 μM U-46619 (15-20 min) in the absence and following pretreatment of the tissue with the L-VOCC blocker diltiazem (10 μM). In the first set of experiments performed without pretreatment with diltiazem, after a steady level of contraction with 1 μM U-46619 was achieved, 10 μM Y-27632 alone or Y-27632+diltiazem (10 μM each) were applied in PA and MA to assess a relative proportion of Rho-kinase-sensitive and voltage-sensitive components in the contraction resulting from the action of U-46619.

Figures 5.17 and 5.18 respectively show the representative traces and the summary of the results obtained in 3 PA and 3 MA. In the absence of diltiazem, in PA, 10 μM Y-27632 blocked U-46619-induced contraction by ~68% (mean 43.9±11.8%, *n* = 3), and Y-27632+diltiazem (10 μM each) blocked by ~77% (mean 58.6±9.6%, *n* = 3) (Fig. 5.17 A); while in MA, 10 μM Y-27632 blocked U-46619-induced contraction by ~86% (mean 89.3±2.0%, *n* = 3), and Y-27632+diltiazem (10 μM each) blocked by ~99% (mean 99.4±0.2%, *n* = 3) (Fig. 5.17 C).

When the experiment was repeated after pretreatment of the tissue with 10 μM diltiazem, in the PA the U-46619-induced contraction was diminished by ~19 %, however the effect of Y-27632 was similar to that in the absence of diltiazem. Notably, as one would expect, the additional effect of diltiazem was absent (Fig. 5.17 B and D). In MA, Y-27632 in the presence of diltiazem completely relaxed

U-46619-induced contraction without further effect of diltiazem (Fig. 5.17 D). Notably, the presence of the third component of U-46619-induced contraction which was insensitive to both diltiazem and Y-27632 in PA, but not in MA, echoes the effect of these inhibitors on the 4-AP-induced contraction in both arteries described in the previous sections.

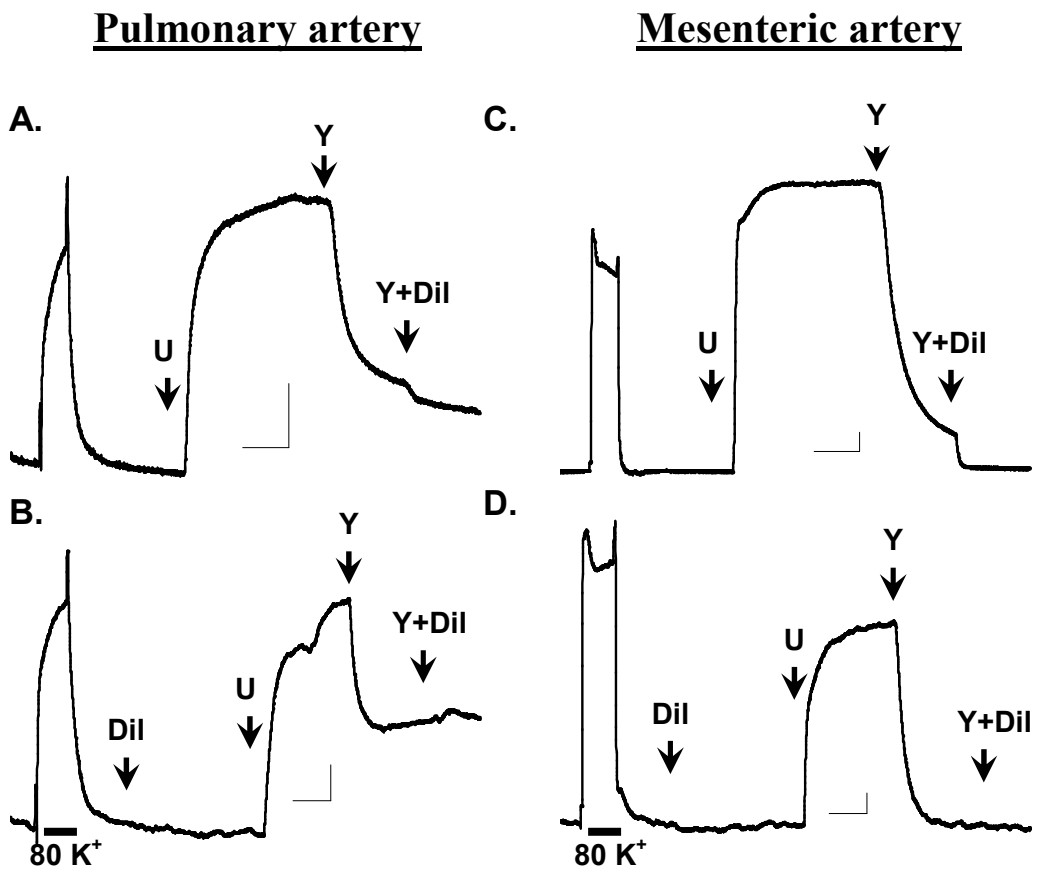

Figure 5.17 Effects of Y-27632 and diltiazem on U-46619-induced contraction in rat PA and MA in the absence (A, C) and presence (B, D) of diltiazem.

Representative traces obtained from PA of 362 (A) and 423 (B) μm i.d. and MA of 274 (C) and 370 (D) μm i.d. showing relaxation of 1 μM U-46619-induced contraction by 10 μM Y-27632 alone or Y-27632+diltiazem (10 μM each). U, U-46619; Y, Y-27632; Dil, diltiazem. Horizontal and vertical scale bars represent 5 min and 1 mN, respectively.

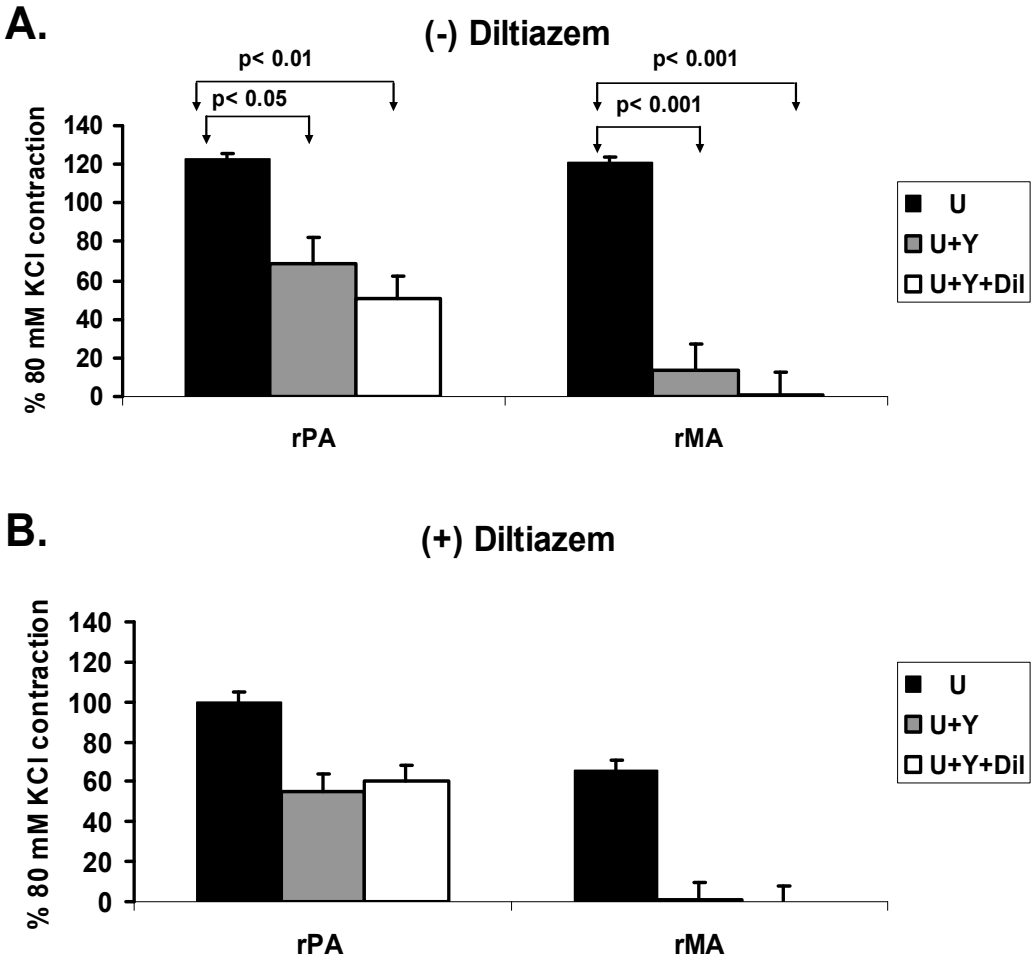

Figure 5.18 Effect of Y-27632 and diltiazem on U-46619-induced contraction in rat PA and MA in the absence and presence of diltiazem.

Graphs summarise and compare normalised tensions produced with 1 μM U-46619 alone, remaining tension after application of 10 μM Y-27632, or Y-27632+diltiazem (10 μM each). (-) Diltiazem, experiments were carried out in absence of diltiazem; (+) Diltiazem, experiments were carried out in the presence of 10 μM diltiazem added before the application of U-46619. U, U-46619, Y, Y-27632, Dil, Diltiazem. Top panel (A) one-way ANOVA with Tukey-Kramer post-hoc test (n = 3), bottom panel (B) no statistics done (n = 2).

5.2.9 Effects of pretreatment with Y-27632 and diltiazem on U-46619-induced contraction in rat PA and MA

In the previous section I demonstrated that a combination of Y-27632 and diltiazem was unable to block the sustained U-46619-induced contraction in PA indicating the presence of a third component. I have also shown that the pretreatment with two inhibitors together completely blocked 4-AP- and high K+-induced contraction. It is therefore logical to evaluate the effect of the combined addition of Y-27632 and diltiazem (10 μM each) on the subsequent contractile response to U-46619.

Figures 5.19 and 5.20 respectively show the examples of the representative experiments and statistical comparison of the averaged data obtained in 4 PAs and 4 MAs. Pretreatment with a combination of Y-27632 and diltiazem (10 μM each) blocked U-46619-induced contraction in PA by 63% (mean 61.1±11.9%, n = 4) with one third of contraction being insensitive to this treatment (Fig. 5.19 B). In contrast, in MA, the contraction was blocked by 95% (mean 95.8±1.2%, n = 4) (Fig. 5.19 E). In both cases, the complete recovery of the U-46619-induced responses was observed.

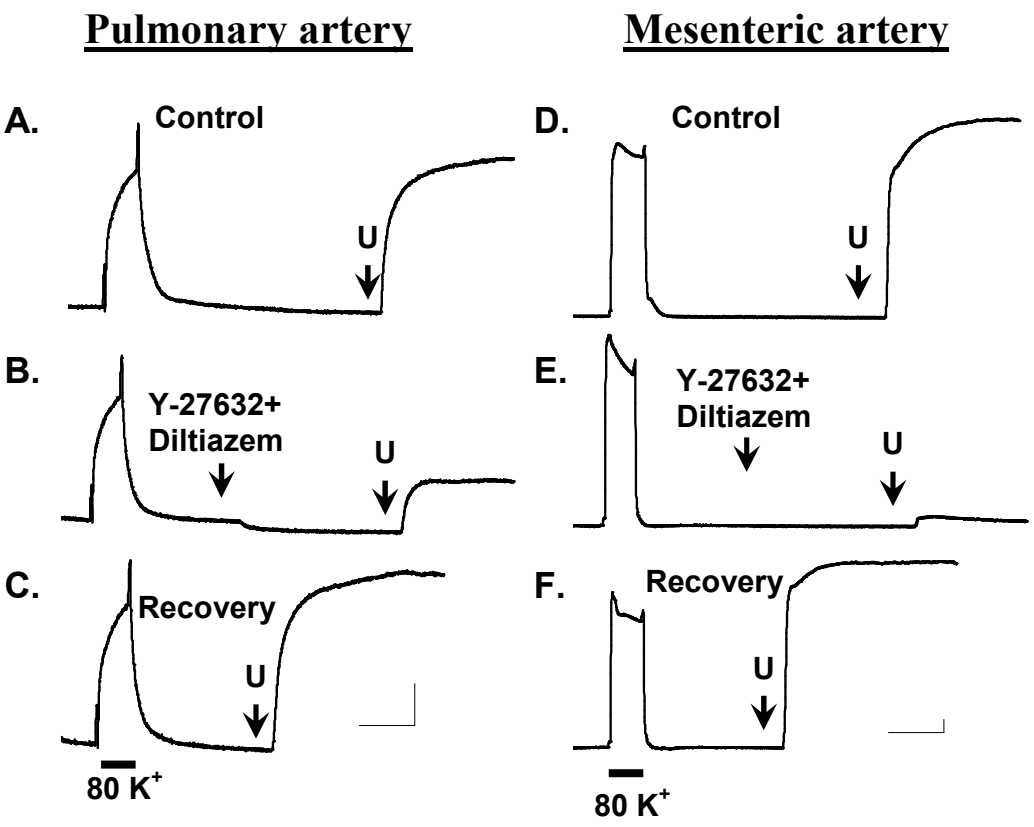

Figure 5.19 Effect of pretreatment with a combination of Y-27632 and diltiazem on U-46619-induced contraction in rat PA and MA.

Representative traces obtained from PA (A-C) of 362 μm i.d. and MA (D-F) of 274 μm i.d. showing contraction elicited by 1 μM U-46619 in the control, in the presence of Y-27632+diltiazem (10 μM each), and following the recovery. U, U-46619 (1 μM). Horizontal and vertical scale bars represent 5 min and 1 mN, respectively.

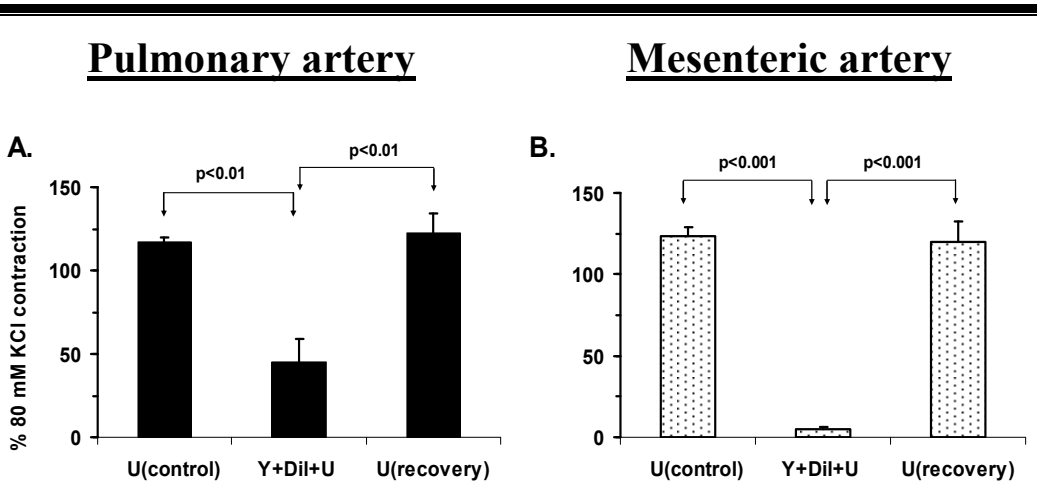

Figure 5.20 Comparison of the effect of pretreatment with Y-27632+diltiazem on U-46619-induced contraction between rat PA and MA.

Graphs summarise and compare normalised tension obtained from PA (A) and MA (B) with 1 μM U-46619 alone (control), with 1 μM U-46619 following the pretreatment with Y-27632+diltiazem (10 μM each) and the recovery. Pre-testament with a combination of Y-27632+diltiazem (10 μM each) was unable to completely block U-46619 response in PA (A) but it blocked U-46619 response entirely in MA (B). Note that the order of the drugs listed on x-axis indicates the order of their application in the experiment. U, U-46619; Y, Y-27632; Dil, diltiazem.

5.2.10 Dependence of the effects of Y-27632 on the level of U-46619-induced contraction in rat PA and MA

The findings described in the previous sections suggest that the effect of Y-27632 was dependent on the level of preconstriction induced by 4-AP and high K^+ specifically in PA. I therefore investigated if similar dependency exists for contractions caused by different concentrations of U-46619. The experiments were carried out under two conditions: 1) in the presence of 10 μM diltiazem in order to eliminate voltage-dependent component, and 2) in the absence of diltiazem. In both cases 10, 20, 100 and 1000 nM of U-46619 were used to obtain increasing levels of contractions; the agonist was applied for 10-15 min to obtain a sustained contraction which was followed by addition of 10 μM Y-27632.

Figures 5.21 and 5.22 respectively show the representative recordings in the presence and in the absence of diltiazem. The statistical comparison of the mean values obtained under both conditions is shown in Fig. 5.23. This analysis clearly shows that Y-27632 caused a greater relaxation at low concentrations of U-46619 in PA in both conditions. In MA, however, the effect of Y-27632 was independent on the degree of preconstriction in the presence of diltiazem (Fig. 5.21 E-H and Fig. 5.23 A). In the absence of the L-VOCC blocker diltiazem, Y-27632 was less effective at high concentration of U-46619 (Fig. 5.22 E-H and Fig. 5.23 B) and the remaining contraction is likely to be mediated by the Ca^{2+} entry via L-VOCC as it can be blocked by subsequent application of diltiazem (Fig. 5.17 C).

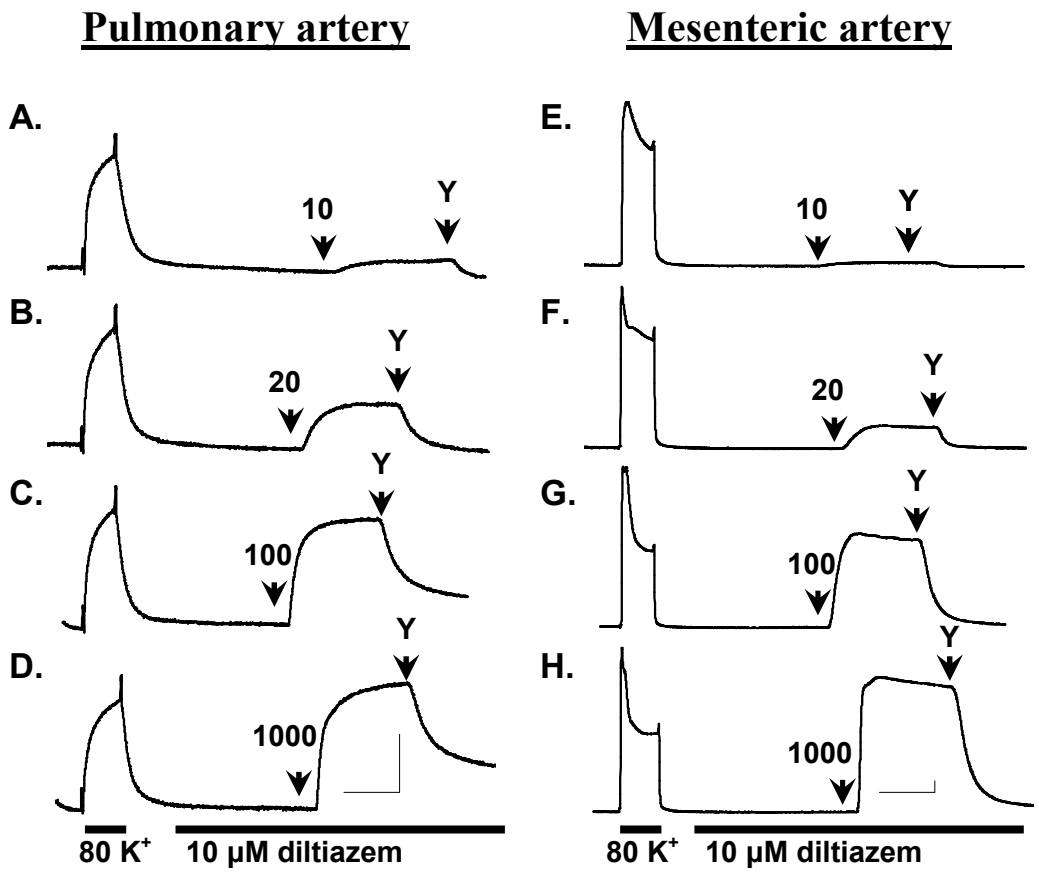

Figure 5.21 Effect of Y-27632 on the levels of U-46619-induced contraction (in the presence of diltiazem) in rat PA and MA.

Representative traces obtained from PA (A-D) of 309 μm i.d. and MA (E-H) of 300 μm i.d. showing relaxation at different levels of U-46619-induced contractions with a 10 μM Y-27632. A-D, in PA, Y-27632 relaxed U-46619 contractions completely at a concentration of 10 and 20 nM while contraction elicited with 100 nM or higher concentrations of U-46619, Y-27632 only partly blocked the response. E-H, in MA, on the other hand, Y-27632 nearly completely blocked any level of U-46619-induced contraction. The numbers next to the arrows indicate concentration of U-46619 in nM. Y, Y-27632 (10 μM). Horizontal and vertical scale bars represent 5 min and 1 mN, respectively.

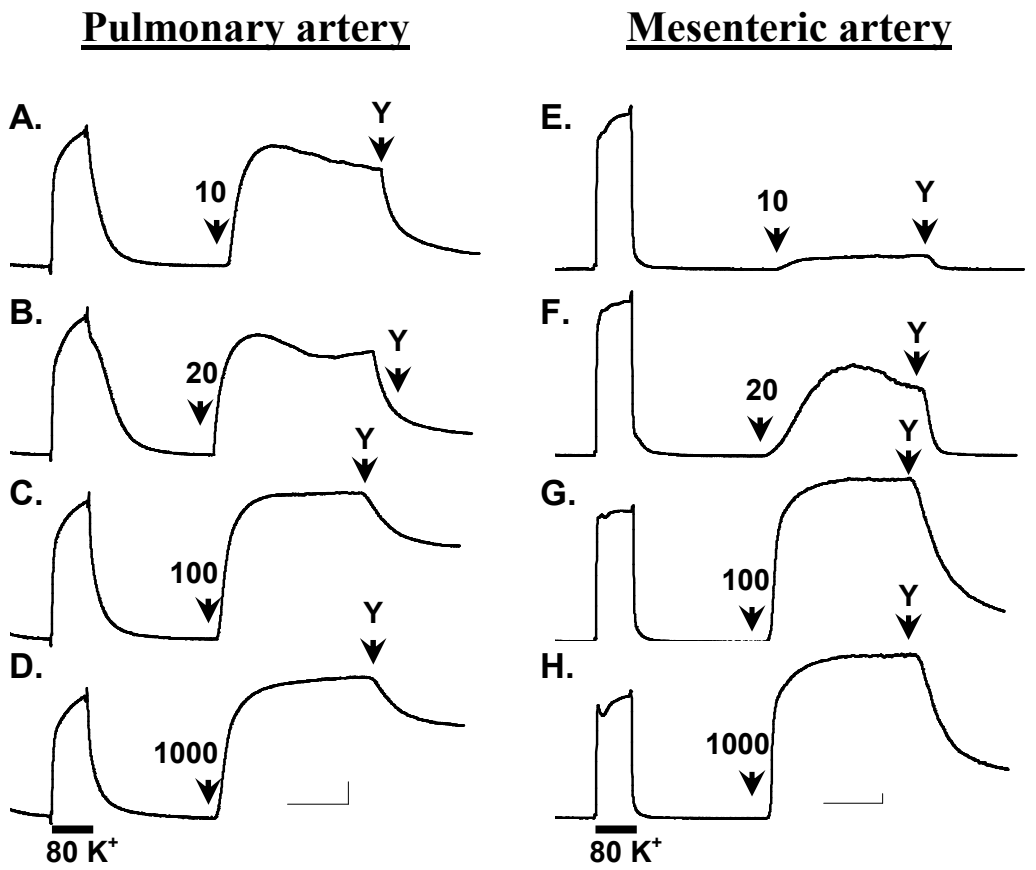

Figure 5.22 Effect of Y-27632 on the levels of U-46619-induced contraction (in the absence of diltiazem) in rat PA and MA.

Representative traces obtained from PA (A-D) of 3338 μm i.d. and MA (E-H) of 215 μm i.d. showing relaxation at different levels of U-46619-induced contractions with a 10 μM Y-27632. A-D, in PA, Y-27632 relaxed U-46619-induced contractions incompletely at any concentration of U-46619 with an increasing insensitivity to Y-27632 with the increase of contraction. E-H, in MA, on the other hand, Y-27632 completely blocked U-46619-induced contractions at 10 and 20 nM while contractions elicited with 100 nM or higher concentrations of U-46619, Y-27632 only partly blocked the contraction. The numbers next to the arrows indicate concentration of U-46619 in nM. Y, Y-27632 (10 μM). Horizontal and vertical scale bars represent 5 min and 1 mN, respectively.

Effect of Y-27632 on U-46619 responses in PA and MA

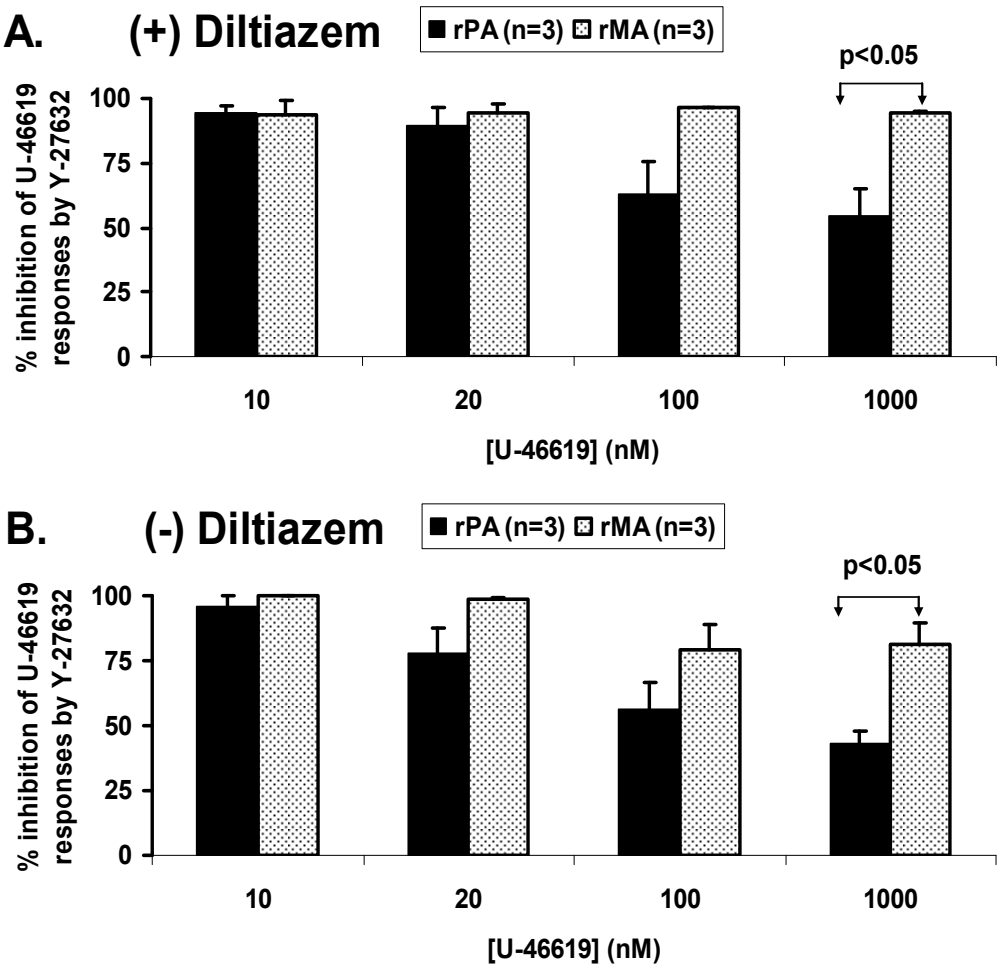

Figure 5.23 Statistical comparisons of the inhibitory effects of Y-27632 on U-46619-induced contractions in rat PA and MA in the presence (A) and absence (B) of diltiazem.

Data expressed as a percentage of inhibition of U-46619-induced contractions by 10 μM Y-27632. Mean data compared between PA and MA with paired Student's *t*-test (n = 3). (+) Diltiazem, experiments were carried out in the presence of 10 μM diltiazem added before addition of U-46619; (-) Diltiazem, experiments were carried out in the absence of diltiazem.

5.3 Discussion

The main observations described in this chapter is that in both pulmonary and systemic arteries contraction elicited by the membrane depolarisation either via inhibition of K^+ channels with 4-AP and linopirdine or using high K^+ has two components: **1)** voltage-dependent and **2)** voltage-independent; the latter involves Rho-kinase dependent Ca^{2+} sensitisation component. There are however several differences between the two type of arteries. *Firstly*, the voltage-dependent and voltage-independent components of 4-AP- or high K^+-induced contractions are additive in PA, but not in MA. *Secondly*, the Rho-kinase-dependent sensitisation has a significantly greater dependence on the pretone in PA than in MA. *Thirdly*, in PA, an additional third component is present in the 4-AP-induced contraction, which is absent in MA. Interestingly, three additive components of contraction elicited by the thromboxane A_2 receptor agonist U-46619 (as distinguished using diltiazem and Y-27632) also exists in PA, and not in MA. Although this may imply the similarity between the contractions caused by 4-AP and U-46619, however the third component of contraction was preserved following the pretreatment with diltiazem and Y-27632 in response to U46619 (Fig. 5.20 A), whereas 4-AP-induced contraction was completely abolished under such conditions (Fig. 5.5 B). This suggests that cellular mechanisms responsible for the third component (which is insensitive to the L-VOCC blockade and to the inhibition of Rho-kinase) in the 4-AP- and U-46619-induced contractions may be different. Previously, it was demonstrated that activation of TP receptors in PA involved both intracellular Ca^{2+} release and activation of non-voltage-dependent Ca^{2+} entry (Liu *et al.*, 1997;Snetkov *et al.*, 2006); both mechanisms could contribute to the described third component of the U-46619-induced contraction.

The novel and most interesting observation presented here is that relaxation of the high K^+ and 4-AP-induced contractions to diltiazem and Y-27632 are additive in PA, but not in MA. This finding provides an important insight into the principal difference between the voltage-dependent and voltage-independent cellular mechanisms which are responsible for maintenance of contraction in the two arteries. Based on this evidence I propose that the voltage-dependent Ca^{2+} entry

and Ca^{2+}-sensitisation via Rho-kinase pathway operates in parallel in the PA, hence termed the *parallel hypothesis*. In the MA, they run in sequence, hence termed *sequential hypothesis*. The two diverse hypotheses are depicted in Fig. 5.24. In both hypotheses Ca^{2+} entry is essential in order to maintain the sustained contraction because the contraction is completely abolished by the pretreatment with diltiazem and Y-27632.

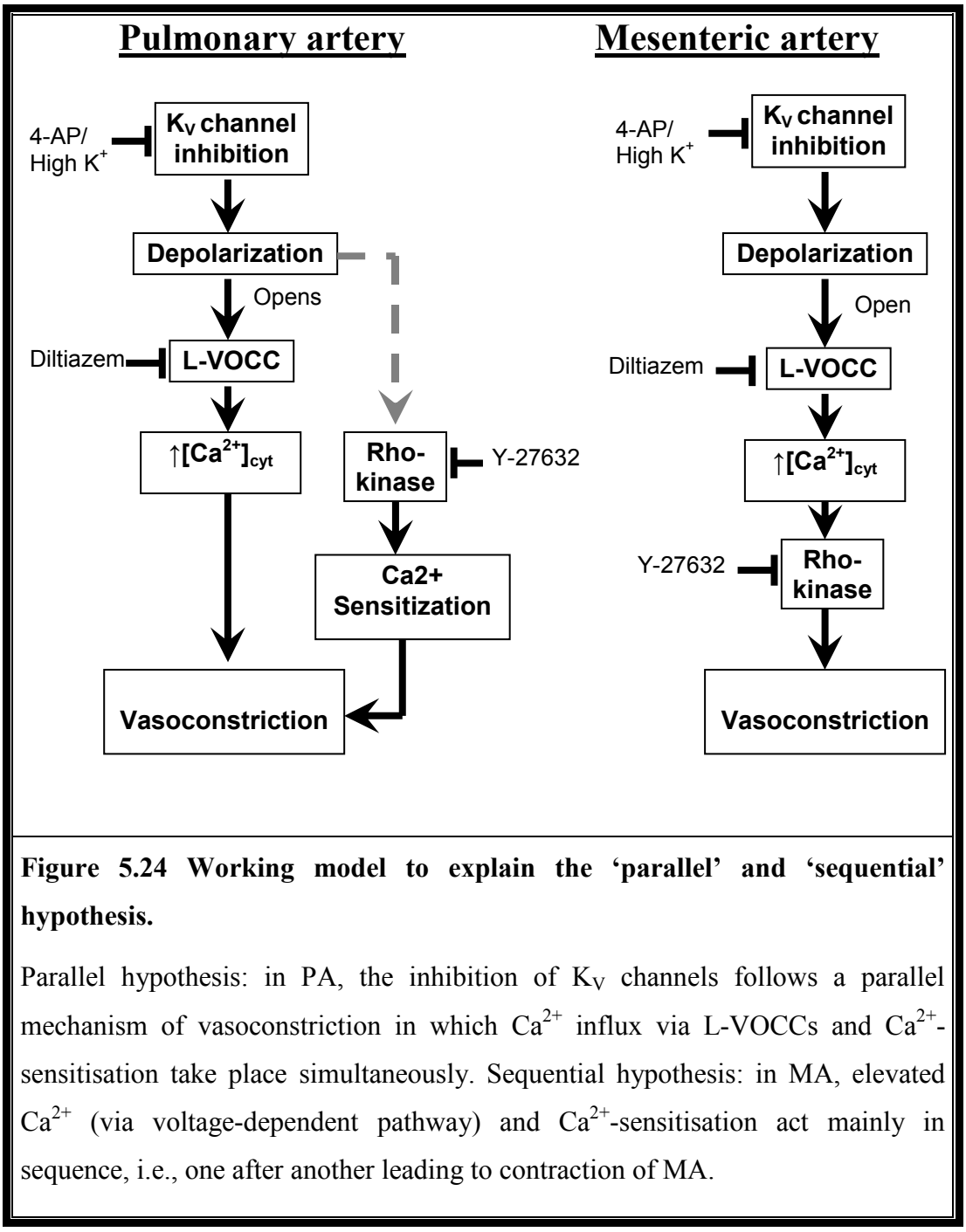

Figure 5.24 Working model to explain the 'parallel' and 'sequential' hypothesis.

Parallel hypothesis: in PA, the inhibition of K_V channels follows a parallel mechanism of vasoconstriction in which Ca^{2+} influx via L-VOCCs and Ca^{2+}-sensitisation take place simultaneously. Sequential hypothesis: in MA, elevated Ca^{2+} (via voltage-dependent pathway) and Ca^{2+}-sensitisation act mainly in sequence, i.e., one after another leading to contraction of MA.

It is worth mentioning that the overall effects of Rho-kinase inhibition described in this study are consistent with previously published works. Several groups demonstrated that Rho-kinase is activated in response to KCl-induced depolarisation (Yuan, 1995;Sakurada *et al.*, 2001;Sakurada *et al.*, 2003). Rho-kinase phosphorylates myosin phosphatase target subunit 1 (MYPT1) and thus downregulates MLCP activity, resulting in Ca^{2+}-sensitisation (Somlyo & Somlyo, 2003;Hilgers & Webb, 2005). In my study, I did not find a significant effect of 4-AP on phosphorylation of MYPT1. However, Y-27632 significantly reduced phosphorylation of MYPT1. The results where 4-AP effect was studied on MLC_{20} phosphorylation were more promising when tissue was stretched but still not conclusive. More experiments will be required to achieve a clearer view regarding phosphorylation of MYPT1 as well as MLC_{20}. There is a significant functional difference in terms of sensitivity to Y-27632 between pulmonary and systemic arteries. For example, agonist-induced contractions in the systemic arteries are more susceptible to Y-27632 (Batchelor *et al.*, 2001;Chan *et al.*, 2009;Freitas *et al.*, 2009) than that in the pulmonary arteries (Alapati *et al.*, 2007;McKenzie *et al.*, 2009). One of the weaknesses of my study is the focus on measuring MLC_{20} phosphorylation, the ultimate indicator of smooth muscle contraction, only in PA. Therefore, it will be important to determine the phosphorylation of MYPT1 in stretched PA and MA in the future works.

The thromboxane A_2 mimetic U-46619 acts via TP receptors (Yang *et al.*, 2004) which leads to an increase in $[Ca^{2+}]_i$ and sensitisation of the contractile proteins to Ca^{2+} (Tosun *et al.*, 1998;Janssen *et al.*, 2001;Somlyo & Somlyo, 2003). One of the signalling molecules activated downstream of the TP receptor in smooth muscle cell is Rho-kinase (Somlyo & Somlyo, 2003) and the involvement of Rho-kinase pathway in U-46619-induced sustained contractile response was demonstrated in PA (Alapati *et al.*, 2007). A study by Cogolludo *et al.* (2003) established a possible link between the TP receptor, K_V channels and Rho-kinase in rat PASMCs. This study provided evidence that U-46619 acting via TP receptor inhibits K_V channel activity and causes membrane depolarisation, leading to opening of L-VOCCs, increase in $[Ca^{2+}]_i$, and contraction of PASMCs (Cogolludo *et al.*, 2003). This opens the possibility that U-46619 may share, at least partly, mechanisms similar to those activated in the presence of 4-AP. The similarity

between the effect of the L-VOCC blocker and the Rho-kinase inhibitor on the U-46619 and 4-AP-induced contractions does not contradict this notion.

In this study, diltiazem was exclusively used because it showed complete reversibility upon the removal of the inhibitor. In a separate set of experiments, 1 μM nifedipine was also used (n = 2, data not shown) demonstrating similar results. Diltiazem also blocked completely linopirdine-induced contraction in depolarised PA and MA (n = 2, data not shown). Similar effects was also observed in previous studies where 1 μM nifedipine was able to completely block linopirdine (10 μM) responses in rat PA (Joshi *et al.*, 2006).

It is worth noting that MA always showed greater sensitivity to either diltiazem or Y-27632, in comparison to PA irrespective of the way how contraction was generated (either with 4-AP, high K^+ or U-46619) (Fig. 5.2, 5.11 and 5.20). It is also notable that for the same tissue there is a significant difference in the sensitivity to Rho-kinase inhibitor Y-27632 depending on the agonist used for inducing sustained contraction as summarised in Fig. 5.25. The present finding is also consistent with the previous report that the relative inhibitory effects of the Rho-kinase inhibitors depends on the agonists used (Chan *et al.*, 2009). The reason for this difference is likely to be inherent to each tissue and could be due to the differences in the kinetics of contraction. It is noteworthy that PA and MA has different kinetics of response to high K^+; PA shows a slow and sustained ('tonic') response whereas MA shows a comparatively fast ('phasic') onset of contraction, which then can decrease with time. This could be due to differences in the role Ca^{2+} channels and the Ca^{2+}-entry pathways between these two arteries (Zheng *et al.*, 2008). The data presented in this study however do not allow answering the question of what cellular mechanisms are involved in the onset of contraction. Further specific studies which will address this very interesting question are needed.

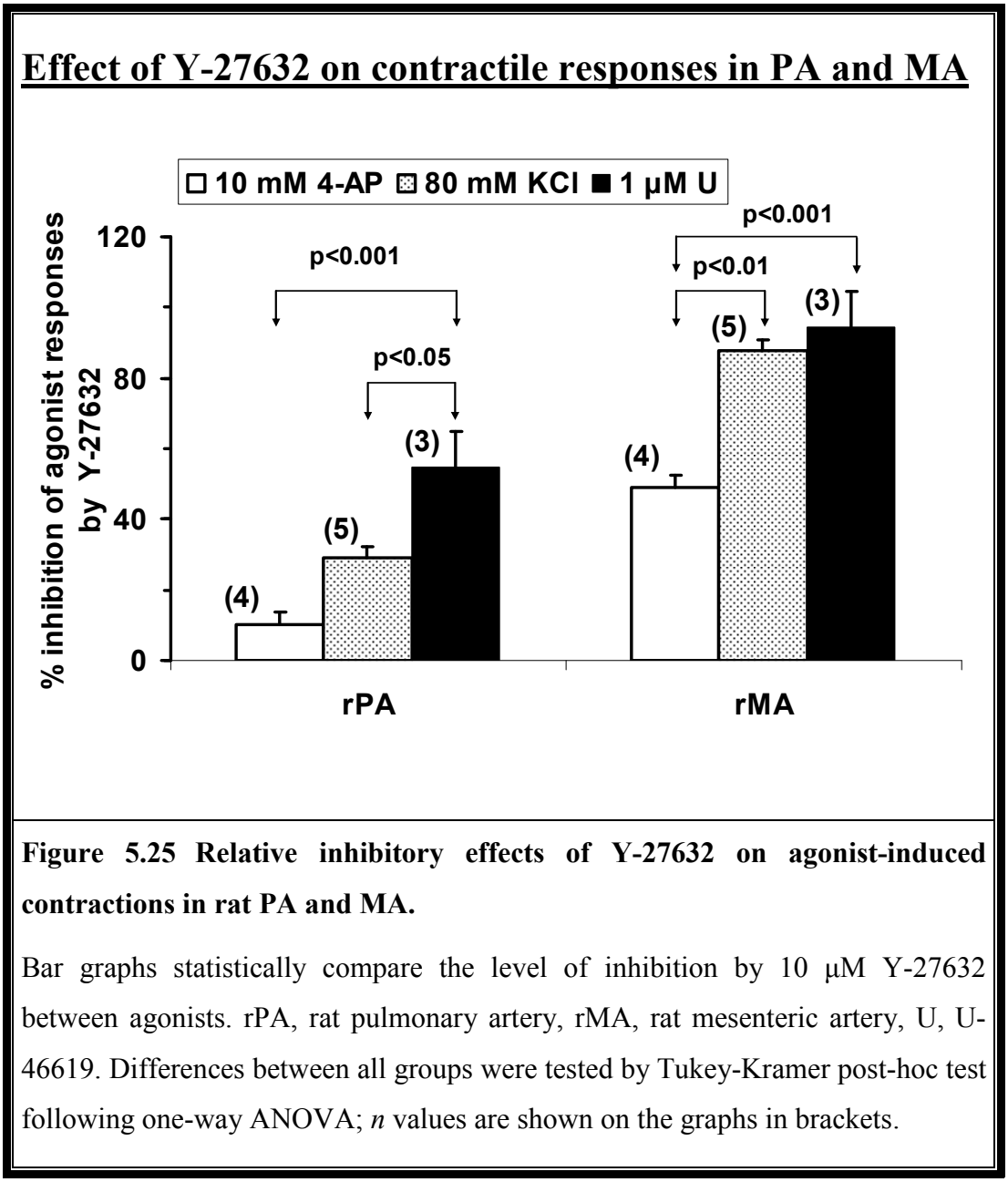

Figure 5.25 Relative inhibitory effects of Y-27632 on agonist-induced contractions in rat PA and MA.

Bar graphs statistically compare the level of inhibition by 10 μM Y-27632 between agonists. rPA, rat pulmonary artery, rMA, rat mesenteric artery, U, U-46619. Differences between all groups were tested by Tukey-Kramer post-hoc test following one-way ANOVA; *n* values are shown on the graphs in brackets.

To address the differences in the sensitivity to Rho-kinase inhibitor Y-27632 between PA and MA at the molecular level, immunohistochemical techniques can be applied in the future works. Immunohistochemical localisation can be performed in PA and MA segments by using specific polyclonal and monoclonal antibodies to Rho-kinase (e.g. ROKα) (Yoon *et al.*, 2010). Comparison of the immunohistochemical expression of ROKα between PA and MA could reveal the possible reason for difference in the sensitivity to Y-27632.

Another observation which demonstrate that contractions induced by 4-AP, high K^+ or U-46619 were attenuated by the Rho-kinase inhibitor Y-27632 to a greater extent at low levels of pretone in PA than in MA is consistent with previous work which showed that Y-27632 inhibited more effectively contractions induced by low concentrations of KCl in rabbit aorta (Sakurada *et al.*, 2003) and by low concentrations of phenylephrine in rabbit femoral artery (Ratz *et al.*, 2005). Such differences in my experiments are unlikely to be due to variation in the expression of RhoA/ROK as was demonstrated for tonic smooth muscle (which had characteristically higher levels of RhoA/ROK) compared to phasic smooth muscle (Patel & Rattan, 2006), because the degree of relaxation was similar at low level of contraction and was consistently greater in MA (showing 'phasic' type of responses). An increase in the receptor-induced activation of RhoA and associated MYPT1 phosphorylation with increased level of contraction (Sakurada *et al.*, 2001;Mizuno *et al.*, 2008) is also unlikely, as both KCl- and U46619-induced contractions demonstrated such dependence in PA (Figs. 5.16 and 5.23). One possible explanation could be Ca^{2+}-dependence of the Rho-kinase activity, which is somehow decreased when $[Ca^{2+}]_i$ is increased. Since there is currently no evidence that Rho-kinase is inhibited by increased $[Ca^{2+}]_i$, these findings therefore provide a foundation for further studies focussed in this direction.

There is also another important implication of the results described in this study related to the specificity of the action of 4-AP, which is often criticised in the literature. In my experimental settings a number of observations strongly suggest that 4-AP acts specifically causing contraction via inhibition of K_V channels in both types of arteries. These include: 1) the similarity between the effects of the L-VOCC blocker and the Rho-kinase inhibitor on the 4-AP, KCl- and U-46619-induced responses; 2) the ability of diltiazem+Y-27632 pretreatment to completely inhibit 4-AP-induced contractions; 3) the differences between the effects of 4-AP in PA and MA measured simultaneously and in identical experimental conditions; and 4) the ability of linopirdine to significantly potentiate the effect of 4-AP specifically in the PA. This set of evidence strongly supports the notion in favour of 4-AP as specific inhibitor of K_V channels in the concentration range used in this study.

One of the unanswered questions is: what is the residual component of the 4-AP-induced contraction in PA? It is interesting that this residual component was ablated by pretreatment with a combination of diltiazem and Y-27632. However, once the contraction is developed ~30% of 4-AP-induced contraction was not sensitive to the combination of both inhibitors. Similar effects of both inhibitors was observed for the contraction induced by U-46619 only in PA, the main difference between the effects of the L-VOCC and Rho-kinase inhibitors in the two cases was the presence of the residual component of the U-46619-induced contraction following the pretreatment with inhibitors in contrast to the 4-AP-induced contraction.

To explore the insensitive 3rd component of 4-AP response in PA several attempts have been taken. To check the possibility if ROS are involved the effect of tiron, a membrane permeable ROS scavenger, on 4-AP-induced contraction was tested. Pretreatment of both arteries with 10 mM tiron did not alter 4-AP-induced responses in either of the two tissue types (data not shown). Similarly, tissue pretreatment with 100 μM pinacidil, a K_{ATP} channel opener, did not affect the 4-AP-induced contraction (data not shown), suggesting that K_{ATP} channels are not involved. Also 100 μM tyrphostin, a widely used tyrosine kinase blocker, alone or even in combination with diltiazem and Y-27632 applied after 4-AP-induced contraction was developed failed to ablate 4-AP responses in PA (data not shown), suggesting that tyrosine kinase is unlikely to be involved.

These differences between PA and MA clearly indicates that the 3rd component of 4-AP-induced contraction is specific for 4-AP, an inhibitor of the K_V channels. Recently, Firth *et al.* showed that K_V channels are functionally and structurally associated with mitochondria specifically in PASMCs (Firth *et al.*, 2008;Firth *et al.*, 2009a). On the basis of these previous reports, I speculated that the insensitive component of 4-AP-induced contraction might be associated with compartmentalisation of K_V channels and mitochondria.

Whether the voltage-independent and Rho-kinase insensitive component of the 4-AP-induced contraction is linked to compartmentalisation phenomenon involving

mitochondria, I investigated the effect of 4-AP in α-toxin and β-escin permeabilised (skinned) tissues. The effect of mitochondrial uncouplers to inhibit mitochondria function was also assessed in the skinned and intact tissue preparations. These results will be described in the following chapter (Chapter 6).

Chapter 6

INTERACTION OF MITOCHONDRIA WITH K_V CHANNELS AND ITS ROLE IN THE METABOLIC REGULATION OF CONTRACTION IN RAT PULMONARY AND MESENTERIC ARTERIES

6.1 Introduction

The results presented in the previous chapter clearly demonstrated the presence of the additional component in the 4-AP-induced contraction, which was insensitive to the inhibition by both L-VOCC and Rho-kinase inhibitors specifically in the PA, and not in the MA. Although similar component was also observed in contraction evoked by U-46619, it was not sensitive to the pretreatment with diltiazem+Y-27632, whereas that seen with the K_V channel blocker 4-AP was completely ablated (compare Fig. 5.5 B and 5.20 A). Also this component of contraction was not significantly affected by CPA, suggesting that Ca^{2+} release from the sarcoplasmic reticulum is unlikely to be responsible. This component was not observed in contractions induced by high K^+, which will impair the overall K^+ efflux indiscriminately through all K^+ channels, but will not inhibit them. The 4-AP specificity of this phenomenon therefore strongly suggests that it is linked to the inhibition of K_V channels specifically in the PA. Smirnov and Aaronson previously reported that activation of K_V channels in rat PASMCs lead to re-distribution of local K^+ concentrations (Smirnov & Aaronson, 1994). Recently, Firth *et al.* presented the evidence that K_V channels are associated with a population of mitochondria which form submembrane compartment and functional coupling between K_V channels and mitochondria (Firth *et al.*,

2008;Firth *et al.*, 2009a). Considering that K^+ ions are crucial for the regulation of normal homeostasis of mitochondria (Garlid & Paucek, 2003), the inhibition of K_V channels with 4-AP would alter the balance of the local subcellular K^+ concentration and in that way influence mitochondrial function. This directly via changing $[Ca^{2+}]_i$, or indirectly via release of active substance (e.g. superoxide or H_2O_2) or via metabolic changes (e.g. changes in the ATP production) could have an impact on contraction. The ROS hypothesis discussed in details in Chapter 1 (section 1.7.2.3) supports the potential ability of ROS to stimulate contraction in PA. Thus, it is well established that mitochondria are responsible for Ca^{2+}-sequestration and release (Duchen, 1999;Nicholls & Budd, 2000).

As vasoconstriction depends upon MLC_{20} phosphorylation which consumes up to 50% of cytosolic ATP (Wingard *et al.*, 1994), a difference in metabolic regulation of contractions in the two types of arteries may contribute to the differences in the 4-AP-induced contraction in PA and MA. Previously, a different role of glycolysis and oxidative phosphorylation was demonstrated in HPV (Leach *et al.*, 2001). In that study, glycolysis was found to be essential for the development of sustained phase (phase-II) of HPV, as the inhibition of glycolysis by iodoacetate or 2-DOG in the absence of glucose abolished phase-II of HPV. On the other hand, inhibition of the mETC by inhibiting cytochrome oxidase with cyanide potentiated the phase-II of HPV (Leach *et al.*, 2001) as well as increased $[Ca^{2+}]_i$ by stimulating Ca^{2+} release from the SR and mitochondria in both pulmonary and systemic artery myocytes (Wang *et al.*, 2003a). This evidence supports a potential ability of altered mitochondria to affect contraction in PA. It has also been demonstrated that inhibition of cellular glycolysis with 2-DOG increases $[Ca^{2+}]_i$ (Bright *et al.*, 1995) and mimics effects of hypoxia on ion channels including K_V channels in PASMCs (Yuan *et al.*, 1994;Yuan *et al.*, 1995a), although similar effects were found in some systemic arteries (Miller *et al.*, 1993).

In the systemic arteries, metabolic blockade generally resulted in a decrease in $[Ca^{2+}]_i$ and vasodilatation. Thus, metabolic blockade with 2-DOG reduced ATP levels in cultured A7r5 vascular smooth muscle cells (Lynch *et al.*, 1996), and caused vasodilatation in rat coronary artery (Conway *et al.*, 1994), and in guinea pig thoracic aorta (Gasser *et al.*, 1993). In systemic arteries, metabolic inhibition

of ATP production, either by inhibiting glycolysis (2-DOG) or mitochondrial oxidative phosphorylation (NaCN, oligomycin), resulted in vasodilation (Gasser *et al.*, 1993). Inhibition of oxidative phosphorylation with rotenone, antimycin A, NaCN attenuated vasoconstriction of the rat tail artery without altering $[Ca^{2+}]_i$ (Tran *et al.*, 1997;Swärd *et al.*, 2002). Similar effects of metabolic inhibition were also observed in the heart. Thus, cyanide, 2-DOG and/or iodoacetate decreased in inward L-type Ca^{2+} current (I_{Ca}), level of $[Ca^{2+}]_i$ and the amplitude of contraction in rat ventricular myocytes (Eisner *et al.*, 1989;Lancaster & Harrison, 1998;Fukumoto *et al.*, 2005).

It is also possible that hypoxia may influence the cellular metabolic state in different manner in the systemic and pulmonary arteries. Otter and Austin (2000) found the differences in the effect of hypoxia and metabolic inhibition on the rat mesenteric arteries of different diameter. Hypoxia caused near maximal relaxation in both large and small mesenteric artery preconstricted with 60 mM KCl, while metabolic inhibition (with cyanide) resulted maximal relaxation of only small mesenteric arteries but in larger vessels the relaxation to cyanide was significantly less compared to that in hypoxic conditions (Otter & Austin, 2000). Hypoxia has been reported not to alter basal levels of $[Ca^{2+}]_i$ in most vascular smooth muscle cells including coronary (Paul *et al.*, 2009), cerebral and mesenteric (Aalkjaer & Lombard, 1995). In pulmonary circulation, however, hypoxia decreased basal level of $[Ca^{2+}]_i$ in conduit pulmonary (Ureña *et al.*, 1996) but increased in small pulmonary artery (Salvaterra & Goldman, 1993;Post *et al.*, 1995;Ureña *et al.*, 1996). On the other hand, metabolic inhibition was found to increase in basal levels of $[Ca^{2+}]_i$ both in systemic artery SMCs (Sward *et al.*, 1993;Lydrup *et al.*, 1994) and PASMCs (Bright *et al.*, 1995).

The above overview of the published evidence suggests not only the existence of a potential crosstalk between the mechanisms contributing to the effects of hypoxia and those which control cellular metabolism in both systemic and pulmonary circulations, but also points out towards potential differences between the two circulations. However, characterisation of metabolic dependence of contraction in intact arteries and direct comparison between pulmonary and systemic circulations has not yet been systematically investigated.

In the experiments presented in this chapter I used several pharmacological tools including mitochondrial uncouplers, membrane permeabilisation technique and metabolic poisons. In this study I employed two selective mitochondrial uncouplers CCCP (carbonyl cyanide 3-chlorophenylhydrazone) and FCCP (carbonyl cyanide 4-trifluoromethoxy phenylhydrazone), which share the same mechanism of action and are widely used pharmacological tools to investigate the involvement of mitochondria in the vascular tension at the cellular level and whole tissue preparations. The mitochondrial uncouplers collapse mitochondrial membrane potential and inhibit mitochondrial function by uncoupling electron transport from oxidative phosphorylation. This will lead to mitochondria depolarisation which could result in an accumulation of cytoplasmic Ca^{2+} as a result of mitochondrial Ca^{2+} release and/or impaired Ca^{2+} sequestration into mitochondria. Thus, application of FCCP, for example, caused an increase in intracellular Ca^{2+} in single PASMCs (Drummond & Tuft, 1999;Kang *et al.*, 2003). Notably, FCCP caused membrane depolarisation mimicking the effect of 4-AP in single cultured PASMCs (Yuan *et al.*, 1995a) whilst CCCP enhanced the effect of hypoxia on intracellular Ca^{2+} increase in rabbit PASMCs (Kang *et al.*, 2002). Yu *et al*. (1998) used FCCP to investigate whether mitochondria contribute to contractions induced by sodium hydrosulfite in intact rat PAs (Yu *et al.*, 1998b). Based on the previous reports, in my study I used both uncouplers to influence mitochondrial function in order to investigate if there is a contribution of mitochondria in contraction to 4-AP in intact pulmonary and mesenteric arteries.

If changes in cytosolic Ca^{2+} are important in the initiation and maintenance of the 4-AP-induced contraction, it will therefore be appropriate to assess this under conditions when $[Ca^{2+}]_i$ is controlled. This can be achieved in intact arteries by employing membrane skinning or permeabilisation technique. I used two different tissue permeabilising agents, α-toxin and β-escin, to evaluate the effect of 4-AP under controlled intracellular Ca^{2+} environment.

To study the metabolic dependence of contraction a range of pharmacological tools, previously used for this purpose, were employed. Cyanides are widely used to investigate the dependence of contraction on oxidative metabolism mediated by

mitochondria in intact arteries (Buescher *et al.*, 1991;Tran *et al.*, 1997;Otter & Austin, 2000;Leach *et al.*, 2001;Swärd *et al.*, 2002). To inhibit glycolysis, the replacement of extracellular glucose with its non-metabolised analogue, 2-DOG is widely used (MacLeod, 1989;Gasser *et al.*, 1993;Conway *et al.*, 1994;Yuan *et al.*, 1995a;Lynch *et al.*, 1996;Zhao *et al.*, 1996;Leach *et al.*, 2001;Fukumoto *et al.*, 2005). Combination of cyanides with 2-DOG is thought to result in complete metabolic blockade of the cell, preventing majority of ATP production (Lancaster & Harrison, 1998). Also, the F_0/F_1 ATP synthetase inhibitor oligomycin is commonly used to selectively inhibit mitochondrial oxidative phosphorylation thereby preventing oxidative ATP production (Nicholls *et al.*, 2003;Wang *et al.*, 2003a;Firth *et al.*, 2009a). In this set of experiments I used sodium cyanide (1 mM) to inhibit oxidative phosphorylation and equimolar replacement of glucose (5.6 mM) with 2-DOG in Krebs solution to inhibit glycolysis. In some experiments, oligomycin (1μM) was also used to selectively inhibit F_0/F_1 ATP synthetase.

The above mentioned pharmacological tools were employed to test the two related hypotheses in this chapter:

1. Whether there is a relationship between K_V channels and mitochondria in intact PA and MA of the rat.
2. Whether there is a difference in the metabolic dependence of contraction between intact PA and MA of the rat.

6.2 Results

6.2.1 Effects of CCCP on 4-AP-induced contraction in non-permeabilised rat PA and MA

The effect of the mitochondrial uncoupler CCCP was investigated in the intact non-permeabilised preparation. Concentration-contraction responses were obtained in PA and MA with a series of increasing concentrations of 4-AP (0.5, 1, 2, 5 and 10 mM) in the absence and presence of 3 μM CCCP. The representative traces demonstrating the effect of CCCP on 4-AP-induced contractions in PA and MA are depicted in Fig. 6.1. Preincubation of the arteries with CCCP potentiated 4-AP responses in PA starting with a concentration as little as 1 mM (Fig. 6.2 A). The effect was significant for contractions elicited by 2, 5 and 10 mM 4-AP in the presence of CCCP compared to the control. On the other hand, in MA, CCCP evoked only a small potentiation of contraction at high concentration of 4-AP. This effect in MA was not however significant (Fig. 6.2 B).

It is worth mentioning that application of 3 μM CCCP alone occasionally constricted both arteries with bigger amplitude in PA. Thus in PA, CCCP alone caused contraction of 0.76±0.40 mN or 12.4±6.5% of 80 mM KCl (n = 10) while in MA the contraction was comparatively smaller (0.20±0.12 mN or 2.2±1.4%, n = 10). However, no significant difference between the two preparations was found.

These results clearly show that mitochondrial uncoupling with CCCP potentiated 4-AP-induced contraction selectively in PA, thus closely resembling the effect of tissue pretreatment with 20 mM KCl and linopirdine described in Chapter 3. One possibility is that mitochondrial uncoupling with CCCP can lead to membrane depolarisation (Yuan *et al.*, 1995a) and $[Ca^{2+}]_i$ increase (Kang *et al.*, 2002).

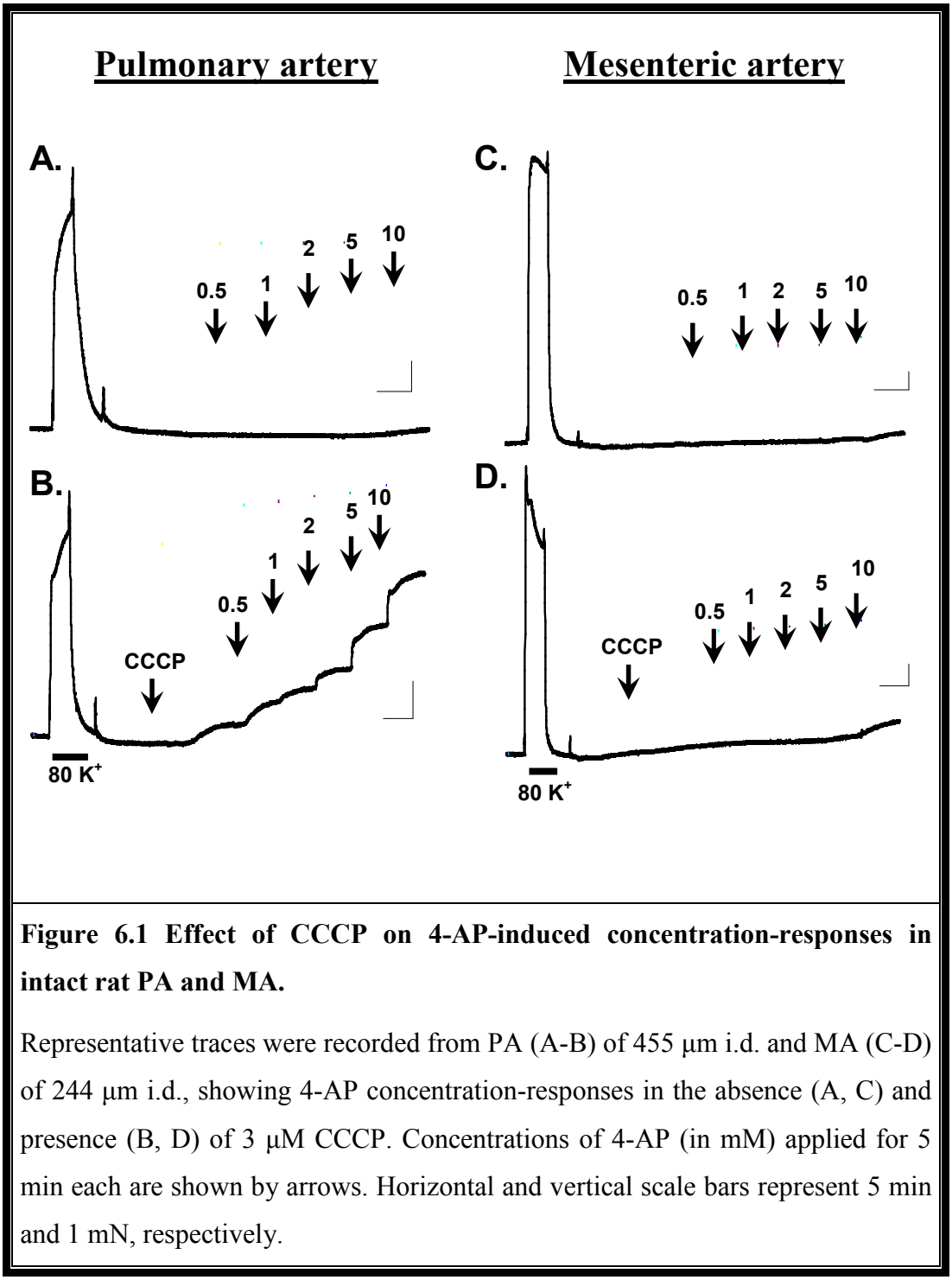

Figure 6.1 Effect of CCCP on 4-AP-induced concentration-responses in intact rat PA and MA.

Representative traces were recorded from PA (A-B) of 455 µm i.d. and MA (C-D) of 244 µm i.d., showing 4-AP concentration-responses in the absence (A, C) and presence (B, D) of 3 µM CCCP. Concentrations of 4-AP (in mM) applied for 5 min each are shown by arrows. Horizontal and vertical scale bars represent 5 min and 1 mN, respectively.

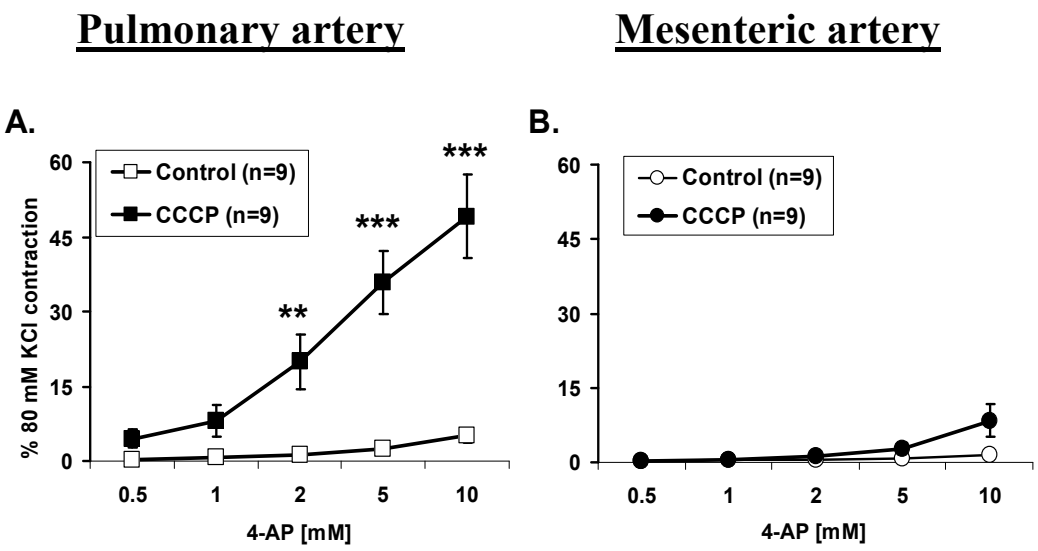

Figure 6.2 Summary of the effect of CCCP on 4-AP-induced contraction in intact rat PA and MA.

Preincubation with 3 μM CCCP significantly potentiated 4-AP concentration responses in PA (A) but not in MA (B). ** $p<0.01$ and *** $p<0.001$ compare 4-AP responses before and after CCCP treatment. Note that some of the error bars are smaller than symbols. Differences between control versus treatment groups for the same concentration of drug were tested by Bonferroni post-hoc test following one-way ANOVA, $n = 9$.

In addition CCCP potentiated K_V channels at more negative potentials (Firth *et al.*, 2008), the effect linked to compartmentalisation of mitochondria in the subplasmalemmal space (Firth *et al.*, 2009a). Both factors will promote facilitation of the 4-AP-induced contraction in accordance with my observations. In order to address the question if 4-AP-induced contraction is linked to changes in $[Ca^{2+}]_i$ independent on membrane depolarisation, the effect of the K_V channel inhibitor was studied in permeabilised preparations under conditions where $[Ca^{2+}]_i$ is tightly controlled.

6.2.2 4-AP-induced contraction in permeabilised rat arteries: role of mitochondria

The experiments were performed in permeabilised preparations using the α-toxin method developed in Prof. Jeremy Ward's laboratory. I myself carried out these experiments at King's College London as a part of ongoing collaboration. In this set of experiments instead of CCCP, another mitochondrial uncoupler FCCP was used to affect mitochondrial function, because this was the drug of the choice in this laboratory.

Following α-toxin permeabilisation, tissues were relaxed with G10 which contains 'zero' calcium. In this state of tissue, application of 10 mM 4-AP produced no further tone at all (data not shown, $n = 3$). It is noteworthy that high concentration of 4-AP does not have any effect on tension on its own in permeabilised tissues. However, when basal Ca^{2+} levels were increased, 10 mM 4-AP elicited further tension both in PA and MA.

Basal Ca^{2+} level was elevated in permeabilised tissues using solutions with different pCa prepared as described in Chapter 2 (Materials and Methods). Because PA showed a higher sensitivity to a given concentration of calcium than MA, PA was preconstricted with pCa 7.2, in some cases 6.8 and MA with pCa 6.4. The main aim of pre-constriction was to achieve a certain level of pretone before proceeding with a specific experimental protocol. As mentioned above, a certain level of pretone was necessary to observe the 4-AP effect because both PA and MA were insensitive to 4-AP in G10 (a Ca^{2+}-free solution). Results were normalised and expressed as percentage of contraction resulted in pCa 4.5 (10 mM Ca^{2+}) which produced a maximum response in both permeabilised tissues.

Elevation of basal Ca^{2+} level itself produced tension both in PA (52.1±8.1%; $n = 10$) and MA (20.0±7.5%, $n = 9$) which was further enhanced to 69.1±8.7% ($n = 10$) in PA and 37.2±10.5% ($n = 9$) in MA upon application of 10 mM 4-AP. However, when arteries were pre-incubated with 3 μM FCCP the 4-AP-induced

tension was significantly suppressed in PA (Fig. 6.3A). Although some reduction in the effect of 4-AP was seen in MA this effect was not significant (Fig. 6.3 B).

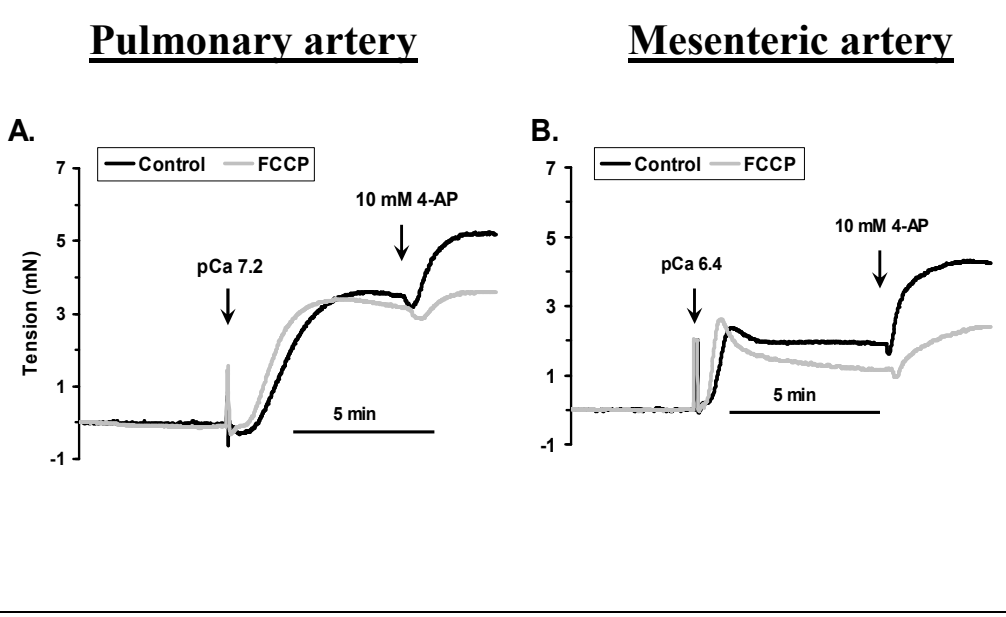

Figure 6.3 Effect of FCCP preincubation in α-toxin permeabilised rat PA and MA.

Representative traces obtained from the same PA (A) and MA (B) showing differences in the response to 4-AP (10 mM) before (black trace) and after (grey trace) incubation with the mitochondrial uncoupler FCCP (3 μM).

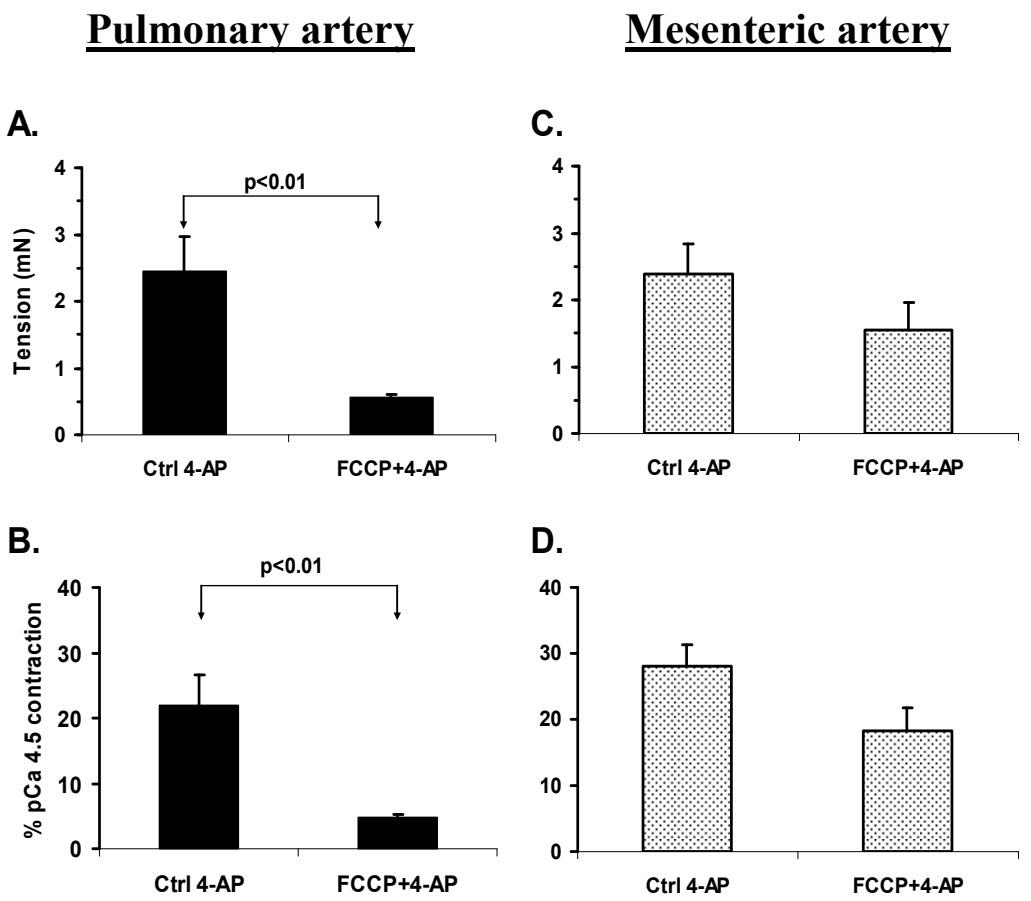

Figure 6.4 Effect of FCCP pretreatment on 4-AP contraction in rat PA and MA.

FCCP, a mitochondrial uncoupler, significantly reduced 4-AP responses in pulmonary artery (A-B) but has no significant effect in mesenteric artery (C-D). Values mean± S.E.M.; paired Student's *t*-test (n = 4).

The changes in 4-AP-induced contraction in the presence and absence of FCCP in α-toxin permeabilised arteries are summarised in Fig. 6.4. FCCP preincubation in PA significantly suppressed both the absolute (from 2.45±0.51 mN to 0.55±0.04 mN, n = 4) and normalised tension (from 21.98±4.54% to 4.91±0.25%, n = 4) produced by 4-AP (Fig. 6.4 A and B, respectively). On average, FCCP reduced 4-AP response by ~78% in PA, and only by ~35% in MA. Importantly, although

similar trend was also in MA, the FCCP-dependent changes in 4-AP-induced contraction were not significant (Fig. 6.4 C-D), suggesting that FCCP has a selective effect on the 4-AP-induced response in PA, and not in MA.

Similar to intact tissues, pretreatment with CPA did not alter 4-AP responses in α-toxin permeabilised tissue (n = 3, data not shown), suggesting the intracellular Ca^{2+} store does not play a significant role in the 4-AP-induced contraction.

Although the differences in the effect of FCCP on the 4-AP-induced contraction in α-toxin permeabilised PA and MA are consistent with the differential effects observed in intact preparations described in the section 6.2.1, the ability of 4-AP to constrict the permeabilised tissue is unexpected. Because there is no membrane potential preserved under this condition, this is unlikely to be due to membrane depolarisation. It is therefore possible that this 4-AP-induced contraction might be a correlate of the 3rd component of contraction which was not sensitive to diltiazem and Y-27632 in the intact preparation. Its selective sensitivity to the mitochondrial uncoupler FCCP, may therefore suggest that it involves mitochondria. It is possible that in α-toxin permeabilised tissues some intracellular compartments might be intact. It has been previously shown that permeabilisation with α-toxin (≤1000 Da) is most gentle compared to saponin and Triton-X (Van Heijs *et al.*, 2000). In order to check if this is the case, the effect of 4-AP was investigated in arteries permeabilised with a saponin ester β-escin to achieve a greater degree of permeabilisation (> 17,000 Da) (Somlyo & Somlyo, 1990).

Representative traces comparing tissue responses to 4-AP using α-toxin and β-escin permeabilisation are depicted in Fig. 6.5 (A-D). In α-toxin permeabilised tissues 10 mM 4-AP significantly increased contraction both in PA (~32%, n = 10) and MA (~85%, n = 9) (Fig. 6.5 A and B, respectively) while in β-escin permeabilised arteries, the 4-AP response was rather decreased by ~10% in PA (n = 7), but slightly increased in MA (~5%, n = 7) (Fig. 6.5 C and D, respectively).

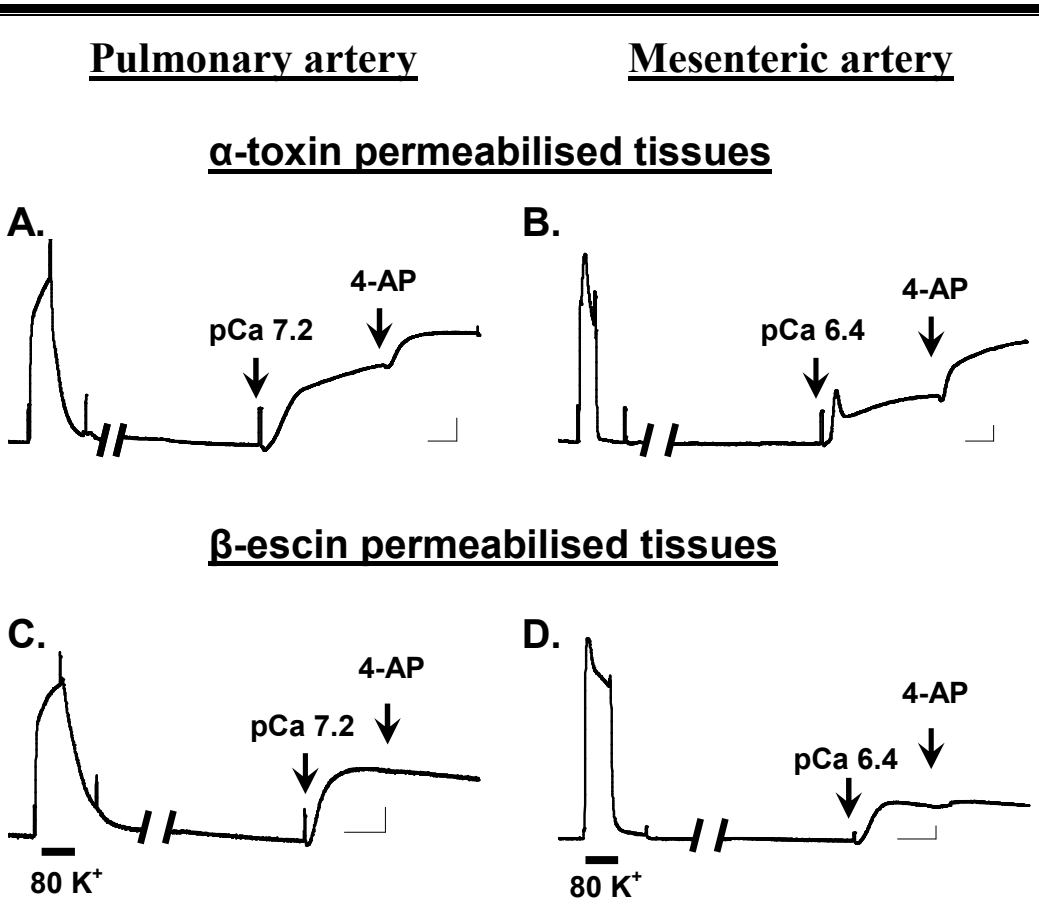

Figure 6.5 Comparison of tissue permeabilisation with α-toxin and β-escin on tissue response to 4-AP.

Representative traces obtained from PA (A, C) and MA (B, D) where α-toxin permeabilised arteries show further contraction in response to 4-AP, whereas β-escin permeabilised arteries show no further contraction to 4-AP. Breaks in line indicate time gap when tissue permeabilisation was performed between high K^+ and test response. Horizontal and vertical scale bars represent 5 min and 1 mN, respectively.

Fig. 6.6 compares the effect of a different degree of permeabilisation achieved with α-toxin and β-escin on the 4-AP-induced contraction. It can be clearly seen that while 4-AP is able to produce a significant level of contraction in both PA and MA permeabilised with α-toxin (Fig. 6.6, A and B, respectively), this ability is completely lost following β-escin permeabilisation (Fig. 6.6 C-D).

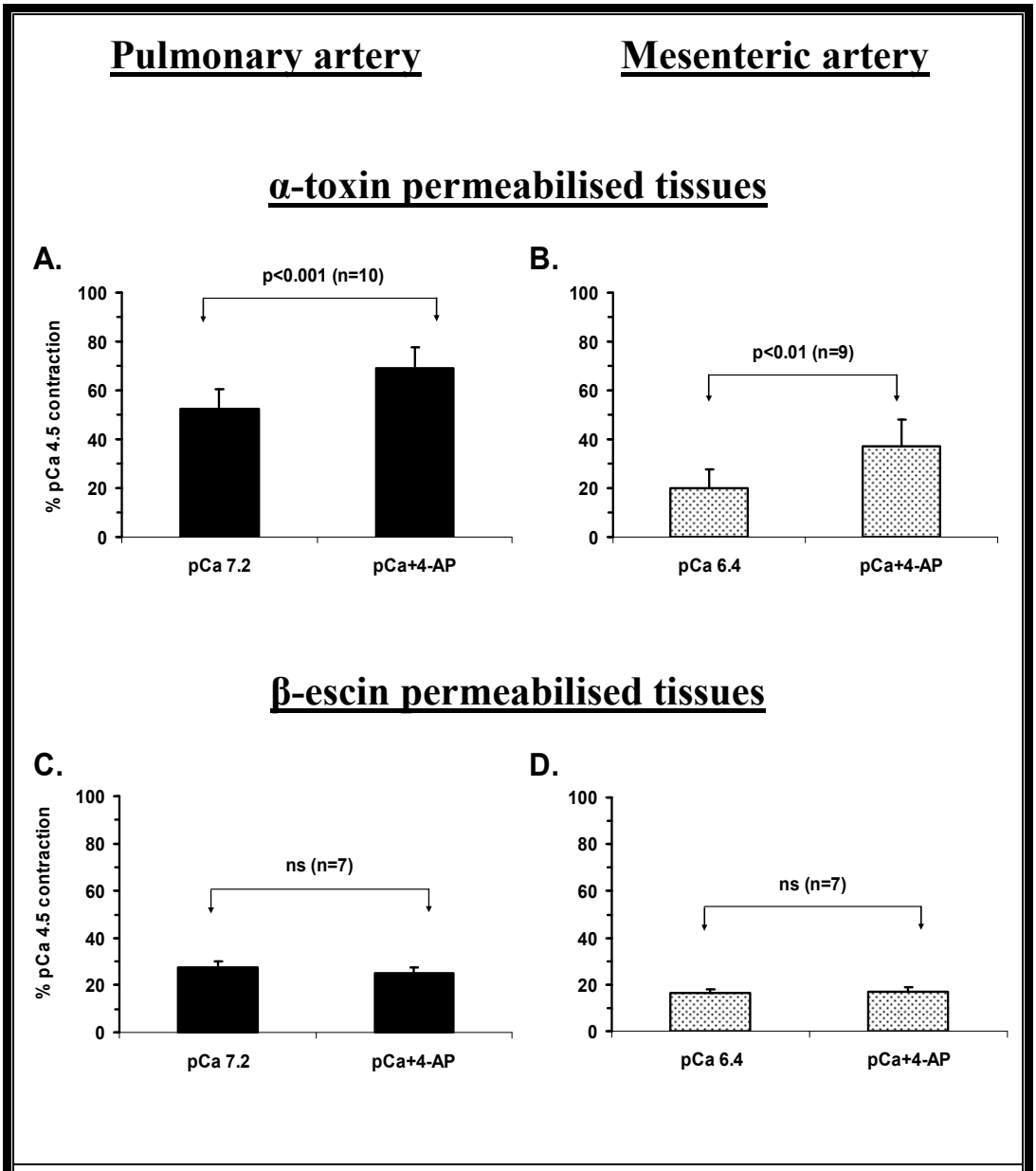

Figure 6.6 Comparison of tissue permeabilisation with α-toxin and β-escin on tissue response to 4-AP.

Note further contraction in response to 4-AP in α-toxin permeabilised arteries (PA and MA), and the lack of responses in β-escin permeabilised arteries. Paired Student's *t*-test; *n* numbers as shown in brackets; ns = not significant at p>0.05.

6.2.3 Effects of mitochondrial uncoupler CCCP on hypoxia-induced contraction in rat PA and MA (non-permeabilised)

The differences in the modulation of 4-AP-induced responses by mitochondrial uncoupling in PA and MA may have direct functional implication in HPV as the mitochondrion is considered as a putative oxygen sensor in HPV (Waypa & Schumacker, 2002;Ward, 2003;Weissmann *et al.*, 2006b). In Chapter 4 I found that the effect of hypoxia was similar in both preparations (PA and MA) preconstricted with low concentration of 4-AP (2 mM) in the presence of linopirdine. It is therefore important to assess whether mitochondrial uncoupling can modulate the effect of hypoxia in PA in the presence of 4-AP and linopirdine, differently to that described in Chapter 4.

Figure 6.7 depicts representative traces showing the results of such experiments. In the absence of CCCP (which was used in this set of experiments) hypoxia induced a transient contraction in the presence of the two K^+ channel inhibitors in both PA (Fig. 6.7 A) and MA (Fig. 6.7 C), i.e. the effects similar to those described in Chapter 4. Tissue pretreatment with 3 μM CCCP revealed dramatic differences in response to hypoxia between the two preparations. In PA, contraction to linopirdine and 4-AP was firstly enhanced (which is consistent with the overall potentiating effect of CCCP on 4-AP-induced contraction described in Section 6.2.1). Importantly, the hypoxic response was also changed from being a transient in the control conditions to becoming a sustained response in the presence of CCCP (Fig. 6.7 B). On the other hand, in MA, hypoxia-induced transient contraction was completely eliminated (Fig. 6.7 D). Figure 6.8 summarises and compares normalised maximal tensions obtained before and after preincubation with CCCP. It can be clearly seen that mitochondrial uncoupling significantly potentiated the hypoxic response in PA by ~2.5 times (tension increased from 22.2±5.7% to 79.6±17.0%, n = 3), whilst no significant change was observed in MA (Fig. 6.8).

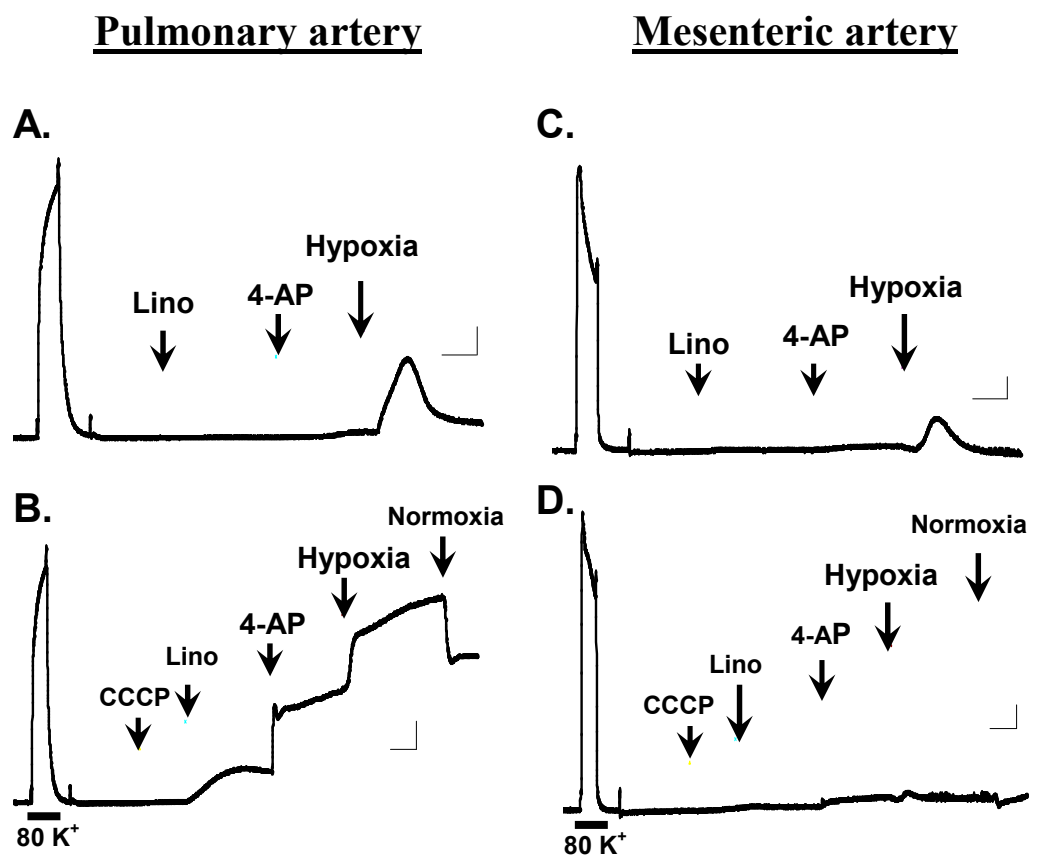

Figure 6.7 Effect of preincubation with CCCP on hypoxia-induced vasoconstriction in rat PA and MA.

Representative traces were obtained from PA (A-B) of 435 μm and MA (C-D) of 368 μm i.d., showing hypoxic vasoconstriction in the presence of 10 μM linopirdine and 2 mM 4-AP with (B and D) or without (A and C) preincubation for 10 min with 3 μM CCCP. Lino, linopirdine; 4-AP, 4-aminopyridine; CCCP, carbonyl cyanide 3-chlorophenylhydrazone (a mitochondrial uncoupler). Horizontal and vertical scale bars represent 5 min and 1 mN, respectively.

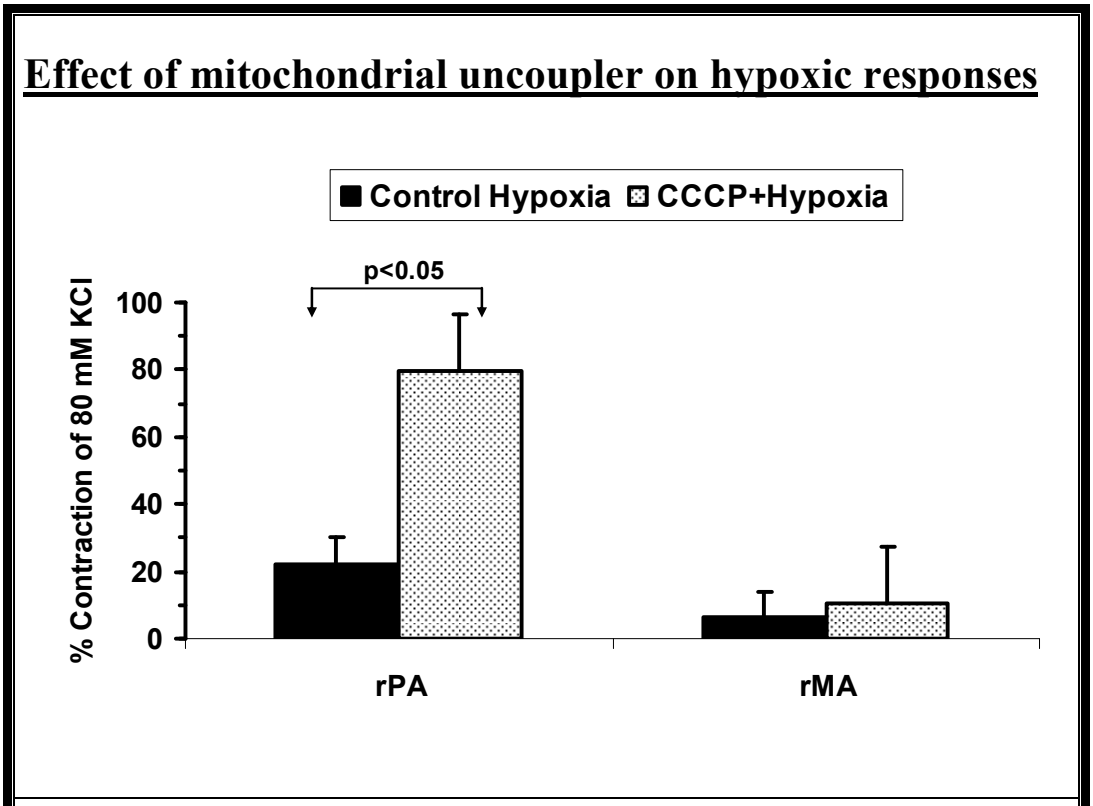

Figure 6.8 Preincubation with CCCP significantly potentiated hypoxic vasoconstriction in rat PA.

Graphs summarise and statistically compare hypoxic vasoconstriction obtained in the presence of 10 μM linopirdine and 2 mM 4-AP (control) followed by incubation of the tissues with 3 μM CCCP for 10 min and repeating the control. Paired Student's *t*-test ($n = 3$).

These results clearly demonstrate the presence of the relationship between hypoxia, inhibition of K_V channels and mitochondria function which are specific to the PA. It is noteworthy that in intact tissue mitochondrial uncoupling potentiated the response to 4-AP, whereas in α-toxin permeabilised preparations mitochondrial uncoupling inhibited 4-AP-induced contraction. One possible explanation could be the differences in the mitochondrial metabolism between two preparations (intact vs. permeabilised), because in the permeabilised tissue both $[Ca^{2+}]_i$ and ATP concentration are controlled. To determine if such differences in metabolism exists in two preparations, the effect of agents altering cellular metabolism on high K^+ and 4-AP-induced contractions were investigated.

6.2.4 Metabolic dependence of high K^+ (80 mM KCl)-induced contraction in rat PA and MA

To investigate if the inhibition of cellular metabolism differentially affect contraction in PA and MA, the contraction of the arteries to high K^+ (80 mM KCl applied for 15 min) was studied in the absence or in the presence of 2-DOG (5.6 mM, equimolar glucose substitution to inhibit glycolysis), NaCN (1 mM, to inhibit the mETC complex IV) or combination of NaCN and the inhibitor of ATP synthetase oligomycin (1 μM, to inhibit oxidative phosphorylation).

Figure 6.9 A and 6.9 E show representative traces demonstrating the effect of prolonged (15 min) application of 80 mM KCl in control conditions on PA and MA, respectively. It is noteworthy that contraction to prolonged exposure to high K^+ (15 min) exhibited biphasic responses in MA under control conditions, whilst in PA in the presence of metabolic inhibitors (Fig. 6.9 B-D). To assess this effect quantitatively, the peak of contraction and contraction at 15 min were measured in the presence of inhibitors, normalised to the peak KCl contraction measured in control conditions and expressed as a percentage. Notably, a distinct difference was found in the kinetics of the responses between PA and MA. In PA, high K^+-induced contraction was suppressed by metabolic inhibition but was maintained at a steady level for the total 15 min period of exposure (Fig. 6.9 B-D). On the other hand, in MA, the initial peak contraction was suppressed much less by the metabolic inhibitors, but the subsequent contraction was not sustained and progressively declined in the presence of 80 mM KCl (Fig. 6.9 F-H).

The metabolic inhibition of the peak and sustained contractions in PA and MA are statistically compared in Fig. 6.10. 2-DOG, NaCN and a combination of NaCN and oligomycin significantly suppressed the maximal peak contraction induced by high K^+ in both PA (Fig. 6.10 A) and MA (Fig. 6.10 C). In PA, the replacement of glucose with 2-DOG and the inhibition of oxidative phosphorylation with NaCN caused a similar decrease in high K^+-induced contraction (41.7±7.5%, n = 5 vs. 48.0±12.8%, n = 3). The effect of NaCN was not further enhanced by addition of

oligomycin (50.0±4.5%, *n* = 8) (Fig. 6.10 A). Qualitatively similar effects were observed in MA with 2-DOG (84.0±4.24%, *n* = 5), NaCN (77.5±8.6%, *n* = 3) and NaCN+oligomycin (83.2±3.0%, *n* = 8), except a greater degree of the inhibition observed in this tissue (Fig. 6.10 C).

Notably, in PA the effect of all metabolic inhibitors on the sustained KCl-contraction was quantitatively similar to that of the peak contraction (Fig. 6.10 A and B, respectively), whereas in MA, the inhibition of the sustained phase was approximately 3 times greater than that of the peak phase of contraction (Fig. 6.10 C and D, respectively). The analysis of the inhibition of the sustained phase of high K^+ contraction clearly showed a significantly greater suppression in MA than in PA for all metabolic inhibitors (Fig. 6.11).

These results clearly demonstrate that the maintenance of contraction in PA is significantly less dependent on cellular metabolism compared to that in MA.

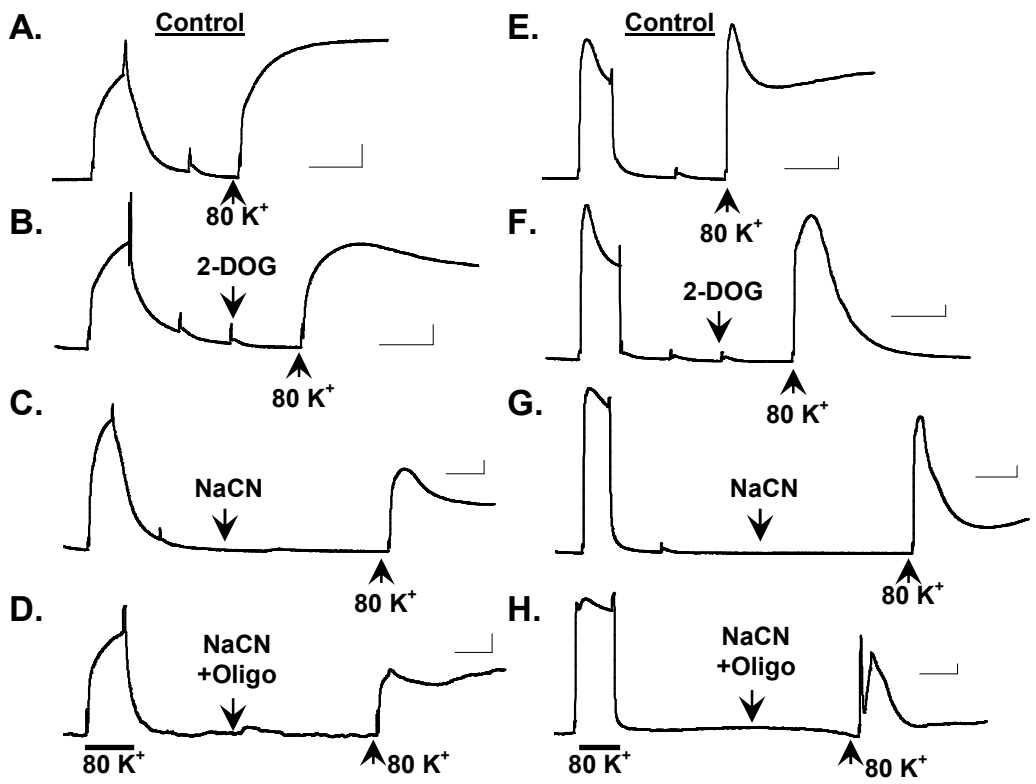

Figure 6.9 Effect of metabolic inhibitors on high K^+-induced contraction in rat PA and MA.

Representative traces were obtained from PA of 455 μm (A, B), 398 μm (C) and 293 μm (D) i.d.; and MA of 343 μm (E, F), 339 μm (G) and 224 μm i.d., showing contractile response to 80 mM KCl in control conditions (A, E), in the presence of 2-DOG (B, F), 1 mM NaCN (C, G) and in 1 mM NaCN +1 μM oligomycin (D, H). 2-DOG, 2-deoxyglucose (equimolar replacement of 5.6 mM glucose in Krebs solution); NaCN, sodium cyanide; Oligo, oligomycin. Horizontal and vertical scale bars represent 5 min and 1 mN, respectively.

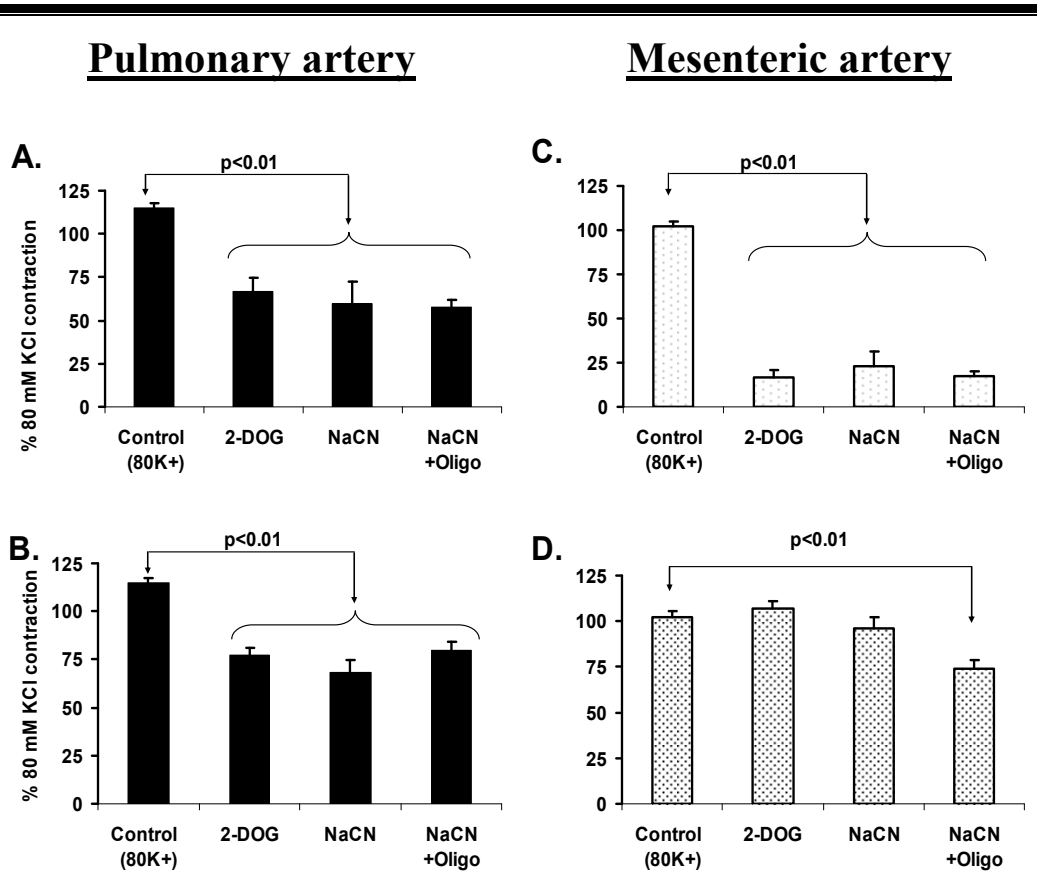

Figure 6.10 Metabolic inhibitions of the contraction induced by high K^+ in rat PA and MA.

The graphs summarise and compare the metabolic inhibition of the sustained phase (A and C) and the peak phase (B and D) of 80 mM KCl-induced contractions in PA (A-B) and MA (C-D). 2-DOG, 2-deoxyglucose; NaCN, sodium cyanide; Oligo, oligomycin. Differences between control versus treatment groups were tested by Dunnett post-hoc test following one-way ANOVA, n = 3-13 (Control, n = 13; 2-DOG, n = 5; NaCN, n = 3; and NaCN+Oligo, n = 8).

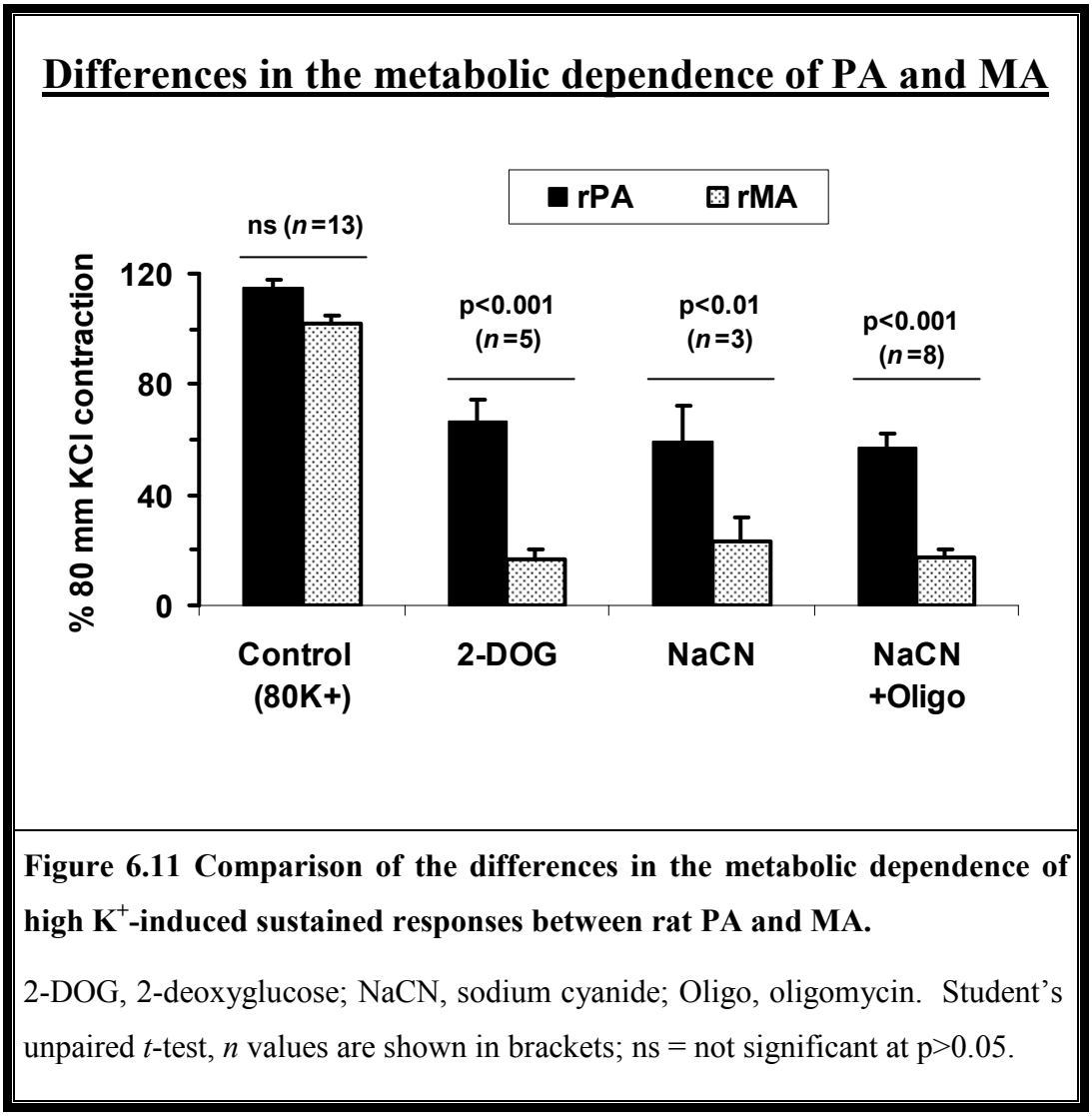

Figure 6.11 Comparison of the differences in the metabolic dependence of high K^+-induced sustained responses between rat PA and MA.

2-DOG, 2-deoxyglucose; NaCN, sodium cyanide; Oligo, oligomycin. Student's unpaired *t*-test, *n* values are shown in brackets; ns = not significant at p>0.05.

6.2.5 Metabolic dependence of 4-AP-induced contraction in rat PA

Since 4-AP-induced vasoconstriction shares common mechanisms with that induced by high K^+, the effect of metabolic inhibitors on the 4-AP-induced contraction was therefore investigated. This set of experiments was performed only in PA to investigate whether metabolic inhibition has any effect on the residual component (3^{rd} component) of the sustained contraction which was not inhibited by Y-27632 and diltiazem conversely to MA. I hypothesised that this component may be associated with metabolic regulation in PA.

In this set of experiments, 10 μM linopirdine was routinely used to maximise 4-AP-induced contraction and occasionally linopirdine alone produced a measurable level of tone (e.g. Figs. 6.12 A and 6.14 A). Although on some occasions a small increase in tone upon application of 2-DOG, NaCN or 2-DOG+NaCN was observed, overall no significant effect of the metabolic inhibitors was noted. 4-AP-induced contractions obtained in the presence of metabolic inhibitors 2-DOG (5.6 mM) or NaCN (1 mM) added alone or in combination were compared with the control 4-AP-induced contraction. Representative traces showing the effects of metabolic inhibitors on 4-AP-induced contraction are depicted in Fig. 6.12. It can be seen from the figure that 2-DOG and NaCN incompletely and similarly inhibited 4-AP-induced contraction by 58.2±9.7% (n = 10) and 55.6±8.7% (n = 8), respectively. Combined application of both drugs caused further suppression of the contraction (72.4±10.5%, n = 3), although it was not significantly different from the effects of metabolic inhibitors used alone (Fig. 6.13). Overall, the similarity between the effects caused by the inhibition of the glycolytic (2-DOG-sensitive) and oxidative phosphorylation (NaCN-sensitive) pathways could suggest that they are not additive.

It is worth mentioning that oscillations were often observed in the presence of NaCN (Fig. 6.12 C) but not in 2-DOG. Six out of the total eight preparations showed oscillations similar to those demonstrated in Fig. 6.12 C.

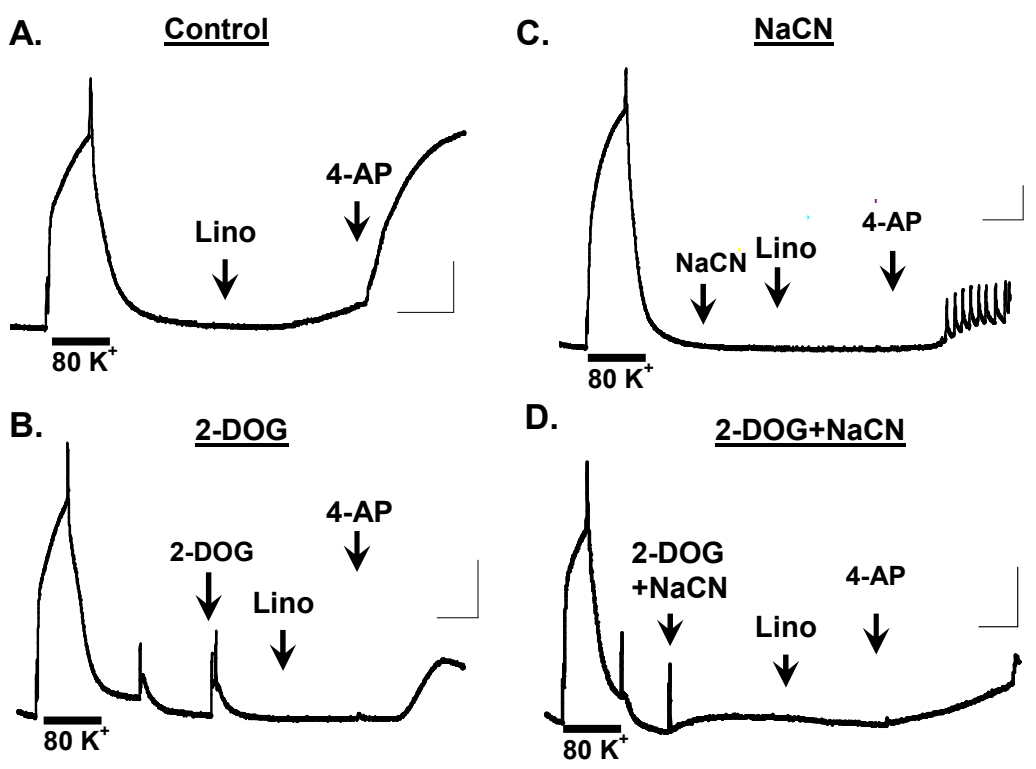

Figure 6.12 Effect of 2-deoxyglucose and sodium cyanide on 4-AP-induced contraction in rat PA.

A-D, representative traces obtained form PA of 487 μm i.d. (A and B), 395 μm i.d. (C) and 393 μm i.d. (D) showing contractile response induced by 10 mM 4-AP in control conditions (A), in the presence of 2-DOG (B), 1 mM NaCN (C) and 2-DOG+1 mM NaCN (D). Lino, linopirdine; 4-AP, 4-aminopyridine, NaCN, Sodium cyanide; 2-DOG, 2-deoxyglucose (equimolar replacement of 5.6 mM glucose in Krebs solution). Horizontal and vertical scale bars represent 5 min and 1 mN, respectively. Note that the transient peaks in B and D upon addition of 2-DOG are artefacts of changing solutions in the experimental chamber.

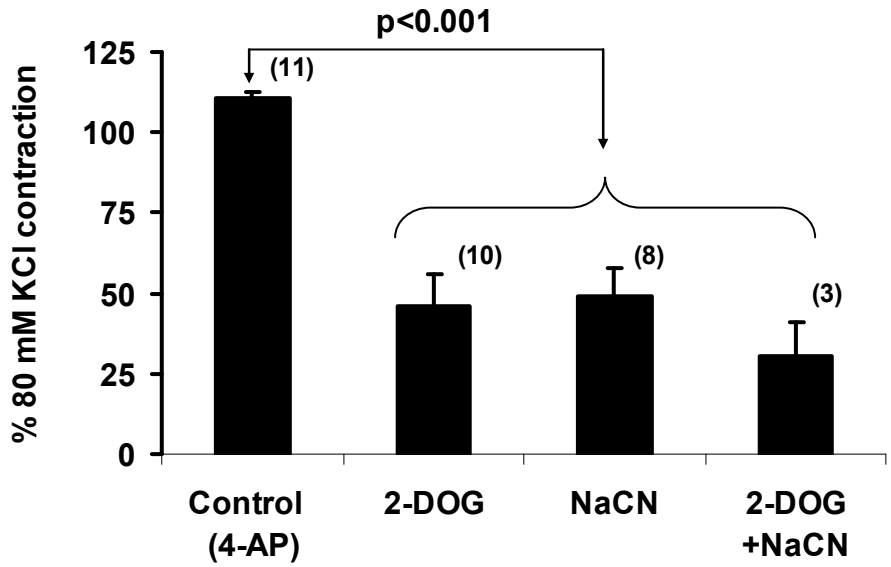

Figure 6.13 Summary of the effects of metabolic inhibitors on 4-AP-induced contraction in rat PA.

Graphs summarise and statistically compare between contraction elicited by 4-AP (control) and that in the presence of different metabolic inhibitors. 4-AP, 4-aminopyridine, 2-DOG, 2-deoxyglucose; NaCN, Sodium cyanide. Differences between control and treatment groups were tested by Dunnett post-hoc test following one-way ANOVA; *n* values are shown on the graphs.

The above results suggest that the metabolic inhibition with either 2-DOG, NaCN or their combination blocked only ~50% of the 4-AP-induced contraction. The similarity of the effects between the inhibitors suggests that their effects are not additive. To assess the nature of the 4-AP-induced contraction remaining in the presence of the metabolic inhibitors, the effect of the Rho-kinase inhibitor Y-27632 was investigated first. In this set of experiments, 2-DOG was chosen as a tool to inhibit cellular metabolism. The 4-AP responses were recorded in the presence of 2-DOG (5.6 mM) alone, Y-27632 (10 μM) alone or in the presence of the combination of these two agents.

The representative traces showing the inhibitory effects of 2-DOG or Y-27632 alone or their combination on 4-AP-induced contraction are depicted in Fig. 6.14. Y-27632 and 2-DOG blocked the 4-AP-induced contraction to a similar degree by 50.3±4.0%, (n = 7) and 56.8±5.9%, (n = 10), respectively. Most notably, however, the combination of these two agents almost completely abolished the 4-AP-induced contraction (97.7±4.8%, n = 6) (Fig. 6.15), suggesting that the Ca^{2+} sensitisation component and the component sensitive to cellular metabolism are independent. Notably, a nearly complete inhibition of the 4-AP-induced contraction following the pretreatment of PA with 2-DOG+Y-27632, resembles the complete block of the 4-AP-induced contraction as a result of the pretreatment with diltiazem+Y-27632 described in Chapter 5 (Figures 5.4 and 5.5). Therefore, it is possible that the 2-DOG-sensitive pathway could target the same pathway as diltiazem, i.e. Ca^{2+} entry via L-VOCCs.

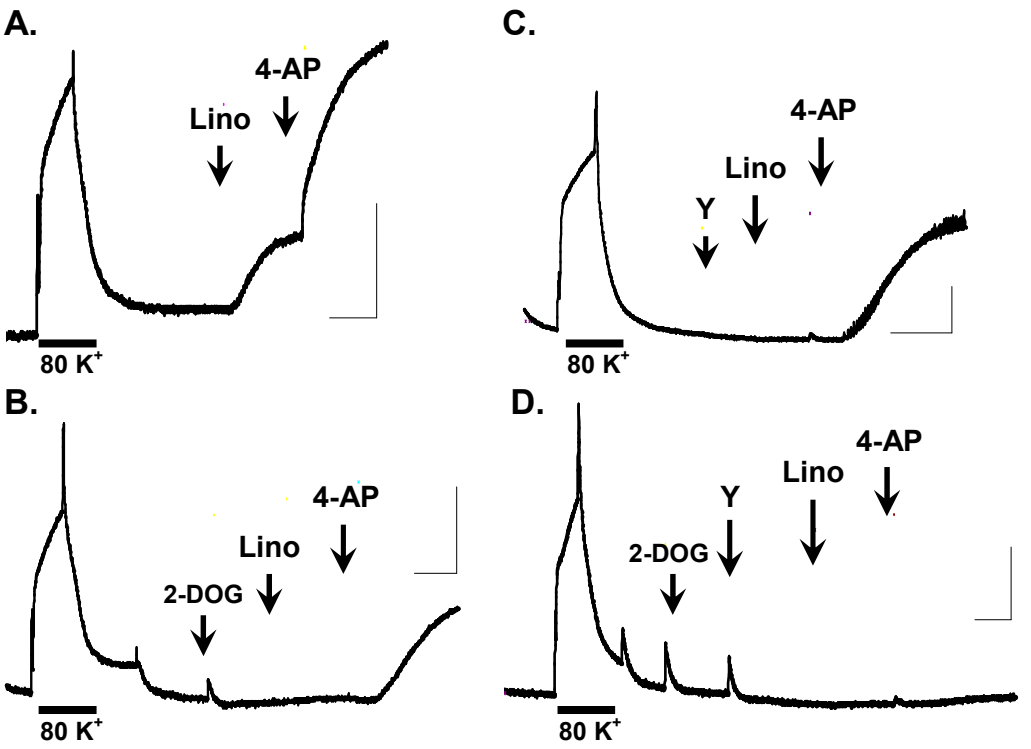

Figure 6.14 Effect of 2-DOG and Rho-kinase inhibitor Y-27632 on 4-AP-induced contraction in rat PA.

A-D, Representative traces were obtained from PA of 373 μm (A, B), 399 μm (C), and 391 μm (D) i.d., showing contractile response elicited by inhibition of K_V channels in control conditions (A), in the presence of 2-DOG (B), in the presence of 10 μM Y-27632 (C) and in the presence of 2-DOG+10 μM Y-27632 (D). Lino, 10 μM linopirdine; 4-AP, 10 mM 4-aminopyridine; Y, Y-27632; 2-DOG, 2-deoxyglucose. Horizontal and vertical scale bars represent 5 min and 1 mN, respectively.

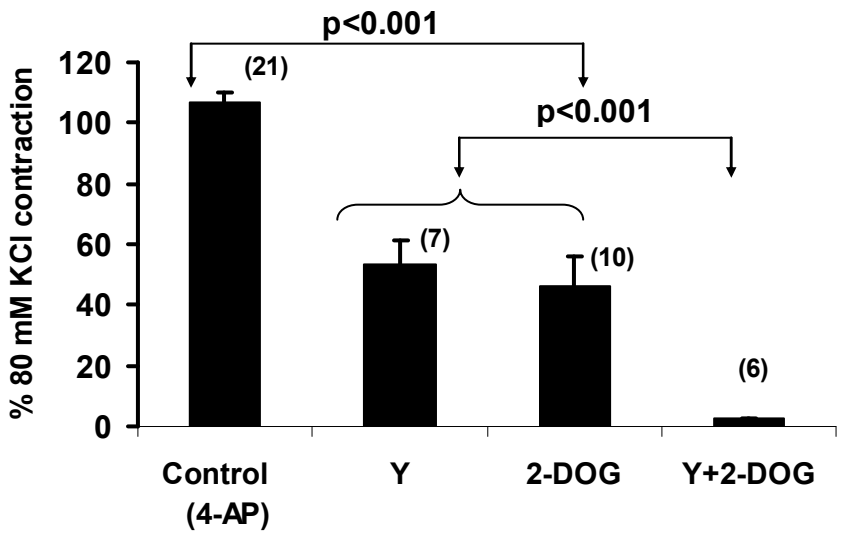

Figure 6.15 The dependence of 4-AP-induced contraction on Rho-kinase-mediated Ca^{2+} sensitisation and glycolytic metabolism in rat PA.

Graphs summarise and statistically compare the effect of Rho-kinase inhibitor Y-27632 (10 μM), 2-DOG and combination of these two on 4-AP elicited contraction in PA. Y, Y-27632 (10 μM), 2-DOG, 2-deoxyglucose. Differences between all groups were tested by Tukey-Kramer post-hoc test following one-way ANOVA; *n* values are shown on the graphs.

6.2.6 Effects of 2-DOG and NaCN on contraction evoked by U-46619 in rat PA

If 2-DOG selectively inhibits L-VOCC-mediated pathway, as suggested in the previous section, then contraction which does not involve the activation of this pathway should be non-sensitive to 2-DOG pretreatment. To investigate this possibility in PA, the effect of 2-DOG and NaCN was studied on contraction produced by a stable analogue of thromboxane A_2 mimetic U-46619 in the presence of 10 μM diltiazem (added 5 min prior to U-46619) to block the Ca^{2+}-entry via L-type Ca^{2+} channels. The effect of 2-DOG was also compared with that caused by the inhibitor of oxidative phosphorylation NaCN.

The representative traces and summary graphs of this set of experiments are shown in Fig. 6.16. The results shown in Fig. 6.16 B clearly shows that contraction recorded under such conditions was completely insensitive to 2-DOG, thus supporting the proposed hypothesis. On the other hand, U-46619 contraction was virtually completely abolished by NaCN (Fig. 6.16 C). The summary of the results is shown in Fig. 6.16 D. Note that the low *n* number (due to time constraints) does not allow to perform statistical analysis of this set of data. Nevertheless, these results clearly suggest the existence of at least two independent pathways (i.e., glycolytic and oxidative phosphorylation) which contribute at different levels in the regulation and maintenance of contraction in PA.

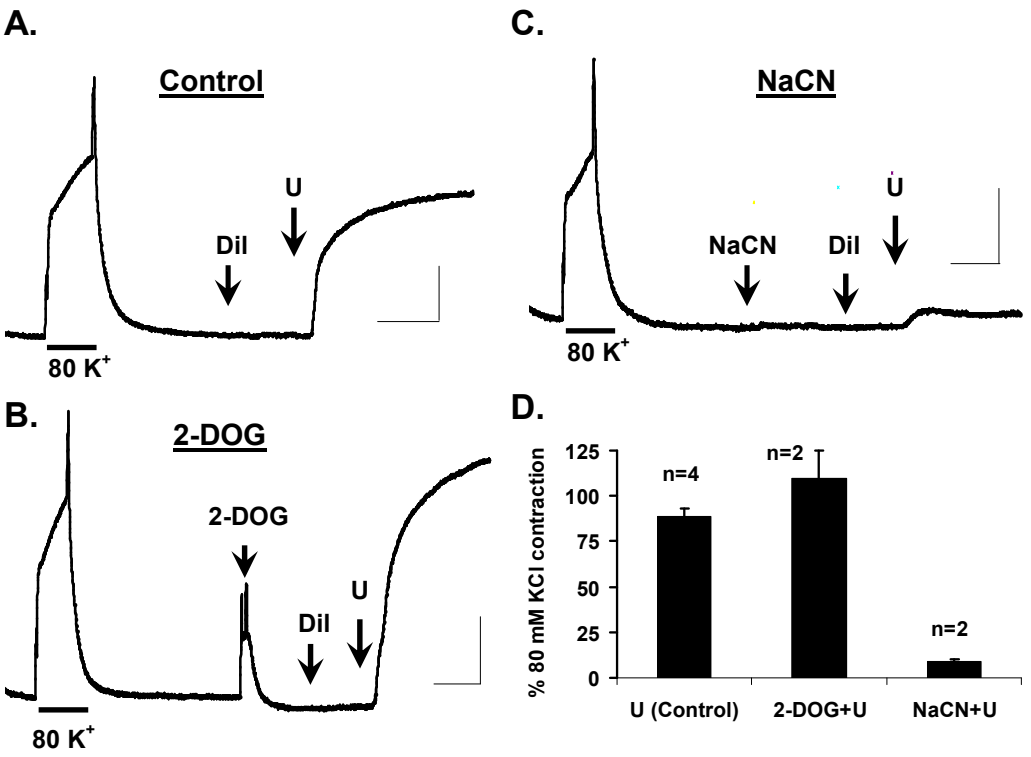

Figure 6.16 Metabolic inhibition of contraction to U-46619 in rat PA.

A-C, Representative traces were obtained from PA of 420 μm i.d., showing contractile response induced by 1 μM U-46619 in the presence of 10 μM diltiazem in control conditions (A), in the presence of 2-DOG (B), and in the presence of 1 mM NaCN (C). **D**, Compares the results obtained from two to four different rings of PA. Dil, 10 μM diltiazem; U, 1 μM U-46619; 2-DOG, 2-deoxyglucose; NaCN, 1 mM sodium cyanide. Horizontal and vertical scale bars represent 5 min and 1 mN, respectively.

6.3 Discussion

The main findings of this chapter can be summarised as following:

1) In intact arteries, mitochondrial uncoupling significantly potentiated 4-AP-induced contraction only in PA, and not in MA, indicating the presence of specific interactions between mitochondria and inhibition of K_V channels in PA.

2) 4-AP-induced contraction was dependent on the degree of tissue permeabilisation, being significant in α-toxin permeabilised arteries of both types and absent in β-escin permeabilised preparations which may indicate the presence of intact cellular compartments in α-toxin permeabilised preparations, which has much less disruption of the cell membrane compared to other skinning agents.

3) Mitochondrial uncoupling significantly potentiated and altered hypoxia-induced contraction in the presence of linopirdine and 4-AP significantly in PA, but not in MA, suggesting that the interaction between the putative oxygen sensor mitochondria and the inhibition of K^+ channels could be important in HPV.

4) The investigation of the effects of metabolic inhibition showed that sustained, but not the peak, contraction caused by high K^+ was significantly more metabolic dependent in MA than that in PA. In the PA, contraction to both high K^+ and 4-AP were similarly suppressed by the inhibition of glycolysis (2-DOG) and mitochondrial oxidative phosphorylation (NaCN) alone or in combination, suggesting that the two metabolic pathways are reciprocal.

5) In the PA, the component of the 4-AP-induced contraction, which was insensitive to the metabolic inhibitors, ablated by further addition of the Rho-kinase inhibitor Y-27632, suggesting that Ca^{2+} sensitisation is relatively independent of the cellular metabolism.

It is well documented that 4-AP acts via blocking K_V channels and that K_V channels expressed in inner mitochondrial membranes play an important role in cellular function (Szabo *et al.*, 2005). The results of this chapter demonstrate that the contraction occurring as a result of the blockade of K_V channels with 4-AP could be linked to mitochondrial function. To the best of my knowledge, this is the first demonstration of the existence of such interactions between the K_V channels and mitochondria at the level of a whole multicellular preparation. The ability of CCCP to enhance the 4-AP-induced contraction in PA in a similar manner as 20 mM KCl and 10 μM linopirdine can have several possible explanations. *Firstly*, as it was demonstrated in the previous chapters in intact arteries, and in this chapter in α-toxin-permeabilised arteries, that the 4-AP-induced contraction depends on the level of membrane depolarisation (which increases the number of opened K_V channels) hence a greater 4-AP-induced effect which in turn is associated with increased $[Ca^{2+}]_i$. The maintenance of the contraction to 4-AP will require both factors as 4-AP is not effective in Ca^{2+}-free Krebs in intact preparations, and in zero Ca^{2+} G10 solution in α-toxin-permeabilised arteries. Mitochondrial uncouplers can cause both an increase in intracellular Ca^{2+} (Hughes & Schachter, 1994;Yuan *et al.*, 1996;Drummond & Tuft, 1999;Kamishima *et al.*, 2000;Kamishima & Quayle, 2002;Kang *et al.*, 2003) and membrane depolarisation (Yuan *et al.*, 1995a) in pulmonary and systemic arterial SMCs. The latter could be indirectly due to activation of Ca^{2+}-dependent NSCCs or Cl_{Ca} by elevated $[Ca^{2+}]_i$ (Klöckner & Isenberg, 1991;Greenwood *et al.*, 1997;Bae *et al.*, 1999) leading to membrane depolarisation and activation of K_V channels, hence a greater effect of 4-AP. These effects however would be expected to be similar in PA and MA, which was not the case in my experiments, thus indicating the presence of the mechanism which is specific for PA. *Secondly*, an alternative explanation could be the dependence of the activity of K_V channels on mitochondrial function specifically in PA. This possibility was demonstrated by Firth *et al.* (2008) in single PASMCs, where it was shown that inhibition of mitochondrial function has a dual effect on the K_V current, potentiating at negative potentials and inhibiting at positive voltages. This effect was not observed in MASMCs (Firth *et al.*, 2008). A greater K_V current at rest in PA can explain a greater potency of 4-AP selectively in PA. In intact tissue, however, it is

likely that both mechanisms may contribute to increased 4-AP-induced contraction in the presence of CCCP in PA.

The significance of the mitochondrial involvement in 4-AP-induced contraction in PA was further demonstrated in permeabilised arteries. Tissue permeabilisation is a widely used experimental tool to investigate the role of signalling pathways under controlled intracellular conditions (Kitazawa *et al.*, 1989;Kobayashi *et al.*, 1989;Fu *et al.*, 1998;Evans *et al.*, 1999;Thomas *et al.*, 2005;Snetkov *et al.*, 2006;Knock *et al.*, 2008;Knock *et al.*, 2009). The use of α-toxin and the saponin ester β-escin allows a different degree of tissue permeabilisation while leaving receptor mediated signalling intact [reviewed in (Somlyo & Somlyo, 1990)]. The α-toxin creates holes in the cell membrane allowing molecules of <1000 Da to enter and leave cells while β-escin makes bigger pores allowing molecules of ≥17,000 Da to permeate cells (Kobayashi *et al.*, 1989).

In both type of permeabilisation, the voltage-dependent mechanism of contraction via membrane depolarisation is suppressed as there should be no ion flux across the cell membrane provided that the cell membrane is equally permeabilised across cells. Under such conditions, the ability of 4-AP alone to contract arteries may indicate a non-specific effect of the drug. Indeed, being a weak base, large concentrations of 4-AP (5-10 mM) are able to produce alkalisation of intracellular pH and increase intracellular Ca^{2+} (Guse *et al.*, 1994;Gobet *et al.*, 1995). This process however requires an intact cell membrane and is unlikely to occur in permeabilised preparations as intracellular pH is well controlled. The most strong evidence against the non-specific action of 4-AP under such experimental conditions comes from the ability of FCCP to significantly reduce 4-AP-induced contraction in PA but not in MA, suggesting that mitochondria could be, at least in part, responsible for 4-AP-induced contraction in PA. Although the non-specific action of 4-AP (which may be responsible for the FCCP-insensitive component) cannot be entirely ruled out, such a possibility is unlikely as greater degree of cell permeabilisation with β-escin completely inhibited the effect of 4-AP.

Although it is difficult to explain fully the mechanism underlying the effects of 4-AP and FCCP in permeabilised tissues, the presented evidence do not contradict the hypothesis that the strong functional relationship between mitochondria and K_V channels exists due to the presence of a population of subplasmalemmal mitochondria specifically in PA, and not in MA (Firth *et al.*, 2008;Firth *et al.*, 2009a). Gentle tissue permeabilisation with α-toxin may leave such compartments relatively intact providing the basis for the action of 4-AP in this condition. In β-escin permeabilised tissue this compartmentalisation could be disrupted more substantially thus removing the structural basis for 4-AP action. The ability of 4-AP to produce contraction in MA, which was relatively insensitive to mitochondrial uncoupling, may suggest a different relationship in this type of artery. Because MA was not a primarily focus of this study, its mechanism has not been specifically investigated in this work. One possible explanation could be a close association between mitochondria and SR in systemic arteries that has been documented previously (Kamishima *et al.*, 2000;Gordienko *et al.*, 2001). Further experimentation is required to completely understand both mechanisms. In any case, the experimental approach adopted in my study using different degrees of tissue permeabilisation represent a very useful technique to address certain questions raised for example in the single cell studies at the level of intact preparations.

The interactions between the K_V channel inhibition and mitochondrial uncoupling specifically in PA can have important functional implications in HPV, an adaptation mechanism which is unique to the pulmonary circulation but the mechanisms remain controversial and highly disputable (Robertson *et al.*, 2000b;Moudgil *et al.*, 2005;Waypa & Schumacker, 2005;Aaronson *et al.*, 2006;Sommer *et al.*, 2008;Ward & McMurtry, 2009). The ability of hypoxia to transiently contract both PA and MA has been demonstrated previously (Leach *et al.*, 1994;Robertson *et al.*, 2003) and confirmed in this study (Chapter 4; and Fig. 6.7 A and C). It does not however represent an ability which is unique to PA. The difference in hypoxic responses observed in the presence of CCCP clearly suggest the presence of a specific and synergistic effect between mitochondria function and K_V channel inhibition in PA under hypoxic conditions. As mitochondria, one of the important oxygen sensors in PA (Rounds & McMurtry, 1981;Waypa *et al.*,

2001;Waypa & Schumacker, 2002;Weissmann *et al.*, 2003;Michelakis *et al.*, 2004;Waypa & Schumacker, 2005), are depolarised by hypoxia (Duchen & Biscoe, 1992;Di Lisa *et al.*, 1995) and the K_V channels are known to be blocked by hypoxia (Post *et al.*, 1992;Archer *et al.*, 1993;Weir & Archer, 1995;Olschewski *et al.*, 2002;Archer & Michelakis, 2002;Platoshyn *et al.*, 2006), this synergistic action could be one of the contributing mechanisms to the complex HPV response. In MA, the pretreatment with CCCP under identical condition completely inhibited the transient hypoxic contraction, an observation which supports the well-known relaxatory action of hypoxia in the systemic arteries (Ishida & Honda, 1992;Aalkjaer & Lombard, 1995;Shimizu *et al.*, 2000).

Another important consequence of the action of mitochondrial uncouplers could be uncoupling of electron transport mechanism and oxidative phosphorylation, which could influence metabolism and thus contractility. This possibility is directly supported by the following findings described in this chapter. In PA, the contraction initiated by high K^+ is suppressed and maintained, whereas in MA, the contraction becomes transient with a little effect on the initial peak component. This could indicate stronger metabolic requirements for the maintenance of contraction in MA than in PA. One of the reasons for the difference in the metabolic dependence of contraction in the two tissue types could be the difference in ATP consumption, which could be greater in MA compared to PA. This can be speculated from the observation that the dependence of oxidative energy production for endothelium-dependent relaxation to acetylcholine and adenosine differs between the rat PA and aorta, being greater in the latter (Rodman *et al.*, 1991). The authors suggested that this could be an adaptive mechanism as the maintenance of low pulmonary tone is likely to be less metabolic dependent. Although my experiments do not provide a direct answer to the exact molecular mechanisms responsible for such differences, dissimilar rates of phosphorylation and/or dephosphorylation could be a contributing mechanism. There is very little further published evidence which address this interesting and I believe an important question.

The differences between PA and MA described in this chapter suggest that the rate of consumption of ATP during contraction may be enhanced in MA, and if

less supply of ATP is provided in the presence of metabolic inhibitors the contraction is failed to maintain (Fig. 6.9 E-H). It has previously been suggested that, unlike the systemic artery, PA possesses an additional mechanism which allows an enhanced glycolytic ATP production and glucose uptake (Leach *et al.*, 2002). There is convincing evidence that cellular energy production and utilisation is compartmentalised in smooth muscle cells (Paul, 1983). In PA, ATP production resides largely within mitochondria (Leach *et al.*, 2002). A recent study revealed that PASMCs have a greater number of mitochondria which are compartmentalised closer to the cell membrane compared to mitochondria in MASMCs which are more centrally distributed (Firth *et al.*, 2009a). The role of this subplasmalemmal population of mitochondria in ATP production is not clear. In systemic vasodilation, the total concentration of ATP has been shown to be unchanged during hypoxia (Leach *et al.*, 1998;Shimizu *et al.*, 2000), although the method used (e.g. ^{31}P NMR) is not capable to detect localised changes of ATP within the cell. As metabolic inhibition mimics the effects of hypoxia (Miller *et al.*, 1993), hypoxia *per se* could be considered as an equivalent to a metabolic inhibitor, at least in the pulmonary circulation. It has been reported that hypoxia causes less deterioration in energy state in the pulmonary than in systemic artery (Leach *et al.*, 1998). Several other metabolic markers such as intracellular pH and phosphocreatine are also better conserved or unchanged during hypoxia and HPV in pulmonary arteries (Leach *et al.*, 2000). Furthermore, it has been reported that hypoxia increased glucose uptake into PASMCs during HPV by ~250% whilst glucose uptake into MASMCs remained less than 50% of that in PASMCs whether in normoxia or hypoxia (Leach *et al.*, 2001), possibly reflecting the capacity of pulmonary artery to maintain sustained contraction during metabolic inhibition. These unique properties of PASMCs could indicate the presence of specific mechanisms that allow improved maintenance of cellular energy state, such as enhanced glucose uptake and glycolytic ATP production specifically in PA. This notion is supported by the evidence presented in this chapter.

An interesting additional observation was the presence of oscillations in PA in the response to 4-AP in the presence of cyanide. The exact mechanism however is not clear. Interestingly, CN causes transitions in mitochondrial energetics due to block of ATP production by inhibiting complex IV of the mETC (Aon *et al.*,

2003). However, it is not clear if this process contributed to tension oscillations observed in this study.

The contractile response elicited by K^+ channel inhibition clearly showed involvement of two reciprocal metabolic pathways: glycolysis and mitochondrial oxidative phosphorylation. There is a possible link between these two pathways since glycolysis not only produce ATP but also provides pyruvate for the mitochondrial oxidative phosphorylation which further produces ATP. Such potential interaction between these two pathways could explain a reciprocal action of 2-DOG and cyanide on high K^+- and 4-AP-induced contractions. Glycolytic pathway itself provides relatively little energy (only 2 ATP per each molecule of glucose is derived) compared to subsequent oxidative phosphorylation pathway (upto 38 ATP molecules net) (Leach *et al.*, 2002). However, vascular smooth muscles are exceptional in that they exhibit high levels of glycolysis, which is associated with a large lactate production derived almost entirely from this source. In VSMCs glycolysis generates ~30% of total ATP production during normoxia, and accounts for ~90% of the glucose utilised by the cell (Paul, 1989).

An important observation in this chapter is that inhibition of 4-AP-induced contractions by 2-DOG and Y-27632 are additive in pulmonary artery mirroring the findings that diltiazem and Y-27632 are additive in contraction produced by high K^+ and 4-AP (described in Chapter 5). It is therefore possible that the inhibition of 4-AP-induced contraction by 2-DOG may be due to selective suppression of or interference with the function of L-VOCCs. This hypothesis is supported by the observation that 2-DOG did not have an effect on contraction caused by U-46619 under conditions when L-VOCCS were inhibited by diltiazem. In addition, in ventricular cardiac myocytes, I_{Ca} was found to be regulated by intracellular ATP derived from glycolysis (Losito *et al.*, 1998). This study revealed that a complete metabolic inhibition with 2-DOG and cyanide resulted in a 40% decrease in peak I_{Ca} (Losito *et al.*, 1998). Another notable finding of this chapter is the total blockade of the 4-AP-induced contraction with Y-27632 in the presence of 2-DOG, suggesting that the Ca^{2+}-sensitisation component (Y-27632-sensitive) of contraction is relatively independent of the cellular metabolism because these are completely additive effects. If the Y-27632-sensitive component

was dependent on glycolytic metabolic pathway then Y-27632 and 2-DOG would have a little further change in the 4-AP-induced contraction. It is noteworthy that complete block of 4-AP response also supports the specificity of 4-AP and is consistent with previous evidence supporting this notion.

Interestingly, the voltage-independent component of the U-46619-induced contraction showed different sensitivity to the inhibition of glycolysis (with 2-DOG) and mitochondrial oxidative phosphorylation (with NaCN). Greater dependence of NaCN suggests perhaps different compartmentalisation of energy sources, for example Ca^{2+} re-uptake into the SR using SERCA which utilises ATP for its activity. A high demand of ATP for SERCA activity can be provided via oxidative phosphorylation pathway, hence its higher sensitivity to cyanides. I would like to mention here that due to time constrain these are rather preliminary findings and further experimentation is necessary to elucidate the exact mechanisms.

Chapter 7

INVESTIGATION INTO THE ROLE OF K_V CHANNELS IN THE REGULATION OF CONTRACTILITY IN MOUSE PULMONARY AND SYSTEMIC MESENTERIC ARTERIES

7.1 Introduction

Mouse is a widely used experimental animal model and, genetically, is closely related to humans. In addition to the wild type, transgenic or knock out (KO) mice are increasingly being used to investigate disease mechanisms and in drug discovery. KO mouse models are also increasingly being used to investigate and unveil the mechanisms of HPV and pulmonary hypertension (MacLean *et al.*, 2004;Millen *et al.*, 2006;Morecroft *et al.*, 2009;Morrell *et al.*, 2009;Kelland *et al.*, 2010;MacLean & Dempsie, 2010;Morecroft *et al.*, 2010). Many KO mouse models have already been used to evaluate mechanisms of the modulation of pulmonary vasoconstriction and remodelling in connection to i) altered function of ion channels and transporters (Rios *et al.*, 2005;Dietrich *et al.*, 2005), ii) altered superoxide production (Liu & Folz, 2004;Liu *et al.*, 2006), iii) endothelial nitric oxide synthase disruption (Fagan *et al.*, 1999;Ozaki *et al.*, 2001), and iv) vasoactive and mitogenic agonists such as hypoxia inducible factor 1α and 2α (Yu *et al.*, 1999;Brusselmans *et al.*, 2003). However, to explore the basic physiological phenomenon the wild type mouse model still plays significant role. Recently, several studies have carried out functional characterisation of agonist-induced pulmonary vasoconstriction (Xu *et al.*, 2008), and also characterisation of K_V channels in mouse PASMCs (Ko *et al.*, 2007) using wild type mouse model,

but neither of these studies compared the findings with systemic arteries. Recent evidence revealed that K_V channels in mouse PASMCs possess different pharmacological characteristics, being sensitive to both TEA and to 4-AP (Ko *et al.*, 2007) which is different to the rat model. This pharmacological profile may suggest abundant expression of K_V2 α-subunits in mouse tissue, in comparison to rat PASMCs (Smirnov *et al.*, 2002). Notably, expression of K_V1 and $K_V2.1$ α-subunits was demonstrated in mouse MASMCs (Fountain *et al.*, 2004). Using $K_V1.5$ KO mice Archer *et al.* (2001) found that a K^+ channel containing $K_V1.5$α-subunits is an important effector of HPV in mice. In addition to the abundant expression of 4-AP sensitive $K_V1.5$, mouse PASMCs also express $K_V1.2$ which is sensitive to TEA (Grissmer *et al.*, 1994;Archer *et al.*, 2001). Also, in contrast to rat PASMCs, a greater proportion of BK_{Ca} current is present in mouse vascular tissues (Fountain *et al.*, 2004;Ko *et al.*, 2007). It has been previously demonstrated that BK_{Ca} channels play an important role in the regulation of cerebral vascular tone in mice (Plüger *et al.*, 2000). Notably, KCNQ channels are also expressed in murine vasculature including portal vein (Ohya *et al.*, 2003;Yeung *et al.*, 2008), aorta, carotid, femoral and mesenteric arteries (Yeung *et al.*, 2007). Functional role of KCNQ channels have also been reported in murine non-vascular smooth muscles including myometrium (McCallum *et al.*, 2010) and gastrointestinal tract (Jepps *et al.*, 2009). The ability of specific KCNQ channel inhibitors to constrict mouse PA (mPA) was greater than mouse MA (mMA) (Joshi *et al.*, 2006). Also, KCNQ channel openers were able to cause greater relaxation effects on mPA than on mMA (Morecroft *et al.*, 2009). These reports indirectly suggest that the interaction between the two channel types may be also important in the mouse, i.e. similar to the phenomenon I described in the rat model in this thesis. However, the basic characterisation of the pulmonary vascular reactivity in the mouse model is still lacking. Furthermore, no direct comparison of the involvement of K_V channels in the regulation of excitability and contractility of the murine pulmonary and systemic arteries has been yet undertaken.

To address the question what is the role of K_V channels in intact mPA and mMA, the effects of pharmacological inhibitors of K_V channels 4-AP and TEA (which will inhibit TEA-sensitive K_V channels like $K_V2.1$) were compared between these

two tissue types. In this study, male CD mice (10-12 weeks old) weighing 35-40 g were used. First order intrapulmonary (i. d. 313±26 μm, *n* =7) and 2nd to 3rd order mesenteric arterial rings (i. d. 167±17 μm, *n* = 7) were used for tension measurement. Arterial rings were mounted in the small vessel dual wire myograph (as described in Chapter 2) and set up at tensions equivalent to their mean in vivo resting tension; i.e. ~15 mmHg for mPA (Kelland *et al.*, 2010) and ~100 mmHg for mMA (Madhani *et al.*, 2003). It is notable that due to lack of time the data presented in this chapter are rather preliminary and further studies will be necessary to address a number of questions raised as a result of these experiments.

7.2 Results

7.2.1 Effect of 4-AP on basal tone in mPA and mMA

Arterial rings were preconstricted with 80 mM KCl 3-4 times before the beginning of the experiment. Concentration-response curves were constructed in mPA and mMA with K_V blocker 4-AP adding cumulatively at 0.5, 1, 2, 5 and 10 mM, each concentration applied for 5 min (Fig. 7.1 A). Similar to the rat PA, in mPA as well, only small contraction of 0.56±0.26 mN (*n* = 8) and 1.07±0.23 mN (*n* = 8) was observed at 5 and 10 mM 4-AP, respectively. Membrane depolarisation by pretreatment of the tissue with 20 mM KCl enhanced 4-AP-induced contraction (0.87±0.16 and 1.64±0.16 mN at 5 and 10 mM 4-AP, respectively) (Fig. 7.1 B). The difference was, however, statistically significant only at 10 mM 4-AP (Fig. 7.2 A). Similar trend was observed in mMA treated with increasing concentration of 4-AP in the absence (Fig. 7.1. C) and presence of 20 mM KCl (Fig. 7.1 D). However, in contrast to mPA, no significant difference was observed in mMA even at high concentration of 4-AP when the responses were compared between control and depolarised conditions (Fig. 7.2 B). It is notable that 20 mM KCl *per se* posed only a little contraction with 0.12±0.05 mN (*n* = 6) or ~ 5% of 80 mM KCl contraction in mPA and 0.65±0.16 mN (*n* = 6) or ~19% of 80 mM KCl contraction in mMA.

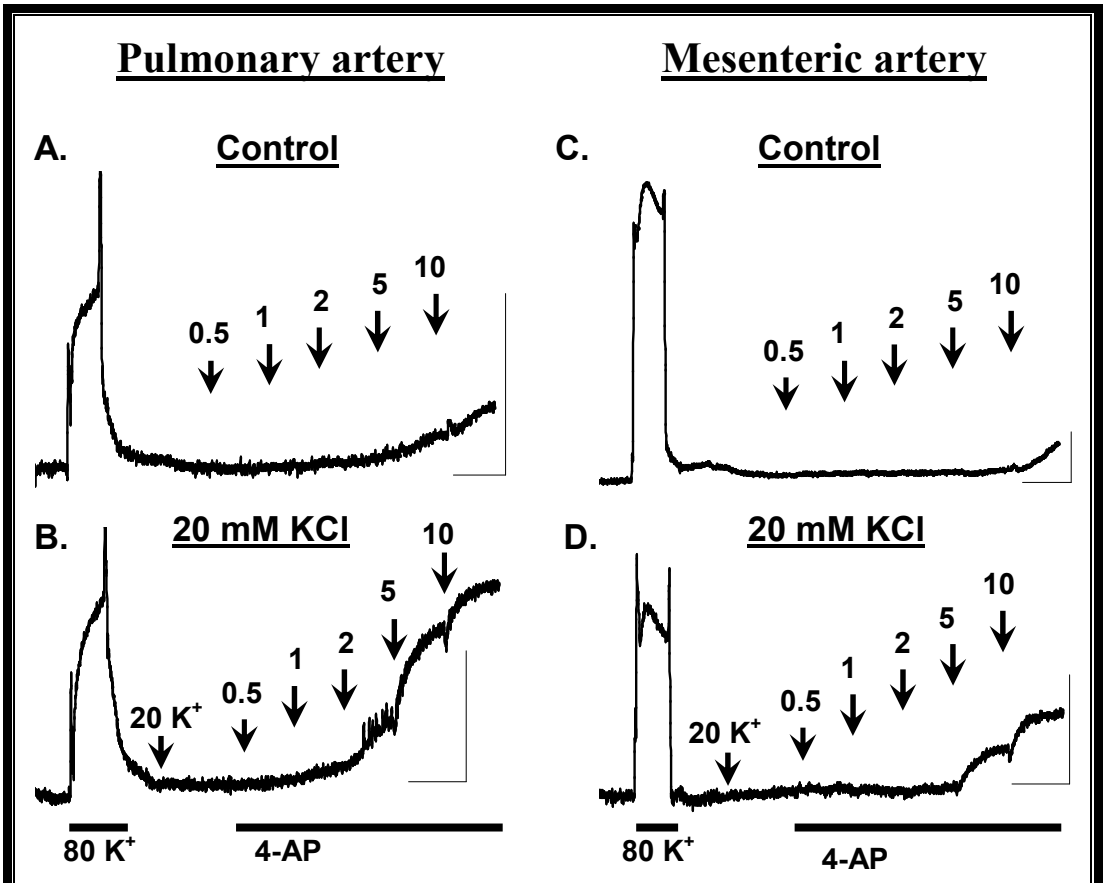

Figure 7.1 Potentiation of 4-AP concentration-contraction responses by low concentration of KCl in mPA and mMA.

Representative traces were obtained from mPA (A-B) and mMA (C-D) in the absence (A, C) and presence (B, D) of 20 mM KCl. Concentrations of 4-AP in mM and time of their application are indicated by arrows. Internal diameters of mPA were 381 μm (A) and 259 μm (B); and of mMA were 207 μm (C) and 115 μm (D). Horizontal and vertical scale bars represent 5 min and 1 mN, respectively.

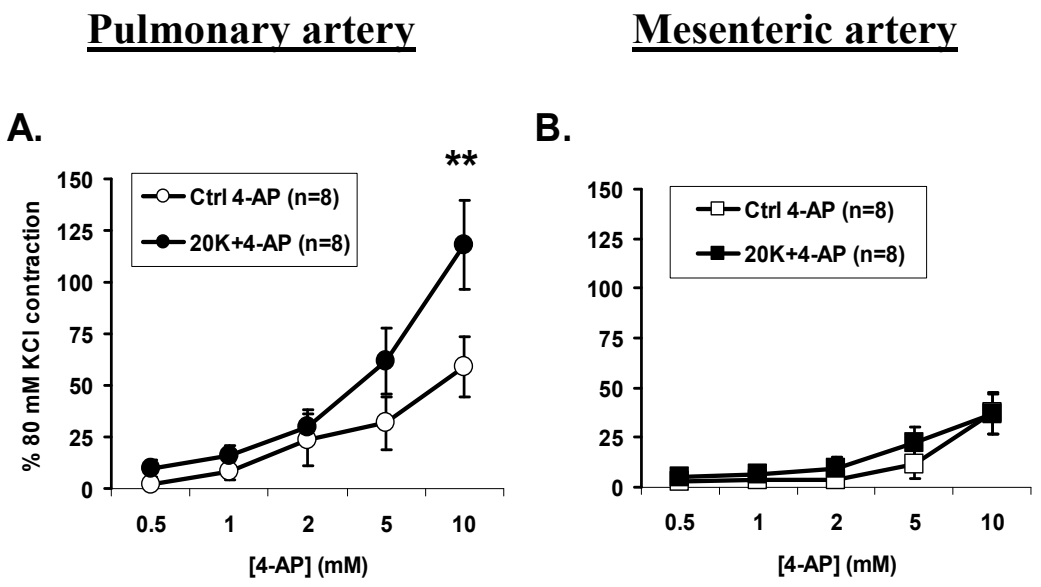

Figure 7.2 Tissue specific differences in potentiation of 4-AP-induced responses by 20 mM KCl.

Concentration-response curves obtained from mPA (A) and mMA rings (B) in the absence and presence of 20 mM KCl. ** ($P < 0.01$) denotes significant potentiation of 4-AP response at 10 mM concentration following treatment with 20 mM KCl in mPA. Differences between control versus treatment groups for the same concentration of drug were tested by Bonferroni post-hoc test following one-way ANOVA, $n = 8$.

Notably, some oscillations were observed in the presence of 10 mM 4-AP in 6 out of 8 mPA in the presence of 20 mM KCl, and 3 out of 8 mPA in the absence of 20 mM KCl. In mMA, however, no oscillations were observed in either condition. The 4-AP-induced oscillatory contractions were blocked by diltiazem suggesting the involvement of L-VOCCs in this process. Interestingly, similar type of oscillations have also occasionally been observed in rat PA but not as common as in mPA, whereas in rat MA oscillations in contraction were observed more frequently.

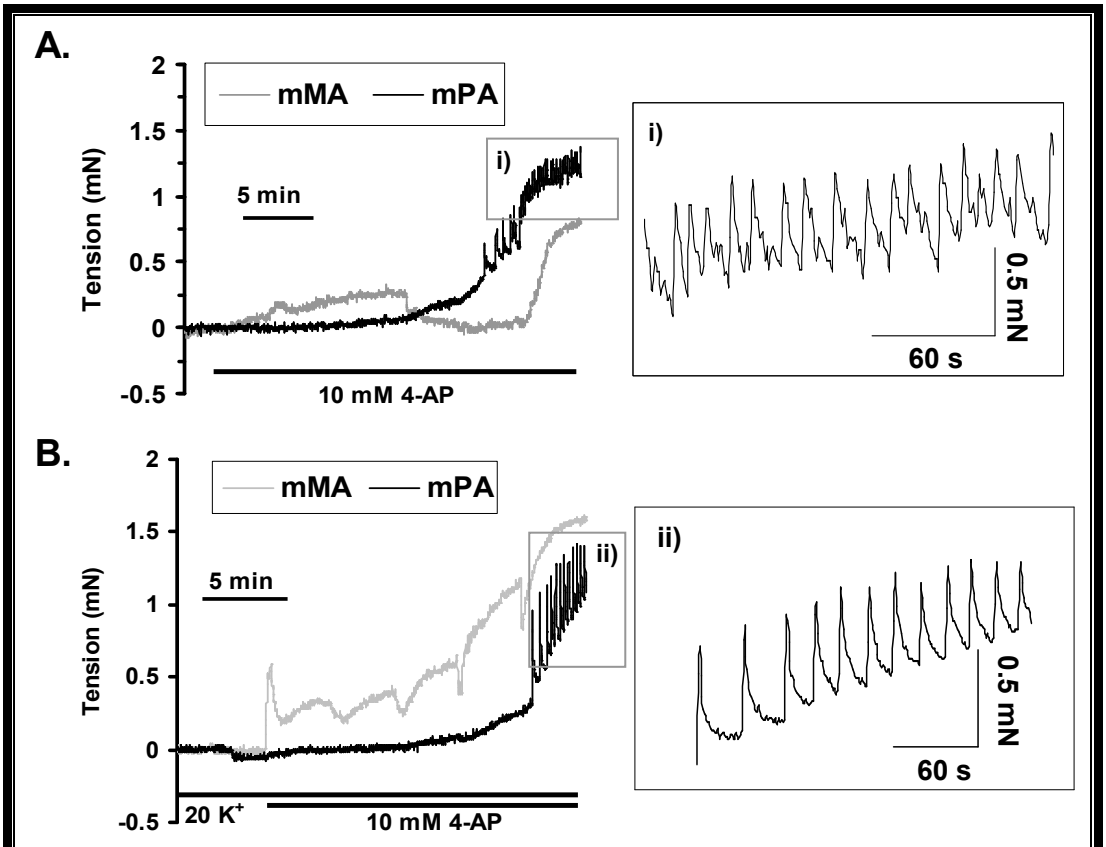

Figure 7.3 Inhibition of K_V channels with 10 mM 4-AP elicits spontaneous oscillations in mPA in the absence (A) and presence (B) of 20 mM KCl.

Representative traces obtained from mPA (black traces) and mMA (grey traces). Internal diameters of mPA were 382 and 320 μm (A and B, respectively) and of mMA were 186 and 140 μm (A and B, respectively). Inserts (i) and (ii) show oscillations at an expanded time scale for A and B, respectively.

Figure 7.3 summarises the characteristics of 4-AP-induced spontaneous oscillations observed in mPA in the absence (Fig. 7.3 A) and presence of 20 mM KCl (Fig. 7.3 B). The amplitude and frequency of oscillations recorded in the absence of 20 mM KCl was 0.55±0.11 mN (n = 3) and 0.50±0.09 Hz (n = 3), respectively. No difference was observed in the amplitude (0.45±0.07 mN, n = 6) and frequency (0.48±0.06 Hz, n = 6) of oscillations in the presence of 20 mM KCl.

7.2.2 Effect of TEA on contractility of mPA and mMA

TEA sensitive K_V channels include $K_V1.1$, $K_V1.2$ $K_V1.3$, $K_V1.6$, $K_V2.1$, $K_V2.2$, $K_V3.1$ and $K_V3.2$ (Gutman *et al.*, 2005). Among these K_V subtypes, the $K_V1.2$ and $K_V2.1$ isoforms are known to be sensitive to TEA (K_d = 560 nM for $K_V1.2$ and K_d =1-3 mM for $K_V2.1$) and are expressed in murine VSMCs (Grissmer *et al.*, 1994;Archer *et al.*, 2001;Ko *et al.*, 2007). To investigate if these isoforms contribute to the regulation of contractility in intact murine vasculature concentration-contraction responses to TEA (1-20 mM) were constructed in mPA and mMA in the absence (Fig. 7.4 A and C) and presence (Fig. 7.4 B and D) of 20 mM KCl. In the absence of 20 mM KCl both mPA and mMA revealed only small contraction to high concentration of TEA. However, in the presence of 20 mM KCl both murine tissues demonstrated increased contractility to TEA although this potentiation did not reach significance at the number of performed experiments (Fig. 7.5).

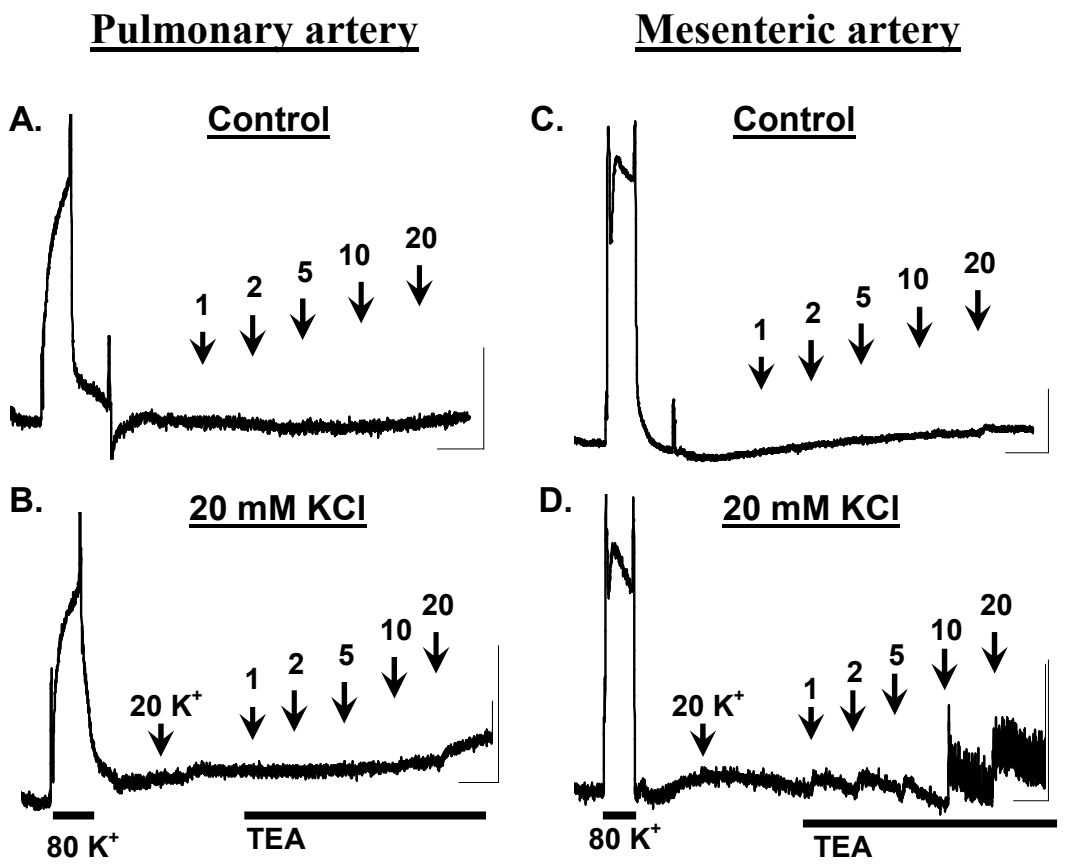

Figure 7.4 Effect of TEA on contractility of mPA and mMA in the absence (A & C) and presence (B & D) of 20 mM KCl.

Representative traces of tension recordings were obtained from mPA (A-B) and mMA (C-D) showing concentration-dependent contraction to TEA. Internal diameters of mPAs were 203 and 259 μm (A and B, respectively) and of mMA were 104 and 115 μm (C and D, respectively). Concentrations of TEA in mM and time of their application are indicated by arrows. 20 K^+, 20 mM KCl; 80 K^+, 80 mM KCl; TEA, tetraethylammonium. Horizontal and vertical scale bars represent 5 min and 1 mN, respectively.

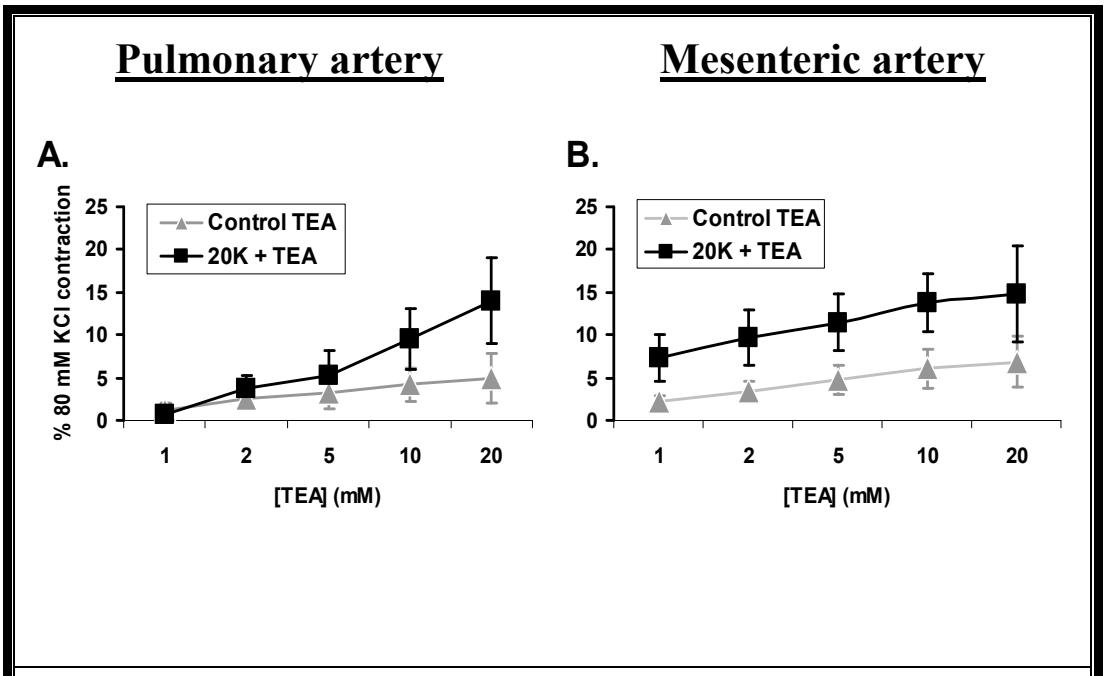

Figure 7.5 Summary of the concentration-contraction responses to TEA in mPA and mMA.

Concentration-contraction responses were obtained from 5 mPA (A) and 5 mMA (B) in the absence and presence of 20 mM KCl showing trend of potentiation of TEA responses in both mPA and mMA in the presence of elevated K^+. 20K, 20 mM KCl; TEA, tetraethylammonium. Differences were not significant with Bonferroni post-hoc test following one-way ANOVA (n = 5).

7.2.3 Comparison of the responses to 4-AP and TEA between PA and MA of mouse and rat

A comparison of the responses to 10 mM 4-AP and 20 mM TEA, expressed as a percentage of contraction elicited by 80 mM KCl, between the two species, rat and mouse, and the two types of tissues, pulmonary and systemic, are tabulated below. In comparison to the rat, mouse vasculature (both PA and MA) was apparently more sensitive to 4-AP and TEA in both stimulated and non-stimulated tissues causing greater contraction in relation of 80 mM KCl responses (Table 7.1).

Table 7.1 Comparison between 4-AP and TEA-induced responses between pulmonary and mesenteric arteries of mouse and rat

	Mouse tissues (% contraction of 80 mM KCl)		**Rat tissues** (% contraction of 80 mM KCl)	
	mPA	**mMA**	**rPA**	**rMA**
4-AP	59±15 (*n* = 8)	37±10 (*n* = 8)	22±7 (*n* = 8)	4±3 (*n* = 8)
20K+4-AP	118±22 (*n* = 8)	37±10 (*n* = 8)	74±9 (*n* = 8)	38±12 (*n* = 8)
TEA	5±3 (*n* = 5)	7±3 (*n* = 5)	5.8, 0.7 (*n* = 2)	1.2, 1.0 (*n* = 2)
20K+TEA	14±5 (*n* = 5)	14±5 (*n* = 5)	10.8, 1.2 (*n* = 2)	1.1, 1.3 (*n* = 2)

Data expressed as Mean±S.E.M.

7.2.4 Comparison of the effect of diltiazem on 4-AP-induced contraction in mPA and mMA

I have previously found (Chapter 3) that in the rat the L-VOCC blockers were inhibiting 4-AP-induced contractions incompletely in the PA, in contrast to the MA. To determine if similar type of action of L-VOCC blockers exists in mouse arteries, the effect of a selective Ca^{2+} channel blocker diltiazem on contraction induced by 4-AP was investigated. Contraction was induced by increasing concentrations of 4-AP in the presence of 20 mM KCl in mPA and mMA as described above. When contraction reached a steady state level in the presence of 10 mM 4-AP, 10 μM diltiazem was applied. Fig. 7.6 A shows that the tension was declined only partly in mPA, but it was declined rapidly and almost completely in mMA (Fig. 7.6 B). Thus, similarly to the rat PA, the 4-AP-induced contraction is only partly voltage-dependent in mPA but almost entirely voltage-dependent in mMA. Application of 10 μM diltiazem decreased the 4-AP-induced contraction only by 35% in mPA (Fig. 7.6 A) whereas the contraction in mMA was reduced by 93% (Fig 7.6 B). These effects on both absolute (Fig. 7.7 A) and normalised (Fig. 7.7 B) tension are summarised in Figure 7.7. Thus, these results suggest similarity between rat and mouse models in relation to 4-AP responses, i.e. a tissue specific and species independent phenomenon.

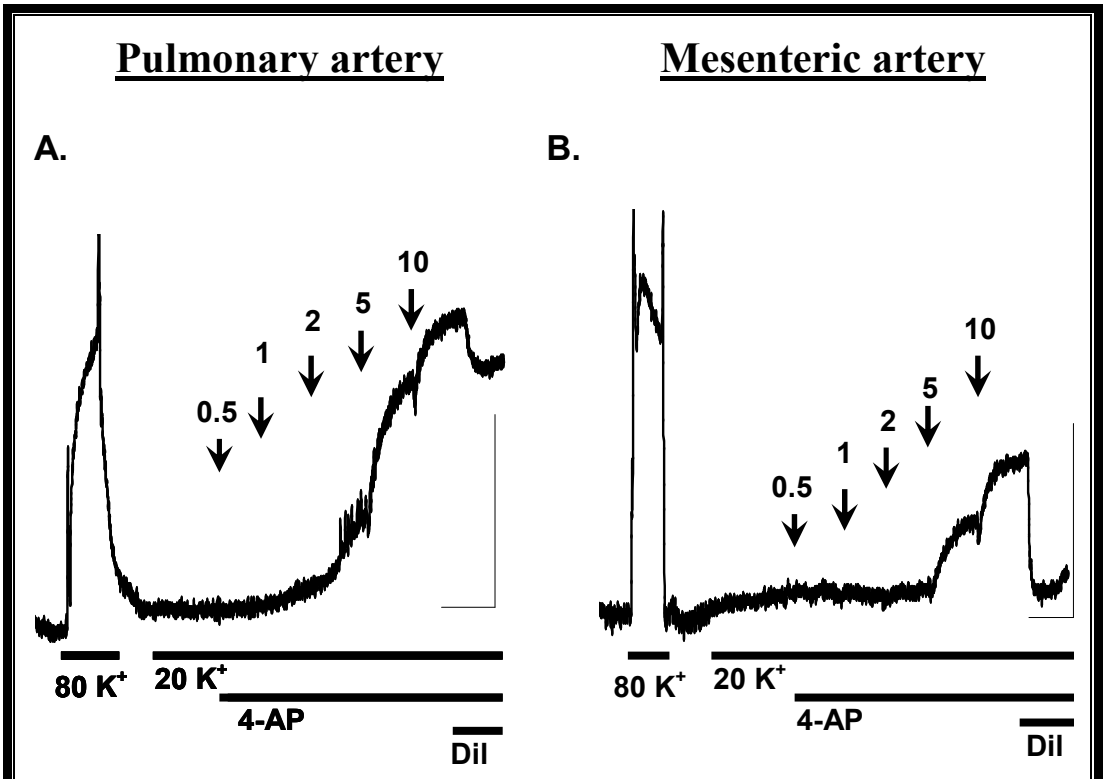

Figure 7.6 Effect of diltiazem on tension induced by 4-AP in mPA and mMA.

Representative traces were obtained from mPA (A) of 259 μm i.d. and mMA (B) of 115 μm i.d., showing the effect of increasing concentrations of 4-AP in the presence of 20 mM KCl followed by addition of 10 μM diltiazem. These traces are taken from the same tissues as shown in figure 7.1 (B and D). Concentrations of 4-AP in mM and time of their application are indicated by arrows. Horizontal and vertical scale bars represent 5 min and 1 mN, respectively.

Diltiazem-insensitive component of 4-AP contractions

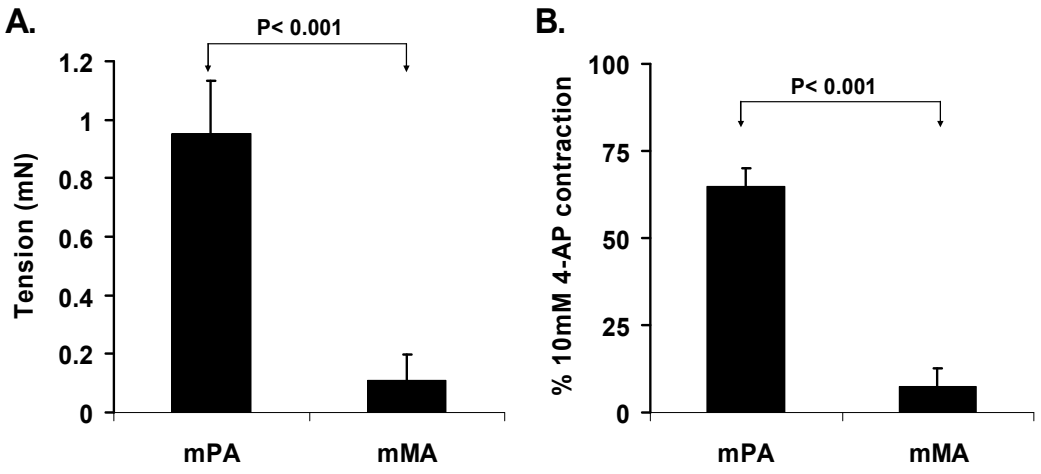

Figure 7.7 Comparison of the diltiazem-insensitive component of 4-AP-induced contraction in mPA and mMA.

A and B show absolute tension and contraction normalised to the peak 4-AP-induced force, respectively. Significance was evaluated with paired Student's *t*-test, $n = 7$).

7.3 Discussion

The main observations described in this chapter can be summarised as follows: ***i)*** contraction to 4-AP was significantly potentiated by 20 mM KCl in mPA; ***ii)*** TEA was able to potentiate contraction in the presence of 20 mM KCl; ***iii)*** application of 4-AP-induced oscillatory activity which were more frequently observed in mPAs compared to mMAs; and ***iv)*** contraction to 4-AP in mPA had a significant diltiazem-insensitive component, which was practically absent in mMAs.

The contractile response to K_V channel blocker (10 mM 4-AP) was increased by ~100% of it's normalised tension and more than 50% of it's absolute tension (mN) in the presence of 20 mM KCl, which itself did not significantly affect the basal tone of mPA. This depolarisation-induced potentiation of 4-AP-induced contraction in the mouse PA was quantitatively similar to that observed in the rat PA in the presence of 20 mM KCl and in the KCNQ channel inhibitor linopirdine (as described in Chapter 3). It is notable that the presence of KCNQ channels was functionally characterised in mouse PAs (Joshi *et al.*, 2006), mouse portal vein smooth muscle cells (Yeung & Greenwood, 2005) and other systemic vasculature of mouse including aorta, carotid artery, femoral artery and mesenteric artery (Yeung *et al.*, 2007). In rat PA and MA, I also observed potentiation of 4-AP responses in the presence of a specific KCNQ channel blocker (10 μM linopirdine) (Chapter 3). Although the effect of linopirdine (or any other KCNQ channel blocker) was not studied in the mouse arteries due to time constrain these preliminary findings from mouse arteries suggest that a similar interaction between the two channel types, K_V and KCNQ, might exist in the pulmonary arteries of both rat and mouse. Overall, however, the similarity of the results obtained in the rat and mouse arteries presented in this study and previously published evidence do not contradict the notion that the mechanism of the regulation of membrane potential by two channel types (K_V and KCNQ) in pulmonary arteries is likely to be species-independent and specific for the pulmonary circulation.

Sensitivity of mPA to TEA is likely to indicate the presence of TEA-sensitive conductances. Low concentrations of TEA (around 1-2 mM) are known to block BK_{Ca} channels (Blatz & Magleby, 1984;Robertson *et al.*, 1993;Nelson & Quayle, 1995). Some voltage-dependent K_V channels such as $K_V3.1b$ which are expressed in PA (Platoshyn *et al.*, 2004) are highly sensitive to TEA. On the other hand, high concentrations of TEA (above 5-10 mM) can block delayed rectifier channels encoded by the members of K_V2 channel subfamily, another type of K_V channels present in PA (Patel *et al.*, 1997;Archer *et al.*, 1998;Smirnov *et al.*, 2002;Hogg *et al.*, 2002). Since TEA constricted mPA only at high concentrations, it is therefore likely that $K_V2.1$ channels are responsible for this effect. On the other hand, a small effect at low concentrations of TEA was observed in mMA. This may suggest the presence of either BK_{Ca} or K_V channels with high TEA-sensitivity in this artery. In any case, these data are consistent with findings published by others where the functional expression of both 4-AP and TEA sensitive channels (K_V2 type) in both mPA and mMA was documented (Fountain *et al.*, 2004;Ko *et al.*, 2007). For the further continuation and advancement in the line of this work here I propose to investigate the possible interplay between the different K_V channels by i) combination of linopirdine with 4-AP and TEA; and ii) utilising KCNQ channel activators (e.g. retigabine, flupirtine) on channel- and receptor-mediated PA contractions. It would also be appropriate to use other more potent and more specific KCNQ channel inhibitors (e.g. XE991) as well as alternative KCNQ openers (e.g. acrylamide S-1) to advance further the knowledge of the functional role of KCNQ channels and their interaction with K_V channels in murine PA, and to compare that with systemic arteries.

One of the most interesting observations in this chapter is the inability of the L-VOCC blocker diltiazem to completely relax 4-AP-induced contraction specifically in mPAs, but not in mMAs. Nearly two third of the 4-AP-induced contraction in mPA was insensitive to diltiazem, while in mMA, 4-AP-induced contraction was nearly entirely abolished with diltiazem. These effects are closely mirroring those in the rat arteries, which are described and characterised in Chapter 3. Such similarities strongly indicate that the principal cellular mechanism responsible for 4-AP-induced contraction is tissue-specific and not species dependent. Because the mouse with a wide availability of genetically

modified types represents an ideal experimental model, it could help in pursuing this issue at the molecular level. Further work is essential to explore these mechanisms in full details.

Tension oscillations in response to 4-AP in mPA is another interesting finding. The oscillatory behaviour of contraction elicited by 4-AP has also been demonstrated previously in normal mPA (Xu *et al.*, 2008). In rat PA oscillations have only been reported in certain conditions such as chronic hypoxia (Bonnet *et al.*, 2001), pulmonary hypertension (Kiyoshi *et al.*, 2003) or endothelin-1-induced vasoconstriction (Hyvelin *et al.*, 1998). I have also occasionally observed oscillations in response to 4-AP in the rat PA (Fig. 6.12 C) but not as often as observed in mouse PA. Interestingly, in the rat MA, oscillations were observed more frequently compared to rat PA (Figs. 3.7 C, 3.15 C and 4.1 B), whereas reversed relation was found in the mouse arteries. Although the mechanism of oscillations has not been specifically addressed in this study, several explanations could be brought forward. Oscillations might occur to maintain a balance between Ca^{2+} influx and extrusion and/or Ca^{2+} release and sequestration (Xu *et al.*, 2008). Cell membrane depolarisation as a result of inhibition of K_V channels with 4-AP may trigger voltage-dependent oscillatory process (Tammaro *et al.*, 2004). Thus, the 4-AP-induced oscillatory contraction suggests that inhibition of voltage-gated K^+ channels and membrane depolarisation may indirectly activate mechanisms or pathways for Ca^{2+} extrusion and sequestration in mPA. Another possibility could be the activation of KCNQ channels in the presence of 4-AP. This could lead to membrane hyperpolarisation, however since the K_V channels are still inhibited, the cell membrane will be destabilised and small depolarisation can occur triggering L-VOCC and thus contraction. Then the process can repeat itself causing oscillatory behaviour. This type of spontaneous contractions has been reported previously by Yeung and Greenwood (2005) in mouse portal vein, where XE991 (10 μM) and linopirdine (50 μM) increased the frequency of contractions and also in some tissues large increase in frequency resulted in a tonic contraction (Yeung & Greenwood, 2005). It would be interesting therefore to investigate the effect of KCNQ channel blockers in the mouse arteries, to assess the role of the KCNQ channels in this oscillatory process.

Chapter 8

CONCLUSION AND FUTURE DIRECTIONS

8.1 Summary

This study was focussed on the investigation and the understanding of the role of K_V channels in intact pulmonary arteries. K_V channels are ubiquitous and are expressed in all known vascular smooth muscles. The main strength of this study which distinguishes it from the previously published works in the pulmonary field is the parallel comparison of the pulmonary and systemic mesenteric arteries recorded under the same experimental conditions. This approach allowed the identification of the mechanisms which are specific to the pulmonary artery and thus provides new insights into the role of the K_V channels in the pulmonary circulation and their contribution to the HPV response.

Figure 8.1 summarises the major mechanistic pathways determined in this study and they can be involved in the normal pulmonary function and in the HPV response.

The role of both K_V and KCNQ channels in the pulmonary function has been proposed, but up-to date the functional significance of each channel type was investigated separately. This is the first study focussed on the interaction between the two channel types and the relative role each channel plays in the control of tissue excitability. The importance of both channel types in the basal tone has been demonstrated specifically in the pulmonary artery. The involvement of both K^+ channels has an important functional implication in the maintenance of the low resistance and low pressure in the pulmonary circulation. This observation may also enhance a future therapeutic use of KCNQ channel activators (e.g. retigabine

and flupirtine which are currently used experimentally) to reduce pulmonary blood pressure in PAH (Joshi *et al.*, 2009;Gurney *et al.*, 2010). In addition, the understanding of this interaction between the two channel types, allowed me to address the important question whether KCNQ channels are affected by hypoxia. The findings are consistent with the notion that the K_V channels are inhibited by hypoxia, whereas the KCNQ channels in the pulmonary artery are likely to be not affected by acute hypoxia. This observation is one of the novel findings of this work.

Another novel finding was the demonstration that the mechanism of contraction resulted from the inhibition of K_V channels by 4-AP is complex and involves both the voltage-dependent (via L-VOCCs) and voltage-independent (Rho-kinase dependent) components in the pulmonary artery. Also another important observation was the presence of the third component of contraction that was not sensitive to L-VOCC blocker and Rho-kinase inhibitor in the pulmonary but not in the mesenteric artery. Furthermore, parallel comparison of the effects of various agents which stimulates and inhibits contraction via the voltage-dependent and voltage-independent manner allowed the proposal for a new hypothesis that describes the principal differences between the maintenance of contraction in these two artery types. In the pulmonary artery, the voltage-dependent and voltage-independent (Ca^{2+} sensitisation) pathways resulting in contraction operate in a parallel manner, whereas, in the mesenteric artery, they occur sequentially.

The investigation of the nature of the third component of the 4-AP-induced contraction in the pulmonary artery, allowed me to hypothesise that it may involve specific interactions between the K_V channels and mitochondria. Such interactions have been recently demonstrated in single PASMCs and not in MASMCs (Firth *et al.*, 2008;Firth *et al.*, 2009a). The evidence presented in this thesis suggests for the first time that such interaction could exist in intact pulmonary arteries and that they may be involved in acute HPV response.

In addition, the results obtained in this work demonstrate the importance of the glycolytic pathway in the regulation of pulmonary contractility initiated by the activation of the voltage-dependent Ca^{2+} entry pathway.

Finally, my preliminary data suggests that the mechanisms described in the rat (including the involvement of the two types of K^+ channels in the regulation of pulmonary vascular tone, and the presence of voltage-dependent and voltage-independent components of contraction) also exist in the mouse pulmonary artery, suggesting that they are not species dependent, and might be the common mechanism intrinsic to the pulmonary circulation.

In conclusion, the findings in this work such as mutually important role of K_V and KCNQ channels in the regulation of pulmonary vascular tone, the existence of specific cellular mechanisms controlling pulmonary contractility and the specific relationship between the K_V channels and mitochondria, which are important in the regulation of normal pulmonary function and in HPV, provide a significant advance in our understanding of the basic mechanisms governing pulmonary excitability and contractility. These can potentially lead to the development of new therapeutic strategies to the treatment of pulmonary related diseases.

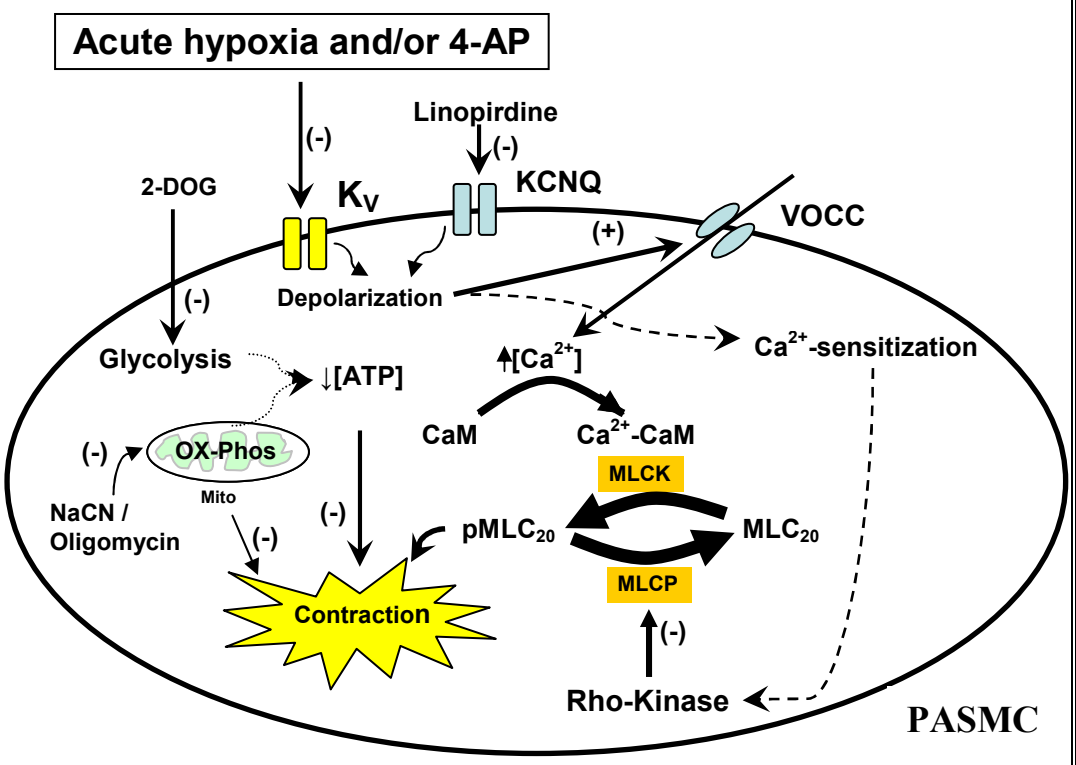

Figure 8.1 Schematic diagram summarising proposed interactions between different intracellular pathways targeted in this study.

2-DOG, 2-deoxyglucose; K_V, voltage-gated K^+ channels; KCNQ, K_V7.1-7.5 channels; VOCC, voltage-operated calcium channel; Mito, mitochondria; Ox-Phos, oxidative phosphorylation; [ATP], net intracellular ATP; [Ca^{2+}], net intracellular calcium; CaM, Calmodulin; MLCK, myosin light chain kinase; MLCP, myosin light chain phosphatase; MLC_{20}, 20 kDa myosin light chain; $pMLC_{20}$, phosphorylated 20 kDa myosin light chain; (-), inhibition or negative effects; (+), opening of a channel or positive effects.

8.2 Future directions

The results of this study not only provide novel and important insights into the function of both the pulmonary and the mesenteric artery, but also set up new intriguing questions which I was not able to address in full in this thesis due to time constrain and limited resources.

The relationship between the K_V channels and mitochondria in the pulmonary artery deserves further investigation. One of the potential approaches could be the investigation of 4-AP responses in tissues where mitochondrial function is impaired (e.g. the use of tissue culture and low concentrations of mitochondrial inhibitors/uncouplers). The role of the glycolytic pathway could be further studied in a similar way.

Mitochondrial function in the pulmonary circulation is frequently linked to ROS. Whether ROS are involved in the above mechanisms has not been addressed in this study and is an important question. The use of novel technologies to quantify ROS, like the recently developed redox-sensitive, ratiometric fluorescent protein sensor (RoGFP) (Waypa *et al.*, 2010), or the use of mitochondria-targeted antioxidant like SkQ1 (Shipounova *et al.*, 2010) will provide new opportunities to investigate this and related questions. The novel mitochondria-targeted antioxidant SkQ1 [10-(60-plastoquinonyl) decyltriphenylphosphonium] selectively accumulates in mitochondria because these organelles form the only negatively charged compartment in the cell. Selective accumulation of SkQ1 in the mitochondria is favoured by high membrane potential of the inner mitochondrial membrane (about 180 mV) together with membrane potential (inside negative) of the plasma membrane and the strong hydrophobicity of SkQ1(Shipounova *et al.*, 2010).

To overcome the limitations and disadvantages of investigations on the isolated cells due to artificial environment and the loss of native cell-cell interactions, the application of new technologies for targeted ROS measurement on the level of the

intact tissue or organ or even whole animals can be helpful. This can be achieved in sophisticated mouse models, where an inducible or conditional knock out or targeted gene deletion can be utilised (Said *et al.*, 2007;Starr *et al.*, 2008;Gayen *et al.*, 2010). Indeed, a strain of mice with mitochondrial dysfunction has been developed (Inoue *et al.*, 2000). Because the mechanisms controlling pulmonary contractility and excitability are likely to be similar between the rodent and murine species (as my results suggest), the use of this and other genetically modified mice could help to answer a number of intriguing questions about exact mechanisms for the interactions between the K_V channels and mitochondria. Although being a challenging task due to small artery sizes, the setting up the mouse model is probably most important to further advance my findings because of the availability of a variety of knock out mice.

The identification of the exact signalling pathways involved in the pulmonary and mesenteric arterial contractions is another very important question in my opinion. However, the complexity and cross interactions between the potential mechanisms involved demand a separate focussed study that combines functional, biochemical and molecular biological techniques. In this type of study, in addition to the standard biochemical and molecular biological techniques (Western blot, RT-PCR), a novel, specific and versatile molecular biological technique called the proximity ligation assay (Soderberg *et al.*, 2006;Soderberg *et al.*, 2007), can be useful in addressing the questions about the molecular composition of the K_V and KCNQ channels that can be heteromultimeric (Zhong *et al.*, 2010a). This approach will be also beneficial for the understanding of the mechanisms responsible for the differences in the maintenance of contraction in the pulmonary and systemic arteries (to investigate the proposed parallel and sequential hypotheses).

The use of the combined measurement of contraction, intracellular Ca^{2+} and/or pH, as well as Po_2 levels will also be important for further understanding of the mechanisms described in this thesis. Such combined approach is widely used to study vascular function (Waypa *et al.*, 2002;Evans *et al.*, 2005;Quayle *et al.*, 2006;Kajimoto *et al.*, 2007). Unfortunately, the required equipments were not available during the time this work was performed.

Chapter 9

REFERENCES

Aalkjaer C & Lombard JH (1995). Effect of hypoxia on force, intracellular pH and Ca^{2+} concentration in rat cerebral and mesenteric small arteries. *J Physiol* **482**, 409-419.

Aalkjaer C & Nilsson H (2005). Vasomotion: cellular background for the oscillator and for the synchronization of smooth muscle cells. *Br J Pharmacol* **144**, 605-616.

Aaronson PI, Robertson TP, Knock GA, Becker S, Lewis TH, Snetkov V, & Ward JP (2006). Hypoxic pulmonary vasoconstriction: mechanisms and controversies. *J Physiol* **570**, 53-58.

Aaronson PI, Robertson TP, & Ward JP (2002). Endothelium-derived mediators and hypoxic pulmonary vasoconstriction. *Respir Physiol Neurobiol* **132**, 107-120.

Abdullah K & Docherty JR (1999). Comparison of the effects of nitric oxide synthase, guanylate cyclase and potassium channel inhibition on vascular contractions in vitro in the rat. *J Auton Pharmacol* **19**, 263-266.

Abe F, Karaki H, & Endoh M (1996). Effects of cyclopiazonic acid and ryanodine on cytosolic calcium and contraction in vascular smooth muscle. *Br J Pharmacol* **118**, 1711-1716.

Accili EA, Kiehn J, Wible BA, & Brown AM (1997). Interactions among inactivating and noninactivating Kvβ subunits, and Kvα1.2, produce potassium currents with intermediate inactivation. *J Biol Chem* **272**, 28232-28236.

Aggarwal SK & MacKinnon R (1996). Contribution of the S4 segment to gating charge in the Shaker K+ channel. *Neuron* **16**, 1169-1177.

Aguilar-Bryan L & Bryan J (1999). Molecular biology of adenosine triphosphate-sensitive potassium channels. *Endocr Rev* **20**, 101-135.

Ahnert-Hilger G & Gratzl M (1988). Controlled manipulation of the cell interior by pore-forming proteins. *Trends Pharmacol Sci* **9**, 195-197.

Aiello EA, Clément-Chomienne O, Sontag DP, Walsh MP, & Cole WC (1996). Protein kinase C inhibits delayed rectifier K^+ current in rabbit vascular smooth muscle cells. *Am J Physiol* **271**, H109-H119.

Aird WC (2008). Endothelium in health and disease. *Pharmacol Rep* **60**, 139-143.

Alapati VR, McKenzie C, Blair A, Kenny D, MacDonald A, & Shaw AM (2007). Mechanisms of U4. *Br J Pharmacol* **151**, 1224-1234.

Albert AP, Saleh SN, Peppiatt-Wildman CM, & Large WA (2007). Multiple activation mechanisms of store-operated TRPC channels in smooth muscle cells. *J Physiol* **583**, 25-36.

Alexander SPH, Mathie A, & Peters JA (2009). Guide to Receptors and Channels (GRAC), 4th edn. *Br J Pharmacol* **158**, S1-S254.

Alioua A, Mahajan A, Nishimaru K, Zarei MM, Stefani E, & Toro L (2002). Coupling of c-Src to large conductance voltage- and Ca^{2+}-activated K^+ channels as a new mechanism of agonist-induced vasoconstriction. *Proc Natl Acad Sci USA* **99**, 14560-14565.

Andreyev AY, Kushnareva YE, & Starkov AA (2005). Mitochondrial metabolism of reactive oxygen species. *Biochemistry (Mosc)* **70**, 200-214.

Aon MA, Cortassa S, Marbán E, & O'Rourke B (2003). Synchronized whole cell oscillations in mitochondrial metabolism triggered by a local release of reactive oxygen species in cardiac myocytes. *J Biol Chem* **278**, 44735-44744.

Archer S & Michelakis E (2002). The mechanism(s) of hypoxic pulmonary vasoconstriction: potassium channels, redox O_2 sensors, and controversies. *News Physiol Sci* **17**, 131-137.

Archer S & Rich S (2000). Primary pulmonary hypertension: a vascular biology and translational research "Work in progress". *Circulation* **102**, 2781-2791.

Archer SL, Gragasin FS, Wu X, Wang S, McMurtry S, Kim DH, Platonov M, Koshal A, Hashimoto K, Campbell WB, Falck JR, & Michelakis ED (2003). Endothelium-derived hyperpolarizing factor in human internal mammary artery is

11,12-epoxyeicosatrienoic acid and causes relaxation by activating smooth muscle BK_{Ca} channels. *Circulation* **107**, 769-776.

Archer SL, Huang J, Henry T, Peterson D, & Weir EK (1993). A redox-based O_2 sensor in rat pulmonary vasculature. *Circ Res* **73**, 1100-1112.

Archer SL, Huang JMC, Reeve HL, Hampl V, Tolarova S, Michelakis E, Weir EK, & Huang JM (1996). Differential distribution of electrophysiologically distinct myocytes in conduit and resistance arteries determines their response to nitric oxide and hypoxia. *Circ Res* **78**, 431-442.

Archer SL, London B, Hampl V, Wu X, Nsair A, Puttagunta L, Hashimoto K, Waite RE, & Michelakis ED (2001). Impairment of hypoxic pulmonary vasoconstriction in mice lacking the voltage-gated potassium channel Kv1.5. *FASEB J* **15**, 1801-1803.

Archer SL, Reeve HL, Michelakis E, Puttagunta L, Waite R, Nelson DP, Dinauer MC, & Weir EK (1999). O_2 sensing is preserved in mice lacking the gp91 phox subunit of NADPH oxidase. *Proc Natl Acad Sci USA* **96**, 7944-7949.

Archer SL, Souil E, Dinh-Xuan AT, Schremmer B, Mercure JV, El Yaagoubi A, Nguyen-Huu L, Reeve HL, & Hampl V (1998). Molecular identification of the role of voltage-gated K^+ channels, Kv1.5 and Kv2.1, in hypoxic pulmonary vasoconstriction and control of resting membrane potential in rat pulmonary artery myocytes. *J Clin Invest* **101**, 2319-2330.

Archer SL, Wu XC, Thébaud B, Nsair A, Bonnet S, Tyrrell B, McMurtry MS, Hashimoto K, Harry G, & Michelakis ED (2004). Preferential expression and function of voltage-gated, O_2-sensitive K^+ channels in resistance pulmonary arteries explains regional heterogeneity in hypoxic pulmonary vasoconstriction: ionic diversity in smooth muscle cells. *Circ Res* **95**, 308-318.

Armstrong CM & Loboda A (2001). A model for 4-aminopyridine action on K channels: similarities to tetraethylammonium ion action. *Biophys J* **81**, 895-904.

Asano M & Nomura Y (2002). Contribution of sarcoplasmic reticulum Ca^{2+} to the activation of Ca^{2+}-activated K^+ channels in the resting state of arteries from spontaneously hypertensive rats. *J Hypertens* **20**, 447-454.

Ayon R, Sones W, Forrest AS, Wiwchar M, Valencik ML, Sanguinetti AR, Perrino BA, Greenwood IA, & Leblanc N (2009). Complex phosphatase regulation of Ca2+-activated Cl- currents in pulmonary arterial smooth muscle cells. *J Biol Chem* **284**, 32507-32521.

Bae YM, Park MK, Lee SH, Ho WK, & Earm YE (1999). Contribution of Ca^{2+}-activated K^+ channels and non-selective cation channels to membrane potential of pulmonary arterial smooth muscle cells of the rabbit. *J Physiol* **514**, 747-758.

Bakhramov A, Evans AM, & Kozlowski RZ (1998). Differential effects of hypoxia on the intracellular Ca^{2+} concentration of myocytes isolated from different regions of the rat pulmonary arterial tree. *Exp Physiol* **83**, 337-347.

Baliga RS, Zhao L, Madhani M, Lopez-Torondel B, Visintin C, Selwood D, Wilkins MR, MacAllister RJ, & Hobbs AJ (2008). Synergy between natriuretic peptides and phosphodiesterase 5 inhibitors ameliorates pulmonary arterial hypertension. *Am J Respir Crit Care Med* **178**, 861-869.

Bardou M, Goirand F, Marchand S, Rouget C, Devillier P, Dumas JP, Morcillo EJ, Rochette L, & Dumas M (2001). Hypoxic vasoconstriction of rat main pulmonary artery: role of endogenous nitric oxide, potassium channels, and phosphodiesterase inhibition. *J Cardiovasc Pharmacol* **38**, 325-334.

Barhanin J, Lesage F, Guillemare E, Fink M, Lazdunski M, & Romey G (1996). K(V)LQT1 and lsK (minK) proteins associate to form the I(Ks) cardiac potassium current. *Nature* **384**, 78-80.

Bari F, Louis TM, & Busija DW (1998). Effects of ischemia on cerebral arteriolar dilation to arterial hypoxia in piglets. *Stroke* **29**, 222-227.

Barman SA, Zhu S, Han G, & White RE (2003). cAMP activates BK_{Ca} channels in pulmonary arterial smooth muscle via cGMP-dependent protein kinase. *Am J Physiol Lung Cell Mol Physiol* **284**, L1004-L1011.

Barman SA, Zhu S, & White RE (2004). Protein kinase C inhibits BK_{Ca} channel activity in pulmonary arterial smooth muscle. *Am J Physiol Lung Cell Mol Physiol* **286**, L149-L155.

Barman SA, Zhu S, & White RE (2005). Hypoxia modulates cyclic AMP activation of BkCa channels in rat pulmonary arterial smooth muscle. *Lung* **183**, 353-361.

Barritt GJ (1999). Receptor-activated Ca^{2+} inflow in animal cells: a variety of pathways tailored to meet different intracellular Ca^{2+} signalling requirements. *Biochem J* **337**, 153-169.

Batchelor TJ, Sadaba JR, Ishola A, Pacaud P, Munsch CM, & Beech DJ (2001). Rho-kinase inhibitors prevent agonist-induced vasospasm in human internal mammary artery. *Br J Pharmacol* **132**, 302-308.

Bauer AJ & Sanders KM (1985). Gradient in excitation-contraction coupling in canine gastric antral circular muscle. *J Physiol* **369**, 283-294.

Beech DJ & Bolton TB (1989). Two components of potassium current activated by depolarization of single smooth muscle cells from the rabbit portal vein. *J Physiol* **418**, 293-309.

Beech DJ, Zhang H, Nakao K, & Bolton TB (1993). Single channel and whole-cell K-currents evoked by levcromakalim in smooth muscle cells from the rabbit portal vein. *Br J Pharmacol* **110**, 583-590.

Bennie RE, Packer CS, Powell DR, Jin N, & Rhoades RA (1991). Biphasic contractile response of pulmonary artery to hypoxia. *Am J Physiol* **261**, L156-L163.

Bentzen BH, Schmitt N, Calloe K, Dalby BW, Grunnet M, & Olesen SP (2006). The acrylamide (S)-1 differentially affects Kv7 (KCNQ) potassium channels. *Neuropharmacology* **51**, 1068-1077.

Bergdahl A, Gomez MF, Wihlborg AK, Erlinge D, Eyjolfson A, Xu SZ, Beech DJ, Dreja K, & Hellstrand P (2005). Plasticity of TRPC expression in arterial smooth muscle: correlation with store-operated Ca2+ entry. *Am J Physiol Cell Physiol* **288**, C872-C880.

Berger MG, Vandier C, Bonnet P, Jackson WF, & Rusch NJ (1998). Intracellular acidosis differentially regulates K_V channels in coronary and pulmonary vascular muscle. *Am J Physiol* **275**, H1351-H1359.

Berne RM (1980). The role of adenosine in the regulation of coronary blood flow. *Circ Res* **47**, 807-813.

Biervert C, Schroeder BC, Kubisch C, Berkovic SF, Propping P, Jentsch TJ, & Steinlein OK (1998). A potassium channel mutation in neonatal human epilepsy. *Science* **279**, 403-406.

Biervert C & Steinlein OK (1999). Structural and mutational analysis of KCNQ2, the major gene locus for benign familial neonatal convulsions. *Hum Genet* **104**, 234-240.

Blatz AL & Magleby KL (1984). Ion conductance and selectivity of single calcium-activated potassium channels in cultured rat muscle. *J Gen Physiol* **84**, 1-23.

Boer C, van Nieuw Amerongen GP, Groeneveld AB, Scheffer GJ, de Lange JJ, Westerhof N, van H, V, & Sipkema P (2004). Smooth muscle F-actin disassembly and RhoA/Rho-kinase signaling during endotoxin-induced alterations in pulmonary arterial compliance. *Am J Physiol Lung Cell Mol Physiol* **287**, L649-L655.

Bolotina V, Gericke M, & Bregestovski P (1991). Kinetic differences between Ca^{2+}-dependent K^+ channels in smooth muscle cells isolated from normal and atherosclerotic human aorta. *Proc R Soc Lond ,B,Biol Sci* **244 (1309)**, 51-55.

Bolotina VM, Najibi S, Palacino JJ, Pagano PJ, & Cohen RA (1994). Nitric oxide directly activates calcium-dependent potassium channels in vascular smooth muscle. *Nature* **368**, 850-853.

Bolton TB (1979). Mechanisms of action of transmitters and other substances on smooth muscle. *Physiol Rev* **59**, 606-718.

Bonnet P, Argibay JA, & Garnier D (1989). Contractile responses to hypoxia of isolated rings from the left branch of rabbit pulmonary artery. *Fundam Clin Pharmacol* **3**, 115-126.

Bonnet P, Gebremedhin D, Rush NJ, & Harder DR (1991). Effects of hypoxia on a potassium channel in cat cerebral arterial muscle cells. *Z Kardiol* **80**, 25-27.

Bonnet S, Dubuis E, Vandier C, Martin S, Marthan R, & Savineau JP (2002). Reversal of chronic hypoxia-induced alterations in pulmonary artery smooth muscle electromechanical coupling upon air breathing. *Cardiovasc Res* **53**, 1019-1028.

Bonnet S, Hyvelin JM, Bonnet P, Marthan R, & Savineau JP (2001). Chronic hypoxia-induced spontaneous and rhythmic contractions in the rat main pulmonary artery. *Am J Physiol Lung Cell Mol Physiol* **281**, L183-L192.

Bonnet S, Michelakis ED, Porter CJ, Andrade-Navarro MA, Thébaud B, Bonnet S, Haromy A, Harry G, Moudgil R, McMurtry MS, Weir EK, & Archer SL (2006). An abnormal mitochondrial-hypoxia inducible factor-1α-Kv channel pathway disrupts oxygen sensing and triggers pulmonary arterial hypertension in fawn hooded rats: similarities to human pulmonary arterial hypertension. *Circulation* **113**, 2630-2641.

Bonnet S, Savineau JP, Barillot W, Dubuis E, Vandier C, & Bonnet P (2003). Role of Ca^{2+}-sensitive K^+ channels in the remission phase of pulmonary hypertension in chronic obstructive pulmonary diseases. *Cardiovasc Res* **60**, 326-336.

Bradford JR & Dean HP (1894). The Pulmonary Circulation. *J Physiol* **16**, 34-158.

Bradford MM (1976). A rapid and sensitive method for the quantitation of microgram quantities of protein utilizing the principle of protein-dye binding. *Anal Biochem* **72**, 248-254.

Brakemeier S, Eichler I, Knorr A, Fassheber T, Kohler R, & Hoyer J (2003). Modulation of Ca^{2+}-activated K^+ channel in renal artery endothelium in situ by nitric oxide and reactive oxygen species. *Kidney Int* **64**, 199-207.

Brayden JE (1996). Potassium channels in vascular smooth muscle. *Clin Exp Pharmacol Physiol* **23**, 1069-1076.

Brayden JE (2002). Functional roles of K_{ATP} channels in vascular smooth muscle. *Clin Exp Pharmacol Physiol* **29**, 312-316.

Brayden JE & Nelson MT (1992). Regulation of arterial tone by activation of calcium-dependent potassium channels. *Science* **256**, 532-535.

Brenner R, Peréz GJ, Bonev AD, Eckman DM, Kosek JC, Wiler SW, Patterson AJ, Nelson MT, & Aldrich RW (2000). Vasoregulation by the β_1 subunit of the calcium-activated potassium channel. *Nature* **407**, 870-876.

Brenner T & O'Shaughnessy KM (2008). Both TASK-3 and TREK-1 two-pore loop K channels are expressed in H295R cells and modulate their membrane potential and aldosterone secretion. *Am J Physiol Endocrinol Metab* **295**, E1480-E1486.

Brevnova EE, Platoshyn O, Zhang S, & Yuan JX (2004). Overexpression of human *KCNA5* increases $I_{K(V)}$ and enhances apoptosis. *Am J Physiol Cell Physiol* **287**, C715-C722.

Bright RT, Salvaterra CG, Rubin LJ, & Yuan X-J (1995). Inhibition of glycolysis by 2-DG increases $[Ca^{2+}]_i$ in pulmonary arterial smooth muscle cells. *Am J Physiol* **269**, L203-L208.

Britton FC, Ohya S, Horowitz B, & Greenwood IA (2002). Comparison of the properties of CLCA1 generated currents and I(Cl(Ca)) in murine portal vein smooth muscle cells. *J Physiol* **539**, 107-117.

Brown DA & Adams PR (1980). Muscarinic suppression of a novel voltage-sensitive K^+ current in a vertebrate neurone. *Nature* **283**, 673-676.

Bruce J, Taggart M, & Austin C (2004). Contractile responses of isolated rat mesenteric arteries to acute episodes of severe hypoxia and subsequent reoxygenation. *Microvasc Res* **68**, 303-312.

Brueggemann LI, Markun DR, Henderson KK, Cribbs LL, & Byron KL (2006). Pharmacological and electrophysiological characterization of store-operated currents and capacitative Ca^{2+} entry in vascular smooth muscle cells. *J Pharmacol Exp Ther* **317**, 488-499.

Brueggemann LI, Moran CJ, Barakat JA, Yeh JZ, Cribbs LL, & Byron KL (2007). Vasopressin stimulates action potential firing by protein kinase C-dependent inhibition of KCNQ5 in A7r5 rat aortic smooth muscle cells. *Am J Physiol Heart Circ Physiol* **292**, H1352-H1363.

Brusselmans K, Compernolle V, Tjwa M, Wiesener MS, Maxwell PH, Collen D, & Carmeliet P (2003). Heterozygous deficiency of hypoxia-inducible factor-2α protects mice against pulmonary hypertension and right ventricular dysfunction during prolonged hypoxia. *J Clin Invest* **111**, 1519-1527.

Buescher PC, Pearse DB, Pillai RP, Litt MC, Mitchell MC, & Sylvester JT (1991). Energy state and vasomotor tone in hypoxic pig lungs. *J Appl Physiol* **70**, 1874-1881.

Burg ED, Remillard CV, & Yuan JX (2006). K+ channels in apoptosis. *J Membr Biol* **209**, 3-20.

Burke MA, Mutharasan RK, & Ardehali H (2008). The sulfonylurea receptor, an atypical ATP-binding cassette protein, and its regulation of the KATP channel. *Circ Res* **102**, 164-176.

Buus NH, VanBavel E, & Mulvany MJ (1994). Differences in sensitivity of rat mesenteric small arteries to agonists when studied as ring preparations or as cannulated preparations. *Br J Pharmacol* **112**, 579-587.

Cachero TG, Morielli AD, & Peralta EG (1998). The small GTP-binding protein RhoA regulates a delayed rectifier potassium channel. *Cell* **93**, 1077-1085.

Calcraft PJ, Ruas M, Pan Z, Cheng X, Arredouani A, Hao X, Tang J, Rietdorf K, Teboul L, Chuang KT, Lin P, Xiao R, Wang C, Zhu Y, Lin Y, Wyatt CN, Parrington J, Ma J, Evans AM, Galione A, & Zhu MX (2009). NAADP mobilizes calcium from acidic organelles through two-pore channels. *Nature* **459**, 596-600.

Carl A, Kenyon JL, Uemura D, Fusetani N, & Sanders KM (1991). Regulation of Ca^{2+}-activated K^+ channels by protein kinase A and phosphatase inhibitors. *Am J Physiol* **261**, C387-C392.

Carter EP, Sato K, Morio Y, & McMurtry IF (2000). Inhibition of K_{Ca} channels restores blunted hypoxic pulmonary vasoconstriction in rats with cirrhosis. *Am J Physiol Lung Cell Mol Physiol* **279**, L903-L910.

Casimiro MC, Knollmann BC, Ebert SN, Vary JC, Jr., Greene AE, Franz MR, Grinberg A, Huang SP, & Pfeifer K (2001). Targeted disruption of the Kcnq1 gene produces a mouse model of Jervell and Lange-Nielsen Syndrome. *Proc Natl Acad Sci U S A* **98**, 2526-2531.

Casteels R, Kitamura K, Kuriyama H, & Suzuki H (1977). The membrane properties of the smooth muscle cells of the rabbit main pulmonary artery. *J Physiol* **271**, 41-61.

Chan CK, Mak JC, Man RY, & Vanhoutte PM (2009). Rho kinase inhibitors prevent endothelium-dependent contractions in the rat aorta. *J Pharmacol Exp Ther* **329**, 820-826.

Chandel NS & Schumacker PT (2000). Cellular oxygen sensing by mitochondria: old questions, new insight. *J Appl Physiol* **88**, 1880-1889.

Charlier C, Singh NA, Ryan SG, Lewis TB, Reus BE, Leach RJ, & Leppert M (1998). A pore mutation in a novel KQT-like potassium channel gene in an idiopathic epilepsy family. *Nat Genet* **18**, 53-55.

Chen Q, Vazquez EJ, Moghaddas S, Hoppel CL, & Lesnefsky EJ (2003). Production of reactive oxygen species by mitochondria: central role of complex III. *J Biol Chem* **278**, 36027-36031.

Cheong A, Dedman AM, & Beech DJ (2001). Expression and function of native potassium channel [$K_V\alpha 1$] subunits in terminal arterioles of rabbit. *J Physiol* **534**, 691-700.

Chipperfield AR & Harper AA (2000). Chloride in smooth muscle. *Prog Biophys Mol Biol* **74**, 175-221.

Chrissobolis S & Sobey CG (2001). Evidence that Rho-kinase activity contributes to cerebral vascular tone in vivo and is enhanced during chronic hypertension: comparison with protein kinase C. *Circ Res* **88**, 774-779.

Chrissobolis S & Sobey CG (2002). Inhibitory effects of protein kinase C on inwardly rectifying K^+- and ATP-sensitive K^+ channel-mediated responses of the basilar artery. *Stroke* **33**, 1692-1697.

Christensen KL & Mulvany MJ (2001). Location of resistance arteries. *J Vasc Res* **38**, 1-12.

Clapp LH (1995). Regulation of glibenclamide-sensitive K^+ current by nucleotide phosphates in isolated rabbit pulmonary myocytes. *Cardiovasc Res* **30**, 460-468.

Clapp LH & Gurney AM (1992). ATP-sensitive K^+ channels regulate resting potential of pulmonary arterial smooth muscle cells. *Am J Physiol* **262**, H916-H920.

Clapp LH & Tinker A (1998). Potassium channels in the vasculature. *Curr Opin Nephrol Hypertens* **7**, 91-98.

Clark JF (1994). The creatine kinase system in smooth muscle. *Mol Cell Biochem* **133-134**, 221-232.

Cogolludo A, Moreno L, Bosca L, Tamargo J, & Perez-Vizcaino F (2003). Thromboxane A_2-induced inhibition of voltage-gated K^+ channels and pulmonary vasoconstriction: role of protein kinase Cζ. *Circ Res* **93**, 656-663.

Cogolludo AL, Moral-Sanz J, van der SS, Frazziano G, van Cleef AN, Menendez C, Zoer B, Moreno E, Roman A, Perez-Vizcaino F, & Villamor E (2009). Maturation of O2 sensing and signaling in the chicken ductus arteriosus. *Am J Physiol Lung Cell Mol Physiol* **297**, L619-L630.

Conway MA, Nelson MT, & Brayden JE (1994). 2-Deoxyglucose-induced vasodilation and hyperpolarization in rat coronary artery are reversed by glibenclamide. *Am J Physiol* **266**, H1322-H1326.

Cooper EC & Jan LY (2003). M-channels: neurological diseases, neuromodulation, and drug development. *Arch Neurol* **60**, 496-500.

Coppock EA, Martens JR, & Tamkun MM (2001). Molecular basis of hypoxia-induced pulmonary vasoconstriction: role of voltage-gated K^+ channels. *Am J Physiol Lung Cell Mol Physiol* **281**, L1-L12.

Coppock EA & Tamkun MM (2001). Differential expression of K_V channel α- and β-subunits in the bovine pulmonary arterial circulation. *Am J Physiol Lung Cell Mol Physiol* **281**, L1350-L1360.

Cornfield DN, Reeve HL, Tolarova S, Weir EK, & Archer SL (1996). Oxygen causes fetal pulmonary vasodilation through activation of a calcium-dependent potassium channel. *Proc Natl Acad Sci USA* **93**, 8089-8094.

Cornfield DN, Stevens T, McMurtry IF, Abman SH, & Rodman DM (1994). Acute hypoxia causes membrane depolarization and calcium influx in fetal pulmonary artery smooth muscle cells. *Am J Physiol* **266**, L469-L475.

Cox DH & Aldrich RW (2000). Role of the β1 subunit in large-conductance Ca^{2+}-activated K^+ channel gating energetics. Mechanisms of enhanced Ca^{2+} sensitivity. *J Gen Physiol* **116**, 411-432.

Cox RH (2005). Molecular determinants of voltage-gated potassium currents in vascular smooth muscle. *Cell Biochem Biophys* **42**, 167-195.

Cox RH & Petrou S (1999). Ca^{2+} influx inhibits voltage-dependent and augments Ca^{2+}-dependent K^+ currents in arterial myocytes. *Am J Physiol* **277**, C51-C63.

Criddle DN, de Moura RS, Greenwood IA, & Large WA (1997). Inhibitory action of niflumic acid on noradrenaline- and 5-hydroxytryptamine-induced pressor responses in the isolated mesenteric vascular bed of the rat. *Br J Pharmacol* **120**, 813-818.

Cui Y, Tran S, Tinker A, & Clapp LH (2002). The molecular composition of K_{ATP} channels in human pulmonary artery smooth muscle cells and their modulation by growth. *Am J Respir Cell Mol Biol* **26**, 135-143.

Daut J, Maier-Rudolph W, von BN, Mehrke G, Gunther K, & Goedel-Meinen L (1990). Hypoxic dilation of coronary arteries is mediated by ATP-sensitive potassium channels. *Science* **247**, 1341-1344.

Davies AR & Kozlowski RZ (2001). Kv channel subunit expression in rat pulmonary arteries. *Lung* **179**, 147-161.

Dawson CA, Grimm DJ, & Linehan JH (1978). Influence of hypoxia on the longitudinal distribution of pulmonary vascular resistance. *J Appl Physiol* **44**, 493-498.

DeFarias FP, Carvalho MF, Lee SH, Kaczorowski GJ, & Suarez-Kurtz G (1996). Effects of the K^+ channel blockers paspalitrem-C and paxilline on mammalian smooth muscle. *Eur J Pharmacol* **314**, 123-128.

Delmas P & Brown DA (2005). Pathways modulating neural KCNQ/M (Kv7) potassium channels. *Nat Rev Neurosci* **6**, 850-862.

Di Lisa F, Blank PS, Colonna R, Gambassi G, Silverman HS, Stern MD, & Hansford RG (1995). Mitochondrial membrane potential in single living adult rat cardiac myocytes exposed to anoxia or metabolic inhibition. *J Physiol* **486**, 1-13.

Dietrich A, Mederos YS, Gollasch M, Gross V, Storch U, Dubrovska G, Obst M, Yildirim E, Salanova B, Kalwa H, Essin K, Pinkenburg O, Luft FC, Gudermann T, & Birnbaumer L (2005). Increased vascular smooth muscle contractility in TRPC6-/- mice. *Mol Cell Biol* **25**, 6980-6989.

Dimopoulos GJ, Semba S, Kitazawa K, Eto M, & Kitazawa T (2007). Ca^{2+}-dependent rapid Ca^{2+} sensitization of contraction in arterial smooth muscle. *Circ Res* **100**, 121-129.

Dipp M, Nye PC, & Evans AM (2001). Hypoxic release of calcium from the sarcoplasmic reticulum of pulmonary artery smooth muscle. *Am J Physiol Lung Cell Mol Physiol* **281**, L318-L325.

Doggrell SA, Wanstall JC, & Gambino A (1999). Functional effects of 4-aminopyridine (4-AP) on pulmonary and systemic vessels from normoxic control and hypoxic pulmonary hypertensive rats. *Naunyn Schmiedeberg's Arch Pharmacol* **360**, 317-323.

Doi S, Damron DS, Ogawa K, Tanaka S, Horibe M, & Murray PA (2000). K^+ channel inhibition, calcium signaling, and vasomotor tone in canine pulmonary artery smooth muscle. *Am J Physiol Lung Cell Mol Physiol* **279**, L242-L251.

Drummond RM & Tuft RA (1999). Release of Ca^{2+} from the sarcoplasmic reticulum increases mitochondrial [Ca^{2+}] in rat pulmonary artery smooth muscle cells. *J Physiol* **516**, 139-147.

Duchen MR (1999). Contributions of mitochondria to animal physiology: from homeostatic sensor to calcium signalling and cell death. *J Physiol* **516**, 1-17.

Duchen MR & Biscoe TJ (1992). Relative mitochondrial membrane potential and $[Ca^{2+}]_i$ in type I cells isolated from the rabbit carotid body. *J Physiol* **450**, 33-61.

Dumas JP, Bardou M, Goirand F, & Dumas M (1999). Hypoxic pulmonary vasoconstriction. *Gen Pharmacol* **33**, 289-297.

Duprat F, Lesage F, Fink M, Reyes R, Heurteaux C, & Lazdunski M (1997). TASK, a human background K^+ channel to sense external pH variations near physiological pH. *EMBO J* **16**, 5464-5471.

Earl RA, Zaczek R, Teleha CA, Fisher BN, Maciag CM, Marynowski ME, Logue AR, Tam SW, Tinker WJ, Huang SM, & Chorvat RJ (1998). 2-Fluoro-4-pyridinylmethyl analogues of linopirdine as orally active acetylcholine release-enhancing agents with good efficacy and duration of action. *J Med Chem* **41**, 4615-4622.

Edwards DH & Griffith TM (1997). Entrained ion transport systems generate the membrane component of chaotic agonist-induced vasomotion. *Am J Physiol* **273**, H909-H920.

Edwards G, Ibbotson T, & Weston AH (1993). Levcromakalim may induce a voltage-independent K-current in rat portal veins by modifying the gating properties of the delayed rectifier. *Br J Pharmacol* **110**, 1037-1048.

Eisner DA, Nichols CG, O'Neill SC, Smith GL, & Valdeolmillos M (1989). The effects of metabolic inhibition on intracellular calcium and pH in isolated rat ventricular cells. *J Physiol* **411**, 393-418.

El-Awady MSH, Smirnov SV, & Watson ML (2008). Desensitization of the soluble guanylyl cyclase/cGMP pathway by lipopolysaccharide in rat isolated pulmonary artery but not aorta. *Br J Pharmacol* **155**, 1164-1173.

Elble RC, Ji G, Nehrke K, DeBiasio J, Kingsley PD, Kotlikoff MI, & Pauli BU (2002). Molecular and functional characterization of a murine calcium-activated chloride channel expressed in smooth muscle. *J Biol Chem* **277**, 18586-18591.

Elliott DA, Ong BY, Bruni JE, & Bose D (1989). Role of endothelium in hypoxic contraction of canine basilar artery. *Br J Pharmacol* **96**, 949-955.

Emile LB (2003). Arteries and Veins. In *Medical Physiology*, eds. Walter FB & Emile LB, pp. 447-482. Saunders, Philadelphia.

England SK, Wooldridge TA, Stekiel WJ, & Rusch NJ (1993). Enhanced single-channel K^+ current in arterial membranes from genetically hypertensive rats. *Am J Physiol* **264**, H1337-H1345.

Eroschenko VP (2005)., 10th ed., pp. 107-119. Lippincott Williams & Wilkins, Philadelphia.

Evans AM (2006a). AMP-activated protein kinase and the regulation of Ca^{2+} signalling in O_2-sensing cells. *J Physiol* **574**, 113-123.

Evans AM (2006b). AMP-activated protein kinase underpins hypoxic pulmonary vasoconstriction and carotid body excitation by hypoxia in mammals. *Exp Physiol* **91**, 821-827.

Evans AM, Cobban HJ, & Nixon GF (1999). ET_A receptors are the primary mediators of myofilament calcium sensitization induced by ET-1 in rat pulmonary artery smooth muscle: a tyrosine kinase independent pathway. *Br J Pharmacol* **127**, 153-160.

Evans AM, Hardie DG, Galione A, Peers C, Kumar P, & Wyatt CN (2006). AMP-activated protein kinase couples mitochondrial inhibition by hypoxia to cell-specific Ca2+ signalling mechanisms in oxygen-sensing cells. *Novartis Found Symp* **272**, 234-252.

Evans AM, Mustard KJ, Wyatt CN, Peers C, Dipp M, Kumar P, Kinnear NP, & Hardie DG (2005). Does AMP-activated protein kinase couple inhibition of mitochondrial oxidative phosphorylation by hypoxia to calcium signaling in O_2-sensing cells? *J Biol Chem* **280**, 41504-41511.

Evans AM, Osipenko ON, & Gurney AM (1996). Properties of a novel K^+ current that is active at resting potential in rabbit pulmonary artery smooth muscle cells. *J Physiol* **496**, 407-420.

Fagan KA, Oka M, Bauer NR, Gebb SA, Ivy DD, Morris KG, & McMurtry IF (2004). Attenuation of acute hypoxic pulmonary vasoconstriction and hypoxic pulmonary hypertension in mice by inhibition of Rho-kinase. *Am J Physiol Lung Cell Mol Physiol* **287**, L656-L664.

Fagan KA, Tyler RC, Sato K, Fouty BW, Morris KG, Jr., Huang PL, McMurtry IF, & Rodman DM (1999). Relative contributions of endothelial, inducible, and neuronal NOS to tone in the murine pulmonary circulation. *Am J Physiol* **277**, L472-L478.

Feng J, Ito M, Ichikawa K, Isaka N, Nishikawa M, Hartshorne DJ, & Nakano T (1999). Inhibitory phosphorylation site for Rho-associated kinase on smooth muscle myosin phosphatase. *J Biol Chem* **274**, 37385-37390.

Fike CD & Kaplowitz MR (1994). Developmental differences in vascular responses to hypoxia in lungs of rabbits. *J Appl Physiol* **77**, 507-516.

Firth AL, Gordienko DV, Yuill KH, & Smirnov SV (2009a). Cellular localization of mitochondria contributes to Kv channel mediated regulation of cellular excitability in the pulmonary, but not mesenteric circulation. *Am J Physiol Lung Cell Mol Physiol* **296**, L347-L360.

Firth AL, Platoshyn O, Brevnova EE, Burg ED, Powell F, Haddad GH, & Yuan JX (2009b). Hypoxia selectively inhibits KCNA5 channels in pulmonary artery smooth muscle cells. *Ann N Y Acad Sci* **1177**, 101-111.

Firth AL, Remillard CV, & Yuan JX (2007). TRP channels in hypertension. *Biochim Biophys Acta* **1772**, 895-906.

Firth AL, Yuill KH, & Smirnov SV (2008). Mitochondria dependent regulation of Kv currents in rat pulmonary artery smooth muscle cells. *Am J Physiol Lung Cell Mol Physiol* **295**, L61-L70.

Forrest AS, Angermann JE, Raghunathan R, Lachendro C, Greenwood IA, & Leblanc N (2010). Intricate interaction between store-operated calcium entry and calcium-activated chloride channels in pulmonary artery smooth muscle cells. *Adv Exp Med Biol* **661**, 31-55.

Fountain SJ, Cheong A, Flemming R, Mair L, Sivaprasadarao A, & Beech DJ (2004). Functional up-regulation of KCNA gene family expression in murine mesenteric resistance artery smooth muscle. *J Physiol* **556**, 29-42.

Freitas MR, Eto M, Kirkbride JA, Schott C, Sassard J, & Stoclet JC (2009). Y27632, a Rho-activated kinase inhibitor, normalizes dysregulation in alpha1-adrenergic receptor-induced contraction of Lyon hypertensive rat artery smooth muscle. *Fundam Clin Pharmacol* **23**, 169-178.

Frings S, Reuter D, & Kleene SJ (2000). Neuronal Ca2+ -activated Cl- channels--homing in on an elusive channel species. *Prog Neurobiol* **60**, 247-289.

Fu X, Gong MC, Jia T, Somlyo AV, & Somlyo AP (1998). The effects of the Rho-kinase inhibitor Y-27632 on arachidonic acid-, GTPγS-, and phorbol ester-induced Ca^{2+}-sensitization of smooth muscle. *FEBS Lett* **440**, 183-187.

Fukumoto GH, Lamp ST, Motter C, Bridge JH, Garfinkel A, & Goldhaber JI (2005). Metabolic inhibition alters subcellular calcium release patterns in rat ventricular myocytes: implications for defective excitation-contraction coupling during cardiac ischemia and failure. *Circ Res* **96**, 551-557.

Gao YD & Garcia ML (2003). Interaction of agitoxin2, charybdotoxin, and iberiotoxin with potassium channels: selectivity between voltage-gated and Maxi-K channels. *Proteins* **52**, 146-154.

Gardener MJ, Johnson IT, Burnham MP, Edwards G, Heagerty AM, & Weston AH (2004). Functional evidence of a role for two-pore domain potassium channels in rat mesenteric and pulmonary arteries. *Br J Pharmacol* **142**, 192-202.

Gardiner SM, Kemp PA, March JE, Fallgren B, & Bennett T (1996). Effects of glibenclamide on the regional haemodynamic actions of alpha-trinositol and its influence on responses to vasodilators in conscious rats. *Br J Pharmacol* **117**, 507-515.

Garland JG & McPherson GA (1992). Evidence that nitric oxide does not mediate the hyperpolarization and relaxation to acetylcholine in the rat small mesenteric artery. *Br J Pharmacol* **105**, 429-435.

Garlid KD & Paucek P (2003). Mitochondrial potassium transport: the K^+ cycle. *Biochim Biophys Acta* **1606**, 23-41.

Gasser R, Klein W, & Kickenweiz E (1993). Vasodilative response to hypoxia and simulated ischemia is mediated by ATP-sensitive K^+ channels in guinea pig thoracic aorta. *Angiology* **44**, 228-243.

Gayen JR, Zhang K, RamachandraRao SP, Mahata M, Chen Y, Kim HS, Naviaux RK, Sharma K, Mahata SK, & O'connor DT (2010). Role of reactive oxygen species in hyperadrenergic hypertension: biochemical, physiological, and pharmacological evidence from targeted ablation of the chromogranin a (Chga) gene. *Circ Cardiovasc Genet* **3**, 414-425.

Gebremedhin D, Kaldunski M, Jacobs ER, Harder DR, & Roman RJ (1996). Coexistence of two types of Ca^{2+}-activated K^+ channels in rat renal arterioles. *Am J Physiol* **270**, F69-F81.

Gelband CH & Hume JR (1992). Ionic currents in single smooth muscle cells of the canine renal artery. *Circ Res* **71**, 745-758.

German WJ & Stanfield CL (2005). *Principles of Human Physiology*, 2nd ed., pp. 541-577. Pearson Benjamin Cummings, San Francisco.

Giangiacomo KM, Garcia ML, & McManus OB (1992). Mechanism of iberiotoxin block of the large-conductance calcium-activated potassium channel from bovine aortic smooth muscle. *Biochemistry* **31**, 6719-6727.

Gibor G, Yakubovich D, Peretz A, & Attali B (2004). External barium affects the gating of KCNQ1 potassium channels and produces a pore block via two discrete sites. *J Gen Physiol* **124**, 83-102.

Glavind-Kristensen M, Matchkov V, Hansen VB, Forman A, Nilsson H, & Aalkjaer C (2004). KATP-channel-induced vasodilation is modulated by the Na,K-pump activity in rabbit coronary small arteries. *Br J Pharmacol* **143**, 872-880.

Gobet I, Lippai M, Tomkowiak M, Durocher Y, Leclerc C, Moreau M, & Guerrier P (1995). 4-aminopyridine acts as a weak base and a Ca^{2+} mobilizing agent in triggering oocyte meiosis reinitiation and activation in the Japanese clam *Ruditapes philippinarum*. *Int J Dev Biol* **39**, 485-491.

Goldstein SA, Bayliss DA, Kim D, Lesage F, Plant LD, & Rajan S (2005). International Union of Pharmacology. LV. Nomenclature and molecular relationships of two-P potassium channels. *Pharmacol Rev* **57**, 527-540.

Gollasch M, Ried C, Bychkov R, Luft FC, & Haller H (1996). K^+ currents in human coronary artery vascular smooth muscle cells. *Circ Res* **78**, 676-688.

Gomez-Viquez L, Guerrero-Serna G, Garcia U, & Guerrero-Hernandez A (2003). SERCA pump optimizes Ca2+ release by a mechanism independent of store filling in smooth muscle cells. *Biophys J* **85**, 370-380.

Gonczi M, Szentandrassy N, Johnson IT, Heagerty AM, & Weston AH (2006). Investigation of the role of TASK-2 channels in rat pulmonary arteries; pharmacological and functional studies following RNA interference procedures. *Br J Pharmacol* **147**, 496-505.

Gonzalez JM, Jost LJ, Rouse D, & Suki WN (1996). Plasma membrane and sarcoplasmic reticulum Ca-ATPase and smooth muscle. *Miner Electrolyte Metab* **22**, 345-348.

Gordienko DV, Greenwood IA, & Bolton TB (2001). Direct visualization of sarcoplasmic reticulum regions discharging Ca^{2+}sparks in vascular myocytes. *Cell Calcium* **29**, 13-28.

Greenwood IA, Helliwell RM, & Large WA (1997). Modulation of Ca^{2+}-activated Cl^- currents in rabbit portal vein smooth muscle by an inhibitor of mitochondrial Ca^{2+} uptake. *J Physiol* **505**, 53-64.

Greenwood IA & Leblanc N (2007). Overlapping pharmacology of Ca^{2+}-activated Cl^- and K^+ channels. *Trends Pharmacol Sci* **28**, 1-5.

Greenwood IA, Leblanc N, Gordienko DV, & Large WA (2002). Modulation of $I_{Cl(Ca)}$ in vascular smooth muscle cells by oxidizing and cysteine-reactive reagents. *Pflügers Arch* **443**, 473-482.

Greenwood IA & Ohya S (2009). New tricks for old dogs: KCNQ expression and role in smooth muscle. *Br J Pharmacol* **156**, 1196-1203.

Greyner H & Dzialowski EM (2008). Mechanisms mediating the oxygen-induced vasoreactivity of the ductus arteriosus in the chicken embryo. *Am J Physiol Regul Integr Comp Physiol* **295**, R1647-R1659.

Griffith TM & Edwards DH (1993). Modulation of chaotic pressure oscillations in isolated resistance arteries by EDRF. *Eur Heart J* **14 Suppl I**, 60-67.

Grissmer S, Nguyen AN, Aiyar J, Hanson DC, Mather RJ, Gutman GA, Auperin DD, & Chandy KG (1994). Pharmacological characterization of five cloned voltage-gated K^+ channels, types Kv1.1, 1.2, 1.3, 1.5, and 3.1, stably expressed in mammalian cell lines. *Mol Pharmacol* **45**, 1227-1234.

Guibert C, Ducret T, & Savineau JP (2008). Voltage-independent calcium influx in smooth muscle. *Prog Biophys Mol Biol* **98**, 10-23.

Guibert C, Flemming R, & Beech DJ (2002). Prevention of a hypoxic $Ca^{2+}{}_i$ response by SERCA inhibitors in cerebral arterioles. *Br J Pharmacol* **135**, 927-934.

Gulbis JM, Mann S, & MacKinnon R (1999). Structure of a voltage-dependent K^+ channel β subunit. *Cell* **97**, 943-952.

Gulbis JM, Zhou M, Mann S, & MacKinnon R (2000). Structure of the cytoplasmic β subunit - T1 assembly of voltage-dependent K^+ channels. *Science* **289**, 123-127.

Gupte RS, Rawat DK, Chettimada S, Cioffi DL, Wolin MS, Gerthoffer WT, McMurtry IF, & Gupte SA (2010). Activation of glucose-6-phosphate dehydrogenase promotes acute hypoxic pulmonary artery contraction. *J Biol Chem* **285**, 19561-19571.

Gurney A & Manoury B (2009). Two-pore potassium channels in the cardiovascular system. *Eur Biophys J* **38**, 305-318.

Gurney AM (2002). Multiple sites of oxygen sensing and their contributions to hypoxic pulmonary vasoconstriction. *Respir Physiol Neurobiol* **132**, 43-53.

Gurney AM & Joshi S (2006). The role of twin pore domain and other K+ channels in hypoxic pulmonary vasoconstriction. *Novartis Found Symp* **272**, 218-228.

Gurney AM, Joshi S, & Manoury B (2010). KCNQ potassium channels: new targets for pulmonary vasodilator drugs? *Adv Exp Med Biol* **661**, 405-417.

Gurney AM, Osipenko ON, MacMillan D, & Kempsill FE (2002). Potassium channels underlying the resting potential of pulmonary artery smooth muscle cells. *Clin Exp Pharmacol Physiol* **29**, 330-333.

Gurney AM, Osipenko ON, MacMillan D, McFarlane KM, Tate RJ, & Kempsill FE (2003). Two-pore domain K channel, TASK-1, in pulmonary artery smooth muscle cells. *Circ Res* **93**, 957-964.

Guse AH, Roth E, & Emmrich F (1994). Ca^{2+} release and Ca^{2+} entry induced by rapid cytosolic alkalinization in Jurkat T-lymphocytes. *Biochem J* **301**, 83-88.

Gustafsson H, Bulow A, & Nilsson H (1994). Rhythmic contractions of isolated, pressurized small arteries from rat. *Acta Physiol Scand* **152**, 145-152.

Gustafsson H, Mulvany MJ, & Nilsson H (1993). Rhythmic contractions of isolated small arteries from rat: influence of the endothelium. *Acta Physiol Scand* **148**, 153-163.

Gutman GA, Chandy KG, Grissmer S, Lazdunski M, McKinnon D, Pardo LA, Robertson GA, Rudy B, Sanguinetti MC, Stühmer W, & Wang X (2005).

International Union of Pharmacology. LIII. Nomenclature and molecular relationships of voltage-gated potassium channels. *Pharmacol Rev* **57**, 473-508.

Han W, Tang X, Wu H, Liu Y, & Zhu D (2007). Role of ERK1/2 signaling pathways in 4-aminopyridine-induced rat pulmonary vasoconstriction. *Eur J Pharmacol* **569**, 138-144.

Hart PJ, Overturf KE, Russell SN, Carl A, Hume JR, & Sanders KM (1993). Cloning and expression of a $K_v1.2$ class delayed rectifier K^+ channel from canine colonic smooth muscle. *Proc Natl Acad Sci USA* **90**, 9659-9663.

Hartshorne DJ (1998). Myosin phosphatase: subunits and interactions. *Acta Physiol Scand* **164**, 483-493.

Hartzell C, Putzier I, & Arreola J (2005). Calcium-activated chloride channels. *Annu Rev Physiol* **67**, 719-758.

Hartzell HC, Yu K, Xiao Q, Chien LT, & Qu Z (2009). Anoctamin/TMEM16 family members are Ca2+-activated Cl- channels. *J Physiol* **587**, 2127-2139.

Hasunuma K, Rodman DM, & McMurtry IF (1991). Effects of K^+ channel blockers on vascular tone in the perfused rat lung. *Am Rev Respir Dis* **144**, 884-887.

Heizmann CW (1992). Calcium-binding proteins: basic concepts and clinical implications. *Gen Physiol Biophys* **11**, 411-425.

Herget J, Suggett AJ, Leach E, & Barer GR (1978). Resolution of pulmonary hypertension and other features induced by chronic hypoxia in rats during complete and intermittent normoxia. *Thorax* **33**, 468-473.

Herrera GM & Walker BR (1998). Involvement of L-type calcium channels in hypoxic relaxation of vascular smooth muscle. *J Vasc Res* **35**, 265-273.

Hester RL & Hammer LW (2002). Venular-arteriolar communication in the regulation of blood flow. *Am J Physiol Regul Integr Comp Physiol* **282**, R1280-R1285.

Hilgers RH, Todd J, Jr., & Webb RC (2007). Increased PDZ-RhoGEF/RhoA/Rho kinase signaling in small mesenteric arteries of angiotensin II-induced hypertensive rats. *J Hypertens* **25**, 1687-1697.

Hilgers RH & Webb RC (2005). Molecular aspects of arterial smooth muscle contraction: focus on Rho. *Exp Biol Med (Maywood)* **230**, 829-835.

Hillier SC, Graham JA, Hanger CC, Godbey PS, Glenny RW, & Wagner WW, Jr. (1997). Hypoxic vasoconstriction in pulmonary arterioles and venules. *J Appl Physiol* **82**, 1084-1090.

Himpens B, De Smedt H, & Casteels R (1992). Kinetics of nucleocytoplasmic Ca^{2+} transients in DDT1 MF-2 smooth muscle cells. *Am J Physiol* **263**, C978-C985.

Hirano K (2007). Current topics in the regulatory mechanism underlying the Ca2+ sensitization of the contractile apparatus in vascular smooth muscle. *J Pharmacol Sci* **104**, 109-115.

Hislop A & Reid L (1978). Normal structure and dimensions of the pulmonary arteries in the rat. *J Anat* **125**, 71-83.

Hogg DS, Davies AR, McMurray G, & Kozlowski RZ (2002). $K_V2.1$ channels mediate hypoxic inhibition of I_{KV} in native pulmonary arterial smooth muscle cells of the rat. *Cardiovasc Res* **55**, 349-360.

Holden WE & McCall E (1984). Hypoxia-induced contractions of porcine pulmonary artery strips depend on intact endothelium. *Exp Lung Res* **7**, 101-112.

Hong KW, Pyo KM, Lee WS, Yu SS, & Rhim BY (1994). Pharmacological evidence that calcitonin gene-related peptide is implicated in cerebral autoregulation. *Am J Physiol* **266**, H11-H16.

Hong Z, Weir EK, Nelson DP, & Olschewski A (2004). Subacute hypoxia decreases voltage-activated potassium channel expression and function in pulmonary artery myocytes. *Am J Respir Cell Mol Biol* **31**, 337-343.

Horowitz A, Menice CB, Laporte R, & Morgan KG (1996). Mechanisms of smooth muscle contraction. *Physiol Rev* **76**, 967-1003.

Hoth M & Penner R (1992). Depletion of intracellular calcium stores activates a calcium current in mast cells. *Nature* **355**, 353-356.

Hughes AD & Schachter M (1994). Multiple pathways for entry of calcium and other divalent cations in a vascular smooth muscle cell line (A7r5). *Cell Calcium* **15**, 317-330.

Hugnot JP, Salinas M, Lesage F, Guillemare E, de Weille J, Heurteaux C, Mattei MG, & Lazdunski M (1996). Kv8.1, a new neuronal potassium channel subunit with specific inhibitory properties towards Shab and Shaw channels. *EMBO J* **15**, 3322-3331.

Hulme JT, Coppock EA, Felipe A, Martens JR, & Tamkun MM (1999). Oxygen sensitivity of cloned voltage-gated K^+ channels expressed in the pulmonary vasculature. *Circ Res* **85**, 489-497.

Hunte C, Palsdottir H, & Trumpower BL (2003). Protonmotive pathways and mechanisms in the cytochrome bc_1 complex. *FEBS Lett* **545**, 39-46.

Hyvelin JM, Guibert C, Marthan R, & Savineau JP (1998). Cellular mechanisms and role of endothelin-1-induced calcium oscillations in pulmonary arterial myocytes. *Am J Physiol* **275**, L269-L282.

Inoue K, Nakada K, Ogura A, Isobe K, Goto Y, Nonaka I, & Hayashi JI (2000). Generation of mice with mitochondrial dysfunction by introducing mouse mtDNA carrying a deletion into zygotes. *Nat Genet* **26**, 176-181.

Inoue R, Jensen LJ, Shi J, Morita H, Nishida M, Honda A, & Ito Y (2006). Transient receptor potential channels in cardiovascular function and disease. *Circ Res* **99**, 119-131.

Ishida Y & Honda H (1992). Underlying mechanisms for hypoxia-induced relaxation of the guinea-pig isolated aorta. *Jpn J Pharmacol* **58 Suppl 2**, 307P.

Ishida Y & Honda H (1993). Inhibitory action of 4-aminopyridine on Ca(2+)-ATPase of the mammalian sarcoplasmic reticulum. *J Biol Chem* **268**, 4021-4024.

Ishikawa T, Hume JR, & Keef KD (1993). Modulation of K+ and Ca2+ channels by histamine H1-receptor stimulation in rabbit coronary artery cells. *J Physiol* **468**, 379-400.

Ishizaka H & Kuo L (1996). Acidosis-induced coronary arteriolar dilation is mediated by ATP-sensitive potassium channels in vascular smooth muscle. *Circ Res* **78**, 50-57.

Isomoto S, Kondo C, Yamada M, Matsumoto S, Higashiguchi O, Horio Y, Matsuzawa Y, & Kurachi Y (1996). A novel sulfonylurea receptor forms with BIR (Kir6.2) a smooth muscle type ATP-sensitive K+ channel. *J Biol Chem* **271**, 24321-24324.

Ito M, Nakano T, Erdodi F, & Hartshorne DJ (2004). Myosin phosphatase: structure, regulation and function. *Mol Cell Biochem* **259**, 197-209.

Jabr RI, Toland H, Gelband CH, Wang XX, & Hume JR (1997). Prominent role of intracellular Ca^{2+} release in hypoxic vasoconstriction of canine pulmonary artery. *Br J Pharmacol* **122**, 21-30.

Jackson WF (1993). Arteriolar tone is determined by activity of ATP-sensitive potassium channels. *Am J Physiol* **265**, H1797-H1803.

Jackson WF (2000a). Hypoxia does not activate ATP-sensitive K^+ channels in arteriolar muscle cells. *Microcirculation* **7**, 137-145.

Jackson WF (2000b). Ion channels and vascular tone. *Hypertension* **35**, 173-178.

Janssen LJ, Lu-Chao H, & Netherton S (2001). Excitation-contraction coupling in pulmonary vascular smooth muscle involves tyrosine kinase and Rho kinase. *Am J Physiol Lung Cell Mol Physiol* **280**, L666-L674.

Jentsch TJ (2000). Neuronal KCNQ potassium channels: physiology and role in disease. *Nat Rev Neurosci* **1**, 21-30.

Jepps TA, Greenwood IA, Moffatt JD, Sanders KM, & Ohya S (2009). Molecular and functional characterization of Kv7 K+ channel in murine gastrointestinal smooth muscles. *Am J Physiol Gastrointest Liver Physiol* **297**, G107-G115.

JERVELL A & LANGE-NIELSEN F (1957). Congenital deaf-mutism, functional heart disease with prolongation of the Q-T interval and sudden death. *Am Heart J* **54**, 59-68.

Jiang Y, Ruta V, Chen J, Lee A, & MacKinnon R (2003). The principle of gating charge movement in a voltage-dependent K^+ channel. *Nature* **423**, 42-48.

Jin L, Ying Z, Hilgers RH, Yin J, Zhao X, Imig JD, & Webb RC (2006). Increased RhoA/Rho-kinase signaling mediates spontaneous tone in aorta from angiotensin II-induced hypertensive rats. *J Pharmacol Exp Ther* **318**, 288-295.

Jin N, Packer CS, & Rhoades RA (1992). Pulmonary arterial hypoxic contraction: signal transduction. *Am J Physiol* **263**, L73-L78.

Joshi S, Balan P, & Gurney AM (2006). Pulmonary vasoconstrictor action of KCNQ potassium channel blockers. *Respir Res* **7**, 31.

Joshi S, Sedivy V, Hodyc D, Herget J, & Gurney AM (2009). KCNQ modulators reveal a key role for KCNQ potassium channels in regulating the tone of rat pulmonary artery smooth muscle. *J Pharmacol Exp Ther* **329**, 368-376.

Juhaszova M, Shimizu H, Borin ML, Yip RK, Santiago EM, Lindenmayer GE, & Blaustein MP (1996). Localization of the Na^+-Ca^{2+} exchanger in vascular smooth muscle, and in neurons and astrocytes. *Ann N Y Acad Sci* **779**, 318-335.

Kajimoto H, Hashimoto K, Bonnet SN, Haromy A, Harry G, Moudgil R, Nakanishi T, Rebeyka I, Thebaud B, Michelakis ED, & Archer SL (2007). Oxygen activates the Rho/Rho-kinase pathway and induces RhoB and ROCK-1 expression in human and rabbit ductus arteriosus by increasing mitochondria-derived reactive oxygen species: a newly recognized mechanism for sustaining ductal constriction. *Circulation* **115**, 1777-1788.

Kamishima T, Davies NW, & Standen NB (2000). Mechanisms that regulate $[Ca^{2+}]_i$ following depolarization in rat systemic arterial smooth muscle cells. *J Physiol* **522**, 285-295.

Kamishima T & Quayle JM (2002). Mitochondrial Ca^{2+} uptake is important over low $[Ca^{2+}]_i$ range in arterial smooth muscle. *Am J Physiol Heart Circ Physiol* **283**, H2431-H2439.

Kamm KE & Stull JT (2001). Dedicated myosin light chain kinases with diverse cellular functions. *J Biol Chem* **276**, 4527-4530.

Kanatsuka H, Sekiguchi N, Sato K, Akai K, Wang Y, Komaru T, Ashikawa K, & Takishima T (1992). Microvascular sites and mechanisms responsible for reactive hyperemia in the coronary circulation of the beating canine heart. *Circ Res* **71**, 912-922.

Kang TM, Park MK, & Uhm DY (2002). Characterization of hypoxia-induced $[Ca^{2+}]_i$ rise in rabbit pulmonary arterial smooth muscle cells. *Life Sci* **70**, 2321-2333.

Kang TM, Park MK, & Uhm DY (2003). Effects of hypoxia and mitochondrial inhibition on the capacitative calcium entry in rabbit pulmonary arterial smooth muscle cells. *Life Sci* **72**, 1467-1479.

Karaki H, Ozaki H, Hori M, Mitsui-Saito M, Amano K, Harada K, Miyamoto S, Nakazawa H, Won KJ, & Sato K (1997). Calcium movements, distribution, and functions in smooth muscle. *Pharmacol Rev* **49**, 157-230.

Karamsetty MR, Wadsworth RM, & Kane KA (1998). Effect of K^+ channel blocking drugs and nitric oxide synthase inhibition on the response to hypoxia in rat pulmonary artery rings. *J Auton Pharmacol* **18**, 49-56.

Kato M & Staub NC (1966). Response of small pulmonary arteries to unilobar hypoxia and hypercapnia. *Circ Res* **19**, 426-440.

Kelland NF, Bagnall AJ, Morecroft I, Gulliver-Sloan FH, Dempsie Y, Nilsen M, Yanagisawa M, MacLean MR, Kotelevtsev YV, & Webb DJ (2010). Endothelial ET(B) limits vascular remodelling and development of pulmonary hypertension during hypoxia. *J Vasc Res* **47**, 16-22.

Kharkovets T, Hardelin JP, Safieddine S, Schweizer M, El-Amraoui A, Petit C, & Jentsch TJ (2000). KCNQ4, a K+ channel mutated in a form of dominant deafness, is expressed in the inner ear and the central auditory pathway. *Proc Natl Acad Sci U S A* **97**, 4333-4338.

Kim D, Fujita A, Horio Y, & Kurachi Y (1998). Cloning and functional expression of a novel cardiac two-pore background K^+ channel (cTBAK-1). *Circ Res* **82**, 513-518.

Kinnear NP, Wyatt CN, Clark JH, Calcraft PJ, Fleischer S, Jeyakumar LH, Nixon GF, & Evans AM (2008). Lysosomes co-localize with ryanodine receptor subtype 3 to form a trigger zone for calcium signalling by NAADP in rat pulmonary arterial smooth muscle. *Cell Calcium* **44**, 190-201.

Kinoshita H & Katusic ZS (1997). Role of potassium channels in relaxations of isolated canine basilar arteries to acidosis. *Stroke* **28**, 433-437.

Kirber MT, Guerrero-Hernández A, Bowman DS, Fogarty KE, Tuft RA, Singer JJ, & Fay FS (2000). Multiple pathways responsible for the stretch-induced increase in Ca^{2+} concentration in toad stomach smooth muscle cells. *J Physiol* **524**, 3-17.

Kirber MT, Ordway RW, Clapp LH, Walsh JV, Jr., & Singer JJ (1992). Both membrane stretch and fatty acids directly activate large conductance Ca^{2+}-activated K^+ channels in vascular smooth muscle cells. *FEBS Lett* **297**, 24-28.

Kirkup AJ, Edwards G, & Weston AH (1996). Investigation of the effects of 5-nitro-2-(3-phenylpropylamino)-benzoic acid (NPPB) on membrane currents in rat portal vein. *Br J Pharmacol* **117**, 175-183.

Kitamura K & Yamazaki J (2001). Chloride channels and their functional roles in smooth muscle tone in the vasculature. *Jpn J Pharmacol* **85**, 351-357.

Kitazawa T, Kobayashi S, Horiuti K, Somlyo AV, & Somlyo AP (1989). Receptor-coupled, permeabilized smooth muscle. Role of the phosphatidylinositol cascade, G-proteins, and modulation of the contractile response to Ca^{2+}. *J Biol Chem* **264**, 5339-5342.

Kitazono T, Ago T, Kamouchi M, Santa N, Ooboshi H, Fujishima M, & Ibayashi S (2002). Increased activity of calcium channels and Rho-associated kinase in the basilar artery during chronic hypertension in vivo. *J Hypertens* **20**, 879-884.

Kiyoshi A, Ishikawa T, Hayashi K, Iwatsuki Y, Ishii K, & Nakayama K (2003). Rhythmical contractions in pulmonary arteries of monocrotaline-induced pulmonary hypertensive rats. *Pflügers Arch* **447**, 142-149.

Kizub IV, Pavlova OO, Johnson CD, Soloviev AI, & Zholos AV (2010). Rho kinase and protein kinase C involvement in vascular smooth muscle myofilament calcium sensitization in arteries from diabetic rats. *Br J Pharmacol*.

Klaas M & Wadsworth R (1989). Contraction followed by relaxation in response to hypoxia in the sheep isolated middle cerebral artery. *Eur J Pharmacol* **168**, 187-192.

Klöckner U & Isenberg G (1991). Endothelin depolarizes myocytes from porcine coronary and human mesenteric arteries through a Ca-activated chloride current. *Pflügers Arch* **418**, 168-175.

Knock GA, Shaifta Y, Snetkov VA, Vowles B, Drndarski S, Ward JP, & Aaronson PI (2008). Interaction between *src* family kinases and rho-kinase in agonist-induced Ca^{2+}-sensitization of rat pulmonary artery. *Cardiovasc Res* **77**, 570-579.

Knock GA, Snetkov VA, Shaifta Y, Connolly M, Drndarski S, Noah A, Pourmahram GE, Becker S, Aaronson PI, & Ward JP (2009). Superoxide constricts rat pulmonary arteries via Rho-kinase-mediated Ca^{2+} sensitization. *Free Radic Biol Med* **46**, 633-642.

Knot HJ, Standen NB, & Nelson MT (1998). Ryanodine receptors regulate arterial diameter and wall [Ca^{2+}] in cerebral arteries of rat via Ca^{2+}-dependent K^+ channels. *J Physiol* **508**, 211-221.

Ko EA, Burg ED, Platoshyn O, Msefya J, Firth AL, & Yuan JX (2007). Functional characterization of voltage-gated K^+ channels in mouse pulmonary artery smooth muscle cells. *Am J Physiol Cell Physiol* **293**, C928-C937.

Ko EA, Han J, Jung ID, & Park WS (2008). Physiological roles of K^+ channels in vascular smooth muscle cells. *J Smooth Muscle Res* **44**, 65-81.

Kobayashi S, Kitazawa T, Somlyo AV, & Somlyo AP (1989). Cytosolic heparin inhibits muscarinic and α-adrenergic Ca^{2+} release in smooth muscle. Physiological role of inositol 1,4,5- trisphosphate in pharmacomechanical coupling. *J Biol Chem* **264**, 17997-18004.

Kobrinsky E, Stevens L, Kazmi Y, Wray D, & Soldatov NM (2006). Molecular rearrangements of the Kv2.1 potassium channel termini associated with voltage gating. *J Biol Chem* **281**, 19233-19240.

Konduri GG, Bakhutashvili I, Eis A, & Gauthier KM (2009). Impaired voltage gated potassium channel responses in a fetal lamb model of persistent pulmonary hypertension of the newborn. *Pediatr Res* **66**, 289-294.

Koo GC, Blake JT, Shah K, Staruch MJ, Dumont F, Wunderler D, Sanchez M, McManus OB, Sirotina-Meisher A, Fischer P, Boltz RC, Goetz MA, Baker R, Bao J, Kayser F, Rupprecht KM, Parsons WH, Tong XC, Ita IE, Pivnichny J, Vincent S, Cunningham P, Hora D, Feeney W, & Kaczorowski G (1999). Correolide and derivatives are novel immunosuppressants blocking the lymphocyte Kv1.3 potassium channels. *Cell Immunol* **197**, 99-107.

Korovkina VP & England SK (2002a). Detection and implications of potassium channel alterations. *Vascul Pharmacol* **38**, 3-12.

Korovkina VP & England SK (2002b). Molecular diversity of vascular potassium channel isoforms. *Clin Exp Pharmacol Physiol* **29**, 317-323.

Korshunov SS, Skulachev VP, & Starkov AA (1997). High protonic potential actuates a mechanism of production of reactive oxygen species in mitochondria. *FEBS Lett* **416**, 15-18.

Kovitz KL, Aleskowitch TD, Sylvester JT, & Flavahan NA (1993). Endothelium-derived contracting and relaxing factors contribute to hypoxic responses of pulmonary arteries. *Am J Physiol* **265**, H1139-H1148.

Koyama M, Ito M, Feng J, Seko T, Shiraki K, Takase K, Hartshorne DJ, & Nakano T (2000). Phosphorylation of CPI-17, an inhibitory phosphoprotein of smooth muscle myosin phosphatase, by Rho-kinase. *FEBS Lett* **475**, 197-200.

Kubisch C, Schroeder BC, Friedrich T, Lutjohann B, El-Amraoui A, Marlin S, Petit C, & Jentsch TJ (1999). KCNQ4, a novel potassium channel expressed in sensory outer hair cells, is mutated in dominant deafness. *Cell* **96**, 437-446.

Kunichika N, Yu Y, Remillard CV, Platoshyn O, Zhang S, & Yuan JX (2004). Overexpression of *TRPC1* enhances pulmonary vasoconstriction induced by capacitative Ca^{2+} entry. *Am J Physiol Lung Cell Mol Physiol* **287**, L962-L969.

Lancaster MK & Harrison SM (1998). Changes in contraction, cytosolic Ca2+ and pH during metabolic inhibition and upon restoration of mitochondrial respiration in rat ventricular myocytes. *Exp Physiol* **83**, 349-360.

Landry DW & Oliver JA (1992). The ATP-sensitive K+ channel mediates hypotension in endotoxemia and hypoxic lactic acidosis in dog. *J Clin Invest* **89**, 2071-2074.

Langton PD, Nelson MT, Huang Y, & Standen NB (1991). Block of calcium-activated potassium channels in mammalian arterial myocytes by tetraethylammonium ions. *Am J Physiol* **260**, H927-H934.

Large WA & Wang Q (1996). Characteristics and physiological role of the Ca^{2+}-activated Cl^- conductance in smooth muscle. *Am J Physiol* **271**, C435-C454.

Lazor R, Feihl F, Waeber B, Kucera P, & Perret C (1996). Endothelin-1 does not mediate the endothelium-dependent hypoxic contractions of small pulmonary arteries in rats. *Chest* **110**, 189-197.

Leach RM, Hill HM, Snetkov VA, Robertson TP, & Ward JP (2001). Divergent roles of glycolysis and the mitochondrial electron transport chain in hypoxic pulmonary vasoconstriction of the rat: identity of the hypoxic sensor. *J Physiol* **536**, 211-224.

Leach RM, Hill HS, Snetkov VA, & Ward JP (2002). Hypoxia, energy state and pulmonary vasomotor tone. *Respir Physiol Neurobiol* **132**, 55-67.

Leach RM, Robertson TP, Twort CH, & Ward JPT (1994). Hypoxic vasoconstriction in rat pulmonary and mesenteric arteries. *Am J Physiol* **266**, L223-L231.

Leach RM, Sheehan DW, Chacko VP, & Sylvester JT (1998). Effects of hypoxia on energy state and pH in resting pulmonary and femoral arterial smooth muscles. *Am J Physiol* **275**, L1051-L1060.

Leach RM, Sheehan DW, Chacko VP, & Sylvester JT (2000). Energy state, pH, and vasomotor tone during hypoxia in precontracted pulmonary and femoral arteries. *Am J Physiol Lung Cell Mol Physiol* **278**, L294-L304.

Leblanc N, Ledoux J, Saleh S, Sanguinetti A, Angermann J, O'Driscoll K, Britton F, Perrino BA, & Greenwood IA (2005). Regulation of calcium-activated chloride channels in smooth muscle cells: a complex picture is emerging. *Can J Physiol Pharmacol* **83**, 541-556.

Lee CH, Rahimian R, Szado T, Sandhu J, Poburko D, Behra T, Chan L, & van Breemen C (2002). Sequential opening of IP_3-sensitive Ca^{2+} channels and SOC during α-adrenergic activation of rabbit vena cava. *Am J Physiol Heart Circ Physiol* **282**, H1768-H1777.

Lee MP, Ravenel JD, Hu RJ, Lustig LR, Tomaselli G, Berger RD, Brandenburg SA, Litzi TJ, Bunton TE, Limb C, Francis H, Gorelikow M, Gu H, Washington K, Argani P, Goldenring JR, Coffey RJ, & Feinberg AP (2000). Targeted disruption of the Kvlqt1 gene causes deafness and gastric hyperplasia in mice. *J Clin Invest* **106**, 1447-1455.

Lee S, Park M, So I, & Earm YE (1994). NADH and NAD modulated Ca^{2+}-activated K^+ channels in small pulmonary arterial smooth muscle cells of the rabbit. *Pflügers Arch* **427**, 378-380.

Lerche C, Scherer CR, Seebohm G, Derst C, Wei AD, Busch AE, & Steinmeyer K (2000). Molecular cloning and functional expression of KCNQ5, a potassium channel subunit that may contribute to neuronal M-current diversity. *J Biol Chem* **275**, 22395-22400.

Lesage F & Lazdunski M (2000). Molecular and functional properties of two-pore-domain potassium channels. *Am J Physiol Renal Physiol* **279**, F793-F801.

Lesh RE, Nixon GF, Fleischer S, Airey JA, Somlyo AP, & Somlyo AV (1998). Localization of ryanodine receptors in smooth muscle. *Circ Res* **82**, 175-185.

Lewis RS (2007). The molecular choreography of a store-operated calcium channel. *Nature* **446**, 284-287.

Li L, Eto M, Lee MR, Morita F, Yazawa M, & Kitazawa T (1998). Possible involvement of the novel CPI-17 protein in protein kinase C signal transduction of rabbit arterial smooth muscle. *J Physiol* **508**, 871-881.

Li W & Aldrich RW (2004). Unique inner pore properties of BK channels revealed by quaternary ammonium block. *J Gen Physiol* **124**, 43-57.

Li Y, Um SY, & McDonald TV (2006). Voltage-gated potassium channels: regulation by accessory subunits. *Neuroscientist* **12**, 199-210.

Lin MJ, Leung GP, Zhang WM, Yang XR, Yip KP, Tse CM, & Sham JS (2004). Chronic hypoxia-induced upregulation of store-operated and receptor-operated Ca^{2+} channels in pulmonary arterial smooth muscle cells: a novel mechanism of hypoxic pulmonary hypertension. *Circ Res* **95**, 496-505.

Liu F, Wu JY, Beasley D, & Orr JA (1997). TxA_2-induced pulmonary artery contraction requires extracellular calcium. *Respir Physiol* **109**, 155-166.

Liu H, Chen H, Yang X, & Cheng J (2001a). ATP sensitive K+ channel may be involved in the protective effects of preconditioning in isolated guinea pig cardiomyocytes. *Chin Med J (Engl)* **114**, 178-182.

Liu JQ & Folz RJ (2004). Extracellular superoxide enhances 5-HT-induced murine pulmonary artery vasoconstriction. *Am J Physiol Lung Cell Mol Physiol* **287**, L111-L118.

Liu JQ, Zelko IN, Erbynn EM, Sham JS, & Folz RJ (2006). Hypoxic pulmonary hypertension: role of superoxide and NADPH oxidase (gp91phox). *Am J Physiol Lung Cell Mol Physiol* **290**, L2-L10.

Liu Q, Sham JS, Shimoda LA, & Sylvester JT (2001b). Hypoxic constriction of porcine distal pulmonary arteries: endothelium and endothelin dependence. *Am J Physiol Lung Cell Mol Physiol* **280**, L856-L865.

Liu R, Ueda M, Okazaki N, & Ishibe Y (2001c). Role of potassium channels in isoflurane- and sevoflurane-induced attenuation of hypoxic pulmonary vasoconstriction in isolated perfused rabbit lungs. *Anesthesiology* **95**, 939-946.

Liu W & Saint DA (2004). Heterogeneous expression of tandem-pore K+ channel genes in adult and embryonic rat heart quantified by real-time polymerase chain reaction. *Clin Exp Pharmacol Physiol* **31**, 174-178.

Liu Y & Gutterman DD (2002). The coronary circulation in diabetes: influence of reactive oxygen species on K^+ channel-mediated vasodilation. *Vascul Pharmacol* **38**, 43-49.

Lopez-Barneo J, Pardal R, & Ortega-Saenz P (2001). Cellular mechanism of oxygen sensing. *Annu Rev Physiol* **63**, 259-287.

Losito VA, Tsushima RG, Diaz RJ, Wilson GJ, & Backx PH (1998). Preferential regulation of rabbit cardiac L-type Ca^{2+} current by glycolytic derived ATP via a direct allosteric pathway. *J Physiol* **511**, 67-78.

Lu T, Wang XL, He T, Zhou W, Kaduce TL, Katusic ZS, Spector AA, & Lee HC (2005). Impaired arachidonic acid-mediated activation of large-conductance Ca2+-activated K+ channels in coronary arterial smooth muscle cells in Zucker Diabetic Fatty rats. *Diabetes* **54**, 2155-2163.

Lu W, Wang J, Shimoda LA, & Sylvester JT (2008). Differences in STIM1 and TRPC expression in proximal and distal pulmonary arterial smooth muscle are associated with differences in Ca^{2+} responses to hypoxia. *Am J Physiol Lung Cell Mol Physiol* **295**, L104-L113.

Lu Y, Zhang J, Tang G, & Wang R (2001). Modulation of voltage-dependent K^+ channel current in vascular smooth muscle cells from rat mesenteric arteries. *J Membr Biol* **180**, 163-175.

Lydrup ML, Sward K, & Hellstrand P (1994). Effect of glibenclamide on membrane response to metabolic inhibition in smooth muscle of rat portal vein. *J Vasc Res* **31**, 82-91.

Lynch RM, Carrington W, Fogarty KE, & Fay FS (1996). Metabolic modulation of hexokinase association with mitochondria in living smooth muscle cells. *Am J Physiol* **270**, C488-C499.

Mackie AR, Brueggemann LI, Henderson KK, Shiels AJ, Cribbs LL, Scrogin KE, & Byron KL (2008). Vascular KCNQ potassium channels as novel targets for the control of mesenteric artery constriction by vasopressin, based on studies in single cells, pressurized arteries, and in vivo measurements of mesenteric vascular resistance. *J Pharmacol Exp Ther* **325**, 475-483.

Mackie AR & Byron KL (2008). Cardiovascular KCNQ (Kv7) potassium channels: physiological regulators and new targets for therapeutic intervention. *Mol Pharmacol* **74**, 1171-1179.

MacKinnon R (1991). New insights into the structure and function of potassium channels. *Curr Opin Neurobiol* **1**, 14-19.

MacKinnon R, Heginbotham L, & Abramson T (1990). Mapping the receptor site for charybdotoxin, a pore-blocking potassium channel inhibitor. *Neuron* **5**, 767-771.

MacLean MR & Dempsie Y (2010). The serotonin hypothesis of pulmonary hypertension revisited. *Adv Exp Med Biol* **661**, 309-322.

MacLean MR, Deuchar GA, Hicks MN, Morecroft I, Shen S, Sheward J, Colston J, Loughlin L, Nilsen M, Dempsie Y, & Harmar A (2004). Overexpression of the 5-hydroxytryptamine transporter gene: effect on pulmonary hemodynamics and hypoxia-induced pulmonary hypertension. *Circulation* **109**, 2150-2155.

MacLean MR & McCulloch KM (1998). Influence of applied tension and nitric oxide on responses to endothelins in rat pulmonary resistance arteries: effect of chronic hypoxia. *Br J Pharmacol* **123**, 991-999.

MacLeod KT (1989). Effects of hypoxia and metabolic inhibition on the intracellular sodium activity of mammalian ventricular muscle. *J Physiol* **416**, 455-468.

Madden JA, Dawson CA, & Harder DR (1985). Hypoxia-induced activation in small isolated pulmonary arteries from the cat. *J Appl Physiol* **59**, 113-118.

Madden JA, Vadula MS, & Kurup VP (1992). Effects of hypoxia and other vasoactive agents on pulmonary and cerebral artery smooth muscle cells. *Am J Physiol* **263**, L384-L393.

Madhani M, Scotland RS, MacAllister RJ, & Hobbs AJ (2003). Vascular natriuretic peptide receptor-linked particulate guanylate cyclases are modulated by nitric oxide-cyclic GMP signalling. *Br J Pharmacol* **139**, 1289-1296.

Maingret F, Fosset M, Lesage F, Lazdunski M, & Honoré E (1999). TRAAK is a mammalian neuronal mechano-gated K^+ channel. *J Biol Chem* **274**, 1381-1387.

Maingret F, Lauritzen I, Patel AJ, Heurteaux C, Reyes R, Lesage F, Lazdunski M, & Honoré E (2000). TREK-1 is a heat-activated background K^+ channel. *EMBO J* **19**, 2483-2491.

Maljevic S, Wuttke TV, Seebohm G, & Lerche H (2010). KV7 channelopathies. *Pflugers Arch* **460**, 277-288.

Malli R, Frieden M, Osibow K, Zoratti C, Mayer M, Demaurex N, & Graier WF (2003). Sustained Ca^{2+} transfer across mitochondria is essential for mitochondrial Ca^{2+} buffering, sore-operated Ca^{2+} entry, and Ca^{2+} store refilling. *J Biol Chem* **278**, 44769-44779.

Mandegar M, Remillard CV, & Yuan JX (2002). Ion channels in pulmonary arterial hypertension. *Prog Cardiovasc Dis* **45**, 81-114.

Mandegar M & Yuan JX (2002). Role of K^+ channels in pulmonary hypertension. *Vascul Pharmacol* **38**, 25-33.

Manoury B, Tamuleviciute A, & Tammaro P (2010). TMEM16A/anoctamin 1 protein mediates calcium-activated chloride currents in pulmonary arterial smooth muscle cells. *J Physiol* **588**, 2305-2314.

Marchenko SM & Sage SO (1994). Smooth muscle cells affect endothelial membrane potential in rat aorta. *Am J Physiol* **267**, H804-H811.

Marin J, Encabo A, Briones A, Garcia-Cohen EC, & Alonso MJ (1999). Mechanisms involved in the cellular calcium homeostasis in vascular smooth muscle: calcium pumps. *Life Sci* **64**, 279-303.

Marriott JF & Marshall JM (1990). Differential effects of hypoxia upon contractions evoked by potassium and noradrenaline in rabbit arteries in vitro. *J Physiol* **422**, 1-13.

Marshall BE (1990). Hypoxic pulmonary vasoconstriction. *Acta Anaesthesiol Scand Suppl* **94**, 37-41.

Marshall BE, Marshall C, Benumof J, & Saidman LJ (1981). Hypoxic pulmonary vasoconstriction in dogs: effects of lung segment size and oxygen tension. *J Appl Physiol* **51**, 1543-1551.

Masumoto A, Hirooka Y, Shimokawa H, Hironaga K, Setoguchi S, & Takeshita A (2001). Possible involvement of Rho-kinase in the pathogenesis of hypertension in humans. *Hypertension* **38**, 1307-1310.

Matsuno-Yagi A & Hatefi Y (1993). Studies on the mechanism of oxidative phosphorylation. Different effects of F0 inhibitors on unisite and multisite ATP hydrolysis by bovine submitochondrial particles. *J Biol Chem* **268**, 1539-1545.

Mauban JR, Remillard CV, & Yuan JX (2005). Hypoxic pulmonary vasoconstriction: role of ion channels. *J Appl Physiol* **98**, 415-420.

McCallum LA, Pierce SL, England SK, Greenwood IA, & Tribe RM (2010). The contribution of Kv7 channels to pregnant mouse and human myometrial contractility. *J Cell Mol Med*.

McDaniel SS, Platoshyn O, Wang J, Yu Y, Sweeney M, Krick S, Rubin LJ, & Yuan JX (2001). Capacitative Ca^{2+} entry in agonist-induced pulmonary vasoconstriction. *Am J Physiol Lung Cell Mol Physiol* **280**, L870-L880.

McElroy SP, Gurney AM, & Drummond RM (2008). Pharmacological profile of store-operated Ca(2+) entry in intrapulmonary artery smooth muscle cells. *Eur J Pharmacol* **584**, 10-20.

McGregor E, Gosling M, Beattie DK, Ribbons DM, Davies AH, & Powell JT (2002). Circumferential stretching of saphenous vein smooth muscle enhances vasoconstrictor responses by Rho kinase-dependent pathways. *Cardiovasc Res* **53**, 219-226.

McKenzie C, MacDonald A, & Shaw AM (2009). Mechanisms of U46619-induced contraction of rat pulmonary arteries in the presence and absence of the endothelium. *Br J Pharmacol* **157**, 581-596.

McMurtry IF, Bauer NR, Fagan KA, Nagaoka T, Gebb SA, & Oka M (2003). Hypoxia and Rho/Rho-kinase signaling. Lung development versus hypoxic pulmonary hypertension. *Adv Exp Med Biol* **543**, 127-137.

McMurtry IF, Davidson AB, Reeves JT, & Grover RF (1976). Inhibition of hypoxic pulmonary vasoconstriction by calcium antagonists in isolated rat lungs. *Circ Res* **38**, 99-104.

McMurtry IF, Petrun MD, & Reeves JT (1978). Lungs from chronically hypoxic rats have decreased pressor response to acute hypoxia. *Am J Physiol* **235**, H104-H109.

McNamara PJ, Murthy P, Kantores C, Teixeira L, Engelberts D, van V, Kavanagh BP, & Jankov RP (2008). Acute vasodilator effects of Rho-kinase inhibitors in neonatal rats with pulmonary hypertension unresponsive to nitric oxide. *Am J Physiol Lung Cell Mol Physiol* **294**, L205-L213.

McPherson GA (1985). Analysis of radioligand binding experiments. A collection of computer programs for the IBM PC. *J Pharmacol Methods* **14**, 213-228.

Means AR (1994). Calcium, calmodulin and cell cycle regulation. *FEBS Lett* **347**, 1-4.

Medhurst AD, Rennie G, Chapman CG, Meadows H, Duckworth MD, Kelsell RE, Gloger II, & Pangalos MN (2001). Distribution analysis of human two pore domain potassium channels in tissues of the central nervous system and periphery. *Brain Res Mol Brain Res* **86**, 101-114.

Mellemkjaer S & Nielsen-Kudsk JE (1994). Glibenclamide inhibits hypoxic relaxation of isolated porcine coronary arteries under conditions of impaired glycolysis. *Eur J Pharmacol* **270**, 307-312.

Michelakis ED, Hampl V, Nsair A, Wu X, Harry G, Haromy A, Gurtu R, & Archer SL (2002a). Diversity in mitochondrial function explains differences in vascular oxygen sensing. *Circ Res* **90**, 1307-1315.

Michelakis ED, McMurtry MS, Wu XC, Dyck JR, Moudgil R, Hopkins TA, Lopaschuk GD, Puttagunta L, Waite R, & Archer SL (2002b). Dichloroacetate, a metabolic modulator, prevents and reverses chronic hypoxic pulmonary hypertension in rats: role of increased expression and activity of voltage-gated potassium channels. *Circulation* **105**, 244-250.

Michelakis ED, Thébaud B, Weir EK, & Archer SL (2004). Hypoxic pulmonary vasoconstriction: redox regulation of O_2-sensitive K^+ channels by a mitochondrial O_2-sensor in resistance artery smooth muscle cells. *J Mol Cell Cardiol* **37**, 1119-1136.

Mickelson JR & Louis CF (1996). Malignant hyperthermia: excitation-contraction coupling, Ca2+ release channel, and cell Ca2+ regulation defects. *Physiol Rev* **76**, 537-592.

Millen J, MacLean MR, & Houslay MD (2006). Hypoxia-induced remodelling of PDE4 isoform expression and cAMP handling in human pulmonary artery smooth muscle cells. *Eur J Cell Biol* **85**, 679-691.

Miller AL, Morales E, Leblanc NR, & Cole WC (1993). Metabolic inhibition enhances Ca^{2+}-activated K^+ current in smooth muscle cells of rabbit portal vein. *Am J Physiol* **265**, H2184-H2195.

Miller C, Moczydlowski E, Latorre R, & Phillips M (1985). Charybdotoxin, a protein inhibitor of single Ca2+-activated K+ channels from mammalian skeletal muscle. *Nature* **313**, 316-318.

Minami K, Fukuzawa K, & Nakaya Y (1993a). Protein kinase C inhibits the Ca^{2+}-activated K^+ channel of cultured porcine coronary artery smooth muscle cells. *Biochem Biophys Res Commun* **190**, 263-269.

Minami K, Fukuzawa K, Nakaya Y, Zeng XR, & Inoue I (1993b). Mechanism of activation of the Ca^{2+}-activated K^+ channel by cyclic AMP in cultured porcine coronary artery smooth muscle cells. *Life Sci* **53**, 1129-1135.

Minke B (2006). TRP channels and Ca2+ signaling. *Cell Calcium* **40**, 261-275.

Mitchell P (1961). Coupling of phosphorylation to electron and hydrogen transfer by a chemi-osmotic type of mechanism. *Nature* **191**, 144-148.

Mizuno Y, Isotani E, Huang J, Ding H, Stull JT, & Kamm KE (2008). Myosin light chain kinase activation and calcium sensitization in smooth muscle in vivo. *Am J Physiol Cell Physiol* **295**, C358-C364.

Moreau R, Komeichi H, Kirstetter P, Yang S, upetit-Faisant B, Cailmail S, & Lebrec D (1994). Effects of glibenclamide on systemic and splanchnic haemodynamics in conscious rats. *Br J Pharmacol* **112**, 649-653.

Morecroft I, Murray A, Nilsen M, Gurney AM, & MacLean MR (2009). Treatment with the Kv7 potassium channel activator flupirtine is beneficial in two independent mouse models of pulmonary hypertension. *Br J Pharmacol* **157**, 1241-1249.

Morecroft I, Pang L, Baranowska M, Nilsen M, Loughlin L, Dempsie Y, Millet C, & MacLean MR (2010). In vivo effects of a combined 5-HT1B receptor/SERT antagonist in experimental pulmonary hypertension. *Cardiovasc Res* **85**, 593-603.

Morgan KG & Gangopadhyay SS (2001). Invited review: cross-bridge regulation by thin filament-associated proteins. *J Appl Physiol* **91**, 953-962.

Morio Y & McMurtry IF (2002). Ca^{2+} release from ryanodine-sensitive store contributes to mechanism of hypoxic vasoconstriction in rat lungs. *J Appl Physiol* **92**, 527-534.

Morrell NW, Adnot S, Archer SL, Dupuis J, Jones PL, MacLean MR, McMurtry IF, Stenmark KR, Thistlethwaite PA, Weissmann N, Yuan JX, & Weir EK (2009). Cellular and molecular basis of pulmonary arterial hypertension. *J Am Coll Cardiol* **54**, S20-S31.

Motulsky HJ (1999). *Analysing Data with GraphPad Prism.* GraphPad Software Inc., www.graphpad.com., San Diego, CA.

Moudgil R, Michelakis ED, & Archer SL (2005). Hypoxic pulmonary vasoconstriction. *J Appl Physiol* **98**, 390-403.

Moudgil R, Michelakis ED, & Archer SL (2006). The role of K^+ channels in determining pulmonary vascular tone, oxygen sensing, cell proliferation, and apoptosis: implications in hypoxic pulmonary vasoconstriction and pulmonary arterial hypertension. *Microcirculation* **13**, 615-632.

Mukai Y, Shimokawa H, Matoba T, Kandabashi T, Satoh S, Hiroki J, Kaibuchi K, & Takeshita A (2001). Involvement of Rho-kinase in hypertensive vascular disease: a novel therapeutic target in hypertension. *FASEB J* **15**, 1062-1064.

Mulvany MJ (1988). Biophysical aspects of resistance vessels studied in spontaneous and renal hypertensive rats. *Acta Physiol Scand* **571**, 129-137.

Mulvany MJ (1999). Vascular remodelling of resistance vessels: can we define this? *Cardiovasc Res* **41**, 9-13.

Mulvany MJ & Aalkjaer C (1990). Structure and function of small arteries. *Physiol Rev* **70**, 921-961.

Mulvany MJ & Halpern W (1977). Contractile properties of small arterial resistance vessels in spontaneously hypertensive and normotensive rats. *Circ Res* **41**, 19-26.

Mulvany MJ, Nilsson H, & Flatman JA (1982). Role of membrane potential in the response of rat small mesenteric arteries to exogenous noradrenaline stimulation. *J Physiol* **332**, 363-373.

Muranyi A, Derkach D, Erdodi F, Kiss A, Ito M, & Hartshorne DJ (2005). Phosphorylation of Thr695 and Thr850 on the myosin phosphatase target subunit: inhibitory effects and occurrence in A7r5 cells. *FEBS Lett* **579**, 6611-6615.

Murphy ME & Brayden JE (1995). Nitric oxide hyperpolarizes rabbit mesenteric arteries via ATP-sensitive potassium channels. *J Physiol* **486**, 47-58.

Murray TR, Chen L, Marshall BE, & Macarak EJ (1990). Hypoxic contraction of cultured pulmonary vascular smooth muscle cells. *Am J Respir Cell Mol Biol* **3**, 457-465.

Naeije R & Brimioulle S (2001). Physiology in medicine: importance of hypoxic pulmonary vasoconstriction in maintaining arterial oxygenation during acute respiratory failure. *Crit Care* **5**, 67-71.

Nagaoka T, Fagan KA, Gebb SA, Morris KG, Suzuki T, Shimokawa H, McMurtry IF, & Oka M (2005). Inhaled Rho kinase inhibitors are potent and selective vasodilators in rat pulmonary hypertension. *Am J Respir Crit Care Med* **171**, 494-499.

Nagaoka T, Morio Y, Casanova N, Bauer N, Gebb S, McMurtry I, & Oka M (2004). Rho/Rho-kinase signaling mediates increased basal pulmonary vascular tone in chronically hypoxic rats. *Am J Physiol Lung Cell Mol Physiol* **287**, L665-L672.

Nakashima M & Vanhoutte PM (1995). Isoproterenol causes hyperpolarization through opening of ATP- sensitive potassium channels in vascular smooth muscle of the canine saphenous vein. *J Pharmacol Exp Ther* **272**, 379-384.

Namm DH & Zucker JL (1973). Biochemical alterations caused by hypoxia in the isolated rabbit aorta. Correlation with changes in arterial contractility. *Circ Res* **32**, 464-470.

Nankervis CA & Miller CE (1998). Developmental differences in response of mesenteric artery to acute hypoxia in vitro. *Am J Physiol* **274**, G694-G699.

Narishige T, Egashira K, Akatsuka Y, Katsuda Y, Numaguchi K, Sakata M, & Takeshita A (1993). Glibenclamide, a putative ATP-sensitive K+ channel blocker, inhibits coronary autoregulation in anesthetized dogs. *Circ Res* **73**, 771-776.

Nelson MT, Cheng H, Rubart M, Santana LF, Bonev AD, Knot HJ, & Lederer WJ (1995). Relaxation of arterial smooth muscle by calcium sparks. *Science* **270**, 633-637.

Nelson MT, Huang Y, Brayden JE, Hescheler J, & Standen NB (1990). Arterial dilations in response to calcitonin gene-related peptide involve activation of K^+ channels. *Nature* **344**, 770-773.

Nelson MT & Quayle JM (1995). Physiological roles and properties of potassium channels in arterial smooth muscle. *Am J Physiol* **268**, C799-C822.

Neyroud N, Tesson F, Denjoy I, Leibovici M, Donger C, Barhanin J, Faure S, Gary F, Coumel P, Petit C, Schwartz K, & Guicheney P (1997). A novel mutation in the potassium channel gene KVLQT1 causes the Jervell and Lange-Nielsen cardioauditory syndrome. *Nat Genet* **15**, 186-189.

Ng FL, Davis AJ, Jepps TA, Harhun MI, Yeung SY, Wan A, Reddy M, Melville D, Nardi A, Khong TK, & Greenwood IA (2010). Expression and function of the K(+) channel KCNQ genes in human arteries. *Br J Pharmacol*.

Ng LC & Gurney AM (2001). Store-operated channels mediate Ca^{2+} influx and contraction in rat pulmonary artery. *Circ Res* **89**, 923-929.

Ng LC, Wilson SM, & Hume JR (2005). Mobilization of sarcoplasmic reticulum stores by hypoxia leads to consequent activation of capacitative Ca^{2+} entry in isolated canine pulmonary arterial smooth muscle cells. *J Physiol* **563**, 409-419.

Nicholls DG & Budd SL (2000). Mitochondria and neuronal survival. *Physiol Rev* **80**, 315-360.

Nicholls DG, Vesce S, Kirk L, & Chalmers S (2003). Interactions between mitochondrial bioenergetics and cytoplasmic calcium in cultured cerebellar granule cells. *Cell Calcium* **34**, 407-424.

Niki I, Yokokura H, Sudo T, Kato M, & Hidaka H (1996). Ca2+ signaling and intracellular Ca2+ binding proteins. *J Biochem* **120**, 685-698.

Nilius B & Droogmans G (2003). Amazing chloride channels: an overview. *Acta Physiol Scand* **177**, 119-147.

Nilsson H, Videbæk LM, Toma C, & Mulvany MJ (1998). Role of intracellular calcium for noradrenaline-induced depolarization in rat mesenteric small arteries. *J Vasc Res* **35**, 36-44.

Ning LW & Liang W (2009). Blockade of voltage-sensitive K+ channels increases contractility more in transverse than in longitudinal rat detrusor strips. *Urology* **73**, 400-404.

Nishida M, Cadene M, Chait BT, & MacKinnon R (2007). Crystal structure of a Kir3.1-prokaryotic Kir channel chimera. *EMBO J* **26**, 4005-4015.

Noack T, Edwards G, Deitmer P, & Weston AH (1992). Potassium channel modulation in rat portal vein by ATP depletion: a comparison with the effects of levcromakalim (BRL 38227). *Br J Pharmacol* **107**, 945-955.

Noma A (1983). ATP-regulated K+ channels in cardiac muscle. *Nature* **305**, 147-148.

Ogawa Y, Kawabe J, Onodera S, Tobise K, Morita K, Harada T, Hirayama T, & Takeda A (1993). Role of endothelium in biphasic hypoxic response of the isolated pulmonary artery in the rat. *Jpn Circ J* **57**, 228-236.

Ohya S, Horowitz B, & Greenwood IA (2002). Functional and molecular identification of ERG channels in murine portal vein myocytes. *Am J Physiol Cell Physiol* **283**, C866-C877.

Ohya S, Sergeant GP, Greenwood IA, & Horowitz B (2003). Molecular variants of KCNQ channels expressed in murine portal vein myocytes: a role in delayed rectifier current. *Circ Res* **92**, 1016-1023.

Oka M, Fagan KA, Jones PL, & McMurtry IF (2008). Therapeutic potential of RhoA/Rho kinase inhibitors in pulmonary hypertension. *Br J Pharmacol* **155**, 444-454.

Okabe K, Kitamura K, & Kuriyama H (1987). Features of 4-aminopyridine sensitive outward current observed in single smooth muscle cells from the rabbit pulmonary artery. *Pflügers Arch* **409**, 561-568.

Okada Y, Yanagisawa T, & Taira N (1992). KCl-depolarization potentiates the Ca^{2+} sensitization by endothelin-1 in canine coronary artery. *Jpn J Pharmacol* **60**, 403-405.

Olschewski A, Hong Z, Nelson DP, & Weir EK (2002). Graded response of K^+ current, membrane potential, and $[Ca^{2+}]_i$ to hypoxia in pulmonary arterial smooth muscle. *Am J Physiol Lung Cell Mol Physiol* **283**, L1143-L1150.

Olschewski A, Li Y, Tang B, Hanze J, Eul B, Bohle RM, Wilhelm J, Morty RE, Brau ME, Weir EK, Kwapiszewska G, Klepetko W, Seeger W, & Olschewski H (2006). Impact of TASK-1 in human pulmonary artery smooth muscle cells. *Circ Res* **98**, 1072-1080.

Omote M, Kajimoto N, & Mizusawa H (1993). The ionic mechanism of phenylephrine-induced rhythmic contractions in rabbit mesenteric arteries treated with ryanodine. *Acta Physiol Scand* **147**, 9-13.

Orallo F (1996). Regulation of cytosolic calcium levels in vascular smooth muscle. *Pharmacol Ther* **69**, 153-171.

Orchard CH, Sanchez de Leon R, & Sykes MK (1983). The relationship between hypoxic pulmonary vasoconstriction and arterial oxygen tension in the intact dog. *J Physiol* **338**, 61-74.

Orio P, Rojas P, Ferreira G, & Latorre R (2002). New disguises for an old channel: MaxiK channel beta-subunits. *News Physiol Sci* **17**, 156-161.

Osipenko ON, Alexander D, MacLean MR, & Gurney AM (1998). Influence of chronic hypoxia on the contributions of non-inactivating and delayed rectifier K currents to the resting potential and tone of rat pulmonary artery smooth muscle. *Br J Pharmacol* **124**, 1335-1337.

Osipenko ON, Evans AM, & Gurney AM (1997). Regulation of the resting potential of rabbit pulmonary artery myocytes by a low threshold, O_2-sensing potassium current. *Br J Pharmacol* **120**, 1461-1470.

Osipenko ON, Tate RJ, & Gurney AM (2000). Potential role for Kv3.1b channels as oxygen sensors. *Circ Res* **86**, 534-540.

Otter D & Austin C (1999). Mechanisms of hypoxic vasodilatation of isolated rat mesenteric arteries: a comparison with metabolic inhibition. *J Physiol* **516**, 249-259.

Otter D & Austin C (2000). Hypoxia, metabolic inhibition, and isolated rat mesenteric tone: influence of arterial diameter. *Microvasc Res* **59**, 107-114.

Ottschytsch N, Raes A, Van Hoorick D, & Snyders DJ (2002). Obligatory heterotetramerization of three previously uncharacterized Kv channel α-subunits identified in the human genome. *Proc Natl Acad Sci USA* **99**, 7986-7991.

Owsianik G, Talavera K, Voets T, & Nilius B (2006). Permeation and selectivity of TRP channels. *Annu Rev Physiol* **68**, 685-717.

Ozaki M, Kawashima S, Yamashita T, Ohashi Y, Rikitake Y, Inoue N, Hirata KI, Hayashi Y, Itoh H, & Yokoyama M (2001). Reduced hypoxic pulmonary vascular remodeling by nitric oxide from the endothelium. *Hypertension* **37**, 322-327.

Ozaki M, Marshall C, Amaki Y, & Marshall BE (1998). Role of wall tension in hypoxic responses of isolated rat pulmonary arteries. *Am J Physiol* **275**, L1069-L1077.

Parekh AB (2003). Mitochondrial regulation of intracellular Ca2+ signaling: more than just simple Ca2+ buffers. *News Physiol Sci* **18**, 252-256.

Parekh AB & Putney JW, Jr. (2005). Store-operated calcium channels. *Physiol Rev* **85**, 757-810.

Patel AJ & Honoré E (2001). Molecular physiology of oxygen-sensitive potassium channels. *Eur Respir J* **18**, 221-227.

Patel AJ, Lazdunski M, & Honoré E (1997). Kv2.1/Kv9.3, a novel ATP-dependent delayed-rectifier K^+ channel in oxygen-sensitive pulmonary artery myocytes. *EMBO J* **16**, 6615-6625.

Patel CA & Rattan S (2006). Spontaneously tonic smooth muscle has characteristically higher levels of RhoA/ROK compared with the phasic smooth muscle. *Am J Physiol Gastrointest Liver Physiol* **291**, G830-G837.

Patel HH, Remillard CV, & Yuan JXJ (2004). Hypoxic regulation of K^+ channel expression and function in pulmonary artery smooth muscle cells. In *Hypoxic Pulmonary Vasoconstriction: Cellular and Molecular Mechanisms*, ed. Yuan JXJ, pp. 165-198. Kluwer Academic Publishers, Boston, MA.

Paul RJ (1983). Functional compartmentalization of oxidative and glycolytic metabolism in vascular smooth muscle. *Am J Physiol* **244**, C399-C409.

Paul RJ (1989). Smooth muscle energetics. *Annu Rev Physiol* **51**, 331-349.

Paul RJ, Bowman PS, Parr AJ, Ishida Y, Wardle RL, & Gu M (2009). Hypoxic vasorelaxation in porcine coronary artery is not mediated by reactive oxygen species. *The FASEB Journal* **23**, 1032.

Peake MD, Harabin AL, Brennan NJ, & Sylvester JT (1981). Steady-state vascular responses to graded hypoxia in isolated lungs of five species. *J Appl Physiol* **51**, 1214-1219.

Pedersen SF, Owsianik G, & Nilius B (2005). TRP channels: an overview. *Cell Calcium* **38**, 233-252.

Peinado VI, Paris R, Ramirez J, Roca J, Rodriguez-Roisin R, & Barbera JA (2008). Expression of BK(Ca) channels in human pulmonary arteries: relationship with remodeling and hypoxic pulmonary vasoconstriction. *Vascul Pharmacol* **49**, 178-184.

Peng HL, Jensen PE, Nilsson H, & Aalkjær C (1998). Effect of acidosis on tension and $[Ca^{2+}]_i$ in rat cerebral arteries: is there a role for membrane potential? *Am J Physiol* **274**, H655-H662.

Peng W, Hoidal JR, & Farrukh IS (1999). Role of a novel K_{Ca} opener in regulating K^+ channels of hypoxic human pulmonary vascular cells. *Am J Respir Cell Mol Biol* **20**, 737-745.

Peng W, Karwande SV, Hoidal JR, & Farrukh IS (1996). Potassium currents in cultured human pulmonary arterial smooth muscle cells. *J Appl Physiol* **80**, 1187-1196.

Petkova-Kirova P, Gagov H, Krien U, Duridanova D, Noack T, & Schubert R (2000). 4-Aminopyridine affects rat arterial smooth muscle BK_{Ca} currents by changing intracellular pH. *Br J Pharmacol* **131**, 1643-1650.

Platoshyn O, Brevnova EE, Burg ED, Yu Y, Remillard CV, & Yuan JX (2006). Acute hypoxia selectively inhibits KCNA5 channels in pulmonary artery smooth muscle cells. *Am J Physiol Cell Physiol* **290**, C907-C916.

Platoshyn O, Golovina VA, Bailey CL, Limsuwan A, Krick S, Juhaszova M, Seiden JE, Rubin LJ, & Yuan JX (2000). Sustained membrane depolarization and pulmonary artery smooth muscle cell proliferation. *Am J Physiol Cell Physiol* **279**, C1540-C1549.

Platoshyn O, Remillard CV, Fantozzi I, Mandegar M, Sison TT, Zhang S, Burg E, & Yuan JX (2004). Diversity of voltage-dependent K^+ channels in human pulmonary artery smooth muscle cells. *Am J Physiol Lung Cell Mol Physiol* **287**, L226-L238.

Platoshyn O, Yu Y, Golovina VA, McDaniel SS, Krick S, Li L, Wang JY, Rubin LJ, & Yuan X-J (2001). Chronic hypoxia decreases K_V channel expression and function in pulmonary artery myocytes. *Am J Physiol Lung Cell Mol Physiol* **280**, L801-L812.

Platoshyn O, Yu Y, Ko EA, Remillard CV, & Yuan JX (2007). Heterogeneity of hypoxia-mediated decrease in $I_{K(V)}$ and increase in $[Ca^{2+}]_{cyt}$ in pulmonary artery smooth muscle cells. *Am J Physiol Lung Cell Mol Physiol* **293**, L402-L416.

Plüger S, Faulhaber J, Fürstenau M, Löhn M, Waldschütz R, Gollasch M, Haller H, Luft FC, Ehmke H, & Pongs O (2000). Mice with disrupted BK channel β1 subunit gene feature abnormal Ca^{2+} spark/STOC coupling and elevated blood pressure. *Circ Res* **87**, E53-E60.

Polson JB & Strada SJ (1996). Cyclic nucleotide phosphodiesterases and vascular smooth muscle. *Annu Rev Pharmacol Toxicol* **36**, 403-427.

Pongs O, Leicher T, Berger M, Roeper J, Bahring R, Wray D, Giese KP, Silva AJ, & Storm JF (1999). Functional and molecular aspects of voltage-gated K^+ channel β subunits. *Ann N Y Acad Sci* **868**, 344-355.

Post JM, Gelband CH, & Hume JR (1995). $[Ca^{2+}]_i$ inhibition of K^+ channels in canine pulmonary artery. Novel mechanism for hypoxia-induced membrane depolarization. *Circ Res* **77**, 131-139.

Post JM, Hume JR, Archer SL, & Weir EK (1992). Direct role for potassium channel inhibition in hypoxic pulmonary vasoconstriction. *Am J Physiol* **262**, C882-C890.

Post MA, Kirsch GE, & Brown AM (1996). Kv2.1 and electrically silent Kv6.1 potassium channel subunits combine and express a novel current. *FEBS Lett* **399**, 177-182.

Pozeg ZI, Michelakis ED, McMurtry MS, Thébaud B, Wu XC, Dyck JR, Hashimoto K, Wang S, Moudgil R, Harry G, Sultanian R, Koshal A, & Archer SL (2003). In vivo gene transfer of the O_2-sensitive potassium channel Kv1.5 reduces pulmonary hypertension and restores hypoxic pulmonary vasoconstriction in chronically hypoxic rats. *Circulation* **107**, 2037-2044.

Priest RM, Robertson TP, Leach RM, & Ward JP (1998). Membrane potential-dependent and -independent vasodilation in small pulmonary arteries from chronically hypoxic rats. *J Pharmacol Exp Ther* **285**, 975-982.

Pugsley MK & Tabrizchi R (2000). The vascular system. An overview of structure and function. *J Pharmacol Toxicol Methods* **44**, 333-340.

Putney JW, Jr. (2007). Recent breakthroughs in the molecular mechanism of capacitative calcium entry (with thoughts on how we got here). *Cell Calcium* **42**, 103-110.

Putzke C, Wemhoner K, Sachse FB, Rinne S, Schlichthorl G, Li XT, Jae L, Eckhardt I, Wischmeyer E, Wulf H, Preisig-Muller R, Daut J, & Decher N (2007). The acid-sensitive potassium channel TASK-1 in rat cardiac muscle. *Cardiovasc Res* **75**, 59-68.

Quayle JM, Bonev AD, Brayden JE, & Nelson MT (1995). Pharmacology of ATP-sensitive K^+ currents in smooth muscle cells from rabbit mesenteric artery. *Am J Physiol* **269**, C1112-C1118.

Quayle JM, Dart C, & Standen NB (1996). The properties and distribution of inward rectifier potassium currents in pig coronary arterial smooth muscle. *J Physiol* **494 (Pt 3)**, 715-726.

Quayle JM, Nelson MT, & Standen NB (1997). ATP-sensitive and inwardly rectifying potassium channels in smooth muscle. *Physiol Rev* **77**, 1165-1232.

Quayle JM, Turner MR, Burrell HE, & Kamishima T (2006). Effects of hypoxia, anoxia, and metabolic inhibitors on K_{ATP} channels in rat femoral artery myocytes. *Am J Physiol Heart Circ Physiol* **291**, H71-H80.

Quintero M, Colombo SL, Godfrey A, & Moncada S (2006). Mitochondria as signaling organelles in the vascular endothelium. *Proc Natl Acad Sci U S A* **103**, 5379-5384.

Raj U & Shimoda L (2002). Oxygen-dependent signaling in pulmonary vascular smooth muscle. *Am J Physiol Lung Cell Mol Physiol* **283**, L671-L677.

Rang H.P., Dale MM, Ritter JM, & Flower RJ (2007). *Rang and Dale's Pharmacology*, 6th ed., pp. 54-71.

Rathore R, Zheng YM, Niu CF, Liu QH, Korde A, Ho YS, & Wang YX (2008). Hypoxia activates NADPH oxidase to increase [ROS]i and [Ca2+]i through the mitochondrial ROS-PKCε signaling axis in pulmonary artery smooth muscle cells. *Free Radic Biol Med* **45**, 1223-1231.

Ratz PH, Berg KM, Urban NH, & Miner AS (2005). Regulation of smooth muscle calcium sensitivity: KCl as a calcium-sensitizing stimulus. *Am J Physiol Cell Physiol* **288**, C769-C783.

Reading SA, Earley S, Waldron BJ, Welsh DG, & Brayden JE (2005). TRPC3 mediates pyrimidine receptor-induced depolarization of cerebral arteries. *Am J Physiol Heart Circ Physiol* **288**, H2055-H2061.

Reeve HL, Michelakis E, Nelson DP, Weir EK, & Archer SL (2001). Alterations in a redox oxygen sensing mechanism in chronic hypoxia. *J Appl Physiol* **90**, 2249-2256.

Reeve HL, Weir EK, Nelson DP, Peterson DA, & Archer SL (1995). Opposing effects of oxidants and antioxidants on K^+ channel activity and tone in rat vascular tissue. *Exp Physiol* **80**, 825-834.

Reid RA, Moyle J, & Mitchell P (1966). Synthesis of adenosine triphosphate by a protonmotive force in rat liver mitochondria. *Nature* **212**, 257-258.

Remillard CV & Leblanc N (1996). Mechanism of inhibition of delayed rectifier K^+ current by 4-aminopyridine in rabbit coronary myocytes. *J Physiol* **491**, 383-400.

Remillard CV & Yuan JX (2004). Activation of K^+ channels: an essential pathway in programmed cell death. *Am J Physiol Lung Cell Mol Physiol* **286**, L49-L67.

RILEY RL (1951). Pulmonary gas exchange. *Am J Med* **10**, 210-220.

Rios EJ, Fallon M, Wang J, & Shimoda LA (2005). Chronic hypoxia elevates intracellular pH and activates Na^+/H^+ exchange in pulmonary arterial smooth muscle cells. *Am J Physiol Lung Cell Mol Physiol* **289**, L867-L874.

Robbins J (2001). KCNQ potassium channels: physiology, pathophysiology, and pharmacology. *Pharmacol Ther* **90**, 1-19.

Robertson BE, Kozlowski RZ, & Nye PC (1992). Opposing actions of tolbutamide and glibenclamide on hypoxic pulmonary vasoconstriction. *Comp Biochem Physiol* **102**, 459-462.

Robertson BE & Nelson MT (1994). Aminopyridine inhibition and voltage dependence of K^+ currents in smooth muscle cells from cerebral arteries. *Am J Physiol* **267**, C1589-C1597.

Robertson BE, Schubert R, Hescheler J, & Nelson MT (1993). cGMP-dependent protein kinase activates Ca-activated K channels in cerebral artery smooth muscle cells. *Am J Physiol* **265**, C299-C303.

Robertson TP, Aaronson PI, & Ward JP (2003). Ca^{2+} sensitization during sustained hypoxic pulmonary vasoconstriction is endothelium dependent. *Am J Physiol Lung Cell Mol Physiol* **284**, L1121-L1126.

Robertson TP, Aaronson PI, & Ward JPT (1995). Hypoxic vasoconstriction and intracellular Ca^{2+} in pulmonary arteries: evidence for PKC-independent Ca^{2+} sensitization. *Am J Physiol* **268**, H301-H307.

Robertson TP, Dipp M, Ward JP, Aaronson PI, & Evans AM (2000a). Inhibition of sustained hypoxic vasoconstriction by Y-27632 in isolated intrapulmonary arteries and perfused lung of the rat. *Br J Pharmacol* **131**, 5-9.

Robertson TP, Hague D, Aaronson PI, & Ward JP (2000b). Voltage-independent calcium entry in hypoxic pulmonary vasoconstriction of intrapulmonary arteries of the rat. *J Physiol* **525**, 669-680.

Robertson TP, Mustard KJ, Lewis TH, Clark JH, Wyatt CN, Blanco EA, Peers C, Hardie DG, & Evans AM (2008). AMP-activated protein kinase and hypoxic pulmonary vasoconstriction. *Eur J Pharmacol* **595**, 39-43.

Rodman DM, Mallet J, & McMurtry IF (1991). Difference in effect of inhibitors of energy metabolism on endothelium-dependent relaxation of rat pulmonary artery and aorta. *Am J Respir Cell Mol Biol* **4**, 237-242.

Rodman DM, Yamaguchi T, Hasunuma K, O'Brien RF, & McMurtry IF (1990). Effects of hypoxia on endothelium-dependent relaxation of rat pulmonary artery. *Am J Physiol* **258**, L207-L214.

Rodman DM, Yamaguchi T, O'Brien RF, & McMurtry IF (1989). Hypoxic contraction of isolated rat pulmonary artery. *J Pharmacol Exp Ther* **248**, 952-959.

Rodrigo GC & Standen NB (2005). ATP-sensitive potassium channels. *Curr Pharm Des* **11**, 1915-1940.

Rottenberg H & Scarpa A (1974). Calcium uptake and membrane potential in mitochondria. *Biochemistry* **13**, 4811-4817.

Rounds S & McMurtry IF (1981). Inhibitors of oxidative ATP production cause transient vasoconstriction and block subsequent pressor responses in rat lungs. *Circ Res* **48**, 393-400.

Roura-Ferrer M, Sole L, Martinez-Marmol R, Villalonga N, & Felipe A (2008). Skeletal muscle Kv7 (KCNQ) channels in myoblast differentiation and proliferation. *Biochem Biophys Res Commun* **369**, 1094-1097.

Rubanyi GM & Vanhoutte PM (1985). Hypoxia releases a vasoconstrictor substance from the canine vascular endothelium. *J Physiol* **364**, 45-56.

Rueda A, Garcia L, Soria-Jasso LE, rias-Montano JA, & Guerrero-Hernandez A (2002). The initial inositol 1,4,5-trisphosphate response induced by histamine is strongly amplified by Ca(2+) release from internal stores in smooth muscle. *Cell Calcium* **31**, 161-173.

Russell SN, Overturf KE, & Horowitz B (1994). Heterotetramer formation and charybdotoxin sensitivity of two K^+ channels cloned from smooth muscle. *Am J Physiol* **267**, C1729-C1733.

Said SI, Hamidi SA, Dickman KG, Szema AM, Lyubsky S, Lin RZ, Jiang YP, Chen JJ, Waschek JA, & Kort S (2007). Moderate pulmonary arterial hypertension in male mice lacking the vasoactive intestinal peptide gene. *Circulation* **115**, 1260-1268.

Sakurada S, Okamoto H, Takuwa N, Sugimoto N, & Takuwa Y (2001). Rho activation in excitatory agonist-stimulated vascular smooth muscle. *Am J Physiol Cell Physiol* **281**, C571-C578.

Sakurada S, Takuwa N, Sugimoto N, Wang Y, Seto M, Sasaki Y, & Takuwa Y (2003). Ca^{2+}-dependent activation of Rho and Rho kinase in membrane depolarization-induced and receptor stimulation-induced vascular smooth muscle contraction. *Circ Res* **93**, 548-556.

Saleh SN, Albert AP, Peppiatt CM, & Large WA (2006). Angiotensin II activates two cation conductances with distinct TRPC1 and TRPC6 channel properties in rabbit mesenteric artery myocytes. *J Physiol* **577**, 479-495.

Saleh SN, Albert AP, Peppiatt-Wildman CM, & Large WA (2008). Diverse properties of store-operated TRPC channels activated by protein kinase C in vascular myocytes. *J Physiol* **586**, 2463-2476.

Saleh SN & Greenwood IA (2005). Activation of chloride currents in murine portal vein smooth muscle cells by membrane depolarization involves intracellular calcium release. *Am J Physiol Cell Physiol* **288**, C122-C131.

Salinas M, de Weille J, Guillemare E, Lazdunski M, & Hugnot JP (1997a). Modes of regulation of *Shab* K^+ channel activity by the Kv8.1 subunit. *J Biol Chem* **272**, 8774-8780.

Salinas M, Duprat F, Heurteaux C, Hugnot JP, & Lazdunski M (1997b). New modulatory α subunits for mammalian *Shab* K^+ channels. *J Biol Chem* **272**, 24371-24379.

Salter KJ, Turner JL, Albarwani S, Clapp LH, & Kozlowski RZ (1995). Ca^{2+}-activated Cl^- and K^+ channels and their modulation by endothelin-1 in rat pulmonary arterial smooth muscle cells. *Exp Physiol* **80**, 815-824.

Salvaterra CG & Goldman WF (1993). Acute hypoxia increases cytosolic calcium in cultured pulmonary arterial myocytes. *Am J Physiol* **264**, L323-L328.

Sanguinetti MC, Curran ME, Zou A, Shen J, Spector PS, Atkinson DL, & Keating MT (1996). Coassembly of K(V)LQT1 and minK (IsK) proteins to form cardiac I(Ks) potassium channel. *Nature* **384**, 80-83.

Sansom SC & Stockand JD (1994). Differential Ca^{2+} sensitivities of BK(Ca) isochannels in bovine mesenteric vascular smooth muscle. *Am J Physiol* **266**, C1182-C1189.

Sato K, Morio Y, Morris KG, Rodman DM, & McMurtry IF (2000). Mechanism of hypoxic pulmonary vasoconstriction involves ET_A receptor-mediated inhibition of K_{ATP} channel. *Am J Physiol Lung Cell Mol Physiol* **278**, L434-L442.

Sauzeau V, Le Jeune H, Cario-Toumaniantz C, Smolenski A, Lohmann SM, Bertoglio J, Chardin P, Pacaud P, & Loirand G (2000). Cyclic GMP-dependent protein kinase signaling pathway inhibits RhoA-induced Ca^{2+} sensitization of contraction in vascular smooth muscle. *J Biol Chem* **275**, 21722-21729.

Scarpa A & Azzone GF (1970). The mechanism of ion translocation in mitochondria. 4. Coupling of K+ efflux with Ca2+ uptake. *Eur J Biochem* **12**, 328-335.

Schach C, Xu M, Platoshyn O, Keller SH, & Yuan JX (2007). Thiol oxidation causes pulmonary vasodilation by activating K^+ channels and inhibiting store-operated Ca^{2+} channels. *Am J Physiol Lung Cell Mol Physiol* **292**, L685-L698.

Schenzer A, Friedrich T, Pusch M, Saftig P, Jentsch TJ, Grotzinger J, & Schwake M (2005). Molecular determinants of KCNQ (Kv7) K+ channel sensitivity to the anticonvulsant retigabine. *J Neurosci* **25**, 5051-5060.

Schroeder BC, Hechenberger M, Weinreich F, Kubisch C, & Jentsch TJ (2000). KCNQ5, a novel potassium channel broadly expressed in brain, mediates M-type currents. *J Biol Chem* **275**, 24089-24095.

Schubert R, Krien U, & Gagov H (2001). Protons inhibit the BK_{Ca} channel of rat small artery smooth muscle cells. *J Vasc Res* **38**, 30-38.

Searle GJ, Hartness ME, Hoareau R, Peers C, & Kemp PJ (2002). Lack of contribution of mitochondrial electron transport to acute O_2 sensing in model airway chemoreceptors. *Biochem Biophys Res Commun* **291**, 332-337.

Seasholtz TM, Wessel J, Rao F, Rana BK, Khandrika S, Kennedy BP, Lillie EO, Ziegler MG, Smith DW, Schork NJ, Brown JH, & O'connor DT (2006). Rho kinase polymorphism influences blood pressure and systemic vascular resistance in human twins: role of heredity. *Hypertension* **47**, 937-947.

Sell M, Boldt W, & Markwardt F (2002). Desynchronising effect of the endothelium on intracellular Ca^{2+} concentration dynamics in vascular smooth muscle cells of rat mesenteric arteries. *Cell Calcium* **32**, 105-120.

Shigemori K, Ishizaki T, Matsukawa S, Sakai A, Nakai T, & Miyabo S (1996). Adenine nucleotides via activation of ATP-sensitive K^+ channels modulate hypoxic response in rat pulmonary artery. *Am J Physiol* **270**, L803-L809.

Shimizu S, Bowman PS, Thorne G, III, & Paul RJ (2000). Effects of hypoxia on isometric force, intracellular Ca^{2+}, pH, and energetics in porcine coronary artery. *Circ Res* **86**, 862-870.

Shipounova IN, Svinareva DA, Petrova TV, Lyamzaev KG, Chernyak BV, Drize NI, & Skulachev VP (2010). Reactive oxygen species produced in mitochondria are involved in age-dependent changes of hematopoietic and mesenchymal progenitor cells in mice. A study with the novel mitochondria-targeted antioxidant SkQ1. *Mech Ageing Dev* **131**, 415-421.

Shuttleworth TJ (2009). Arachidonic acid, ARC channels, and Orai proteins. *Cell Calcium* **45**, 602-610.

Shyng SL & Nichols CG (1998). Membrane phospholipid control of nucleotide sensitivity of K_{ATP} channels. *Science* **282**, 1138-1141.

Singh NA, Charlier C, Stauffer D, DuPont BR, Leach RJ, Melis R, Ronen GM, Bjerre I, Quattlebaum T, Murphy JV, McHarg ML, Gagnon D, Rosales TO, Peiffer A, Anderson VE, & Leppert M (1998). A novel potassium channel gene, KCNQ2, is mutated in an inherited epilepsy of newborns. *Nat Genet* **18**, 25-29.

Slater EC & Cleland KW (1953). The effect of calcium on the respiratory and phosphorylative activities of heart-muscle sarcosomes. *Biochem J* **55**, 566-590.

Smirnov SV & Aaronson PI (1992). Ca^{2+}-activated and voltage-gated K^+ currents in smooth muscle cells isolated from human mesenteric arteries. *J Physiol* **457**, 431-454.

Smirnov SV & Aaronson PI (1994). Alteration of the transmembrane K^+ gradient during development of delayed rectifier in isolated rat pulmonary arterial cells. *J Gen Physiol* **104**, 241-264.

Smirnov SV, Beck R, Tammaro P, Ishii T, & Aaronson PI (2002). Electrophysiologically distinct smooth muscle cell subtypes in rat conduit and resistance pulmonary arteries. *J Physiol* **538**, 867-878.

Smirnov SV, Robertson TP, Ward JPT, & Aaronson PI (1994). Chronic hypoxia is associated with reduced delayed rectifier K^+ current in rat pulmonary artery muscle cells. *Am J Physiol* **266**, H365-H370.

Snetkov VA, Aaronson PI, Ward JPT, Knock GA, & Robertson TP (2003). Capacitative calcium entry as a pulmonary specific vasoconstrictor mechanism in small muscular arteries of the rat. *Br J Pharmacol* **140**, 97-106.

Snetkov VA, Knock GA, Baxter L, Thomas GD, Ward JP, & Aaronson PI (2006). Mechanisms of the prostaglandin $F_{2\alpha}$-induced rise in $[Ca^{2+}]i$ in rat intrapulmonary arteries. *J Physiol* **571**, 147-163.

Sobey CG (2001). Potassium channel function in vascular disease. *Arterioscler Thromb Vasc Biol* **21**, 28-38.

Soderberg O, Gullberg M, Jarvius M, Ridderstrale K, Leuchowius KJ, Jarvius J, Wester K, Hydbring P, Bahram F, Larsson LG, & Landegren U (2006). Direct observation of individual endogenous protein complexes in situ by proximity ligation. *Nat Methods* **3**, 995-1000.

Soderberg O, Leuchowius KJ, Kamali-Moghaddam M, Jarvius M, Gustafsdottir S, Schallmeiner E, Gullberg M, Jarvius J, & Landegren U (2007). Proximity

ligation: a specific and versatile tool for the proteomic era. *Genet Eng (N Y)* **28**, 85-93.

Somlyo AP & Somlyo AV (1990). Flash photolysis studies of excitation-contraction coupling, regulation, and contraction in smooth muscle. *Annu Rev Physiol* **52**, 857-874.

Somlyo AP & Somlyo AV (1994). Signal transduction and regulation in smooth muscle. *Nature* **372**, 231-236.

Somlyo AP & Somlyo AV (2000). Signal transduction by G-proteins, rho-kinase and protein phosphatase to smooth muscle and non-muscle myosin II. *J Physiol* **522**, 177-185.

Somlyo AP & Somlyo AV (2003). Ca^{2+} sensitivity of smooth muscle and nonmuscle myosin II: modulated by G proteins, kinases, and myosin phosphatase. *Physiol Rev* **83**, 1325-1358.

Somlyo AV & Somlyo AP (1968). Electromechanical and pharmacomechanical coupling in vascular smooth muscle. *J Pharmacol Exp Ther* **159**, 129-145.

Sommer N, Dietrich A, Schermuly RT, Ghofrani HA, Gudermann T, Schulz R, Seeger W, Grimminger F, & Weissmann N (2008). Regulation of hypoxic pulmonary vasoconstriction: basic mechanisms. *Eur Respir J* **32**, 1639-1651.

Son YK, Park WS, Kim SJ, Earm YE, Kim N, Youm JB, Warda M, Kim E, & Han J (2006). Direct inhibition of a PKA inhibitor, H-89 on KV channels in rabbit coronary arterial smooth muscle cells. *Biochem Biophys Res Commun* **341**, 931-937.

Stanbrook HS & McMurtry IF (1983). Inhibition of glycolysis potentiates hypoxic vasoconstriction in rat lungs. *J Appl Physiol* **55**, 1467-1473.

Standen NB & Quayle JM (1998). K^+ channel modulation in arterial smooth muscle. *Acta Physiol Scand* **164**, 549-557.

Starr A, Graepel R, Keeble J, Schmidhuber S, Clark N, Grant A, Shah AM, & Brain SD (2008). A reactive oxygen species-mediated component in neurogenic vasodilatation. *Cardiovasc Res* **78**, 139-147.

Staub NC (1985). Site of hypoxic pulmonary vasoconstriction. *Chest* **88**, 240S-245S.

Stehno-Bittel L & Sturek M (1992). Spontaneous sarcoplasmic reticulum calcium release and extrusion from bovine, not porcine, coronary artery smooth muscle. *J Physiol* **451**, 49-78.

Stenmark KR & McMurtry IF (2005). Vascular remodeling versus vasoconstriction in chronic hypoxic pulmonary hypertension: a time for reappraisal? *Circ Res* **97**, 95-98.

Stock D, Gibbons C, Arechaga I, Leslie AG, & Walker JE (2000). The rotary mechanism of ATP synthase. *Curr Opin Struct Biol* **10**, 672-679.

Sun PW, Kyoung SY, Kim N, Boum YJ, Joo H, Warda M, Ko JH, Earm YE, & Han J (2006). The protein kinase A inhibitor, H-89, directly inhibits KATP and Kir channels in rabbit coronary arterial smooth muscle cells. *Biochem Biophys Res Commun* **340**, 1104-1110.

Suzuki H & Twarog BM (1982). Membrane properties of smooth muscle cells in pulmonary arteries of the rat. *Am J Physiol* **242**, H900-H906.

Swärd K, Dreja K, Lindqvist A, Persson E, & Hellstrand P (2002). Influence of mitochondrial inhibition on global and local $[Ca^{2+}]_i$ in rat tail artery. *Circ Res* **90**, 792-799.

Swärd K, Dreja K, Susnjar M, Hellstrand P, Hartshorne DJ, & Walsh MP (2000). Inhibition of Rho-associated kinase blocks agonist-induced Ca^{2+} sensitization of myosin phosphorylation and force in guinea-pig ileum. *J Physiol* **522**, 33-49.

Sward K, Josefsson M, Lydrup ML, & Hellstrand P (1993). Effects of metabolic inhibition on cytoplasmic calcium and contraction in smooth muscle of rat portal vein. *Acta Physiol Scand* **148**, 265-272.

Sweeney M, Yu Y, Platoshyn O, Zhang S, McDaniel SS, & Yuan JX (2002). Inhibition of endogenous TRP1 decreases capacitative Ca^{2+} entry and attenuates pulmonary artery smooth muscle cell proliferation. *Am J Physiol Lung Cell Mol Physiol* **283**, L144-L155.

Sweeney M & Yuan JX (2000). Hypoxic pulmonary vasoconstriction: role of voltage-gated potassium channels. *Respir Res* **1**, 40-48.

Szabadkai G & Duchen MR (2008). Mitochondria: the hub of cellular Ca2+ signaling. *Physiology (Bethesda)* **23**, 84-94.

Szabadkai G, Simoni AM, Bianchi K, De S, Leo S, Wieckowski MR, & Rizzuto R (2006). Mitochondrial dynamics and Ca^{2+} signaling. *Biochim Biophys Acta* **1763**, 442-449.

Szabo I, Bock J, Jekle A, Soddemann M, Adams C, Lang F, Zoratti M, & Gulbins E (2005). A novel potassium channel in lymphocyte mitochondria. *J Biol Chem* **280**, 12790-12798.

Szewczyk A & Wojtczak L (2002). Mitochondria as a pharmacological target. *Pharmacol Rev* **54**, 101-127.

Takahashi Y, Watanabe H, Murakami M, Ohba T, Radovanovic M, Ono K, Iijima T, & Ito H (2007). Involvement of transient receptor potential canonical 1 (TRPC1) in angiotensin II-induced vascular smooth muscle cell hypertrophy. *Atherosclerosis* **195**, 287-296.

Takuwa Y (1996). Regulation of vascular smooth muscle contraction. The roles of Ca2+, protein kinase C and myosin light chain phosphatase. *Jpn Heart J* **37**, 793-813.

Tammaro P, Smith AL, Hutchings SR, & Smirnov SV (2004). Pharmacological evidence for a key role of voltage-gated K+ channels in the function of rat aortic smooth muscle cells. *Br J Pharmacol* **143**, 303-317.

Tanaka Y, Meera P, Song M, Knaus HG, & Toro L (1997). Molecular constituents of maxi K_{Ca} channels in human coronary smooth muscle: predominant $\alpha + \beta$ subunit complexes. *J Physiol* **502**, 545-557.

Tang XD, Garcia ML, Heinemann SH, & Hoshi T (2004). Reactive oxygen species impair Slo1 BK channel function by altering cysteine-mediated calcium sensing. *Nat Struct Mol Biol* **11**, 171-178.

Tasker PN, Michelangeli F, & Nixon GF (1999). Expression and distribution of the type 1 and type 3 inositol 1, 4, 5-trisphosphate receptor in developing vascular smooth muscle. *Circ Res* **84**, 536-542.

Tennant M & McGeachie JK (1990). Blood vessel structure and function: a brief update on recent advances. *Aust N Z J Surg* **60**, 747-753.

Teramoto N (2006). Physiological roles of ATP-sensitive K+ channels in smooth muscle. *J Physiol* **572**, 617-624.

Terraz S, Baechtold F, Renard D, Barsi A, Rosselet A, Gnaegi A, Liaudet L, Lazor R, Haefliger JA, Schaad N, Perret C, Kucera P, Markert M, & Feihl F (1999). Hypoxic contraction of small pulmonary arteries from normal and endotoxemic rats: fundamental role of NO. *Am J Physiol* **276**, H1207-H1214.

Thomas GD, Snetkov VA, Patel R, Leach RM, Aaronson PI, & Ward JP (2005). Sphingosylphosphorylcholine-induced vasoconstriction of pulmonary artery: activation of non-store-operated Ca^{2+} entry. *Cardiovasc Res* **68**, 56-64.

Tosun M, Paul RJ, & Rapoport RM (1998). Role of extracellular Ca^{++} influx *via* L-type and non-L-type Ca^{++} channels in thromboxane A_2 receptor-mediated contraction in rat aorta. *J Pharmacol Exp Ther* **284**, 921-928.

Tran NN, Robert A, Atkinson J, & Capdeville-Atkinson C (1997). Inhibition of oxidative phosphorylation, vascular tone, and $[Ca^{2+}]_i$ in the perfused rat tail artery. *Am J Physiol* **273**, C834-C842.

Treiman M, Caspersen C, & Christensen SB (1998). A tool coming of age: thapsigargin as an inhibitor of sarco-endoplasmic reticulum Ca^{2+}-ATPases. *Trends Pharmacol Sci* **19**, 131-135.

Trepakova ES, Csutora P, Hunton DL, Marchase RB, Cohen RA, & Bolotina VM (2000). Calcium influx factor directly activates store-operated cation channels in vascular smooth muscle cells. *J Biol Chem* **275**, 26158-26163.

Tucker SJ, Gribble FM, Zhao C, Trapp S, & Ashcroft FM (1997). Truncation of Kir6.2 produces ATP-sensitive K+ channels in the absence of the sulphonylurea receptor. *Nature* **387**, 179-183.

Turner JL & Kozlowski RZ (1997). Relationship between membrane potential, delayed rectifier K^+ currents and hypoxia in rat pulmonary arterial myocytes. *Exp Physiol* **82**, 629-645.

Turrens JF (1997). Superoxide production by the mitochondrial respiratory chain. *Biosci Rep* **17**, 3-8.

Turrens JF (2003). Mitochondrial formation of reactive oxygen species. *J Physiol* **552**, 335-344.

Turrens JF, Alexandre A, & Lehninger AL (1985). Ubisemiquinone is the electron donor for superoxide formation by complex III of heart mitochondria. *Arch Biochem Biophys* **237**, 408-414.

Uehata M, Ishizaki T, Satoh H, Ono T, Kawahara T, Morishita T, Tamakawa H, Yamagami K, Inui J, Maekawa M, & Narumiya S (1997). Calcium sensitization of smooth muscle mediated by a Rho-associated protein kinase in hypertension. *Nature* **389**, 990-994.

Ureña J, Franco-Obregón A, & López-Barneo J (1996). Contrasting effects of hypoxia on cytosolic Ca^{2+} spikes in conduit and resistance myocytes of the rabbit pulmonary artery. *J Physiol* **496**, 103-109.

Vaandrager AB & de Jonge HR (1996). Signalling by cGMP-dependent protein kinases. *Mol Cell Biochem* **157**, 23-30.

Vadula MS, Kleinman JG, & Madden JA (1993). Effect of hypoxia and norepinephrine on cytoplasmic free Ca^{2+} in pulmonary and cerebral arterial myocytes. *Am J Physiol* **265**, L591-L597.

Van Heijs BG, Blangé T, Jongsma HJ, & De Beer EL (2000). The length dependency of calcium activated contractions in the femoral artery smooth muscle studied with different methods of skinning. *J Muscle Res Cell Motil* **21**, 59-66.

Vanhoutte PM, Luscher TF, & Graser T (1991). Endothelium-dependent contractions. *Blood Vessels* **28**, 74-83.

Volk KA, Matsuda JJ, & Shibata EF (1991). A voltage-dependent potassium current in rabbit coronary artery smooth muscle cells. *J Physiol* **439**, 751-768.

Von Euler US & Liljestrand G (1946). Observations on the pulmonary arterial blood pressure in the cat. *Acta Physiol Scand* **12**, 301-320.

Wadsworth RM (1994). Vasoconstrictor and vasodilator effects of hypoxia. *Trends Pharmacol Sci* **15**, 47-53.

Waldron GJ & Cole WC (1999). Activation of vascular smooth muscle K^+ channels by endothelium-derived relaxing factors. *Clin Exp Pharmacol Physiol* **26**, 180-184.

Walker RL, Hume JR, & Horowitz B (2001). Differential expression and alternative splicing of TRP channel genes in smooth muscles. *Am J Physiol Cell Physiol* **280**, C1184-C1192.

Wallner M, Meera P, Ottolia M, Kaczorowski GJ, Latorre R, Garcia ML, Stefani E, & Toro L (1995). Characterization of and modulation by a beta-subunit of a

human maxi KCa channel cloned from myometrium. *Receptors Channels* **3**, 185-199.

Wallner M, Meera P, & Toro L (1996). Determinant for β-subunit regulation in high-conductance voltage-activated and Ca^{2+}-sensitive K^+ channels: an additional transmembrane region at the N terminus. *Proc Natl Acad Sci USA* **93**, 14922-14927.

Walsh C, Barrow S, Voronina S, Chvanov M, Petersen OH, & Tepikin A (2009). Modulation of calcium signalling by mitochondria. *Biochim Biophys Acta* **1787**, 1374-1382.

Walter FB (2003). Ventilation and Perfusion of the Lungs. In *Medical Physiology*, eds. Walter F Boron & Emile L Boulpaep, pp. 686-711. Saunders, Philadelphia.

Wang HS, Pan Z, Shi W, Brown BS, Wymore RS, Cohen IS, Dixon JE, & McKinnon D (1998). KCNQ2 and KCNQ3 potassium channel subunits: molecular correlates of the M-channel. *Science* **282**, 1890-1893.

Wang J, Shimoda LA, & Sylvester JT (2004). Capacitative calcium entry and TRPC channel proteins are expressed in rat distal pulmonary arterial smooth muscle. *Am J Physiol Lung Cell Mol Physiol* **286**, L848-L858.

Wang J, Shimoda LA, Weigand L, Wang W, Sun D, & Sylvester JT (2005a). Acute hypoxia increases intracellular [Ca2+] in pulmonary arterial smooth muscle by enhancing capacitative Ca2+ entry. *Am J Physiol Lung Cell Mol Physiol* **288**, L1059-L1069.

Wang J, Weigand L, Wang W, Sylvester JT, & Shimoda LA (2005b). Chronic hypoxia inhibits Kv channel gene expression in rat distal pulmonary artery. *Am J Physiol Lung Cell Mol Physiol* **288**, L1049-L1058.

Wang Q, Curran ME, Splawski I, Burn TC, Millholland JM, VanRaay TJ, Shen J, Timothy KW, Vincent GM, de JT, Schwartz PJ, Toubin JA, Moss AJ, Atkinson DL, Landes GM, Connors TD, & Keating MT (1996). Positional cloning of a novel potassium channel gene: KVLQT1 mutations cause cardiac arrhythmias. *Nat Genet* **12**, 17-23.

Wang R, Wu L, & Wang Z (1997). The direct effect of carbon monoxide on K_{Ca} channels in vascular smooth muscle cells. *Pflügers Arch* **434**, 285-291.

Wang YX, Dhulipala PK, & Kotlikoff MI (2000). Hypoxia inhibits the Na^+/Ca^{2+} exchanger in pulmonary artery smooth muscle cells. *FASEB J* **14**, 1731-1740.

Wang YX, Zheng YM, Abdullaev I, & Kotlikoff MI (2003a). Metabolic inhibition with cyanide induces calcium release in pulmonary artery myocytes and *Xenopus* oocytes. *Am J Physiol Cell Physiol* **284**, C378-C388.

Wang Z, Jin N, Ganguli S, Swartz DR, Li L, & Rhoades RA (2001). Rho-kinase activation is involved in hypoxia-induced pulmonary vasoconstriction. *Am J Respir Cell Mol Biol* **25**, 628-635.

Wang Z, Lanner MC, Jin N, Swartz D, Li L, & Rhoades RA (2003b). Hypoxia inhibits myosin phosphatase in pulmonary arterial smooth muscle cells: role of Rho-kinase. *Am J Respir Cell Mol Biol* **29**, 465-471.

Wanstall JC & O'Brien E (1996). In vitro hypoxia on rat pulmonary artery: effects on contractions to spasmogens and role of $K_{ATP\ channels}$. *Eur J Pharmacol* **303**, 71-78.

Ward JP (2003). Mitochondria and oxygen sensing: fueling the controversy. *J Physiol* **548**, 664.

Ward JP (2008). Oxygen sensors in context. *Biochim Biophys Acta* **1777**, 1-14.

Ward JP & Aaronson PI (1999). Mechanisms of hypoxic pulmonary vasoconstriction: can anyone be right? *Respir Physiol* **115**, 261-271.

Ward JP, Knock GA, Snetkov VA, & Aaronson PI (2004a). Protein kinases in vascular smooth muscle tone-role in the pulmonary vasculature and hypoxic pulmonary vasoconstriction. *Pharmacol Ther* **104**, 207-231.

Ward JP & McMurtry IF (2009). Mechanisms of hypoxic pulmonary vasoconstriction and their roles in pulmonary hypertension: new findings for an old problem. *Curr Opin Pharmacol* **9**, 287-296.

Ward JP & Robertson TP (1995). The role of the endothelium in hypoxic pulmonary vasoconstriction. *Exp Physiol* **80**, 793-801.

Ward JP, Snetkov VA, & Aaronson PI (2004b). Calcium, mitochondria and oxygen sensing in the pulmonary circulation. *Cell Calcium* **36**, 209-220.

Waypa GB, Chandel NS, & Schumacker PT (2001). Model for hypoxic pulmonary vasoconstriction involving mitochondrial oxygen sensing. *Circ Res* **88**, 1259-1266.

Waypa GB, Marks JD, Guzy R, Mungai PT, Schriewer J, Dokic D, & Schumacker PT (2010). Hypoxia triggers subcellular compartmental redox signaling in vascular smooth muscle cells. *Circ Res* **106**, 526-535.

Waypa GB, Marks JD, Mack MM, Boriboun C, Mungai PT, & Schumacker PT (2002). Mitochondrial reactive oxygen species trigger calcium increases during hypoxia in pulmonary arterial myocytes. *Circ Res* **91**, 719-726.

Waypa GB & Schumacker PT (2002). O_2 sensing in hypoxic pulmonary vasoconstriction: the mitochondrial door re-opens. *Respir Physiol Neurobiol* **132**, 81-91.

Waypa GB & Schumacker PT (2005). Hypoxic pulmonary vasoconstriction: redox events in oxygen sensing. *J Appl Physiol* **98**, 404-414.

Waypa GB & Schumacker PT (2006). Role for mitochondrial reactive oxygen species in hypoxic pulmonary vasoconstriction. *Novartis Found Symp* **272**, 176-192.

Weber DS & Webb RC (2001). Enhanced relaxation to the rho-kinase inhibitor Y-27632 in mesenteric arteries from mineralocorticoid hypertensive rats. *Pharmacol* **63**, 129-133.

Wei AD, Gutman GA, Aldrich R, Chandy KG, Grissmer S, & Wulff H (2005). International Union of Pharmacology. LII. Nomenclature and molecular relationships of calcium-activated potassium channels. *Pharmacol Rev* **57**, 463-472.

Weigand L, Foxson J, Wang J, Shimoda LA, & Sylvester JT (2005). Inhibition of hypoxic pulmonary vasoconstriction by antagonists of store-operated Ca^{2+} and nonselective cation channels. *Am J Physiol Lung Cell Mol Physiol* **289**, L5-L13.

Weir EK & Archer SL (1995). The mechanism of acute hypoxic pulmonary vasoconstriction: the tale of two channels. *FASEB J* **9**, 183-189.

Weir EK, Hong Z, Porter VA, & Reeve HL (2002). Redox signaling in oxygen sensing by vessels. *Respir Physiol Neurobiol* **132**, 121-130.

Weir EK & Olschewski A (2006). Role of ion channels in acute and chronic responses of the pulmonary vasculature to hypoxia. *Cardiovasc Res* **71**, 630-641.

Weissmann N, Dietrich A, Fuchs B, Kalwa H, Ay M, Dumitrascu R, Olschewski A, Storch U, Schnitzler M, Ghofrani HA, Schermuly RT, Pinkenburg O, Seeger W, Grimminger F, & Gudermann T (2006a). Classical transient receptor potential channel 6 (TRPC6) is essential for hypoxic pulmonary vasoconstriction and alveolar gas exchange. *Proc Natl Acad Sci USA* **103**, 19093-19098.

Weissmann N, Ebert N, Ahrens M, Ghofrani HA, Schermuly RT, Hänze J, Fink L, Rose F, Conzen J, Seeger W, & Grimminger F (2003). Effects of mitochondrial inhibitors and uncouplers on hypoxic vasoconstriction in rabbit lungs. *Am J Respir Cell Mol Biol* **29**, 721-732.

Weissmann N, Grimminger F, Olschewski A, & Seeger W (2001). Hypoxic pulmonary vasoconstriction: a multifactorial response? *Am J Physiol Lung Cell Mol Physiol* **281**, L314-L317.

Weissmann N, Grimminger F, Walmrath D, & Seeger W (1995). Hypoxic vasoconstriction in buffer-perfused rabbit lungs. *Respir Physiol* **100**, 159-169.

Weissmann N, Sommer N, Schermuly RT, Ghofrani HA, Seeger W, & Grimminger F (2006b). Oxygen sensors in hypoxic pulmonary vasoconstriction. *Cardiovasc Res* **71**, 620-629.

Wellman GC, Quayle JM, & Standen NB (1998). ATP-sensitive K^+ channel activation by calcitonin gene-related peptide and protein kinase A in pig coronary arterial smooth muscle. *J Physiol* **507**, 117-129.

Wilson AJ, Jabr RI, & Clapp LH (2000). Calcium modulation of vascular smooth muscle ATP-sensitive K^+ channels: role of protein phosphatase-2B. *Circ Res* **87**, 1019-1025.

Wilson DP, Susnjar M, Kiss E, Sutherland C, & Walsh MP (2005). Thromboxane A2-induced contraction of rat caudal arterial smooth muscle involves activation of Ca2+ entry and Ca2+ sensitization: Rho-associated kinase-mediated phosphorylation of MYPT1 at Thr-855, but not Thr-697. *Biochem J* **389**, 763-774.

Wilson HL, Dipp M, Thomas JM, Lad C, Galione A, & Evans AM (2001). ADP-ribosyl cyclase and cyclic ADP-ribose hydrolase act as a redox sensor: a primary role for cADPR in hypoxic pulmonary vasoconstriction. *J Biol Chem* **276**, 11180-11188.

Winder SJ, Allen BG, Clement-Chomienne O, & Walsh MP (1998). Regulation of smooth muscle actin-myosin interaction and force by calponin. *Acta Physiol Scand* **164**, 415-426.

Wingard CJ, Paul RJ, & Murphy RA (1994). Dependence of ATP consumption on cross-bridge phosphorylation in swine carotid smooth muscle. *J Physiol* **481 (Pt 1)**, 111-117.

Wray D (2009). Intracellular regions of potassium channels: Kv2.1 and heag. *Eur Biophys J* **38**, 285-292.

Wuttke TV, Seebohm G, Bail S, Maljevic S, & Lerche H (2005). The new anticonvulsant retigabine favors voltage-dependent opening of the Kv7.2 (KCNQ2) channel by binding to its activation gate. *Mol Pharmacol* **67**, 1009-1017.

Wyatt CN & Buckler KJ (2004). The effect of mitochondrial inhibitors on membrane currents in isolated neonatal rat carotid body type I cells. *J Physiol* **556**, 175-191.

Wyatt CN & Evans AM (2007). AMP-activated protein kinase and chemotransduction in the carotid body. *Respir Physiol Neurobiol* **157**, 22-29.

Wyatt CN, Mustard KJ, Pearson SA, Dallas ML, Atkinson L, Kumar P, Peers C, Hardie DG, & Evans AM (2007). AMP-activated protein kinase mediates carotid body excitation by hypoxia. *J Biol Chem* **282**, 8092-8098.

Xu C, Lu Y, Tang G, & Wang R (1999). Expression of voltage-dependent K^+ channel genes in mesenteric artery smooth muscle cells. *Am J Physiol* **277**, G1055-G1063.

Xu M, Platoshyn O, Makino A, Dillmann WH, Akassoglou K, Remillard CV, & Yuan JX (2008). Characterization of agonist-induced vasoconstriction in mouse pulmonary artery. *Am J Physiol Heart Circ Physiol* **294**, H220-H228.

Xu SZ & Beech DJ (2001). TrpC1 is a membrane-spanning subunit of store-operated Ca^{2+} channels in native vascular smooth muscle cells. *Circ Res* **88**, 84-87.

Xu X & Lee KS (1994). Characterization of the ATP-inhibited K+ current in canine coronary smooth muscle cells. *Pflugers Arch* **427**, 110-120.

Yamazaki J, Duan D, Janiak R, Kuenzli K, Horowitz B, & Hume JR (1998). Functional and molecular expression of volume-regulated chloride channels in canine vascular smooth muscle cells. *J Physiol* **507**, 729-736.

Yanagisawa T & Okada Y (1994). KCl depolarization increases Ca^{2+} sensitivity of contractile elements in coronary arterial smooth muscle. *Am J Physiol* **267**, H614-H621.

Yang C, Kwan YW, Chan SW, Lee SM, & Leung GP (2010a). Potentiation of EDHF-mediated relaxation by chloride channel blockers. *Acta Pharmacol Sin* **31**, 1303-1311.

Yang D, Gluais P, Zhang JN, Vanhoutte PM, & Feletou M (2004). Endothelium-dependent contractions to acetylcholine, ATP and the calcium ionophore A 23187 in aortas from spontaneously hypertensive and normotensive rats. *Fundam Clin Pharmacol* **18**, 321-326.

Yang WP, Levesque PC, Little WA, Conder ML, Ramakrishnan P, Neubauer MG, & Blanar MA (1998). Functional expression of two KvLQT1-related potassium channels responsible for an inherited idiopathic epilepsy. *J Biol Chem* **273**, 19419-19423.

Yang XR, Lin MJ, & Sham JS (2010b). Physiological functions of transient receptor potential channels in pulmonary arterial smooth muscle cells. *Adv Exp Med Biol* **661**, 109-122.

Yang Y, Murphy TV, Ella SR, Grayson TH, Haddock R, Hwang YT, Braun AP, Peichun G, Korthuis RJ, Davis MJ, & Hill MA (2009). Heterogeneity in function of small artery smooth muscle BKCa: involvement of the beta1-subunit. *J Physiol* **587**, 3025-3044.

Yang Z, Zhang Z, Xu Y, Li Y, & Ye T (2006). Relationship of intracellular free Ca2+ concentration and calcium-activated chloride channels of pulmonary artery smooth muscle cells in rats under hypoxic conditions. *J Huazhong Univ Sci Technolog Med Sci* **26**, 172-4, 191.

Yeung S, Schwake M, Pucovsky V, & Greenwood I (2008). Bimodal effects of the Kv7 channel activator retigabine on vascular K^+ currents. *Br J Pharmacol* **155**, 62-72.

Yeung SY & Greenwood IA (2005). Electrophysiological and functional effects of the KCNQ channel blocker XE991 on murine portal vein smooth muscle cells. *Br J Pharmacol* **146**, 585-595.

Yeung SY & Greenwood IA (2007). Pharmacological and biophysical isolation of K+ currents encoded by ether-a-go-go-related genes in murine hepatic portal vein smooth muscle cells. *Am J Physiol Cell Physiol* **292**, C468-C476.

Yeung SY, Pucovsky V, Moffatt JD, Saldanha L, Schwake M, Ohya S, & Greenwood IA (2007). Molecular expression and pharmacological identification of a role for K_v7 channels in murine vascular reactivity. *Br J Pharmacol* **151**, 758-770.

Yoon H, Lee D, Chun K, Yoon H, & Yoo J (2010). Effect of stress on the expression of rho-kinase and collagen in rat bladder tissue. *Korean J Urol* **51**, 132-138.

Young KA, Ivester C, West J, Carr M, & Rodman DM (2006). BMP signaling controls PASMC KV channel expression in vitro and in vivo. *Am J Physiol Lung Cell Mol Physiol* **290**, L841-L848.

Yu AY, Shimoda LA, Iyer NV, Huso DL, Sun X, McWilliams R, Beaty T, Sham JS, Wiener CM, Sylvester JT, & Semenza GL (1999). Impaired physiological responses to chronic hypoxia in mice partially deficient for hypoxia-inducible factor 1alpha. *J Clin Invest* **103**, 691-696.

Yu CA, Xia D, Kim H, Deisenhofer J, Zhang L, Kachurin AM, & Yu L (1998a). Structural basis of functions of the mitochondrial cytochrome bc1 complex. *Biochim Biophys Acta* **1365**, 151-158.

Yu MF, Gorenne I, Su X, Moreland RS, & Kotlikoff MI (1998b). Sodium hydrosulfite contractions of smooth muscle are calcium and myosin phosphorylation independent. *Am J Physiol* **275**, L976-L982.

Yuan JX (2001). Oxygen-sensitive K^+ channel(s): where and what? *Am J Physiol Lung Cell Mol Physiol* **281**, L1345-L1349.

Yuan XJ, Wang J, Juhaszova M, Gaine SP, & Rubin LJ (1998a). Attenuated K+ channel gene transcription in primary pulmonary hypertension. *Lancet* **351**, 726-727.

Yuan XJ, Wang J, Juhaszova M, Golovina VA, & Rubin LJ (1998b). Molecular basis and function of voltage-gated K+ channels in pulmonary arterial smooth muscle cells. *Am J Physiol* **274**, L621-L635.

Yuan X-J (1995). Voltage-gated K^+ currents regulate resting membrane potential and $[Ca^{2+}]_i$ in pulmonary arterial myocytes. *Circ Res* **77**, 370-378.

Yuan X-J, Goldman WF, Tod ML, Rubin LJ, & Blaustein MP (1993). Hypoxia reduces potassium currents in cultured rat pulmonary but not mesenteric arterial myocytes. *Am J Physiol* **264**, L116-L123.

Yuan X-J, Sugiyama T, Goldman WF, Rubin LJ, & Blaustein MP (1996). A mitochondrial uncoupler increases K_{Ca} currents but decreases K_V currents in pulmonary artery myocytes. *Am J Physiol* **270**, C321-C331.

Yuan X-J, Tod ML, Rubin LJ, & Blaustein MP (1994). Deoxyglucose and reduced glutathione mimic effects of hypoxia on K^+ and Ca^{2+} conductances in pulmonary artery cells. *Am J Physiol* **267**, L52-L63.

Yuan X-J, Tod ML, Rubin LJ, & Blaustein MP (1995a). Hypoxic and metabolic regulation of voltage-gated K^+ channels in rat pulmonary artery smooth muscle cells. *Exp Physiol* **80**, 803-813.

Yuan X-J, Tod ML, Rubin LJ, & Blaustein MP (1995b). Inhibition of cytochrome P-450 reduces voltage-gated K^+ currents in pulmonary arterial myocytes. *Am J Physiol* **268**, C259-C270.

Yuan X-J, Wang J, Juhaszova M, Golovina VA, & Rubin LJ (1998c). Molecular basis and function of voltage-gated K^+ channels in pulmonary arterial smooth muscle cells. *Am J Physiol* **274**, L621-L635.

Zaritsky JJ, Eckman DM, Wellman GC, Nelson MT, & Schwarz TL (2000). Targeted disruption of Kir2.1 and Kir2.2 genes reveals the essential role of the inwardly rectifying K^+ current in K^+-mediated vasodilation. *Circ Res* **87**, 160-166.

Zhang Y, Oltman CL, Lu T, Lee HC, Dellsperger KC, & VanRollins M (2001). EET homologs potently dilate coronary microvessels and activate BK(Ca) channels. *Am J Physiol Heart Circ Physiol* **280**, H2430-H2440.

Zhao Y, Packer CS, & Rhoades RA (1996). The vein utilizes different sources of energy than the artery during pulmonary hypoxic vasoconstriction. *Exp Lung Res* **22**, 51-63.

Zheng YM, Wang QS, Liu QH, Rathore R, Yadav V, & Wang YX (2008). Heterogeneous gene expression and functional activity of ryanodine receptors in resistance and conduit pulmonary as well as mesenteric artery smooth muscle cells. *J Vasc Res* **45**, 469-479.

Zhong XZ, bd-Elrahman KS, Liao CH, El-Yazbi AF, Walsh EJ, Walsh MP, & Cole WC (2010a). Stromatoxin-sensitive, Heteromultimeric Kv2.1/Kv9.3 Channels Contribute to Myogenic Control of Cerebral Arterial Diameter. *J Physiol*.

Zhong XZ, Harhun MI, Olesen SP, Ohya S, Moffatt JD, Cole WC, & Greenwood I (2010b). Participation of KCNQ (Kv7) Potassium Channels in Myogenic Control of Cerebral Arterial Diameter. *J Physiol*.

Zoccarato F, Cavallini L, Deana R, & Alexandre A (1988). Pathways of hydrogen peroxide generation in guinea pig cerebral cortex mitochondria. *Biochem Biophys Res Commun* **154**, 727-734.

Zor T & Selinger Z (1996). Linearization of the Bradford protein assay increases its sensitivity: theoretical and experimental studies. *Anal Biochem* **236**, 302-308.